THE ELECTROSTATIC PROBLEM FOR PIECEWISE CONSTANT CONDUCTIVITIES IN TWO DIMENSIONS: NUMERICAL METHODS AND OPTIMAL REGULARITY

BY

KYLE WALLER BOWER

A thesis submitted in conformity with
the requirements for the degree of
Doctor of Philosophy
Graduate Department of Mathematics
University of Toronto

ABSTRACT

The Electrostatic Problem for Piecewise Constant Conductivities in Two Dimensions: Numerical Methods and Optimal Regularity

Kyle Waller Bower

Doctor of Philosophy

Graduate Department of Mathematics

University of Toronto

2024

We present a numerical method for solving the elliptic partial differential equation problem for the electrostatic potential with piecewise constant conductivity and a Neumann boundary condition. This setting is often considered in studies of the Electrical Impedance Tomography (EIT) inverse problem. Our aim is to provide an accessible and self-contained presentation of both an integral equation formulation of the problem and a numerical method for solving it, which we hope will facilitate the adoption of such methods in the EIT community. Our method employs an integral equation approach for which we derive a system of well-conditioned integral equations by representing the solution as a sum of single layer potentials. The fast multipole method is used to accelerate the generalized minimal residual method solution of the integral equations. For efficiency, we adapt the grid of the Nyström method based on the spectral resolution of the layer charge density. Additionally, we present a method for evaluating the solution, based on up-sampling and the boundary element method, that is efficient and accurate throughout the domain, circumventing the

close-evaluation problem. To support the design choices of the numerical method, we derive regularity estimates with bounds explicitly in terms of the conductivities and the geometries of the boundaries between their regions. The resulting method is fast and accurate for solving for the electrostatic potential in media with piecewise constant conductivities. We also provide analytical results for the system of equations for the charge densities. Firstly, we establish existence and uniqueness to this system of equations. Secondly, we derive regularity for the charge densities along each interface. We show that assuming that the interface has $\mathcal{C}^k$ regularity, then the charge density is of regularity H^k (*i.e.*, in the Hilbert space of order k). Furthermore, we generalize our results by considering the case where the piecewise constant regions of conductivity overlap and we study the behaviour of the solution to leading order at points of intersection between two transversely intersecting interfaces of regions of piecewise constant conductivity.

Dedicated to my parents for their love and support.

ACKNOWLEDGEMENTS

First and foremost, I would like to thank my advisors Adam R. Stinchcombe and Spyros Alexakis for their expertise and guidance without which none of this would have been possible. Working with them has been both intellectually stimulating and insightful. I will be forever grateful for their care and guidance which has allowed me to become the mathematician I am today.

I would like to thank my committee members Kirill Serkh and Adrian Nachman for their invaluable knowledge and advice. I would like to thank Teemu Tyni for his work on the inverse solver. Additionally, I want to thank the faculty and staff at the Department of Mathematics for making my time at the University of Toronto a profoundly fulfilling and enjoyable time. In particular, I would like to thank Jemima Merisca for making me feel welcome from my first day in Toronto and for always generously volunteering her time to help me with any administrative issues I had.

Thank you to my family and friends for their love and support over all these years.

I acknowledge the Government of Ontario and the Department of Mathematics at the University of Toronto for their generous financial support during my studies.

PUBLICATIONS

Parts of this thesis have been or will be published in other places. The content of Chapter 2 has been submitted for publication and is available on the arXiv: https://arxiv.org/abs/2205.15354. The content of Chapter 3 will be submitted for publication.

CONTENTS

1

INTRODUCTION

The electrical impedance tomography (EIT) problem, also known as the inverse electrical conductivity problem, is the problem of determining the electrical conductivity $\sigma(x) > 0$ in a region $\Omega \subset \mathbb{R}^n$ from measurements of the electric potential $u(x)$ on the boundary $\partial\Omega$, given an injected current $\partial u(x)/\partial n$ on the boundary. The map from the injected current to the observed voltage is known as the Neumann-to-Dirichlet or current-to-voltage map, and the potential $u(x)$ satisfies the conductivity equation

$$\nabla \cdot (\sigma(x)\nabla u(x)) = 0, \quad x \in \Omega, \tag{1.1}$$

and depends in a nonlinear way on the conductivity $\sigma(x)$.

In Calderón's seminal paper [Cal80], he proved that, for the linearized problem, the conductivity can be determined uniquely from the Neumann-to-Dirichlet map. Since then, it has been shown that the conductivity is globally determined by the Neumann-to-Dirichlet map in two dimensions [Nac96b], three dimensions [SU87], for piecewise smooth conductivities [KV84, KV85, Isa88], and even for conductivities that are only bounded [AP06]. The EIT problem is known to be unstable, in the sense that a large perturbation to the conductivity inside Ω can result in only a small change to the Neumann-to-Dirichlet map (see, for example, [Ale88]). Nonetheless, a significant amount of information can be obtained about the conductivity, and the expected low cost and lack of any known side effects on the human body make EIT a potentially attractive imaging modality in medicine (see, for example, [CIN99]).

Since the EIT problem is unstable, any algorithm for solving it must restrict itself to looking for conductivities in some compact space, so that the inverse problem is well-posed in the sense of Tikhonov (see, for example, [TA77]). The spaces to which the conductivity belong are inextricably linked to the numerical method. Many regularization methods assume smooth solutions, including methods which use Tikhonov regularization [DZKK10] and methods which regularize the solution using integral equation formulations (see, for example, [CPS04]). Other methods explicitly represent the conductivity inside the region as a smooth function, using, for example, a sum of basis functions localized by smooth cutoff functions (see [BBP96]). As it turns out, spaces of smooth conductivities are not

particularly realistic when it comes to practical applications. Conductivities often have large discontinuous jumps between regions on which they are smooth—tumors, for example, are many times more conductive than normal tissue (see [SSBS88] and [ZG03]). Such considerations make the piecewise constant conductivity assumption an attractive choice. An enormous variety of methods and approaches have been proposed based on the piecewise constant conductivity assumption, of which the following is only a sample [CIN+90, CZ99, CT04, ALS20, BMPS18, KLMS08, FY20a, HU13a, Bru01].

Whatever the method for the inverse problem, the solution of the forward problem, in which the electric potential is determined from a known conductivity and injected current, is essential for validation and benchmarking, and forms an essential component of many inverse solvers. In the case of piecewise constant conductivities, the forward problem has been solved by the finite element method [TNM+14], the finite difference method [LL94], and the finite volume method [DZB+05]. The boundary element method (BEM) has also been applied to the corresponding integral equation formulations [dMFH00], which are derived by first reformulating the forward problem as a system of partial differential equations with interface boundary conditions connecting the various regions, and then representing the solution to this system by layer-potentials on the boundaries of the regions (see, for example, [CK13]). Such integral equations, when discretized, lead to well-conditioned, dense linear systems, which can be solved rapidly using the fast multipole method (FMM) (see, for example, [GR87, Mar19]).

The resulting reduction in the dimensionality of the problem and their favourable conditioning make integral equation formulations an attractive target for numerical methods. Boundary element methods solve these integral equations in two dimensions by approximating the boundaries by polylines (see, for example, [Liu09a]), but when the boundaries are smooth, the number of elements must be quite large, reducing their overall computational efficiency. Boundary integral equation methods (BIEMs), on the other hand, represent the boundaries and layer-potential densities by high order spectral expansions, and so can require far fewer degrees of freedom, but the evaluation of the resulting layer potentials close to their sources is highly involved and is the subject of contemporary research [HO08a, aKB21].

The integral equation formulations of transmission problems have been studied extensively from the point of view of both boundary integral equation methods and boundary element methods, and many fast and accurate solvers have been constructed. However, this work has mainly focused on acoustic and electromagnetic scattering [GB13, HX11, GHL14, PAB14]

and crack problems [YNK01, ON08, WYW05], with the notable exception of the work of Zakharov and Kalinin [ZK09] who studied the Laplace equation in a piecewise homogeneous medium. As far as we are aware, no boundary integral equation method has yet been proposed which simultaneously addresses all of the particular features of the forward electrical conductivity problem, including: the presence of large numbers of inclusions, which may be close to touching, the smooth boundaries of the inclusions, the finite extent of the domain, the moderate accuracy requirements of the method, and the need for reasonably accurate evaluation of the induced potential close to and on the boundaries of the regions. Furthermore, while the fast multipole method is not unknown in electrical impedance tomography, it has only been used in order to accelerate an application of an inverse solver, rather than to accelerate a forward solver (see [BM04]).

This thesis is organized as follows: In Chapter 2 we prove regularity of the solution to Eq. (1.1) at points across and near smooth interfaces between regions of piecewise constant conductivity and discuss our numerical methods in detail. In Chapter 3 we study the behaviour of the solution to Eq. (1.1) to leading order at points of intersection between two transversely intersecting interfaces of regions of piecewise constant conductivity. The conclusions follow in Chapter 4.

2

FORWARD CONDUCTIVITY PROBLEM FOR NON-OVERLAPPING REGIONS

2.1 INTRODUCTION

This chapter is motivated by the challenge of the Electrical Impedance Tomography (EIT) inverse problem, which is often studied in the setting of piecewise constant conductivities.

The general EIT problem in two dimensions is as follows. One has a conductive body $\Omega \subset \mathbb{R}^2$, where the conductivity at each point $\boldsymbol{x} \in \Omega$ is assumed isotropic and thus given by a positive number $\sigma(\boldsymbol{x}) > 0$. The distribution of the electrostatic potential u inside the body is described by the elliptic partial differential equation

$$L_\sigma(u) := \nabla \cdot (\sigma(\boldsymbol{x}) \nabla u(\boldsymbol{x})) = 0, \quad \boldsymbol{x} \in \Omega. \tag{2.1}$$

This is coupled to a boundary condition. In this chapter we consider the Neumann condition of injections of current. Letting $\boldsymbol{n}(\boldsymbol{x})$ be the outward-pointing unit normal to $\partial\Omega$, the Neumann boundary condition is

$$\sigma(\boldsymbol{x}) \frac{\partial u}{\partial \boldsymbol{n}}(\boldsymbol{x}) = b_0(\boldsymbol{x}), \quad \boldsymbol{x} \in \partial\Omega, \tag{2.2}$$

with $b_0(\boldsymbol{x})$ given subject to the constraint $\int_{\partial\Omega} b_0(\boldsymbol{x}) \, \mathrm{d}\ell(\boldsymbol{x}) = 0$. We can denote the solution to this problem by $u_\sigma(b_0)$, to stress the dependence on the conductivity $\sigma(\boldsymbol{x})$ and the injected current $b_0(\boldsymbol{x})$.

In this Neumann model of EIT, we seek to reconstruct (or approximate) $\sigma(\boldsymbol{x})$ given a finite number of sample measurements. An example of this would be to consider points $P_j \in \partial\Omega$, $j \in \{1, \ldots, J\}$ and a set of injections $b_0^i(\boldsymbol{x})$, $i \in \{1, \ldots, I\}$ of current. Assume that for each of the I injections we measure the voltage $u_\sigma(b_0^i)(P_j)$ at the J points (having grounded somewhere). This gives $I \cdot J$ data points concerning the conductivity $\sigma(\boldsymbol{x})$. We then seek to reconstruct, to some approximation, the conductivity $\sigma(\boldsymbol{x})$

from these $I \cdot J$ pieces of data. The pieces of data can be seen as samples of the Neumann-to-Dirichlet map $b_0 \mapsto u_\sigma(b_0)|_{\partial\Omega}$ associated to the operator $L_\sigma(u)$. We remark that this Neumann model is not the only model for EIT; another model is the related Complete Electrode Model (CEM) [BKIN07, TSA24], which considers the same equation (2.1) but imposes a different boundary condition. The CEM model is a more realistic model when the current injections are performed by electrodes, but since the case of Neumann injections has received more attention we focus on the Neumann setting here.

A successful resolution to the EIT problem (*i.e.*, a *good* reconstruction of $\sigma(\boldsymbol{x})$ given a finite set of boundary measurements $\{u_\sigma(b_0^i)(P_j)\}_{i\leq I, j\leq J}$) has potential real-world applications. In the Direct Current Resistivity (DCR) method used in geophysics, electrode arrays are placed on the Earth's surface or inside boreholes with the aim of determining the vertical distribution of resistivity in the ground. The typical assumption is that geological structures consist of pockets of various materials with differing constant conductivities (see Table 4.3-2 in [KLV07]). This same imaging modality is also used to image cross-sections of industrial processes and is known as Electrical Capacitance Tomography (ECT). In ECT, the capacitances of multi-electrode sensors surrounding an industrial vessel or pipe are used to determine the makeup of the materials inside (see, for example, [YP02]). Typically, the contents consist of a multiphase flow, and the usual assumption is that there are two materials inside the pipe or vessel with different constant permittivities: the flow itself, and either inclusions of a different material or voids (bubbles) (see [MTF15]).

We also note that weaker versions of this problem are also of interest. One such problem is where one does not try to reconstruct $\sigma(\boldsymbol{x})$ with any precision, but to just detect very coarse features of $\sigma(\boldsymbol{x})$. One such pursuit is for stroke detection [ACL+20].

A number of approaches have been tried to numerically solve the EIT problem, which we briefly review momentarily. However prior to doing so, let us note that given the finite number of measurements available, one frequently wants to either *restrict* the class of conductivities to a finite-dimensional space [Har19], or to impose a regularization to promote closeness to a subspace in a larger space of all possible conductivities $\sigma(\boldsymbol{x})$ [LÖS18]. As already discussed, a common assumption is that $\sigma(\boldsymbol{x})$ is piecewise constant. This is the class of conductivities that we will be considering in this chapter.

In addition to serving as a convenient model for real-world conductivities, the assumption of piecewise constant $\sigma(\boldsymbol{x})$ also ties in well with some of the methods that have been introduced to solve the EIT inverse problem. In particular the factorization method [Kir05, KG07] can be tried

to identify islands on which a sharp jump of conductivity occurs relative to a known (often constant) background conductivity. Another recent approach to EIT also considers piecewise constant conductivities which in addition are *layered*, and utilizes a one-dimensional method to identify the layers [Gar20, HS10, HU13b].

Furthermore, it is very common to *test* solvers of the EIT problem on real-world data which *are* piecewise constant. An example of this is in FIPS data set [HKM+17]. These data sets are frequently in two dimensions, where a well-studied approach is the d-bar method, based on Nachman's resolution of the Calderón problem [SMI00, Nac96a, KLMS09].

We also mention certain deep learning approaches to the EIT problem, which also seek to learn the map sending piecewise constant conductivities to their corresponding Neumann-to-Dirichlet (ND) operator (or, more correctly, the inverse of this map) [AMS22, FY20b, WLC19, HH18].

All these works make clear the significance of the piecewise constant conductivities setting to the EIT inverse problem. The significance for EIT of a fast and efficient solver specific to piecewise constant conductivities is in fact two-fold: For inverse solvers that rely *directly* on a fast and accurate forward solver to fit measurements to data, any improved forward solver for piecewise constant conductivities can be expected to provide better results. But even for solvers that do not rely on such direct methods, an improved solver could be useful: For instance for solvers that seek to learn a map from the ND operators to conductivities, the setting of piecewise constant conductivities has been used as a training set (see [HHHK19, CM20]).

Of course one may object that many realistic models have conductivities that are perhaps *close* to piecewise constant but not *quite* so. As we note in Section 2.5.5, in certain examples that we consider, piecewise constant conductivities seem to provide a good approximation for the EIT measurements for conductivities that are *smooth*: We consider the EIT data for conductivities that are C^1 smooth, but transition rapidly between islands of constant conductivity and a background of (different) fixed conductivity. We find that the EIT data of that setting are in fact small perturbations of the EIT data that correspond to the same islands, but where the transition between background and island conductivities is *sharp*.

The solution of (2.1) for piecewise constant $\sigma(\boldsymbol{x})$ is clearly then an important subject in EIT. In the case of piecewise constant conductivities, the forward problem has been solved by the finite element method [TNM+14], the finite difference method [LL94], and the finite volume method [DZB+05]. The boundary element method (BEM) and the boundary integral equation method (BIEM) have also been applied to the corresponding integral

equation formulations (see [dMFH00, YB13]), which are derived by first reformulating the forward problem as a system of partial differential equations with transmission boundary conditions connecting the various regions, and then representing the solution to this system of transmission problems by layer-potentials on the boundaries of the regions (see, for example, [CK13]). Such integral equations, when discretized, generally lead to well-conditioned, dense linear systems, which can be solved rapidly using an iterative linear system solver together with the fast multipole method (FMM), or by a direct approach (see, for example, [GR87, Mar19]).

The reduction in the dimensionality of the problem and their favorable conditioning make integral equation formulations an attractive target for numerical methods. BEMs solve these integral equations by approximating the boundaries by polylines (see, for example, [Liu09b]); however, when the boundaries are smooth, the number of elements must be quite large, which reduces their overall computational efficiency. BIEMs, on the other hand, represent the boundaries and layer-potential densities by high order spectral expansions, and so can require far fewer degrees of freedom, but the evaluation of the resulting layer potentials close to their sources can be fairly involved [HO08b, aKB21].

The integral equation formulations of transmission problems have been studied extensively using the BEM and the BIEM and many fast and accurate solvers have been constructed. Much of this work has focused on acoustic and electromagnetic scattering [GB13, HX11, GHL14, PAB14] and crack problems [YNK01, ON08, WYW05], however, several authors have presented methods specifically for the electrical conductivity problem, including the works of Zakharov and Kalinin [ZK09], Ying and Beale [YB13], and Helsing [Hel11a, Hel11b].

Despite the availability of these papers, boundary integral equation methods have remained essentially unused in the EIT literature. For this, we offer the following possible explanations. Firstly, boundary integral equation formulations are usually presented in the literature without proofs of existence, uniqueness, and regularity. Such proofs are generally confined to more specialized references (see, for example, the discussion of pseudodifferential boundary integral operators in [HW08]), which remain mostly inaccessible to non-specialists. Secondly, papers like [Hel11a, Hel11b] are written with an integral equation method audience in mind, and focus on demonstrating the effectiveness of more advanced and specialized techniques. For example, [Hel11b] solves (2.1) where the conductivity $\sigma(\boldsymbol{x})$ is piecewise constant on a random checkerboard, and while the results are very impressive, the methods described there (include the methods for discretization and preconditioning) are highly specific to this particular checkerboard geometry. Thirdly, the pa-

pers [ZK09] and [YB13], which are aimed at a more general audience, do not solve quite the same problem as the one required in EIT. Both papers only consider Dirichlet boundary conditions, which are easier to handle with integral equation formulations, and neither describe methods for adaptive discretization.

In this chapter, we seek to remedy this situation, providing both a complete and self-contained theory together with an easy-to-use algorithm. In particular, we describe an accessible algorithm for solving the forward electrical conductivity problem which: constructs the solution to the equation (2.1) on domains with numerous inclusions; allows for Neumann boundary conditions; evaluates the solution quickly and accurately; achieves $O(N)$ scaling with the use of the FMM; and solves the problem in an automatically adaptive fashion depending only on a user-specified accuracy.

We illustrate the performance of our algorithm with several numerical examples. We show that the method is highly effective, especially in the low-to-moderate accuracy regime typically required in EIT problems.

Of all of the papers previously cited, the algorithm of this chapter is most closely related to the algorithm proposed in [YB13]. Our algorithm differs in that we consider Neumann boundary conditions; we show that a combination of upsampling and BEM discretization performs well at the accuracy levels required in EIT, yielding a simpler approach compared to their more mathematically involved singularity splitting scheme (see also [BL01]); we evaluate the solution directly from the solved layer potentials; and we construct our Nyström discretization in a fully adaptive fashion.

In this chapter, we also provide a completely self-contained theory with regards to the formulation of a well-conditioned system of boundary integral equations, and to the existence, uniqueness, and regularity of its solutions. First, we describe how the rank-deficiency resulting from the Neumann boundary conditions of the electrical conductivity problem can be resolved by adding an extra term to adjust the resulting system of integral equations. This is done without changing the dimensionality of the system to be solved, and differs from the usual approach of adjoining additional degrees of freedom as well as additional constraints to the system (see, for example, [GGM93, ZK09]). Second, we provide a detailed justification for the choice of rescaling of the integral equations to ensure good conditioning (see also [ZK09]). Third, we provide the proofs of existence and uniqueness to this system of integral equations, and derive $\mathcal{C}^{k,\alpha}$ regularity estimates for the charge densities on the interfaces using energy-type methods. While the behaviour of such systems of boundary integral equations is considered well-understood, regularity results are

typically stated in more general settings (see, for example, [HW08, Cos88]), where the dependency of the constants on the physical parameters of the problem is often suppressed. Our $\mathcal{C}^{k,\alpha}$ estimates provide bounds explicitly in terms of the conductivities and the geometries of the boundaries between regions, and are highly illuminating with respect to numerical and practical applications. We also provide stronger estimates for the case of concentric circles, which is a ubiquitous test case for inverse methods in EIT (see, for example, [KLMS08, CII90, MS03]). Our proofs are also reasonably short and should be accessible to an applied audience.

This chapter is organized as follows. In Section 2.2, we describe the forward electrical conductivity problem. In Section 2.3, we derive the corresponding system of boundary integral equations and modify it so that it is both solvable and well-conditioned. Our numerical method is presented in Section 2.4. We provide numerical experiments in Section 2.5. In Section 2.6, we prove existence and uniqueness, and provide regularity estimates for both the case of general regions and the case of concentric circular regions of constant conductivity. The conclusions follow in Section 2.7.

2.2 PROBLEM SETTING

Let $\Omega \subset \mathbb{R}^2$ be a simply connected and bounded domain with smooth boundary $\partial\Omega$. We consider the conductivity equation (2.1) for which $u : \Omega \to \mathbb{R}$ is the unknown scalar potential and $\sigma : \Omega \to \mathbb{R}^+$ is the electrical conductivity. We consider the case in which the domain consists of finitely many regions of piecewise constant conductivity *i.e.*, $\sigma = \sigma_i$ on region E_i for $i = 0, 1, \ldots, N$. The Neumann boundary condition is (2.2) in which $b_0 : \partial\Omega \to \mathbb{R}$ is the injected current. We consider the case for which $b_0 \in \mathcal{C}^{0,1}$ is a Lipschitz function. We use $\boldsymbol{n}$ to denote the unit outward normal vector to the boundary and use $\frac{\partial}{\partial \boldsymbol{n}}$ or $\partial_{\boldsymbol{n}}$ for the corresponding normal derivative.

We introduce a tree structure, a connected acyclic undirected graph, to describe the layout of the regions of constant conductivity. The *descendants* of a region are those regions that are entirely within it. Let p_i denote the unique *parent* of region E_i for $i = 1, \ldots, N$. Note that $\boldsymbol{n}$ will point towards a region's parent. Let region 0 be the root region in the tree. This is the region on whose boundary the Neumann boundary condition is imposed. The conductivity jumps across the outer boundary of region $i \neq 0$ from σ_i to σ_{p_i}. Leaves of the tree correspond to simply connected regions that do not contain any other regions. Figure 2.1 shows an example layout of regions and the corresponding tree of regions.

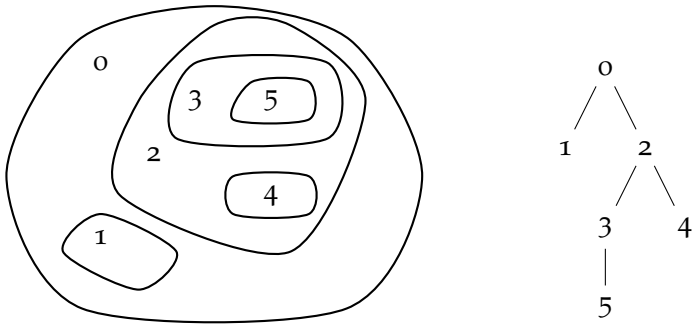

Figure 2.1: An example layout of regions and the corresponding tree of regions. The outer boundary of the root of the tree, here region 0, is the boundary of the domain. Each region shares an interface with its children in the tree. The sets of descendants are $S_0 = \{1,2,3,4,5\}, S_1 = \{\}, S_2 = \{3,4,5\}, S_3 = \{5\}, S_4 = \{\}, S_5 = \{\}$.

We seek to solve an elliptic interface problem by finding u such that:

$$\Delta u = 0 \text{ in } \Omega \setminus \cup_{i=0}^{N} \partial\Omega_i \tag{2.3}$$

$$\sigma_0 \partial_{\boldsymbol{n}} u = b_0 \text{ on } \partial\Omega_0 \tag{2.4}$$

$$[u] = 0 \text{ on } \partial\Omega_i, \quad i = 1, \ldots, N \tag{2.5}$$

$$[\sigma \partial_{\boldsymbol{n}} u] = b_i \text{ on } \partial\Omega_i, \quad i = 1, \ldots, N \tag{2.6}$$

in which Ω_i is the union of region E_i and all its descendants. We require $\partial\Omega_i \in \mathcal{C}^2$ and $b_i \in \mathcal{C}^{0,1}$ for $i = 0, \ldots, N$. Additionally, we require that no region intersects the outer boundary $\partial\Omega_0$. For any function $\xi : \Omega \to \mathbb{R}$ and $\boldsymbol{x}_0 \in \partial\Omega_i$, we define $[\xi](\boldsymbol{x}_0)$ to be $\xi^+(\boldsymbol{x}_0) - \xi^-(\boldsymbol{x}_0)$ where $\xi^+(\boldsymbol{x}_0)$ is the limit of $\xi(\boldsymbol{x})$ as $\boldsymbol{x} \to \boldsymbol{x}_0$ from $\Omega \setminus \Omega_i$ and $\xi^-(\boldsymbol{x}_0)$ is the limit of $\xi(\boldsymbol{x})$ as $\boldsymbol{x} \to \boldsymbol{x}_0$ from Ω_i. We require $\int_{\partial\Omega_i} b_i(\boldsymbol{x}) \, \mathrm{d}\ell_{\boldsymbol{x}} = 0$ for $i = 0, \ldots, N$ so that the PDE problem is well-posed up to an additive constant.

The weak formulation of the PDE problem (2.3)-(2.6) will be discussed in Section 2.6.

2.3 A BOUNDARY INTEGRAL FORMULATION

We recast the PDE problem, equations (2.3)-(2.6), as a boundary integral equation of the second kind [Atk97]. The resulting system of integral

equations is given in (2.38) and (2.39). Using an indirect approach, we represent the solution as the sum of $N+1$ single layer potentials

$$u(\boldsymbol{x}) = \sum_{j=0}^{N} \mathcal{S}_{\partial\Omega_j}[\gamma_j](\boldsymbol{x}). \tag{2.7}$$

The single layer potential with charge density $\gamma_j \in \mathcal{C}(\partial\Omega_j)$ is defined as

$$\mathcal{S}_{\partial\Omega_j}[\gamma_j](\boldsymbol{x}) := \int_{\partial\Omega_j} G(\boldsymbol{x},\boldsymbol{y})\gamma_j(\boldsymbol{y})\, \mathrm{d}\ell_{\boldsymbol{y}}, \tag{2.8}$$

with the two-dimensional free space Green's function

$$G(\boldsymbol{x},\boldsymbol{y}) = \frac{1}{2\pi}\log|\boldsymbol{x}-\boldsymbol{y}|. \tag{2.9}$$

Since the single layer potential is harmonic off of $\partial\Omega_j$ and continuous across $\partial\Omega_j$, the sum of single layer potentials in (2.7) automatically satisfies (2.3) and (2.5).

As a consequence of (2.7), the charge density on an interface is equal to the jump in normal derivatives of the solution across the interface *i.e.*,

$$\gamma_i = [\partial_{\boldsymbol{n}} u] = \partial_{\boldsymbol{n}^+} u - \partial_{\boldsymbol{n}^-} u \text{ on } \partial\Omega_i, \quad i = 1,\ldots,N. \tag{2.10}$$

The normal derivative of a single layer potential on $\partial\Omega_i$ is readily computed using the adjoint of the Neumann-Poincaré operator,

$$\mathcal{K}^*_{\partial\Omega_i}[\gamma_i](\boldsymbol{x}) := \frac{1}{2\pi}\int_{\partial\Omega_i} \frac{(\boldsymbol{x}-\boldsymbol{y})\cdot\boldsymbol{n}(\boldsymbol{x})}{|\boldsymbol{x}-\boldsymbol{y}|^2}\gamma_i(\boldsymbol{y})\, \mathrm{d}\ell_{\boldsymbol{y}}, \quad \boldsymbol{x}\in\partial\Omega_i. \tag{2.11}$$

A standard result from potential theory [Kre14, CDH16] is that for $\boldsymbol{x}\in\partial\Omega_i$

$$\partial_{\boldsymbol{n}^\pm}\mathcal{S}_{\partial\Omega_i}[\gamma_i](\boldsymbol{x}) = \mathcal{K}^*_{\partial\Omega_i}[\gamma_i](\boldsymbol{x}) \pm \frac{1}{2}\gamma_i(\boldsymbol{x}), \tag{2.12}$$

provided that $\partial\Omega_i$ is $\mathcal{C}^2$ and $\gamma_i \in \mathcal{C}(\partial\Omega_i)$. The kernel of the adjoint of the Neumann-Poincaré operator,

$$K(\boldsymbol{x},\boldsymbol{y}) = \frac{1}{2\pi}\frac{(\boldsymbol{x}-\boldsymbol{y})\cdot\boldsymbol{n}(\boldsymbol{x})}{|\boldsymbol{x}-\boldsymbol{y}|^2}, \tag{2.13}$$

has a removable discontinuity at $\boldsymbol{x}=\boldsymbol{y}\in\partial\Omega_i$. This discontinuity is removed by defining

$$K(\boldsymbol{x},\boldsymbol{x}) := \frac{\kappa(\boldsymbol{x})}{4\pi}, \tag{2.14}$$

in which κ is the curvature at point $\boldsymbol{x} \in \partial\Omega_i$. Since the interfaces are in $\mathcal{C}^2$, do not self-intersect, and do not intersect with other interfaces, $\boldsymbol{x} = \boldsymbol{y}$ implies $\boldsymbol{n}(\boldsymbol{x}) = \boldsymbol{n}(\boldsymbol{y})$ and $K(\boldsymbol{x}, \boldsymbol{y}) \in \mathcal{C}^2$.

On the boundary of each region $\partial\Omega_i$, there is a single layer of charge with density γ_i. Enforcing the boundary condition (2.4) and the interfaces conditions (2.6) provide a system of integral equations that determine $\gamma_0, \ldots, \gamma_N$. The normal derivative of the single layer potential $\mathcal{S}_{\partial\Omega_j}[\gamma_j]$ at point $\boldsymbol{x} \in \partial\Omega_i, i \in \{0, \ldots, N\}$ is

$$\partial_{\boldsymbol{n}^\pm} \mathcal{S}_{\partial\Omega_j}[\gamma_j](\boldsymbol{x}) = \int_{\partial\Omega_j} K(\boldsymbol{x}, \boldsymbol{y}) \gamma_j(\boldsymbol{y}) \, \mathrm{d}\ell_{\boldsymbol{y}} \pm \frac{1}{2} \gamma_j(\boldsymbol{x}) \delta_{ij}, \tag{2.15}$$

in which δ_{ij} is the Kronecker delta. Substituting (2.7) and (2.15) into (2.4) and (2.6) gives a system of integral equations for the charge densities,

$$-\frac{1}{2}\sigma_0 \gamma_0(\boldsymbol{x}) + \sigma_0 \sum_{j=0}^{N} \int_{\partial\Omega_j} K(\boldsymbol{x}, \boldsymbol{y}) \gamma_j(\boldsymbol{y}) \, \mathrm{d}\ell_{\boldsymbol{y}} = b_0(\boldsymbol{x}), \quad \boldsymbol{x} \in \partial\Omega_0, \tag{2.16}$$

$$\frac{1}{2} \left(\sigma_{p_i} + \sigma_i\right) \gamma_i(\boldsymbol{x}) + \left(\sigma_{p_i} - \sigma_i\right) \sum_{j=0}^{N} \int_{\partial\Omega_j} K(\boldsymbol{x}, \boldsymbol{y}) \gamma_j(\boldsymbol{y}) \, \mathrm{d}\ell_{\boldsymbol{y}} = b_i(\boldsymbol{x}), \quad \boldsymbol{x} \in \partial\Omega_i, \tag{2.17}$$

$$\text{for } i = 1, \ldots, N.$$

The system of equations (2.16) and (2.17) is ill-posed, owing exclusively to the well-known non-uniqueness for the Neumann problem for equations of this type. In particular, solutions are only defined up to an additive constant.

We will resolve this issue here, by making a suitable change to the system. Prior to doing this, it is instructive to derive that the total charge on any inner interface must vanish as a consequence of the system (2.16) and (2.17). The non-uniqueness is entirely captured in the freedom to define a weighted integral of the charge density on the outer boundary arbitrarily, as we will see later.

Denote the total charge on $\partial\Omega_i$ by C_i *i.e.*,

$$C_i := \int_{\partial\Omega_i} \gamma_i(\boldsymbol{x}) \, \mathrm{d}\ell_{\boldsymbol{x}}, \quad \text{for } i = 0, \ldots, N. \tag{2.18}$$

We will show that the integral equations (2.17) imply that $C_i = 0$ for all $i = 1, \ldots, N$. We integrate the integral equations (2.17) along $\partial\Omega_i$ and use

the requirement that $\int_{\partial\Omega_i} b_i(\boldsymbol{x})\ \mathrm{d}\ell_{\boldsymbol{x}} = 0$ for $i \in \{1,\ldots,N\}$ to obtain the system of equations

$$0 = \frac{1}{2}(\sigma_{p_i} + \sigma_i)C_i + (\sigma_{p_i} - \sigma_i)\sum_{j=0}^{N}\int_{\partial\Omega_i}\int_{\partial\Omega_j} K(\boldsymbol{x},\boldsymbol{y})\gamma_j(\boldsymbol{y})\ \mathrm{d}\ell_{\boldsymbol{y}}\ \mathrm{d}\ell_{\boldsymbol{x}}, \quad (2.19)$$
$$\text{for } i = 1,\ldots,N.$$

Since $\boldsymbol{y} \in \partial\Omega_j$, the divergence theorem and in the case when $\boldsymbol{y} \in \partial\Omega_i$ slightly modifying the contour can be used to compute the integral

$$\int_{\partial\Omega_i} K(\boldsymbol{x},\boldsymbol{y})\ \mathrm{d}\ell_{\boldsymbol{x}} = \begin{cases} 1, & \boldsymbol{y} \in \mathrm{int}(\Omega_i) \\ \frac{1}{2}, & \boldsymbol{y} \in \partial\Omega_i \\ 0, & \boldsymbol{y} \in \mathrm{ext}(\Omega_i) \end{cases}. \quad (2.20)$$

Swapping the order of integration in (2.19) and using (2.20) leads to the system of equations

$$0 = \sigma_{p_i}C_i + (\sigma_{p_i} - \sigma_i)\sum_{j\in S_i} C_j, \quad \text{for } i = 1,\ldots,N, \quad (2.21)$$

in which $S_i \subseteq \{0,\ldots,N\}$ is the set of all regions that are descendants of region E_i as illustrated in Figure 2.1. These equations immediately give us that for any region E_i that has no descendants *i.e.*, a leaf of our tree of regions, $C_i = 0$. Then, for any parent region p_i whose descendants all have $C_i = 0$, we must also have $C_{p_i} = 0$. By induction, we get $C_i = 0$ for all $i = 1,\ldots,N$.

Subsequently, we will show that the freedom in selecting the total charge on the outer boundary is equivalent to choosing the additive constant for the PDE problem. We will begin by showing that the freedom in selecting a weighted integral of the charge density on the outer boundary is equivalent to choosing the additive constant for the PDE problem. Assume we have two solutions to the system of integral equations (2.16) and (2.17). We will denote these two solutions by u_1 and u_2. Define u to be the difference between the two solutions *i.e.*, $u = u_1 - u_2$.

Then u satisfies the same problem as before (2.3)-(2.6) with all the right hand sides being zero. Any solution to the system (2.3)-(2.6) is a solution of the weak formulation of the elliptic interface problem. The only solution to the weak problem with all the right hand sides being zero is the constant solution $u = d$.

Let us denote the charge densities corresponding to the difference of the two solutions to the integral equations system (2.16) and (2.17) by $\delta\gamma_i, i = 0,\ldots,N$. Since we know that the solution u must be a constant,

we have using (2.10) that $\delta\gamma_i = 0$ for all $i \geq 1$. Therefore, using (2.7) and (2.8) u satisfies the formula

$$u(\boldsymbol{x}) = \int_{\partial\Omega_0} G(\boldsymbol{x}, \boldsymbol{y}) \delta\gamma_0(\boldsymbol{y}) \, \mathrm{d}\ell_y, \tag{2.22}$$

in which $\delta\gamma_0$ is the charge density on the outer boundary. Integrating u along $\partial\Omega_0$ and swapping the order of integration gives

$$\begin{aligned} d \cdot \text{length}(\partial\Omega_0) &= \int_{\partial\Omega_0} u(\boldsymbol{x}) \, d\ell_x && (2.23)\\ &= \int_{\partial\Omega_0} \int_{\partial\Omega_0} G(\boldsymbol{x}, \boldsymbol{y}) \delta\gamma_0(\boldsymbol{y}) \, d\ell_y \, d\ell_x && (2.24)\\ &= \int_{\partial\Omega_0} w(\boldsymbol{y}) \delta\gamma_0(\boldsymbol{y}) \, d\ell_y && (2.25) \end{aligned}$$

in which $w(\boldsymbol{y}) := \int_{\partial\Omega_0} G(\boldsymbol{x}, \boldsymbol{y}) \, \mathrm{d}\ell_x$. If $\partial\Omega_0$ is a circle of radius R, then $w(\boldsymbol{y})$ is constant and identically equal to $R \log R$. This computation is as follows:

$$\begin{aligned} w &= \frac{1}{2\pi} \int_0^{2\pi} \log |\langle R\cos\theta, R\sin\theta\rangle - \langle R, 0\rangle| R \, d\theta && (2.26)\\ &= \frac{1}{2\pi} \int_0^{2\pi} \log |\langle R\cos\theta - R, R\sin\theta\rangle| R \, d\theta && (2.27)\\ &= \frac{1}{2\pi} \int_0^{2\pi} \log \left(\sqrt{(R\cos\theta - R)^2 + (R\sin\theta)^2} \right) R \, d\theta && (2.28)\\ &= \frac{R}{4\pi} \int_0^{2\pi} \log \left((R\cos\theta - R)^2 + (R\sin\theta)^2 \right) \, d\theta && (2.29)\\ &= \frac{R}{4\pi} \int_0^{2\pi} \log \left(2R^2(1 - \cos\theta) \right) \, d\theta && (2.30)\\ &= \frac{R}{4\pi} \int_0^{2\pi} \left(2\log(R) + \log(2(1 - \cos\theta)) \right) \, d\theta && (2.31)\\ &= \frac{R}{4\pi} \left[4\pi \log R \right] && (2.32)\\ &= R \log R. && (2.33) \end{aligned}$$

Next we will show that specifying the given weighted integral of the charge density on the outer boundary is equivalent to specifying the total charge on the outer boundary. We note that $\delta\gamma_0$ is the charge density on the boundary of a conductor and is thus continuous and never zero [Pet12]. Hence, $\delta\gamma_0$ is of constant sign. Now we have already shown there is a one-dimensional kernel to our system of integral equations (2.16) and (2.17) consisting of charge densities that yield the constant solution so specifying the total charge on the outer boundary will uniquely specify

the weighted integral of the charge density on the outer boundary and vice versa.

We thus derive that any two solutions to the original problem (2.3)-(2.6) with the same b_i for $i = 0, \ldots, N$ differ by a constant and that specifying the total charge on the outer boundary uniquely specifies a solution to problem (2.3)-(2.6).

For definiteness, we will be imposing that the total charge on the outer boundary $C_0 := \int_{\partial\Omega_0} \gamma_0(\boldsymbol{y}) \, \mathrm{d}\ell_{\boldsymbol{y}} = 0$. We incorporate our choice of $C_0 = 0$ into the system of linear integral equations given in (2.16) and (2.17) by modifying the kernel in (2.13) when $i = j = 0$ by subtracting 1. The integral equations (2.16) and (2.17) for the charge densities with the modified kernel where $C_0 = 0$ become

$$-\frac{1}{2}\sigma_0\gamma_0(\boldsymbol{x}) + \sigma_0 \sum_{j=0}^{N} \int_{\partial\Omega_j} \left[K(\boldsymbol{x},\boldsymbol{y}) - \delta_{0j}\right] \gamma_j(\boldsymbol{y}) \, \mathrm{d}\ell_{\boldsymbol{y}} = b_0(\boldsymbol{x}), \quad \boldsymbol{x} \in \partial\Omega_0, \tag{2.34}$$

$$\frac{1}{2}\left(\sigma_{p_i} + \sigma_i\right)\gamma_i(\boldsymbol{x}) + \left(\sigma_{p_i} - \sigma_i\right) \sum_{j=0}^{N} \int_{\partial\Omega_j} K(\boldsymbol{x},\boldsymbol{y})\gamma_j(\boldsymbol{y}) \, \mathrm{d}\ell_{\boldsymbol{y}} = b_i(\boldsymbol{x}), \quad \boldsymbol{x} \in \partial\Omega_i, \quad \text{for } i = 1, \ldots, N. \tag{2.35}$$

We seek to show that the previous integral equations (2.16) and (2.17) with the additional constraint $C_0 := \int_{\partial\Omega_0} \gamma_0(\boldsymbol{y}) \, \mathrm{d}\ell_{\boldsymbol{y}} = 0$ are equivalent to the modified integral equations (2.34) and (2.35). We first show that a solution to the previous integral equations (2.16) and (2.17) where in addition $C_0 = 0$ yields a solution to the modified integral equations (2.34) and (2.35). Since the only difference between the two systems of integral equations is that (2.34) has an additional term on the left hand side

$$-\int_{\partial\Omega_0} \gamma_0(\boldsymbol{y}) \, \mathrm{d}\ell_{\boldsymbol{y}} \tag{2.36}$$

which is 0 when $C_0 = 0$, a solution to the previous integral equations (2.16) and (2.17) where in addition $C_0 = 0$ yields a solution to the modified integral equations (2.34) and (2.35).

Next, we show the converse that a solution to the modified integral equations (2.34) and (2.35) yields a solution to the previous integral equations (2.16) and (2.17) where in addition $C_0 = 0$. Integrating the integral equation with the modified kernel (2.34) around $\partial\Omega_0$, swapping the order of integration, and using the divergence theorem immediately gives $-\int_{\partial\Omega_0} \gamma_0(\boldsymbol{y}) \, \mathrm{d}\ell_{\boldsymbol{y}} = 0$ which by definition of C_0 implies that $C_0 = 0$. Now, the additional term (2.36) in equation (2.34) vanishes so a solution to

the modified integral equations (2.34) and (2.35) yields a solution to the previous integral equations (2.16) and (2.17).

Thus, the system of modified integral equations (2.34)-(2.35) is equivalent to the original system of integral equations (2.16)-(2.17) with the additional constraint that the total charge on the outer boundary $C_0 = 0$.

2.3.1 *Conditioning of Linear System*

The scenarios we are interested in typically involve conductivities of order 1; however, if two neighbouring conductivities are very similar in value then the resulting system of integral equations will be poorly conditioned. For an inner interface (*i.e.*, $i \geq 1$), if $b_i \equiv [\sigma \partial_{\boldsymbol{n}} u] = 0$, then (2.6) and (2.10) imply that the charge density on interface $\partial\Omega_i$ is

$$\gamma_i = \partial_{\boldsymbol{n}^+} u \left(1 - \frac{\sigma_{p_i}}{\sigma_i}\right). \tag{2.37}$$

This quantity will be very small if $\sigma_{p_i} \approx \sigma_i$ leading to a poorly conditioned system of integral equations. To improve the conditioning of the system of integral equations, we rescale the charge densities to be proportional to $\partial_{\boldsymbol{n}^+} u$ by defining $\phi_i := \gamma_i / \alpha_i$ where $\alpha_i = 1 - \sigma_{p_i}/\sigma_i$ for $i \in \{1, \ldots, N\}$ and $\alpha_0 = 1$. The integral equations for the rescaled charge densities ϕ_i become

$$-\frac{1}{2}\phi_0(\boldsymbol{x}) + \sum_{j=0}^{N} \alpha_j \int_{\partial\Omega_j} \left[K(\boldsymbol{x}, \boldsymbol{y}) - \delta_{0j}\right] \phi_j(\boldsymbol{y}) \, \mathrm{d}\ell_{\boldsymbol{y}} = \frac{b_0(\boldsymbol{x})}{\sigma_0}, \quad \boldsymbol{x} \in \partial\Omega_0, \tag{2.38}$$

$$\frac{1}{2}\alpha_i \frac{(\sigma_{p_i} + \sigma_i)}{\sigma_{p_i} - \sigma_i} \phi_i(\boldsymbol{x}) + \sum_{j=0}^{N} \alpha_j \int_{\partial\Omega_j} K(\boldsymbol{x}, \boldsymbol{y}) \phi_j(\boldsymbol{y}) \, \mathrm{d}\ell_{\boldsymbol{y}} = \frac{b_i(\boldsymbol{x})}{\sigma_{p_i} - \sigma_i}, \quad \boldsymbol{x} \in \partial\Omega_i, \tag{2.39}$$

$$\text{for } i = 1, \ldots, N$$

in which δ_{0j} is the Kronecker delta and K is the kernel of the adjoint of the Neumann-Poincaré operator defined in (2.13) and (2.14). Thus, ϕ_i in view of (2.37) will be proportional to $\partial_{\boldsymbol{n}^+} u$ leading to a well-conditioned system of integral equations.

2.4 NUMERICAL METHODS

This section describes the discretization scheme for the integral equations, specifies the interpolation of the charge densities, documents the adaptive quadrature method used to automatically refine the quadrature grids,

details the solution evaluation, and presents the exact solution for the two non-concentric nested circles case.

2.4.1 *Discretization Scheme*

We employ the Nyström method [Kre14] to discretize the integral equations (2.38)-(2.39). The curves $\partial\Omega_i$ are parameterized in $q \in [0,1]$ and the grid on each curve is denoted $q_{i,m},\ m = 0,\ldots,M_i - 1$ for M_i grid points on curve i. We use two different quadrature schemes. For interfaces that approach other interfaces within a threshold, we use composite quadrature and split the interface into panels. We use Gauss-Legendre quadrature on each panel and Lagrange interpolation for interpolating the charge density. For interfaces that are sufficiently far away from all other interfaces we use uniform grid points, trapezoidal rule quadrature, and trigonometric interpolation for interpolating the charge density. For either interface type, we adaptively refine the panels and increase the number of grid points to meet a given error tolerance.

After discretization, the integral equations (2.38) and (2.39) can be expressed as $A\boldsymbol{\phi} = \boldsymbol{b}$. The entries in $\boldsymbol{b}$ are given by evaluating the functions $b_0, b_1, \ldots, b_N$ at the quadrature nodes and the entries in A are computed from evaluating the kernel (2.13) at the pairs of grid points and applying the quadrature rule.

We solve the system $A\boldsymbol{\phi} = \boldsymbol{b}$ using GMRES [SS86], an iterative method that approximates the solution by the vector in a Krylov subspace with minimal residual. When solving with GMRES, the well-conditioned integral equations give a well-conditioned discrete linear system for which GMRES converges quickly.

We use the `fmm2d` library that implements fast multipole methods in two dimensions [Fla21]. It allows us to compute N-body interactions governed by the Laplace equation, to a specified precision, in two dimensions, on a multi-core shared-memory machine. In particular, `fmm2d` can accelerate evaluation of the sum

$$\sum_{j=1}^{M} c_j \mathcal{K}\left(\boldsymbol{x}_i, \boldsymbol{y}_j\right), \quad \text{for } i = 1, 2 \ldots, N, \tag{2.40}$$

in which there are M arbitrary source locations $\boldsymbol{y}_j \in \mathbb{R}^2$ with corresponding strengths $c_j \in \mathbb{R}$, N target locations $\boldsymbol{x}_i \in \mathbb{R}^2$, and the kernel $\mathcal{K}$ can be the free-space Green's function $G(\boldsymbol{x}, \boldsymbol{y})$ from (2.9) or its derivative $K(\boldsymbol{x}, \boldsymbol{y})$ from (2.13).

2.4.2 *Interpolation of Charge Densities*

The boundary integral method results in estimates of the charge densities on a grid $\gamma_i(q_{i,m})$. When evaluating the singular layer potentials $\mathcal{S}_{\partial\Omega_i}[\gamma_i](\boldsymbol{x}) = \int_{\partial\Omega_i} G(\boldsymbol{x},\boldsymbol{y})\gamma_i(\boldsymbol{y})\,\mathrm{d}\ell_{\boldsymbol{y}}$, the value of the charge density may need to be known off of this grid depending on the quadrature scheme employed.

While we could have opted to use Nyström interpolation [Nys30, DM88, Kre14] in which the integral equations are re-arranged and evaluated for the charge density at non-grid points, we instead choose barycentric Lagrange interpolation [BT04] for the paneled interfaces and trigonometric interpolation [WJMT15] for the uniform interfaces.

Consider the case of a uniform interface first. Let $p_K(q)$ be the trigonometric polynomial of degree K, *i.e.*, a truncated Fourier series. The $2K+1$ unknowns are determined by requiring that the interpolant pass through given values $p_K(q_m) = f_m, m = 0,\ldots,M-1$ with $M = 2K+1$. In the case of the shifted uniform grid $q_m = (m+s)/M,\ m = 0,\ldots,M-1,\ s \in [0,1]$, this interpolant can readily and stably be evaluated using the barycentric formula for trigonometric interpolation [WJMT15],

$$p_K(q) = \frac{\sum_{m=0}^{M-1} (-1)^m f_m F\left(\pi(q-q_m)\right)}{\sum_{m=0}^{M-1} (-1)^m F\left(\pi(q-q_m)\right)}. \tag{2.41}$$

For odd M, $F(q) = \csc(q)$, while for even M, $F(q) = \cot(q)$. We choose $s = \frac{1}{2}$ so as to avoid a possible numerical instability with the barycentric formula [AX17].

In the case of a non-uniform grid $q_m, m = 0,\ldots,M-1$, we opt for a degree $M-1$ Lagrange interpolant using the barycentric formula [BT04],

$$p_{M-1}(q) = \frac{\sum_{m=0}^{M-1} \frac{w_m f_m}{q-q_m}}{\sum_{m=0}^{M-1} \frac{w_m}{q-q_m}}, \tag{2.42}$$

in which

$$w_m = \frac{1}{\prod_{n\neq m}(q_m - q_n)}. \tag{2.43}$$

If the coefficients w_m are precomputed, then interpolation requires only $\mathcal{O}(NM)$ work for N evaluation points.

2.4.3 *Adaptive Grid Refinement*

We use an adaptive strategy to automatically refine the quadrature grids for the integral equations.

For interfaces discretized with uniform grids, we solve the discretized integral equations (2.38)-(2.39) with M uniform grid points and use trigonometric interpolation to approximate the scaled charge densities. We take $M = 2K + 1$ and let $p_K(q)$ be the truncated Fourier series of degree K approximation to the discrete charge densities

$$p_K(q) = \sum_{k=-K}^{K} c_k \exp(2\pi i k q), \tag{2.44}$$

in which the Fourier coefficients are

$$c_k = \int_0^1 p_K(q) \exp(-2\pi i k q) \, \mathrm{d}q. \tag{2.45}$$

If the two highest mode Fourier coefficients $|c_K|$ and $|c_{K-1}|$ are both smaller than a specified tolerance, then the charge densities are well resolved and $p_K(q)$ is taken to be our final approximation of the scaled charge density. Otherwise, we refine the interface and iterate until $|c_K|$ and $|c_{K-1}|$ are both smaller than the specified tolerance. We check that the last two coefficients, rather than just one, are smaller than the threshold so that a symmetry does not mislead us into thinking that the series has converged.

For interfaces discretized with composite quadrature (panels), we solve the discretized integral equations (2.38)-(2.39) with an M point Gauss-Legendre quadrature and examine the truncated Legendre series polynomial of order M approximation to the discrete charge densities on each panel. If either of the last two coefficients in the polynomial approximation are above a specified tolerance, then the panel is refined. After refinement, if the number of quadrature nodes is greater than the maximum allowed on a panel, then we split the panel into four smaller panels. We iterate until the last two coefficients in the polynomial approximation are both below the specified tolerance, indicating that the charge densities are well resolved. Refining based on the size of the coefficients of Legendre series polynomials has been used previously when computing generalized Gaussian quadratures [BGR10].

Each time the grid is refined, the linear system for charge densities needs to be solved again. We reduced the number of GMRES iterations needed to solve this linear system by using an initial guess from interpolating the charge densities from the course grid to the fine grid.

2.4.4 *Solution Evaluation*

Having solved for the charge densities, the solution may be evaluated using (2.7) and the same quadrature scheme used in the Nyström method. This is known as naïve quadrature and is fast and accurate when the evaluation point is not near or on an interface or the boundary. For evaluation points on or near an interface or the boundary, the integrand is logarithmically singular or nearly singular for which the quadrature schemes for smooth integrands perform poorly [Bar14, HO08b].

This so-called close evaluation problem has been addressed with quadratures that are spectrally accurate up to the boundary [HO08b, BWV15], quadrature by expansion [KBGO13] (whose convergence is analyzed in [EGK13]), and adaptive quadrature [Gon09]. We opt for a simpler approach: approximate interfaces or the boundary with line segments near an evaluation point and employ an analytic expression for the single layer potential due to a line segment.

Through explicit integration, the potential at point $\boldsymbol{x}$ due to a single layer of charge on a line segment ΔS, parameterized by arclength s, from $\boldsymbol{X}_1$ at s_1 to $\boldsymbol{X}_2$ at s_2 with a charge density $\gamma(s) = \gamma_1 \frac{s_2 - s}{s_2 - s_1} + \gamma_2 \frac{s - s_1}{s_2 - s_1}$ varying linearly from γ_1 at $\boldsymbol{X}_1$ to γ_2 at $\boldsymbol{X}_2$ is

$$\begin{aligned}\mathcal{S}_{\Delta S}[\gamma(s)](\boldsymbol{x}) =& \frac{1}{2\pi} \frac{\gamma_1 s_2 - \gamma_2 s_1}{s_2 - s_1} \left(s_2 \log(r_2) - s_1 \log(r_1) - s_2 + s_1 + (\theta_2 - \theta_1) d\right) \\ &+ \frac{1}{2\pi} \frac{\gamma_2 - \gamma_1}{s_2 - s_1} \left(\frac{r_2^2}{2} \left(\log(r_2) - \frac{1}{2} \right) - \frac{r_1^2}{2} \left(\log(r_1) - \frac{1}{2} \right) \right),\end{aligned} \tag{2.46}$$

in which: r_1, r_2 are the distances between $\boldsymbol{x}$ and $\boldsymbol{X}_1, \boldsymbol{X}_2$, respectively; d is the perpendicular distance between $\boldsymbol{x}$ and the line segment ΔS; and θ_1, θ_2 are the angles from the perpendicular line to $\boldsymbol{X}_1, \boldsymbol{X}_2$, respectively. The variables in this formula are shown in Figure 2.2a. This formula is given in the Appendix A of [Liu09b] in the case of $\gamma_1 = \gamma_2 = 1$.

The values of the charge densities at the endpoints of each line segment can be obtained by interpolating the charge density solution. If we simply take the values of the unmodified charge densities at the endpoints of the curved segment, then the total charge for the line segment approximation would be reduced as the length of the line segment is shorter than that of the curved segment. To ensure the total charge on each line segment is equal to the total charge on the corresponding curved segment, we estimate the total charge on each curved segment by computing a truncated Legendre (respectively Fourier) series polynomial for panelled (respectively uniform) interfaces. Imposing that the estimated total charge

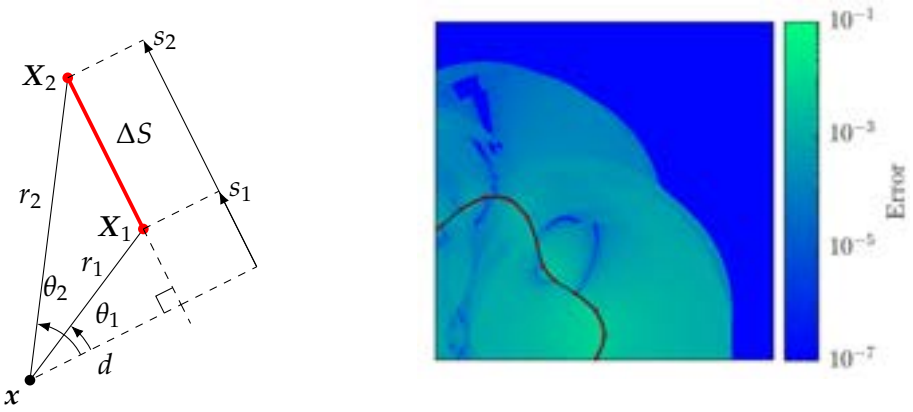

(a) (b)

Figure 2.2: Line segment potential. (a) The variables used in (2.46) to compute the potential at point $\boldsymbol{x}$ due to a single layer of charge on a line segment ΔS, parameterized by arclength s, from $\boldsymbol{X}_1$ at s_1 to $\boldsymbol{X}_2$ at s_2. Here r_1, r_2 are the distances between $\boldsymbol{x}$ and $\boldsymbol{X}_1, \boldsymbol{X}_2$; d is the perpendicular distance between $\boldsymbol{x}$ and the line segment ΔS; and θ_1, θ_2 are the angles from the perpendicular line to $\boldsymbol{X}_1, \boldsymbol{X}_2$. (b) The difference between the single layer potential $\mathcal{S}_\Gamma[1]$ for unit charge density on a curve Γ and the sum of the charge line potentials $\sum_i \mathcal{S}_{\Delta S_i}[1]$ for 36 segments. The difference is negligible outside the boundary of the "5h rule".

on each curved segment equals that on the corresponding line segment yields a system for the charge densities at each endpoint. For an even number of endpoints, this system has a one-dimensional kernel and we choose the solution with minimum ℓ_2-norm.

Following the "5h rule" [Bar14], panels within a distance of five times the local grid spacing to an evaluation point are broken into line segments and evaluated using (2.46). The contributions to the potential due the other panels are evaluated using (2.7). Approximating the curves $\partial\Omega_i$ near the evaluation point as the union of line segments introduces some error especially where the curve has high curvature. This is illustrated in Figure 2.2b, which shows the difference between the single layer potential on a curve Γ and the approximate potential due to 36 line segments. In practical applications, more line segments are used so that the error introduced by this approximation is much smaller.

2.4.5 *Exact Solution to Two Non-Concentric Nested Circles Problem*

We will construct a solution to the two non-concentric nested circles problem using a conformal map to a two concentric nested circles problem. The numerical solution to this problem computed using our method

and using FEniCS [ABH+15] will be compared to the exact solution in Section 2.5.1. The conformal map

$$\tilde{z} = f(z) = \frac{z - \alpha}{1 - \bar{\alpha} z} \tag{2.47}$$

maps the unit disk to the unit disk and the point α to 0. The inverse of this map is

$$z = f^{-1}(\tilde{z}) = \frac{\tilde{z} + \alpha}{1 + \bar{\alpha}\tilde{z}}. \tag{2.48}$$

Let the off-centre circle have a diameter on the x-axis passing through $(0,0)$ and $(a,0)$. Choose

$$\alpha = \frac{\sqrt{1+a} - \sqrt{1-a}}{\sqrt{1+a} + \sqrt{1-a}}, \tag{2.49}$$

the point equidistant between $(0,0)$ and $(a,0)$ in the unit disc model for hyperbolic geometry.

Let us construct some solutions $\tilde{u}(\tilde{r}, \tilde{\theta})$ in the domain with concentric circles. Consider the problem

$$\Delta \tilde{u} = 0 \text{ on } \tilde{r} < 1, \tilde{r} \neq \alpha \tag{2.50}$$

$$\partial_{\tilde{r}} \tilde{u} = \sin(m\tilde{\theta}) \text{ on } \tilde{r} = 1, \tag{2.51}$$

$$\tilde{u}^- = \tilde{u}^+ \text{ on } \tilde{r} = \alpha, \tag{2.52}$$

$$\sigma \partial_{\tilde{r}^-} \tilde{u} = \partial_{\tilde{r}^+} \tilde{u} \text{ on } \tilde{r} = \alpha, \tag{2.53}$$

in which $\sigma = \sigma_1/\sigma_0$ is the ratio of conductivities in the disks of radius α and 1. m is a natural number. By separating variables on the disk, we find the solution

$$\tilde{u}(\tilde{r}, \tilde{\theta}) = \begin{cases} A\tilde{r}^m \sin(m\tilde{\theta}), & \tilde{r} \leq \alpha \\ (B\tilde{r}^m + C\tilde{r}^{-m}) \sin(m\tilde{\theta}), & \alpha \leq \tilde{r} \leq 1 \end{cases}, \tag{2.54}$$

in which $A = \frac{2}{m} \frac{1}{\alpha^{2m}(\sigma-1)+\sigma+1}$, $B = A(\sigma+1)/2$, $C = B - 1/m$.

We obtain a solution to a non-concentric nested circles problem where $u(r,\theta) = \tilde{u}(\tilde{r}, \tilde{\theta})$. The injected current b_0 this implies for the non-concentric problem is

$$b_0(\theta) = \sin\left(m \tan^{-1}\left(\frac{\sin(\theta)(1-\alpha^2)}{\cos(\theta)(1+\alpha^2) - 2\alpha} \right) \right) \frac{1-\alpha^2}{1 - 2\alpha\cos(\theta) + \alpha^2}. \tag{2.55}$$

The charge density on the inner circle is

$$\gamma_1(\tilde{\theta}) = [\partial_{\tilde{r}^+}\tilde{u} - \partial_{\tilde{r}^-}\tilde{u}]_{\tilde{r}=\alpha} = \sin(m\tilde{\theta})\frac{2\alpha^{m-1}(\sigma-1)}{\alpha^{2m}(\sigma-1)+\sigma+1}. \tag{2.56}$$

2.5 NUMERICAL RESULTS

This section illustrates numerically the performance of our method. We compare results obtained using our solver to those obtained using FEniCS [ABH+15], a popular open-source (LGPLv3) computing platform for solving partial differential equations. The finite element meshes used in FEniCS were created in Gmsh [GR09], an open source 2D and 3D finite element mesh generator distributed under the terms of the GNU General Public License (GPL). Gmsh allows one to create customizable finite element meshes that can be refined near each interface to increase accuracy at minimal cost to computation time. We consider four separate test cases.

2.5.1 *Test Case 1: Two Nested Circles*

We consider the case of two nested circles. Figure 2.3 shows the analytic solution to a two circle non-concentric and the corresponding concentric problems, the pointwise difference between the analytic solutions and the boundary integral method solutions, and the pointwise difference between the analytic solutions and the solution computed using FEniCS. Additionally, the finite element mesh created using the frontal Delaunay triangulation [Reb93] in Gmsh and used by FEniCS is shown. The wall time to build and solve the system of equations for the two non-concentric circle problem was 0.23 seconds for our solver and 1.37 seconds for FEniCS and the two concentric circle problem was 0.07 seconds for our solver and 0.83 seconds for FEniCS. Figure 2.4 shows the absolute error in the computed solution using the naïve quadrature (dash-dotted), using adaptive quadrature using the interpolant of the charge densities (solid), and using the charge line potential between each node (dashed) for the case of two concentric circles as a function of distance from the outer boundary. The solution is evaluated at the point $(r,\theta) = (1-\hat{x}, \frac{\pi}{2})$ in polar coordinates. In Fig. 2.4a the point $(r,\theta) = (1, \frac{\pi}{2})$ is at a quadrature node and in Fig. 2.4b we use the same number of quadrature nodes but rotate them so that the same point $(r,\theta) = (1, \frac{\pi}{2})$ is half way between two quadrature nodes. The wall time to evaluate the solution at all 8,000 points used in Figure 2.4 was 0.02 seconds when using the naïve quadrature, 36.16 seconds when using adaptive quadrature, and 0.90 seconds when using the charge line potential. The charge line potential leads to more accurate

results near the boundary than the naïve quadrature and is faster than adaptive quadrature.

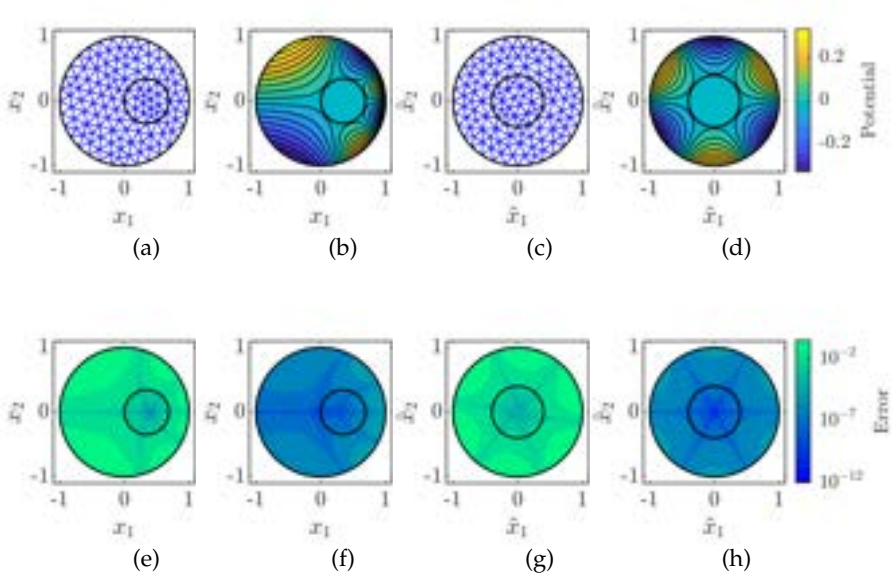

Figure 2.3: Pointwise errors for the nested circles test case. In the non-concentric case, a coarse version of the finite element mesh created in Gmsh and used by FEniCS (a), the contours of the solutions (b), the pointwise error of the numerically computed solutions using FEniCS (e) and using our method (f). The corresponding plots for the concentric case are shown in (c,d,g, and h) respectively. Parameter values are $m = 3, \sigma = 2, \alpha = 0.40$ ($a \approx 0.69$).

2.5.2 *Test Cases 2, 3, and 4: Examples of General Curves*

We consider cases where the conductivity is piecewise constant on regions defined by more general curves. Test case 2 has elliptical regions, test case 3 has clover leaf/starfish curves where the radius of each curve is given in polar coordinates by $r(\theta) = A + B\cos(C\theta)$ for parameters A, B, C, and test case 4 has 155 regions of constant conductivity. In each case, the injected current on the outer boundary is $b_0(\theta) = \cos(6\theta - \pi)\mathbb{1}_{\{|\theta - \pi/2| < \pi/12\}} - \cos(6\theta - \pi)\mathbb{1}_{\{|\theta - 3\pi/2| < \pi/12\}}$. Figure 2.5 displays the regions of constant conductivity and the computed potential using our solver for test cases 2, 3, and 4.

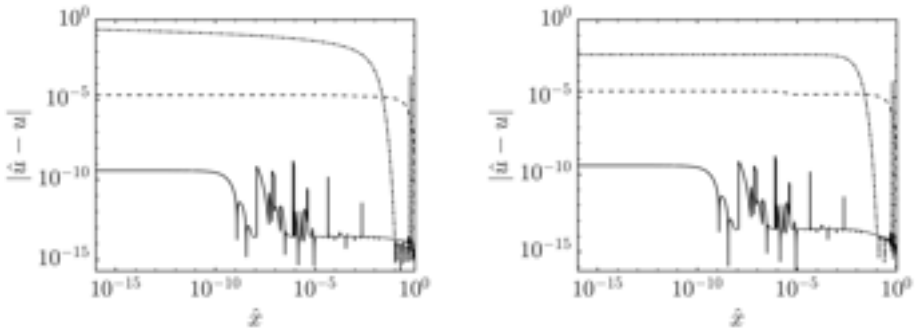

(a) (b)

Figure 2.4: Absolute error in the computed solution using the naïve quadrature (dash-dotted), using adaptive quadrature using the interpolant of the charge densities (solid), and using the charge line potential between each node (dashed) for the case of two concentric circles as a function of distance from the outer boundary. The solution is evaluated at the point $(r, \theta) = (1 - \hat{x}, \frac{\pi}{2})$ in polar coordinates. In (a) the point $(r, \theta) = (1, \frac{\pi}{2})$ is at a quadrature node and in (b) we rotate the quadrature nodes so that the same point is half way between two quadrature nodes. On each interface/boundary 2^8 uniformly spaced nodes were used. For the adaptive quadrature, an adaptive tolerance of 10^{-6} was used.

2.5.3 *Test Cases From the Literature*

We consider the conductivities from Example 2 of Gehre's paper [GJL14] (test case 5) and Nasser's paper [NMIA11] (test case 6). We take the injected current on the outer boundary to be $b_0(\theta) = \cos(8\theta - \pi)\mathbb{1}_{\{|\theta - \pi/2| < \pi/16\}} - \cos(8\theta - \pi)\mathbb{1}_{\{|\theta - 3\pi/2| < \pi/16\}}$ (test case 5) and $b_0(\theta) = \cos(6\theta - \pi)\mathbb{1}_{\{|\theta - \pi/2| < \pi/12\}} - \cos(6\theta - \pi)\mathbb{1}_{\{|\theta - 3\pi/2| < \pi/12\}}$ (test case 6). Figure 2.6 displays the regions of constant conductivity and the computed potential using our solver.

2.5.4 *Grid Refinement and Rescaling Studies*

Figures 2.7a and 2.7b display two refinement studies for our solver. In the first refinement study, the error estimate of the potential u is plotted as a function of M, the number of uniform grid points on each interface, for each of the four test cases. The error estimate is taken to be the absolute difference between the potential difference between the solutions computed at the boundary point $(1, 0)$ with M and $2M$ uniform grid points on each interface. The error is primarily due to solution evaluation error. If higher accuracy in the evaluation is required then using adaptive quadrature will improve the accuracy of the solver albeit at an increased

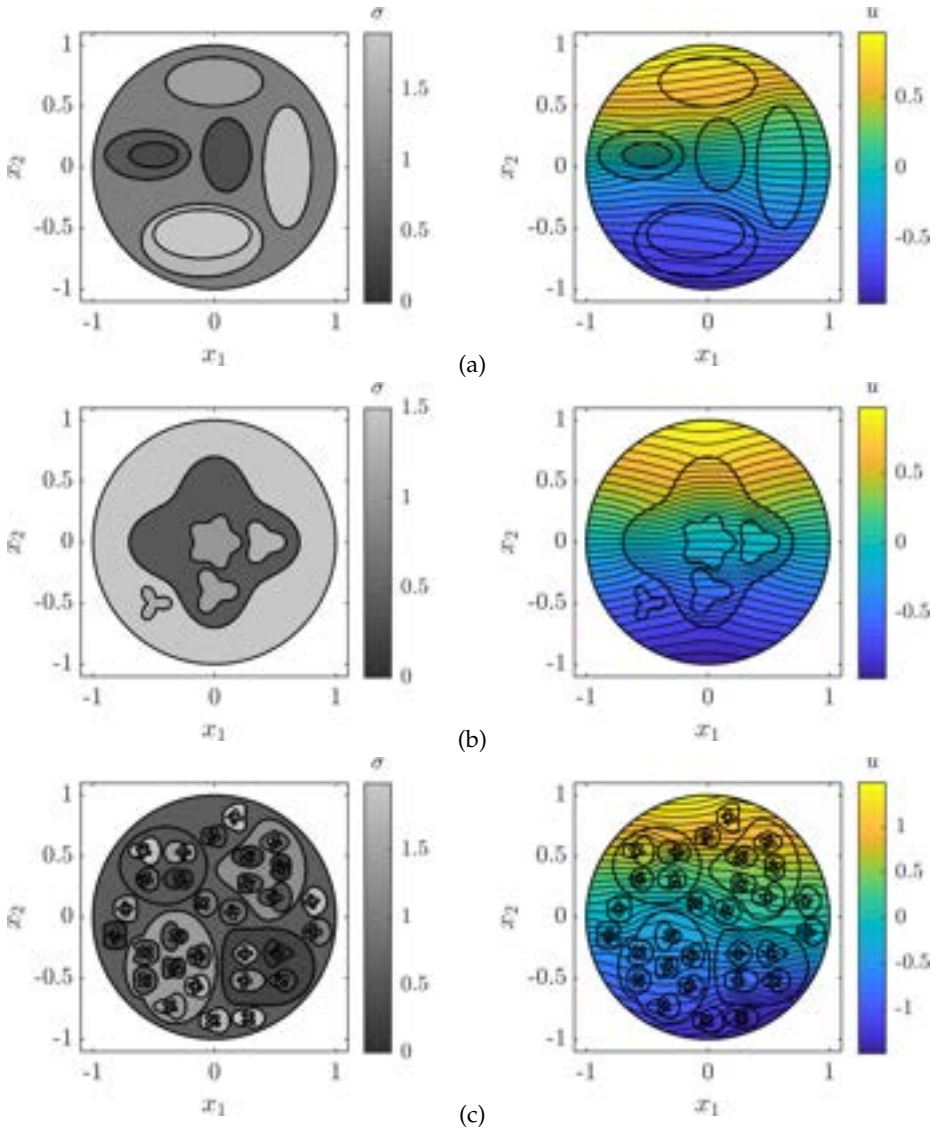

Figure 2.5: Conductivity for the problem (left) and potential computed using our solver (right) for test case 2 (a), test case 3 (b), and test case 4 (c). In all three test cases the injected current on the outer boundary is $b_0(\theta) = \cos(6\theta - \pi)\mathbb{1}_{\{|\theta-\pi/2|<\pi/12\}} - \cos(6\theta - \pi)\mathbb{1}_{\{|\theta-3\pi/2|<\pi/12\}}$.

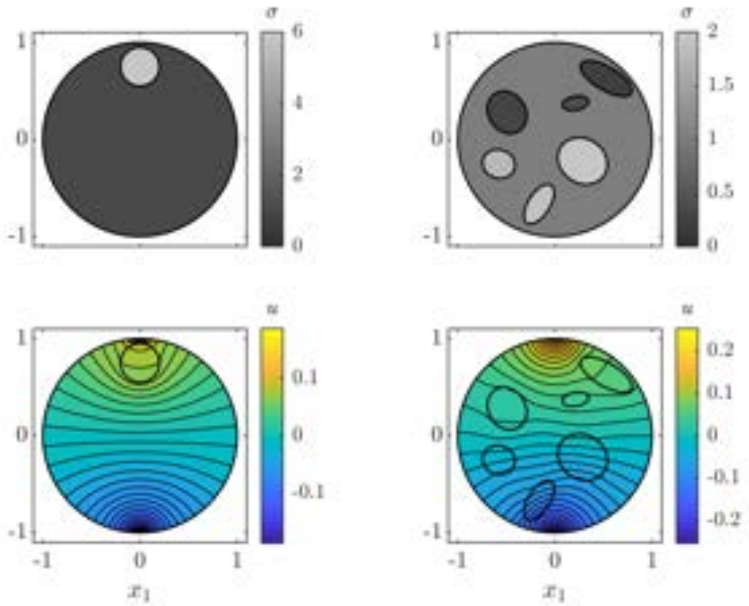

Figure 2.6: Conductivity σ for the problem (top) and potential u computed using our solver (bottom) for test case 5 (a) and 6 (b). The injected current on the outer boundary is $b_0(\theta) = \cos(8\theta - \pi)\mathbb{1}_{\{|\theta-\pi/2|<\pi/16\}} - \cos(8\theta - \pi)\mathbb{1}_{\{|\theta-3\pi/2|<\pi/16\}}$ (test case 5) and $b_0(\theta) = \cos(6\theta - \pi)\mathbb{1}_{\{|\theta-\pi/2|<\pi/12\}} - \cos(6\theta - \pi)\mathbb{1}_{\{|\theta-3\pi/2|<\pi/12\}}$ (test case 6).

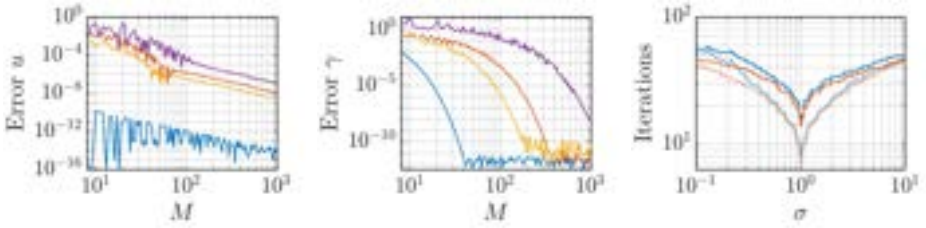

(a) (b) (c)

Figure 2.7: Refinement studies showing (a) the pointwise error estimate of the solution u at the boundary point $(1, 0)$ and (b) the error estimate of the charge density γ as a function of M, the number of uniform grid points on each interface, for all four test cases – 1 (blue), 2 (red), 3 (yellow), 4 (purple). (c) Number of GMRES iterations (with GMRES tolerance, *i.e.*, relative residual error, of 10^{-8} and initial guess of the zero vector) performed with (dotted lines) and without (solid lines) rescaling the charge densities for seven elliptical regions of constant conductivity alternating between 1 and σ. On each of the seven ellipses, $M = 2^5$ (blue lines) or 2^8 (red lines) uniformly spaced nodes were used.

cost to computation time. In the second refinement study, the charge density at each node on each interface/boundary is computed for each M and the maximal difference between these charge densities and the charge densities computed with $2M$ grid points is plotted. The refinement studies show that the charge densities converge spectrally and the potential converges linearly for our solver for all four test cases.

As discussed in Section 2.3.1, especially in the case of close conductivities, scaling the charge densities improves the conditioning of the resulting linear system. A study on the effect of rescaling the charge densities for our solver was performed for the case of the seven elliptical regions of constant conductivity described in test case 2 except with the conductivities alternating between 1 and a variable value σ for nested regions. The number of GMRES iterations performed with and without rescaling the charge densities as a function of the value σ are shown in Figure 2.7c. Rescaling decreased the number of GMRES iterations required to meet the convergence criterion. Note that iterations with a larger number of nodes per interface take longer to complete.

In order to benefit from the improved accuracy that using a larger number of nodes per interface brings without suffering too much increased computation time, we adaptively refine our grid to place more points where the interfaces are close together. Figure 2.8a shows an example of the automatically selected adaptive grid for test case 3. Figure 2.8b demonstrates how the adaptive grid refinement improves accuracy at minimal cost to computation time for test cases 2 and 3. The total wall time for the build and solve averaged over 10 samples is plotted against an error

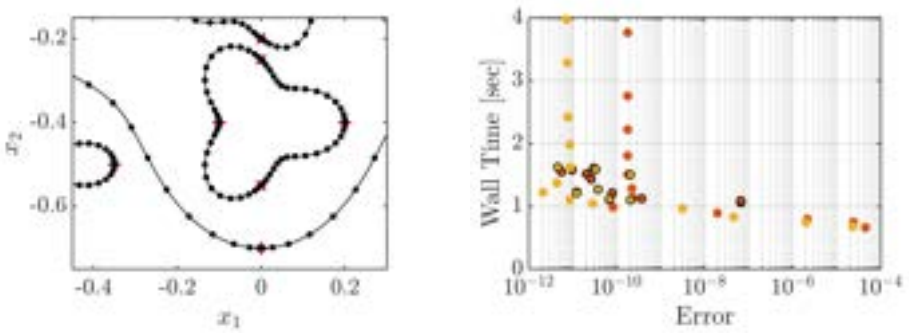

(a) (b)

Figure 2.8: (a) Part of the automatically selected adaptive grid (black dots are the quadrature nodes, red lines are the panel boundaries, black curves are interfaces) for test case 3. (b) Refinement performance plot showing wall time averaged over 10 samples vs error estimate for our solver with (black outline) and without (no outline) adaptively selecting the grid points for test case 2 (red) and 3 (yellow).

estimate – the absolute difference between the potential computed at the origin for the given run and a run computed with higher accuracy. For both test cases, the adaptive method was more efficient ultimately achieving more accurate results with less computation time. All simulations were performed on a desktop PC with a 6-Core 3.59 GHz CPU and 16 GB RAM.

2.5.5 *Effect of Smoothing Out Jumps in Conductivity*

We now propose that the setting of *sharp* jumps in conductivities is a good approximation (in terms of the EIT data) for *steep* but *smooth* transitions in conductivity.

We consider smoothings of piecewise constant conductivity functions. Given islands of constant conductivity inside a constant conductivity medium, the total conductivity function $\sigma(\boldsymbol{x})$ is of course discontinuous. We consider smoothings $\tilde{\sigma}(\boldsymbol{x})$ of these discontinuous functions.

We seek to find whether the EIT data corresponding to $\sigma(\boldsymbol{x})$ and $\tilde{\sigma}(\boldsymbol{x})$ for the same current injection will be sufficiently close. If this were the case, one can imagine our solver for $\sigma(\boldsymbol{x})$ producing adequate approximations to the solution for $\tilde{\sigma}(\boldsymbol{x})$ more efficiently than solvers specifically designed for smooth conductivities since such solvers would require fine grids near the transition regions. We verify in numerical examples that the difference in EIT data between $\sigma(\boldsymbol{x})$ and $\tilde{\sigma}(\boldsymbol{x})$ is indeed very small.

Using FEniCS, we computed the voltage between the north and south pole for five different cases with sharp and smooth jumps in conductivity. The percentage difference between the voltage in the smooth jump and

Case	V_{Sharp}	$V_{0.1}$	$D_{0.1}$	$V_{0.01}$	$D_{0.01}$
1. two concentric circles	1.6901	1.6978	0.4560%	1.6910	0.0534%
2. three concentric circles	1.6827	1.6922	0.5668%	1.6837	0.0596%
3. two ellipses inside disk	1.7672	1.7746	0.4164%	1.7681	0.0475%
4. four ellipses inside disk	1.6354	1.6443	0.5467%	1.6364	0.0636%
5. five ellipses inside disk	1.7529	1.7616	0.5001%	1.7540	0.0615%

Table 2.1: Voltage between the north and south pole for the different cases computed using FEniCS on a unit disk domain. V_{Sharp} is the voltage computed with a sharp jump in conductivity. $V_{0.1}$ and $V_{0.01}$ are the voltages when the conductivity is smoothed out over a region of width 0.1 and 0.01, respectively. $D_{0.1}$ and $D_{0.01}$ denote the percentage difference between the voltage with a smooth jump in conductivity and the voltage with a sharp jump in conductivity, (*i.e.*, percent difference between $V_{0.1}$ and V_{Sharp} and between $V_{0.01}$ and V_{Sharp}, respectively). The injected current is $g(\theta) = \sin(\theta)$ and the FEniCS mesh resolution is 2^7.

the sharp jump case is included. An injected current of $g(\theta) = \sin(\theta)$ and a FEniCS mesh resolution of 2^7 was used. The domain was the unit disk and the conductivities were smoothed out over a region of width 0.1 and 0.01 and the resulting voltages are shown in Table 2.1. A plot of the sharp jump and smoothed out conductivity appears in Fig. 2.9.

We found good agreement between the voltages computed when the conductivity had a smooth jump and a sharp jump. When the conductivities were smoothed out over a region of width 0.1, the resulting voltages differed by only 0.4–0.6% and when smoothing occurred over a region of width 0.01, the resulting voltages differed by a minuscule 0.05–0.06%.

2.6 EXISTENCE AND REGULARITY

In this section we will provide some theoretical study of the system of integral equations (2.38)-(2.39). The following regularity results on the charge densities will guide our choice of quadrature for discretizing the integral equations. The discretization scheme and details of the solution evaluation were discussed in depth in Section 2.4. The conclusions follow in Section 2.7. For now, we aim to show two separate results.

First, we will establish existence and uniqueness to this system of equations. This will be obtained from general PDE theory, and the analogous statement for the system (2.38)-(2.39) will follow as a consequence.

Secondly, we will derive regularity for the charge densities along each interface. The latter result will have two formulations. In both, we

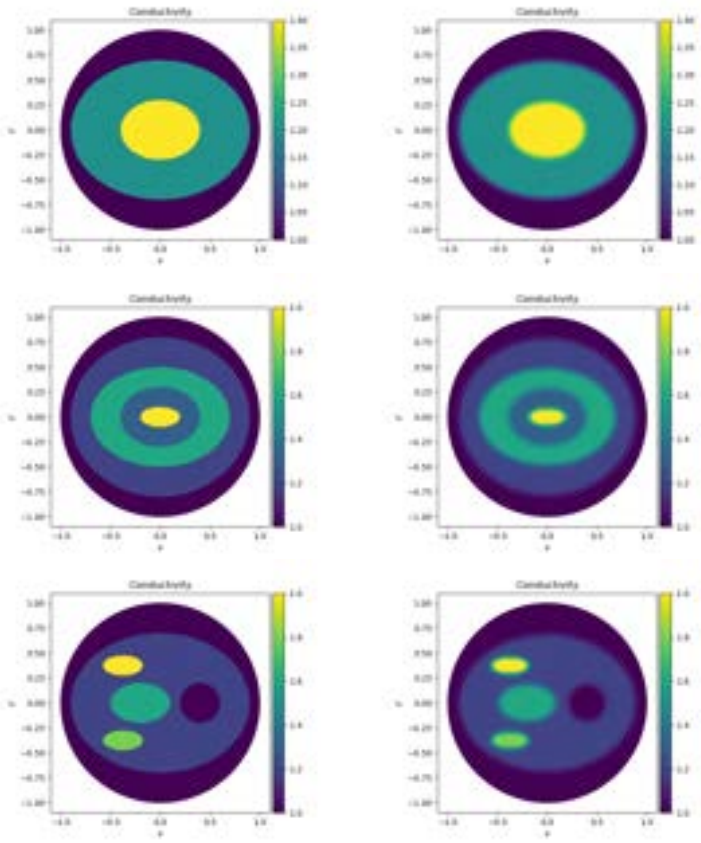

Figure 2.9: Sharp and smooth jump in conductivity. First row - two nested ellipses inside a circle (case 3). Second row - four nested ellipses inside a circle (case 4). Third row - five non-nested ellipses inside a circle (case 5).

will obtain regularity of the charge density functions along an interface, assuming the interface itself enjoys the same regularity. The most general result will be Theorem 2.2 below, which will show that assuming that the interface $\partial\Omega_i$ enjoys $\mathcal{C}^k$ regularity, then the charge density $\gamma_i(x)$ is of regularity H^k (*i.e.*, in the Hilbert space of order k). In particular it will also be of regularity $\mathcal{C}^{k-2}$, by Sobolev embedding. In the second theorem the control we obtain on these norms will be in terms of the L^2-norm of the injected current. In the first Theorem 2.1 we assume that the interfaces are just concentric circles and obtain stronger control making stronger assumptions.

Theorem 2.1. *Consider the solution of problem (2.38)-(2.39), with $\partial\Omega_i$ nested concentric circles inside the unit disk $\mathbb{D}$, injected current $b_0 \in H^k(\partial\mathbb{D})$, and $b_i = 0$ for $i = 1, \dots, N$. Then, the charge densities $\gamma_i(\cdot)$ at each of the inner interfaces are $\mathcal{C}^{k-2}$ regular functions, and their norms are bounded as follows: (θ is the standard polar coordinate)*

$$\|\gamma_i(\theta)\|_{\mathcal{C}^{k-2}(\partial\Omega_i)} \leq \left|1 - \frac{\sigma_{p_i}}{\sigma_i}\right| \frac{M}{\min\{\sigma_0, \dots, \sigma_N\}} \frac{6}{(r_N)^2} \|b_0\|_{H^k(\partial\mathbb{D})} \tag{2.57}$$

in which M is a constant that depends on the constants in the Sobolev embedding, the trace theorem, and the Poincaré inequality on domain $\mathbb{D}$ and r_N is the radius of the innermost circle.

Theorem 2.2. *Consider the solution of problem (2.38)-(2.39), in which $\partial\Omega_i$ are general $\mathcal{C}^k$ curves, $b_0 \in L^2(\partial\Omega)$, and $b_i = 0$ for $i = 1, \dots, N$. Then, the charge densities $\gamma_i(\cdot)$ at each of the inner interfaces are $\mathcal{C}^{k-2}$ regular functions, and their norms are bounded as follows: (s is the arc-length parameter on each curve)*

$$\|\gamma_i(s)\|_{\mathcal{C}^{k-2}(\partial\Omega_i)} \leq \left|1 - \frac{\sigma_{p_i}}{\sigma_i}\right| \frac{M_i}{\min\{\sigma_0, \dots, \sigma_N\}} \rho_{\sigma_i} \|b_0\|_{L^2(\partial\Omega)}. \tag{2.58}$$

Here the constant M_i depends on the shape of the interface $\partial\Omega_i$, the distance δ_i between the curve $\partial\Omega_i$ and its nearest curves, and the order $k \in \mathbb{N}$. ρ_{σ_i} is the maximum ratio of neighbouring conductivities i.e., $\rho_{\sigma_i} := max\{\frac{\sigma_i}{\sigma_{p_i}}, \frac{\sigma_{p_i}}{\sigma_i}\}$.

In particular when an interface $\partial\Omega_i$ is very close to another interface $\partial\Omega_j$, ($j \neq i$) then the constants M_i will increase. The precise constant M_i is given in the proof below.

For comparison, in Theorem 2.1 the constant M does not blow up as two interfaces (circles in that case) approach each other; of course on the other hand, the bounds are in terms of a stronger norm of the injected current.

2.6.1 *Regularity of the Solution at the Interfaces, in the Context of Concentric Circles*

We consider the special case where the regions of piecewise constant conductivity are defined by $N+1 \in \mathbb{N}$ concentric circles, of radii $r_0 = 1 > r_1 > \cdots > r_N > 0$. Figure 2.10 shows the domain and conductivities that we consider.

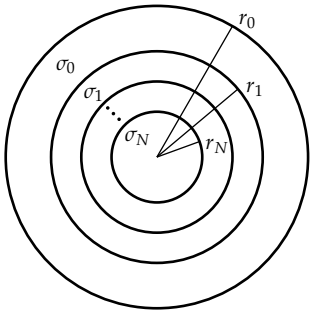

Figure 2.10: Domain for the problem with $N+1$ concentric circular regions of constant conductivity. The conductivity jumps across the outer boundary of region $i \neq 0$, a circle of radius r_i, from σ_i to σ_{i-1}.

We denote the unit disk by $\mathbb{D}$ and we use the standard polar coordinates (r, θ). Let $b_0 \in H^k(\partial\mathbb{D})$ for some $k \in \mathbb{N}$. The weak formulation of (2.1) and (2.2) is

$$\int_{\mathbb{D}} \sigma \langle \nabla u, \nabla \phi \rangle \, \mathrm{d}A = \int_{\partial\mathbb{D}} b_0 \phi \, \mathrm{d}\ell \tag{2.59}$$

for all $\phi \in \mathcal{C}^\infty$ on the closed disk.

Since $\sigma \in L^\infty$, from general PDE theory we obtain that there exists a unique weak solution $u \in H_0^1(\mathbb{D})$ [Eva10]. Setting $\phi = u$ and using the

Cauchy–Schwarz inequality, the trace theorem, and the Poincaré inequality we obtain

$$\begin{aligned}
&\min\{\sigma_0,\dots,\sigma_N\}\int_{\mathbb{D}}|\nabla u|^2\mathrm{d}A \\
&\leq \int_{\mathbb{D}}\sigma|\nabla u|^2\mathrm{d}A && (2.60)\\
&= \int_{\partial\mathbb{D}} b_0 u\ \mathrm{d}\ell && (2.61)\\
&\leq \frac{1}{2}\mu\int_{\partial\mathbb{D}} b_0^2\ \mathrm{d}\ell + \frac{1}{2}\mu^{-1}\int_{\partial\mathbb{D}} u^2\ \mathrm{d}\ell && (2.62)\\
&\leq \frac{1}{2}\mu\int_{\partial\mathbb{D}} b_0^2\ \mathrm{d}\ell + \frac{1}{2}\mu^{-1}c_1^2\|u\|^2_{H^1(\mathbb{D})} && (2.63)\\
&= \frac{1}{2}\mu\int_{\partial\mathbb{D}} b_0^2\ \mathrm{d}\ell + \frac{1}{2}\mu^{-1}c_1^2\left(\int_{\mathbb{D}}|u|^2+|\nabla u|^2\ \mathrm{d}A\right) && (2.64)\\
&\leq \frac{1}{2}\mu\int_{\partial\mathbb{D}} b_0^2\ \mathrm{d}\ell + \frac{1}{2}\mu^{-1}c^2\int_{\mathbb{D}}|\nabla u|^2\ \mathrm{d}A, && (2.65)
\end{aligned}$$

in which c_1 is the trace constant and $\sqrt{\frac{c^2}{c_1^2}-1}$ is the Poincaré constant for the domain $\mathbb{D}$. Thus, choosing $\mu = \frac{c^2}{\min\{\sigma_0,\dots,\sigma_N\}}$ we get the bound

$$\|\nabla u\|_{L^2(\mathbb{D})} \leq \frac{c}{\min\{\sigma_0,\dots,\sigma_N\}}\|b_0\|_{L^2(\partial\mathbb{D})}, \tag{2.66}$$

in which c is a constant depending on the trace constant and Poincaré constant for the domain $\mathbb{D}$.

We seek to prove better regularity for u. First we examine tangential regularity. Let $w\in\mathcal{C}^\infty$ and take $\phi=\partial_\theta^j w$ for some $j\leq k$ in (2.59) *i.e.*

$$\int_{\mathbb{D}}\sigma\langle\nabla u,\nabla\partial_\theta^j w\rangle\ \mathrm{d}A = \int_{\partial\mathbb{D}} b_0\partial_\theta^j w\ \mathrm{d}\ell. \tag{2.67}$$

We integrate by parts in θ to give

$$\int_{\mathbb{D}}\sigma\langle\nabla\partial_\theta^j u,\nabla w\rangle\ \mathrm{d}A = \int_{\partial\mathbb{D}}\partial_\theta^j b_0 w\ \mathrm{d}\ell, \tag{2.68}$$

so $\partial_\theta^j u$ is a weak solution to the same PDE problem (2.1) with Neumann boundary condition $\sigma\partial_{\boldsymbol{n}}u=\partial_\theta^j b_0$ and $\partial_\theta^j u\in H^1(\mathbb{D})$ for $j\leq k$ with the estimate (note that $\int_{\mathbb{D}}\partial_\theta u\ \mathrm{d}A=0$)

$$\|\nabla\partial_\theta^j u\|_{L^2(\mathbb{D})} \leq \frac{c}{\min\{\sigma_0,\dots,\sigma_N\}}\|\partial_\theta^j b_0\|_{L^2(\partial\mathbb{D})}, \tag{2.69}$$

in which c is a constant depending on the trace constant and Poincaré constant for the domain $\mathbb{D}$.

Next we examine normal regularity in the annulus $\Omega_n \setminus \Omega_{n+1}$ up to the interface for $n \in \{0, \dots, N-1\}$. Since $\partial_\theta^j u \in H^1(\mathbb{D})$ we get that $\partial_r \partial_\theta^j u \in L^2(\Omega_n \setminus \Omega_{n+1})$ and $\partial_\theta^{j+1} u \in L^2(\Omega_n \setminus \Omega_{n+1})$ for $j \leq k$. We use the PDE (2.1) to get bounds on $\partial_r^i \partial_\theta^j u$ for $i + j \leq k+1$ and $i \leq 3$. In the annulus $\Omega_n \setminus \Omega_{n+1}$, $\partial_\theta^j u$ is harmonic so

$$\partial_r^2 \partial_\theta^j u = -\frac{1}{r} \partial_r \partial_\theta^j u - \frac{1}{r^2} \partial_\theta^{j+2} u. \tag{2.70}$$

Hence, we can estimate $\partial_r^2 \partial_\theta^j u$ in $L^2(\Omega_n \setminus \Omega_{n+1})$ by

$$\begin{aligned}
&\left\| \partial_r^2 \partial_\theta^j u \right\|_{L^2(\Omega_n \setminus \Omega_{n+1})} \\
&\leq \frac{1}{r_{n+1}} \left\| \partial_r \partial_\theta^j u \right\|_{L^2(\Omega_n \setminus \Omega_{n+1})} + \left(\frac{1}{r_{n+1}} \right)^2 \left\| \partial_\theta^{j+2} u \right\|_{L^2(\Omega_n \setminus \Omega_{n+1})} && (2.71) \\
&\leq \frac{1}{r_{n+1}} \left\| \nabla \partial_\theta^j u \right\|_{L^2(\Omega_n \setminus \Omega_{n+1})} + \left(\frac{1}{r_{n+1}} \right)^2 \left\| \nabla \partial_\theta^{j+1} u \right\|_{L^2(\Omega_n \setminus \Omega_{n+1})} && (2.72)
\end{aligned}$$

for $j \leq k-1$. To get higher normal regularity in the annulus $\Omega_n \setminus \Omega_{n+1}$, we differentiate (2.70) with respect to r which leads to the equation

$$\partial_r^3 \partial_\theta^j u = \frac{1}{r^2} \partial_r \partial_\theta^j u - \frac{1}{r} \partial_r^2 \partial_\theta^j u + \frac{2}{r^3} \partial_\theta^{j+2} u - \frac{1}{r^2} \partial_r \partial_\theta^{j+2} u \tag{2.73}$$

and the corresponding estimate

$$\begin{aligned}
&\left\| \partial_r^3 \partial_\theta^j u \right\|_{L^2(\Omega_n \setminus \Omega_{n+1})} \\
&\leq \left(\frac{1}{r_{n+1}} \right)^2 \left\| \partial_r \partial_\theta^j u \right\|_{L^2(\Omega_n \setminus \Omega_{n+1})} + \frac{1}{r_{n+1}} \left\| \partial_r^2 \partial_\theta^j u \right\|_{L^2(\Omega_n \setminus \Omega_{n+1})} \\
&\quad + 2 \left(\frac{1}{r_{n+1}} \right)^3 \left\| \partial_\theta^{j+2} u \right\|_{L^2(\Omega_n \setminus \Omega_{n+1})} \\
&\quad + \left(\frac{1}{r_{n+1}} \right)^2 \left\| \partial_r \partial_\theta^{j+2} u \right\|_{L^2(\Omega_n \setminus \Omega_{n+1})} && (2.74) \\
&\leq 2 \left(\frac{1}{r_{n+1}} \right)^2 \left\| \nabla \partial_\theta^j u \right\|_{L^2(\Omega_n \setminus \Omega_{n+1})} && (2.75) \\
&\quad + 3 \left(\frac{1}{r_{n+1}} \right)^2 \left\| \nabla \partial_\theta^{j+1} u \right\|_{L^2(\Omega_n \setminus \Omega_{n+1})} \\
&\quad + \left(\frac{1}{r_{n+1}} \right)^2 \left\| \nabla \partial_\theta^{j+2} u \right\|_{L^2(\Omega_n \setminus \Omega_{n+1})}
\end{aligned}$$

for $j \leq k-2$.

We can estimate $\partial_r \partial_\theta^j u$ in H^2 on the annulus $\Omega_n \setminus \Omega_{n+1}$ by

$$\begin{aligned}
\left\|\partial_r \partial_\theta^j u\right\|_{H^2(\Omega_n \setminus \Omega_{n+1})} &= \left\|\partial_r \partial_\theta^j u\right\|_{L^2(\Omega_n \setminus \Omega_{n+1})} + \left\|\partial_r \partial_\theta^{j+1} u\right\|_{L^2(\Omega_n \setminus \Omega_{n+1})} \qquad (2.76)\\
&\quad + \left\|\partial_r \partial_\theta^{j+2} u\right\|_{L^2(\Omega_n \setminus \Omega_{n+1})} + \left\|\partial_r^2 \partial_\theta^j u\right\|_{L^2(\Omega_n \setminus \Omega_{n+1})}\\
&\quad + \left\|\partial_r^2 \partial_\theta^{j+1} u\right\|_{L^2(\Omega_n \setminus \Omega_{n+1})} + \left\|\partial_r^3 \partial_\theta^j u\right\|_{L^2(\Omega_n \setminus \Omega_{n+1})}\\
&\leq \left\|\nabla \partial_\theta^j u\right\|_{L^2(\Omega_n \setminus \Omega_{n+1})} + \left\|\nabla \partial_\theta^{j+1} u\right\|_{L^2(\Omega_n \setminus \Omega_{n+1})} \qquad (2.77)\\
&\quad + \left\|\nabla \partial_\theta^{j+2} u\right\|_{L^2(\Omega_n \setminus \Omega_{n+1})} + \left\|\partial_r^2 \partial_\theta^j u\right\|_{L^2(\Omega_n \setminus \Omega_{n+1})}\\
&\quad + \left\|\partial_r^2 \partial_\theta^{j+1} u\right\|_{L^2(\Omega_n \setminus \Omega_{n+1})} + \left\|\partial_r^3 \partial_\theta^j u\right\|_{L^2(\Omega_n \setminus \Omega_{n+1})}\\
&\leq \left(1 + \frac{1}{r_{n+1}} + 2\left(\frac{1}{r_{n+1}}\right)^2\right) \left\|\nabla \partial_\theta^j u\right\|_{L^2(\Omega_n \setminus \Omega_{n+1})} \qquad (2.78)\\
&\quad + \left(1 + \frac{1}{r_{n+1}} + 4\left(\frac{1}{r_{n+1}}\right)^2\right) \left\|\nabla \partial_\theta^{j+1} u\right\|_{L^2(\Omega_n \setminus \Omega_{n+1})}\\
&\quad + \left(1 + 2\left(\frac{1}{r_{n+1}}\right)^2\right) \left\|\nabla \partial_\theta^{j+2} u\right\|_{L^2(\Omega_n \setminus \Omega_{n+1})}.
\end{aligned}$$

We can estimate $\partial_r \partial_\theta^j u$ in H^2 on the annulus $\Omega \setminus \Omega_N$ by

$$\begin{aligned}
\left\|\partial_r \partial_\theta^j u\right\|_{H^2(\Omega \setminus \Omega_N)} \leq \frac{6}{(r_N)^2} &\left(\left\|\nabla \partial_\theta^j u\right\|_{L^2(\Omega \setminus \Omega_N)} + \left\|\nabla \partial_\theta^{j+1} u\right\|_{L^2(\Omega \setminus \Omega_N)} \right. \qquad (2.79)\\
&\left. + \left\|\nabla \partial_\theta^{j+2} u\right\|_{L^2(\Omega \setminus \Omega_N)}\right).
\end{aligned}$$

2.6.2 *Regularity of the Solution at the Interfaces, in the Context of General C^k Interfaces*

Now we examine regularity of the solution for general C^k interfaces. Let $b_0 \in L^2(\partial\Omega)$. The weak formulation of (2.1) and (2.2) is

$$\int_\Omega \sigma \langle \nabla u, \nabla \phi \rangle \, \mathrm{d}A = \int_{\partial\Omega} b_0 \phi \, \mathrm{d}\ell \qquad (2.80)$$

for all $\phi \in H^1(\Omega)$. Since $\sigma \in L^\infty$, from general PDE theory we obtain that there exists a unique weak solution $u \in H_0^1(\Omega)$ [Eva10]. Setting $\phi = u$ and

using the Cauchy–Schwarz inequality, the trace theorem, and the Poincaré inequality we obtain

$$\|\nabla u\|_{L^2(\Omega)} \leq \frac{c}{\min\{\sigma_0, \ldots, \sigma_N\}} \|b_0\|_{L^2(\partial\Omega)}, \tag{2.81}$$

in which c is a constant depending on the trace constant and Poincaré constant for the domain Ω.

First we will examine tangential regularity. Let $w \in C^\infty(\Omega)$ and let T be a vector field that on $\partial\Omega_i$ is of unit length and tangent to $\partial\Omega_i$ and is zero before the next curve. (Any such vector field T will do for now–we further fix T momentarily). Then take $\phi = T(w)$ in (2.80) *i.e.*

$$\int_\Omega \sigma \langle \nabla u, \nabla T(w) \rangle \, \mathrm{d}A = \int_{\partial\Omega} b_0 T(w) \, \mathrm{d}\ell = 0. \tag{2.82}$$

We integrate by parts with respect to T, to obtain:

$$\begin{aligned} &\int_\Omega \sigma \langle \nabla T(u), \nabla w \rangle \, \mathrm{d}A \\ &= -\int_\Omega \sigma \cdot \mathrm{div}(T) \cdot \langle \nabla u, \nabla w \rangle \, \mathrm{d}A + 2\int_\Omega \sigma \nabla_a T_b \nabla^a u \nabla^b w \, \mathrm{d}A. \end{aligned} \tag{2.83}$$

(We use the Einstein summation convention so a and b are summer from 1 to 2). So formally setting $w = T(u)$ and using the Cauchy–Schwarz inequality we obtain the inequality:

$$\begin{aligned} &\min|\sigma| \cdot \sqrt{\int_\Omega |\nabla T(u)|^2 \, \mathrm{d}A} \\ &\leq \max|\sigma| \cdot (\sup|\mathrm{div}(T)| + 2\sup|\nabla T|) \sqrt{\int_\Omega |\nabla u|^2 \, \mathrm{d}A}. \end{aligned} \tag{2.84}$$

So $\nabla T(u) \in L^2(\Omega)$, with the bound:

$$\|\nabla T(u)\|_{L^2(\Omega)} \leq 4\sup|\nabla T| \cdot \frac{\max|\sigma|}{\min|\sigma|} \|\nabla u\|_{L^2(\Omega)}. \tag{2.85}$$

Iterating we get that the composition

$$T^j(u) \in H^1(\Omega) \tag{2.86}$$

for all $j \leq k$. The constant for each such iteration will increase by a factor

$$4\sup|\nabla T| \cdot \frac{\max|\sigma|}{\min|\sigma|} \tag{2.87}$$

i.e.

$$\|\nabla T^j(u)\|_{L^2(\Omega)} \leq \left(4 \sup |\nabla T| \cdot \frac{\max|\sigma|}{\min|\sigma|}\right)^j \|\nabla u\|_{L^2(\Omega)} \tag{2.88}$$

for $j \leq k$. In particular, we have obtained extra regularity in the direction of the vector field T.

We next use the PDE to obtain regularity for u in the complementary direction. To do this we construct coordinates suitably adapted to each interface and express T in terms of these new coordinates. We consider a unit vector field $\vec{n}$ which is normal to the interface $\partial\Omega_i$. Introduce a coordinate $y \in [0, |\partial\Omega_i|)$ *along* $\partial\Omega_i$ so that $T(y) = 1$. We then introduce Fermi coordinates (x, y) where x is the arclength parameter along the normal lines, with $x = 0$ on $\partial\Omega_i$, and y is extended from $\partial\Omega_i$ to be constant along each such line. We restrict x to lie in a small interval $(-\epsilon, \epsilon)$ so that no two lines normal to $\partial\Omega_i$ intersect over the intervals $x \in (-\epsilon, \epsilon)$. This can be achieved since $\partial\Omega_i$ is assumed to be $\mathcal{C}^2$. Take $0 < \epsilon^* \leq \epsilon$ so that in addition the lines of constant y value with $x \in (-\epsilon^*, \epsilon^*)$ do not intersect any other interface. This can be achieved since all interfaces are mutually disjoint. An example interface with the assigned Fermi coordinates is shown in Figure 2.11.

Define the region $\Omega_i^* := \{(x, y) \in \Omega : y \in [0, |\partial\Omega_i|), x \in (-\epsilon^*, \epsilon^*)\}$. In these coordinates the Euclidean metric on $\partial\Omega_i^*$ is expressed as

$$g_{\mathbb{E}^2} = \mathrm{d}x^2 + g_i(x, y)\mathrm{d}y^2, \tag{2.89}$$

where $g_i(0, y) = 1$ and $g_i(x, y) > 0$ elsewhere. Furthermore, if the interface $\partial\Omega_i \in \mathcal{C}^k$, then g is also bounded in $\mathcal{C}^{k-1}(\Omega_i^*)$ and its $\mathcal{C}^{k-1}(\Omega_i^*)$-norm depends on the $\mathcal{C}^k$ norm of $\partial\Omega_i$.

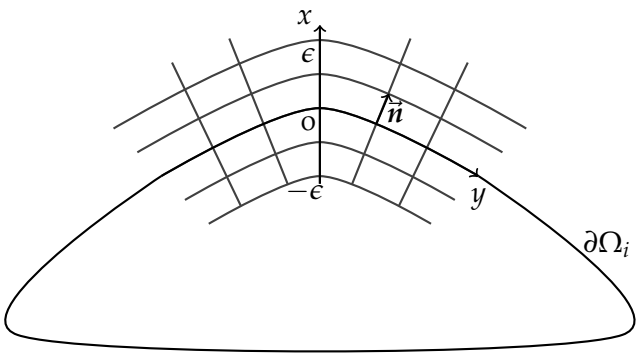

Figure 2.11: An example interface $\partial\Omega_i$ with assigned Fermi coordinates (x, y) where $y \in [0, |\partial\Omega_i|)$ along $\partial\Omega_i$, x is the arc length parameter along the normal lines, with $x = 0$ on $\partial\Omega_i$, and y is extended from $\partial\Omega_i$ to be constant along each such line. Here $\vec{n}$ is a normal vector to curve $\partial\Omega_i$

Then the Laplacian on the region Ω_i^* is

$$\Delta = \partial_x^2 + \frac{1}{2}\frac{\partial_x g_i(x,y)}{g_i(x,y)}\partial_x + [g_i(x,y)]^{-1}\partial_y^2. \tag{2.90}$$

Define χ to be a smooth cutoff function that is 1 when $x \in (-\epsilon^*/2, \epsilon^*/2)$ and 0 when $x = \pm\epsilon^*$. Define the region $\Omega_i^{**} := \{(x,y) \in \Omega : y \in [0, |\partial\Omega_i|), x \in (-\epsilon^*/2, \epsilon^*/2)\}$. Then define $T = \chi\frac{\partial}{\partial y}$. Invoking the bounds in (2.88), we have that:

$$\partial_y^j(u) \in H^1(\Omega_i^{**}) \tag{2.91}$$

for all $j \leq k$. Since $\partial_y^j(u) \in H^1(\Omega_i^{**})$ we have that $\partial_x\partial_y^j(u) \in L^2(\Omega_i^{**})$ for all $j \leq k$. To get bounds on $\partial_x^2\partial_y^j(u) \in L^2(\Omega_i^{**})$ we differentiate (2.90) with respect to y a total of j times. We get the equation

$$\partial_x^2\partial_y^j u = -\partial_y^j\left[\frac{1}{2}\frac{\partial_x g_i(x,y)}{g_i(x,y)}\partial_x u\right] - \partial_y^j\left[[g_i(x,y)]^{-1}\partial_y^2 u\right]. \tag{2.92}$$

Hence, we can estimate $\partial_x^2\partial_y^j u$ in $L^2(\Omega_i^{**})$ by

$$\|\partial_x^2\partial_y^j u\|_{L^2(\Omega_i^{**})} \leq \left\|\partial_y^j\left[\frac{1}{2}\frac{\partial_x g_i(x,y)}{g_i(x,y)}\partial_x u\right]\right\|_{L^2(\Omega_i^{**})} + \left\|\partial_y^j\left[[g_i(x,y)]^{-1}\partial_y^2 u\right]\right\|_{L^2(\Omega_i^{**})}. \tag{2.93}$$

To get higher normal regularity in the region Ω_i^{**}, we differentiate (2.92) with respect to x which leads to the equation

$$\begin{aligned}\partial_x^3\partial_y^j u = &-\frac{1}{2}\partial_y^j\left[[g_i(x,y)]^{-1}\partial_x^2 g_i(x,y)u\right] + \frac{1}{2}\partial_y^j\left[[g_i(x,y)]^{-2}[\partial_x g_i(x,y)]^2 u\right]\\ &-\frac{1}{2}\partial_y^j\left[[g_i(x,y)]^{-1}\partial_x g_i(x,y)\partial_x^2 u\right] + \partial_y^j\left[[g_i(x,y)]^{-2}\partial_x g_i(x,y)\partial_y^2 u\right]\\ &-\partial_y^j\left[[g_i(x,y)]^{-1}\partial_x\partial_y^2 u\right]\end{aligned} \tag{2.94}$$

and the corresponding estimate

$$\begin{aligned}\left\|\partial_x^3\partial_y^j u\right\|_{L^2(\Omega_i^{**})} \leq & \left\|\frac{1}{2}\partial_y^j\left[\left[g_i(x,y)\right]^{-1}\partial_x^2 g_i(x,y)u\right]\right\|_{L^2(\Omega_i^{**})} \\ & + \left\|\frac{1}{2}\partial_y^j\left[\left[g_i(x,y)\right]^{-2}\left[\partial_x g_i(x,y)\right]^2 u\right]\right\|_{L^2(\Omega_i^{**})} \\ & + \left\|\frac{1}{2}\partial_y^j\left[\left[g_i(x,y)\right]^{-1}\partial_x g_i(x,y)\partial_x^2 u\right]\right\|_{L^2(\Omega_i^{**})} \\ & + \left\|\partial_y^j\left[\left[g_i(x,y)\right]^{-2}\partial_x g_i(x,y)\partial_y^2 u\right]\right\|_{L^2(\Omega_i^{**})} \\ & + \left\|\partial_y^j\left[\left[g_i(x,y)\right]^{-1}\partial_x\partial_y^2 u\right]\right\|_{L^2(\Omega_i^{**})}. \end{aligned} \tag{2.95}$$

Repeating the same argument as in the concentric circles case we can estimate $T^j\partial_{\boldsymbol{n}^+}u$ in $H^2(\Omega_i^{**})$ by

$$\|T^j\partial_{\boldsymbol{n}^+}u\|_{H^2(\Omega_i^{**})} \leq \left(4\sup|\nabla T|\cdot\rho_{\sigma_i}\right)^{j+2}\cdot\frac{K_i}{\min\{\sigma_0,\ldots,\sigma_N\}}\|b_0\|_{L^2(\partial\Omega)}, \tag{2.96}$$

in which K_i is a constant that depends on the trace constant and Poincaré constant on domain Ω_i^{**} and ρ_{σ_i} is $\max\{\frac{\sigma_i}{\sigma_{p_i}},\frac{\sigma_{p_i}}{\sigma_i}\}$.

2.6.3 *Regularity of the Solution at the Interface Translates into Regularity of the Charge Densities*

We now derive estimates on the regularity of the charge densities in the two cases – the case of concentric circles and the case of general domains. These estimates will immediately allow us to prove Theorems 2.1 and 2.2.

Firstly, we consider the case of concentric circular domains. Using (2.37), the trace theorem, the Poincaré inequality, and (2.69) we get for $0 \leq j \leq k-2$ the bound

$$\|\partial_\theta^j\gamma_i\|_{\mathcal{C}^0(\partial\Omega_i)} = \left|1-\frac{\sigma_{p_i}}{\sigma_i}\right|\|\partial_r\partial_\theta^j u\|_{\mathcal{C}^0(\partial\Omega_i)} \tag{2.97}$$

$$\leq \left|1-\frac{\sigma_{p_i}}{\sigma_i}\right| c\|\partial_r\partial_\theta^j u\|_{H^2\left(\mathbb{D}\setminus\left(D\left(\mathbf{0},\frac{1}{4}\right)\cap\Omega_N\right)\right)} \tag{2.98}$$

$$\leq \left|1-\frac{\sigma_{p_i}}{\sigma_i}\right|\frac{c\cdot K}{\min\{\sigma_0,\ldots,\sigma_N\}}\frac{6}{(r_N)^2}\|b_0\|_{H^{j+2}(\partial\mathbb{D})}, \tag{2.99}$$

in which c is the Sobolev embedding constant on on disks of size $\frac{1}{2}$ which is uniformly bounded, K is a constant that depends on the trace constant

and Poincaré constant on domain $\mathbb{D}$, r_N is the radius of the innermost circle, and we take the convention $\sigma_{p_0} = 0$. Here $D\left(\mathbf{0}, \frac{1}{4}\right)$ is the disk of radius $\frac{1}{4}$ centred at the origin.

Secondly, we consider the case of general domains. Using (2.37), the trace theorem, the Poincaré inequality, and (2.88) we get for $0 \leq j \leq k-2$ the bound

$$\|T^j \gamma_i\|_{\mathcal{C}^0(\partial\Omega_i)} = \left|1 - \frac{\sigma_{p_i}}{\sigma_i}\right| \|T^j \partial_{\boldsymbol{n}^+} u\|_{\mathcal{C}^0(\partial\Omega_i)} \tag{2.100}$$

$$\leq \left|1 - \frac{\sigma_{p_i}}{\sigma_i}\right| c_i \|T^j \partial_{\boldsymbol{n}^+} u\|_{H^2(\Omega_i^{**})} \tag{2.101}$$

$$\leq \left|1 - \frac{\sigma_{p_i}}{\sigma_i}\right| \left(4 \sup |\nabla T| \cdot \max \rho_{\sigma_i}\right)^{j+2} \cdot \frac{c_i \cdot K_i}{\min\{\sigma_0, \ldots, \sigma_N\}} \|b_0\|_{L^2(\partial\Omega)}, \tag{2.102}$$

in which and ρ_{σ_i} is $\max\{\frac{\sigma_i}{\sigma_{p_i}}, \frac{\sigma_{p_i}}{\sigma_i}\}$, c_i is the Sobolev embedding constant on Ω_i^{**}, K_i is a constant that depends on the trace constant and Poincaré constant on domain Ω_i^{**}, and we take the convention $\sigma_{p_0} = 0$.

Remark: We note that in the special case of concentric circles and for injected currents that are smooth enough as functions of θ on the outer boundary, each extra derivative of our solution is bounded *without* the bounds deteriorating if the two circles are close together. In contrast, in the general case, if two interfaces are close, then the term $\sup |\nabla T|$, for the domain we constructed will necessarily become large. And moreover an interface with large geodesic curvature κ will also cause the constants in the higher-derivatives estimates to deteriorate (*i.e.*, become large). Thus the more general estimate is more versatile, yet more sensitive to the interfaces being either mutually close, or very curved.

2.7 CONCLUSIONS

In this chapter, we presented a novel method for solving the elliptic partial differential equation problem for the electrostatic potential with piecewise constant conductivity. We employ an integral equation approach for which we derive a system of well-conditioned integral equations that can be used to solve the problem. The kernel of the resulting integral operator is smooth.

GMRES is used to solve a linear system for the charge densities at each grid point. Regarding discretion of the integral equations, we employ two different quadrature schemes. In the case where two interfaces are sufficiently close to one another, we use composite quadrature and split

the interface into panels. We then use Gauss-Legendre quadrature on each panel and Lagrange interpolation for interpolating the charge density. For interfaces that are sufficiently far away from all other interfaces we use uniform grid points, trapezoidal rule quadrature, and trigonometric interpolation for interpolating the charge density. An adaptive method allows our solver to achieve higher accuracy even when the curves are close together with acceptably small cost to computation time. In the case of interfaces discretized with uniform grid points we use a truncated Fourier series to approximate the scaled charge densities. On the other hand, in the case of interfaces discretized with composite quadrature (panels) we use a truncated Legendre series polynomial to approximate the scaled charge densities. In either case, if either of the two highest mode coefficients are above a specified threshold, then the interface/panel is refined.

When the evaluation point is not near or on an interface or the boundary, we evaluate the single layer potentials using the same quadrature as used to solve the integral equations. When the evaluation point is near or on an interface or the boundary, we approximate interfaces or the boundary with line segments near the evaluation point and employ an analytic expression for the single layer potential due to a line segment.

To illustrate the effectiveness of our method, we solved the elliptic partial differential equation problem for four test cases. Our method was compared against a popular open-source platform and is shown to be superior since our method produced more accurate results in less computational time. In addition, our method is also shown to easily handle problems of increasingly higher complexity involving up to 155 different regions of constant conductivity.

Numerous avenues of future work exist. One could adapt our method to solve the problem in which the potential u has a prescribed jump across the interfaces by including double layer potentials. Also, the method could be adapted to the three dimensional version of the problem. Each of these generalizations would enable several applications of the method.

In the following chapter, we generalize our method to handle the case of overlapping regions of constant conductivity and we study the behaviour of the solution to Eq. (1.1) to leading order at points of intersection between two transversely intersecting interfaces of regions of piecewise constant conductivity.

3

SINGULAR BEHAVIOUR OF ELECTROSTATIC POTENTIALS AT TRANSVERSELY INTERSECTING INTERFACES

3.1 PROBLEM SETTING

We consider the elliptic partial differential equation for the real-valued electric potential u on a domain $\Omega \subset \mathbb{R}^2$

$$P(u)(\boldsymbol{x}) := \nabla \cdot (\sigma(\boldsymbol{x}) \nabla u(\boldsymbol{x})) = 0, \quad \boldsymbol{x} \in \Omega, \tag{3.1}$$

in which σ is a positive function in L^∞ which in addition is piecewise constant. Our main assumption will consider the geometry of the boundaries of the regions where σ is constant. The Neumann boundary condition is

$$\sigma \frac{\partial u}{\partial \boldsymbol{n}} = b_0 \quad \text{on } \partial\Omega, \tag{3.2}$$

in which $b_0 : \partial\Omega \to \mathbb{R}$ is the real-valued applied current. We use $\boldsymbol{n}$ to denote the unit outward normal vector to the boundary and use $\frac{\partial}{\partial \boldsymbol{n}}$ or $\partial_{\boldsymbol{n}}$ for the corresponding normal derivative. We require $\int_{\partial\Omega} b_0 \, d\ell = 0$ for solvability. Our goal is also to understand the behaviour of the solution at points where the regularity theory in Chapter 2 is not applicable.

Garde [Gar20] considers a class of piecewise constant conductivity coefficients that can be decomposed into a sum of piecewise constant functions on nested sets (layers) with connected complement. This type of conductivity is referred to as a piecewise constant layered conductivity (PCLC). A decomposition of a PCLC type conductivity into each of its layers is shown in Fig. 3.1 [Gar20].

We consider a different class of conductivities than the PCLC class considered by Garde. We remove the requirement that the layers be nested (*i.e.*, we allow the interfaces of two separate layers to intersect) and we require the interfaces to be $\mathcal{C}^2$ smooth. That is, we will consider the class

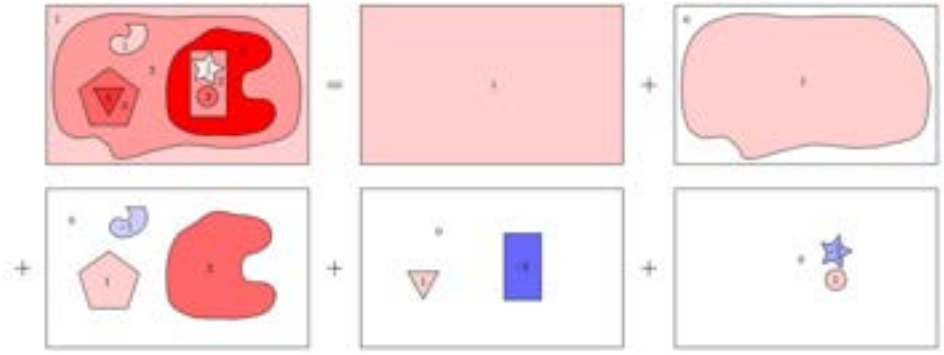

Figure 3.1: Decomposition of a PCLC type conductivity into each of its layers. The numbers represent function values in each of the coloured regions [Gar20].

of piecewise constant conductivity coefficients that can be decomposed into a sum of finitely many piecewise constant functions on not necessarily nested sets (layers) with connected complement and $\mathcal{C}^2$ boundary. The key novelty here is that we allow the boundaries to intersect, transversely. More formally, for a finite set of simply connected regions $\{\Omega_i\}_{i=0}^N$, each with $\mathcal{C}^2$ boundary (*i.e.*, $\partial\Omega_i \in \mathcal{C}^2$), and each contributing σ_i to the total conductivity, we denote the conductivity at any point $\boldsymbol{x} \in \mathbb{R}^2$ by

$$\sigma(\boldsymbol{x}) = \sum_{i=0}^{N} \sigma_i \chi_{\Omega_i}(\boldsymbol{x}), \tag{3.3}$$

in which the indicator function of a subset $A \subseteq \mathbb{R}^2$ is a function $\chi_A : \mathbb{R}^2 \to \{0,1\}$ defined as

$$\chi_A(\boldsymbol{x}) := \begin{cases} 1 & \text{if } \boldsymbol{x} \in A \\ 0 & \text{if } \boldsymbol{x} \notin A \end{cases}. \tag{3.4}$$

We stress that the regions Ω_i can overlap but if the boundaries intersect, then we require that the boundaries necessarily intersect transversely. An example layout of our regions of conductivity is shown in Figure 3.2.

To analyze the solution u to Eq. (3.1) near a point of intersection, we consider a corresponding straight lines model case. The asymptotic behaviour of u near the point of intersection will be fully captured by a model operator on this reduced problem. We now describe the construction of the reduced problem.

Definition 3.1 (Angles at Point of Intersection)**.** Consider $N \in \mathbb{N}$ half-curves c_i for $i = 1, \ldots, N$ which intersect at some point (without loss of generality, say $\mathbf{0} \in \mathbb{R}^2$), forming N successive angles $\widetilde{\omega}_i$, for $i = 1, \ldots, N$

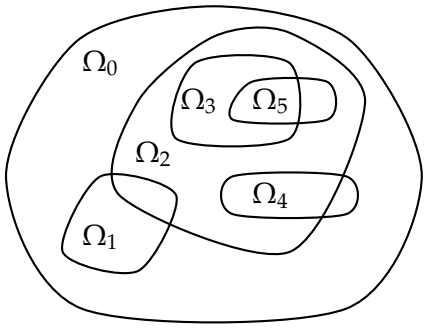

Figure 3.2: An example layout of regions. The boundary of region Ω_0 is the boundary of the domain.

which are all strictly positive (and sum to 2π, *i.e.*, $\sum_{i=1}^{N} \widetilde{\omega}_i = 2\pi$). We define $\omega_i := \sum_{j=1}^{i} \widetilde{\omega}_j$ for $i = 1, \ldots, N$.

An example of the original problem and the corresponding reduced problem is shown in Fig. 3.3.

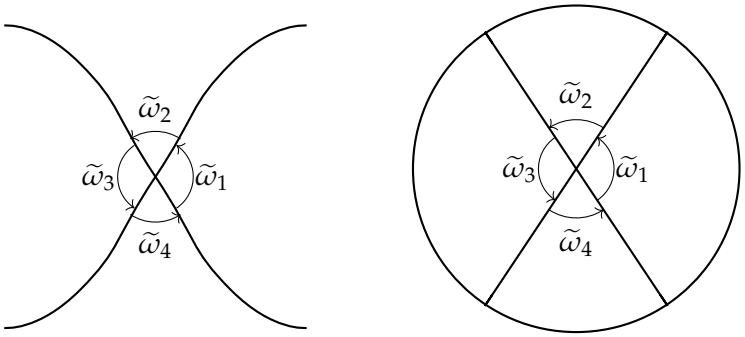

Figure 3.3: The original problem (left) and the reduced problem (right). We note that in the reduced problem, the conductivity will be constant in each sector.

Definition 3.2. Define the model operator $L := -[\tilde{\sigma}(\theta)]^{-1}\partial_\theta(\tilde{\sigma}(\theta)\partial_\theta)$ on $\mathbb{S}^1$ where $\tilde{\sigma}(\theta) := \sigma_i$ when $\theta \in [\omega_{i-1}, \omega_i)$ for $i = 1, \ldots, N$ (adopting the convention that $\omega_0 := \omega_N$).

We now show that L has a sequence of non-negative eigenvalues $0 = \lambda_0 < \lambda_1 < \lambda_2 < \ldots$, and the corresponding eigenspaces $V_0, V_1, \ldots$ are mutually orthogonal, and their joint space $V_0 \oplus V_1 \oplus V_2 \oplus \ldots$ forms a basis of $H^1(\mathbb{S}^1)$.

To do this, let us define the Rayleigh quotient:

$$R[f] = \frac{\int_0^{2\pi} \tilde{\sigma}(\theta) \cdot [\partial_\theta f(\theta)]^2 d\theta}{\int_0^{2\pi} \tilde{\sigma}(\theta)[f(\theta)]^2 d\theta}. \tag{3.5}$$

Then we show that a function $f(\theta)$ that is a critical point of this quotient is an eigenvalue of $L[\cdot]$.

This follows by noting that if f is a critical point of $R[f]$ than there exists a $\lambda \in \mathbb{R}$ so that for all $v \in H^1(\mathbb{S}^1)$:

$$(-\int_0^{2\pi} \partial_\theta(\tilde{\sigma}(\theta) \cdot \partial_\theta f) \cdot v d\theta =) \int_0^{2\pi} \tilde{\sigma}(\theta) \partial_\theta f \cdot \partial_\theta v d\theta = \int_0^{2\pi} \tilde{\sigma}(\theta) f(\theta) \cdot v(\theta) d\theta.$$

This shows that such an $f(\theta)$ is an eigenfunction of L, with eigenvalue λ.

Note that by [Eva10], the first eigenvalue is simple, and by inspection $\lambda_0 = 0$ with $V_0 = Span(1)$.

We point out that considering the L^2-norm with respect to the measure $\tilde{\sigma}(\theta)d\theta$, *i.e.*,

$$\|f(\theta)\|_{L^2(\tilde{\sigma}(\theta)d\theta)} = \sqrt{\int_0^{2\pi} |f(\theta)|^2 \tilde{\sigma}(\theta) d\theta}, \tag{3.6}$$

and also $H^1(\tilde{\sigma}(\theta)d\theta)$ $\Big($with associated norm

$$\|f\|_{H^1(\tilde{\sigma}(\theta)d\theta)} = \sqrt{\|\partial_\theta f\|^2_{L^2(\tilde{\sigma}(\theta)d\theta)} + \|f\|^2_{L^2(\tilde{\sigma}(\theta)d\theta)}}\Big) \tag{3.7}$$

then L is self-adjoint on $H^1(\tilde{\sigma}(\theta)d\theta)$. In particular the eigenfunctions e_k, e_l corresponding to different eigenvalues $0 < \lambda_A < \lambda_B$ will be orthogonal with respect to the inner product $L^2(\tilde{\sigma}(\theta)d\theta)$. In fact we can take all eigenvectors $e_i(\theta)$ (which form a basis for $L^2(\tilde{\sigma}(\theta)d\theta)$)) to be mutually orthogonal with respect to that inner product.

We note that (since all $\sigma_i > 0$ are bounded above and below), the norms $L^2(\tilde{\sigma}(\theta)d\theta)$ and $H^1(\tilde{\sigma}(\theta)d\theta)$ are *equivalent* to the standard norms $L^2(d\theta)$ and $H^1(d\theta)$, but not *identical* to them.

To find these eigenvectors and eigenvalues we perform the standard iterative method: First let λ_0 be the infimum of this quotient $R[f]$ among functions $f(\theta)$ in $H^1(\tilde{\sigma}(\theta)d\theta)$, and let the corresponding space of functions be $V_0 \subset H^1(\tilde{\sigma}(\theta)d\theta)$. Then minimize R over $(V_0)^\perp \subset H^1(\tilde{\sigma}(\theta)d\theta)$. The corresponding space of functions gives the next eigenspace V_1 with an eigenvalue $\lambda_1 > 0$. Then minimize $R[f]$ over the space $(V_0 \oplus V_1)^\perp \subset H^1(\mathbb{S}^1)$; the corresponding space of functions is V_2 and corresponds to the next eigenvalue $\lambda_2 > \lambda_1$, *etc.*

Definition 3.3. We define $e_k(\theta), k \in \mathbb{N}$ to be the orthonormal basis of $L^2(\tilde{\sigma}(\theta)d\theta)$ consisting of the eigenvectors of L on $\mathbb{S}^1$. In particular

$$\int_0^{2\pi} e_i(\theta) \cdot e_j(\theta)\tilde{\sigma}(\theta)d\theta = \delta_{ij}.$$

We choose the ordering so that if $e_i(\theta), e_j(\theta)$ with $i < j$ have corresponding eigenvalues λ, μ then $\lambda \leq \mu$.

We will denote the eigenvalue of $e_k(\theta)$ by λ_{e_k}. Alternatively, we will denote the eigenvalues of L in order of increasing size by $0 = \lambda_0 < \lambda_1 < \lambda_2 < \lambda_3 < \dots$. Let M be the multiplicity of $\lambda_1 > 0$. In particular $e_1(\theta), \dots, e_M(\theta)$ have eigenvalue λ_1.

It turns out that for the special operators L that we consider here (built out of piecewise constant functions $\tilde{\sigma}(\theta)$ on $\mathbb{S}^1$) the eigenvalues λ_{e_k}'s will always satisfy an algebraic system of equations. In Appendix A we show that in the special case where $N = 4$ and $\widetilde{\omega}_i = \frac{\pi}{2}$ for all i, then the eigenvalues λ_{e_k}'s satisfy the specific algebraic system Eqs. (A.24) to (A.31) and the first positive eigenvalue $\lambda_1 < 1$. From this point on, we will make the assumption that $0 < \lambda_1 < 1$.

Definition 3.4. For a disk of radius $\varepsilon > 0$ centred at 0, denoted by $D(0, \varepsilon) \subset \mathbb{R}^2$ and a piecewise constant $\sigma(\theta)$, we define the function space $\dot{H}^2_1(D(0, \varepsilon))$ as follows:

$$\begin{aligned}\dot{H}^2_1(D(0,\varepsilon)) := \{f : \sigma(\theta)\partial_r f, r^{-1}\sigma(\theta)\partial_\theta f, r\sigma(\theta)\partial_r(\partial_r f), \partial_r(\sigma(\theta)\partial_\theta f),\\ r^{-1}\partial_\theta\left(\sigma(\theta)\partial_\theta f\right) \in L^2(D(0,\varepsilon)\}\end{aligned} \tag{3.8}$$

in which r and θ are the standard radial and angular polar coordinates, respectively. Recall that $\sigma(\theta)\partial_\theta f$ is continuous. We note that a more proper notation would be $\dot{H}^2_{1,\sigma(\theta)}(D(0, \varepsilon))$; however, we avoid this for notational simplicity.

The main theorem of this chapter is now stated:

Theorem 3.5 (Main Theorem)**.** *Let u solve Eq. (3.1) at a point of intersection as defined in Definition 3.1. Recall the model operator L on $\mathbb{S}^1$ defined in Definition 3.2. Recall that $e_1(\theta), \dots, e_M(\theta)$ are the eigenfunctions corresponding to the first positive eigenvalue $\lambda_1 > 0$ of L. Assume $\lambda_1 < 1$. Let λ_2 be the second positive eigenvalue of L. Consider the standard polar coordinates (r, θ) centred at the point of intersection. There exists a change of coordinates to (ρ, φ) (which is explicitly defined in Eq. (3.32)) with respect to which the following expansion holds. Then there exists some $(\alpha_1, \dots, \alpha_M) \in \mathbb{R}^M$ such that for*

$$S(\rho) := \left\| \frac{u(\rho,\varphi) - u(\mathbf{0})}{\rho^{\sqrt{\lambda_1}}} - \sum_{k=1}^{M} \alpha_k e_k(\varphi) \right\|_{L^2_\varphi(d\varphi)}, \tag{3.9}$$

we have to leading order

$$S(\rho) = \mathcal{O}(\rho^{\delta}), \tag{3.10}$$

in which $\delta = \min(\sqrt{\lambda_2} - \sqrt{\lambda_1}, \frac{1}{3}\left(1 - \sqrt{\lambda_1}\right)) > 0$.

3.2 GENERAL INTERSECTING CURVES

We will show that the solution $u(\boldsymbol{x})$ to Eq. (3.1) near a point in the case of general intersecting curves (Fig. 3.3 left) and the case of intersecting half-lines (Fig. 3.3 right) are identical to leading order. This will be done in two steps. The first step will be a change of coordinates that will convert the general intersecting curves to straight half-lines. A suitable choice of coordinates allows us to express the operator P with respect to the new coordinates leading to a natural decomposition of the operator:

$$P = \overline{P} + \tilde{P} \tag{3.11}$$

in which $\overline{P}$ is the operator defined in Eq. (3.37) and $\tilde{P}$ is a correction term that vanishes at the point of intersection and involves first and second derivatives. We will refer to P as the original operator. The second step will be to solve this original problem $Pu = 0$.

3.2.1 *Change of Coordinates*

The first step to showing that the case of general intersecting curves (Fig. 3.3 left) is identical to the straight lines case (Fig. 3.3 right) to leading order will be a change of coordinates that will convert the general intersecting curves to straight lines. In particular, the curves c_i will be level sets of a new coordinate φ. Also, the coordinate r will be replaced by a new coordinate ρ which will have the property that $\partial_\rho, \partial_\varphi$ are normal in an open neighbourhood around each curve c_i. In fact our construction of new coordinates (ρ, φ) is performed in a suitable local angle around each c_i and then the coordinates are glued together making use of suitable cutoff functions.

Let us consider the following local problem: Recall the angles of intersection as defined in Definition 3.1. Consider $N \in \mathbb{N}$ half-curves c_i for $i = 1, \ldots, N$ which intersect at some point (say $\mathbf{0} \in \mathbb{R}^2$), forming N successive angles $\widetilde{\omega}_i$, for $i = 1, \ldots, N$ which are all strictly positive (and sum to 2π): $\sum_{i=1}^{N} \widetilde{\omega}_i = 2\pi$. We define $\omega_i := \sum_{j=1}^{i} \widetilde{\omega}_j$ for $i = 1, \ldots, N$. The curves c_i can be expressed in parameterized form:

$$c_i : [0, \delta) \to \mathbb{R}^2,\ c_i(0) = 0,\ \dot{c}_i(t) \neq 0\ \forall t \in [0, \delta) \tag{3.12}$$

for some $\delta > 0$. Here the functions c_i are assumed to be C^k for some $k \geq 2$. For definiteness, let us assume t to be the unique arc-length parameter along the curve c_i.

We consider the conductivity σ defined in the standard polar coordinates (r, θ) by $\sigma(r, \theta) := \sigma_i$ when $\theta \in [\omega_{i-1}, \omega_i)$ for $i = 1, \ldots, N$.

Proposition 3.6. *Consider $N \in \mathbb{N}$ half-curves $\{c_i\}_{i=1}^N$, each parameterized by Eq. (3.12), which intersect at $\mathbf{0} \in \mathbb{R}^2$, forming N successive positive angles $\widetilde{\omega}_i$, for $i = 1, \ldots, N$. Then there exists a change of coordinates function f_{cc} that will transform the general intersecting half-curves to straight half-lines.*

The smoothness of the half-lines can be captured when we express them as a graph over their tangent line at the origin: Consider the straight half-lines $l_i(t)$ which emanate from the origin and are such that l_{i-1} and l_i form an angle $\widetilde{\omega}_i$ at the origin (with the convention that $l_0 = l_N$). Normalize the parameter t on these half-lines to have unit speed. In other words:

$$l_i(t) = t \cdot (\cos \omega_i, \sin \omega_i). \tag{3.13}$$

Associated to each such line l_i, let us consider a complementary direction s, so that s is the (signed) distance function from the line l_i. Then the curve c_i (seen as an un-parameterized object) can be written as a graph:

$$s = b_i(t),\ b_i \in C^2([0, \delta)),\ b_i(0) = 0,\ b_i'(0) = 0 \tag{3.14}$$

(here $'$ stands for $\frac{d}{dt}$). We note the geometric significance of the second derivative of $b_i(t)$ at $t = 0$:

$$b_i''(0) = \kappa_i(0), \tag{3.15}$$

in which κ_i is the (signed) curvature of curve c_i.

Now, let us restrict our attention to a small disc $D(0, \varepsilon)$ centred at the origin of radius ε. By slight abuse of notation, we denote the restrictions of the curves c_i to this disc by c_i again.

We now introduce our change of coordinates:

Lemma 3.7. *There exists a function φ defined in $D(0, \varepsilon)$,*

$$\varphi : D(0, \varepsilon) \to [0, 2\pi)$$

with the property that:

$$\{\varphi = \omega_i\} = c_i,$$

and moreover φ is a 2π-periodic function, in the sense that

$$\frac{d^{(i)}}{d\theta^i}\varphi(r, \theta)\Big|_{\theta=0} = \frac{d^{(i)}}{d\theta^i}\varphi(r, \theta)\Big|_{\theta=2\pi}$$

for all $i \in \mathbb{N}$ and $r \in (0, \varepsilon)$. Furthermore, if we think of φ as a function of the usual polar coordinates (r, θ), then $d\varphi \neq 0$ everywhere.

Proof. Let us construct this function φ. First, we express the curves c_i as graphs of functions in the regular polar coordinates (r, θ). In particular there exist functions $\theta_i(r)$ so that

$$c_i := \{(r, \theta_i(r)), r \in [0, \delta)\}, \tag{3.16}$$

and moreover, we have $\theta_i(r) \in \mathcal{C}^2([0, \delta))$ and also $\theta_i(0) = \omega_i$. We note that for a general C^2 curve,

$$\theta_i(r) = \theta_i(0) + \kappa_i r^2 + o(r^2) \tag{3.17}$$
$$= \omega_i + \kappa_i r^2 + o(r^2). \tag{3.18}$$

Hence,

$$\theta_i(r) - \omega_i = \kappa_i r^2 + o(r^2). \tag{3.19}$$

Let us locally construct φ near curves c_i. We define

$$\varphi_i(r, \theta) = \theta - \theta_i(r) + \omega_i. \tag{3.20}$$

We introduce a cutoff function:

Definition 3.8. Let $\chi(\theta), 0 \leq \chi(\theta) \leq 1$ be a $\mathcal{C}^\infty$-smooth periodic function over $[0, 2\pi)$ which equals 1 in an open neighbourhood around each ω_i and 0 in open neighbourhoods around the midpoints $M_1 = \frac{1}{2}[\omega_1 + \omega_2], \ldots, M_N = \frac{1}{2}[\omega_N + \omega_1]$. We also require that the regions $\{\chi(\theta) = 0\}$ on large enough intervals so that $\{\chi(\theta) \neq 0\} \subset \bigcup_{i=1}^N [\omega_i - \delta, \omega_i + \delta]$.

Let us then define $\tilde{\varphi}_i$ on each of the intervals $[M_{i-1}, M_i]$ for $i = 1, \ldots, N$ (with the convention that $M_0 = M_N$) via the formula:

$$\tilde{\varphi}_i(r, \theta) = \chi(\theta) \cdot \varphi_i(r, \theta) + (1 - \chi(\theta))\theta. \tag{3.21}$$

We note in particular that these functions agree with θ in open neighbourhoods of the points $M_1, \ldots, M_N$. So merely defining φ via the formula:

$$\varphi(r, \theta) = \tilde{\varphi}_i(r, \theta) \text{ for } \theta \in [M_{i-1}, M_i], \tag{3.22}$$

(with the convention that $M_0 = M_N$) defines a $\mathcal{C}^1$ 2π-periodic function on $[0, 2\pi)$.

We also check that $d\varphi(r,\theta) \neq 0$, for all $(r,\theta) \in (0,\delta) \times [0,2\pi)$, provided we take $\delta > 0$ sufficiently small. To check this, it suffices to show that $\partial_\theta \varphi(r,\theta) > 0$, when $\delta > 0$ is taken small enough. We calculate:

$$\partial_\theta \varphi(r,\theta) = \chi'(\theta) \cdot \varphi_i(r,\theta) + \chi(\theta) \cdot \partial_\theta \varphi_i(r,\theta) - \chi'(\theta) \cdot \theta + (1 - \chi(\theta)).$$

Since by taking δ small enough we can make θ_i arbitrarily close to ω_i, the claim follows:

$$\begin{aligned}
\partial_\theta \varphi(r,\theta) &= \chi'(\theta) \cdot [\theta - \theta_i(r) + \omega_i] + \chi(\theta) \cdot \partial_\theta [\theta - \theta_i(r) + \omega_i] \\
&\quad - \chi'(\theta) \cdot \theta + (1 - \chi(\theta)) \\
&= \chi'(\theta) \cdot [\theta - \theta_i(r) + \omega_i] + \chi(\theta) - \chi'(\theta) \cdot \theta + (1 - \chi(\theta)) \\
&= \chi'(\theta) \cdot [-\theta_i(r) + \omega_i] + 1 \\
&\xrightarrow[\delta \to 0^+]{} \chi'(\theta) \cdot [-\omega_i + \omega_i] + 1 \\
&= 1.
\end{aligned}$$

□

We have defined

$$\varphi(r,\theta) = \chi(\theta)\,[-\theta_i(r) + \omega_i] + \theta. \tag{3.23}$$

We now introduce a second coordinate $\rho(r,\theta)$ which will replace r; the pair $(\rho(r,\theta), \varphi(r,\theta))$ will define our desired new coordinates. Let $\rho = \rho(r,\theta)$ unspecified for now. Then

$$d\rho = \frac{\partial \rho}{\partial r} dr + \frac{\partial \rho}{\partial \theta} d\theta. \tag{3.24}$$

We impose $\langle d\rho, d\theta \rangle = 0$ (where $\langle \cdot, \cdot, \rangle$ denotes the inner product of the 1-forms with respect to the Euclidean metric, in a small set $D_i = \{(r,\theta) | \theta \in [\omega_i - \delta, \omega_i + \delta], r \in (0,\varepsilon)\}$ around each c_i). This is equivalent to

$$\frac{\partial \rho}{\partial r}\frac{\partial \varphi}{\partial r} + r^{-2}\frac{\partial \rho}{\partial \theta}\frac{\partial \varphi}{\partial \theta} = 0. \tag{3.25}$$

We chose $\varphi = \theta - \theta_i(r) + \omega_i$ which implies

$$\begin{aligned}
d\varphi &= \frac{\partial \varphi}{\partial \theta} d\theta + \frac{\partial \varphi}{\partial r} dr && (3.26) \\
&= d\theta - \theta_i'(r) dr. && (3.27)
\end{aligned}$$

By Eq. (3.25),

$$\frac{\partial \rho}{\partial r} \cdot \left(-\theta_i'(r)\right) + r^{-2}\frac{\partial \rho}{\partial \theta} \cdot 1 = 0. \tag{3.28}$$

So we need

$$\frac{\partial \rho}{\partial \theta} = r^2 \theta_i'(r) \frac{\partial \rho}{\partial r}. \tag{3.29}$$

We locally solve this equation in the neighbourhoods D_i abound each c_i; we denote these local solutions by $\rho_i(r,\theta)$. In particular we solve for $\rho_i(r,\theta)$ by solving

$$\begin{cases} \left(\partial_\theta - r^2\theta_i'(r)\partial_r\right)\rho_i(r,\theta) & = 0 \\ \rho_i(r,\omega_i) & = r. \end{cases} \tag{3.30}$$

Eq. (3.30) admits a unique solution. Given the $\mathcal{C}^2$ regularity of $\theta_i(r)$ in r and since $\theta_i'(0) = 0$ we derive that $\rho_i(r,\theta) - r = \mathcal{O}(r^3)$, $\partial_r\rho_i(r,\theta) - 1 = \mathcal{O}(r^2)$.

Finally, we build our desired coordinate $\rho(r,\theta)$ out of the locally constructed $\rho_i(r,\theta)$ by means of the cutoff function in Definition 3.8. Let $\rho_i(r,\theta)$ be the function that equals 0 outside the domain of definitions D_i. We then define

$$\rho(r,\theta) = \sum_{i=1}^{N} \chi(\theta)\cdot\rho_i(r,\theta) + (1-\chi(\theta))r. \tag{3.31}$$

Combining Eqs. (3.23) and (3.31) gives us the change of coordinates transformation

$$\begin{cases} \rho(r,\theta) = \sum_{i=1}^{N}\chi(\theta)\cdot\rho_i(r,\theta) + (1-\chi(\theta))r \\ \varphi(r,\theta) = \chi(\theta)\left[-\theta_i(r) + \omega_i\right] + \theta \end{cases}. \tag{3.32}$$

We note that:

Lemma 3.9. *The coordinate system $(\rho(r,\theta),\varphi(r,\theta))$ just constructed has the property that there exist open neighbourhoods $\tilde{D}_i = [\omega_i - \delta', \omega_i + \delta'] \subset D_i$ around each curve c_i where $\langle d\rho, d\varphi\rangle = 0$. In particular in those same neighbourhoods $\partial_\rho \perp \partial_\varphi$ (with respect to the Euclidean metric).*

Moreover we have the bounds

$$\rho(r,\theta) - r = \mathcal{O}(r^3), \tag{3.33}$$
$$\partial_r\rho(r,\theta) - 1 = \mathcal{O}(r^2), \tag{3.34}$$
$$\partial_\theta\rho(r,\theta) = \mathcal{O}(r^3). \tag{3.35}$$

We also make a key remark: The conductivity function $\sigma(x)$ defined in (3.3), expressed now in the new coordinates via $\tilde{\sigma}(\rho(r,\theta),\varphi(r,\theta)) = \sigma(r,\theta)$ is a piecewise constant function *only of φ. Moreover, the current matching condition $\sigma_i\vec{n}(u) = \sigma_{i+1}\vec{n}(u)$ across each interface is now recast as $\sigma_i\partial_\varphi u = \sigma_{i+1}\partial_\varphi u$ at each $\varphi = \omega_i$, $i = 1,\dots,N$.*

Our next goal is to re-express the operator P in terms of the coordinates ρ, φ. With slight abuse of notation, we call the operator expressed with respect to ρ, φ again P. We will show in Proposition 3.13 that this operator can be expressed in the form:

$$P = \overline{P} + \tilde{P} \tag{3.36}$$

in which $\overline{P}$ is the operator:

$$\overline{P}[u(\rho,\varphi)] := \tilde{\sigma}(\varphi)\left(\frac{\partial^2}{\partial\rho^2} + \frac{1}{\rho}\frac{\partial}{\partial\rho}\right)u + \frac{1}{\rho^2}\frac{\partial}{\partial\varphi}\left(\tilde{\sigma}(\varphi)\frac{\partial u}{\partial\varphi}\right) \tag{3.37}$$

and $\tilde{P}$ is the correction term which we will show in Proposition 3.13 can be expressed in polar coordinates:

In the corner-like neighbourhoods $\{(\rho,\varphi)|\varphi \in (\omega_i - \delta, \omega_i + \delta), \rho \in (0,\varepsilon)\}$ around the angles $\varphi = \omega_i$ the operator $\tilde{P}$ can be expressed:

$$\begin{aligned}\tilde{P}f = {} & \mathcal{O}(\rho)\partial_\rho[\tilde{\sigma}(\varphi)\partial_\rho]f + \mathcal{O}(\rho^{-1})\partial_\varphi[\tilde{\sigma}(\varphi)\partial_\varphi]f \\ & + \mathcal{O}(1)\partial_\varphi f + \mathcal{O}(\rho)\partial_\rho f.\end{aligned} \tag{3.38}$$

On the other hand, *away* from the corner-like neighbourhoods around $\varphi = \omega_i$, the operator $\tilde{P}$ can be expressed as:

$$\begin{aligned}\tilde{P}f = {} & \mathcal{O}(\rho^2)\partial_\rho\partial_\rho f + \mathcal{O}(\rho)\partial_\varphi\partial_\rho f + \mathcal{O}(\rho^{-2})\partial_\varphi\partial_\varphi f \\ & + \mathcal{O}(1)\partial_\varphi f + \mathcal{O}(\rho)\partial_\rho f.\end{aligned} \tag{3.39}$$

See Eqs. (3.174) to (3.180) below for a more detailed expression of $\tilde{P}$.

3.2.2 *Regularity Results*

Recall the original problem involving the equation for the electric potential u on a domain $\Omega \subset \mathbb{R}^2$ Eq. (3.1) and the Neumann boundary condition Eq. (3.2):

$$\begin{cases} Pu = 0 & \text{in } \Omega \\ \sigma\frac{\partial u}{\partial n} = b_0 & \text{on } \partial\Omega \end{cases}.$$

We want to study the solution u near the intersection of regions of constant conductivity. Let $\widetilde{\Omega} \subset \Omega$ be a small region around a point of intersection between different regions of constant conductivity. Without

loss of generality, take the point of intersection to be located at the origin. The electric potential u will satisfy

$$\begin{cases} Pu = 0 & \text{in } \widetilde{\Omega} \\ u = \tilde{f} & \text{on } \partial\widetilde{\Omega} \end{cases}, \tag{3.40}$$

in which $\tilde{f}$ is a C^2 piecewise smooth function satisfying the current continuity condition across each interface.

We perform the change of coordinates transformation defined in Lemma 3.9 that converts the general intersecting curves to straight lines. We specifically choose $\widetilde{\Omega}$ in Eq. (3.40) to be the preimage of $D(0,\varepsilon)$ for the change of coordinates transformation. We seek to solve the reduced problem on $D(0,\varepsilon) \subset \mathbb{R}^2$, *i.e.*, the disk of radius $\varepsilon > 0$. We note that any asymptotic behaviour we obtain in ρ for solutions to (3.40) will imply the identical bound for r, in view of the bounds on ρ in terms of r in Lemma 3.9. We make a further convention: all functions spaces H^1, L^2, H^2_1 unless stated otherwise will be considered in the coordinates ρ, φ, and unless otherwise stated the volume form will be $\rho d\rho d\varphi$.

In the new coordinate system (ρ, φ) defined in Eq. (3.32):

$$\begin{cases} Pu = 0 & \text{in } D(0,\varepsilon) \\ u = f & \text{on } \partial D(0,\varepsilon) \end{cases}, \tag{3.41}$$

in which $f(\varphi)$ is piecewise C^2 on each of the intervals $[\varphi_i, \varphi_{i+1}]$ and $\sigma\partial_\varphi u$ is continuous across each juncture φ_i. We note that the current was continuous across each interface before the change of coordinates. We invoke the fact that the current continuity condition is invariant under changes of coordinates. Note that after the change of coordinates, $\rho^{-1}\partial_\varphi$ is the unit normal vector field to the interface, on both sides of the interface. This implies that $\sigma_i\partial_\varphi u$ equals $\sigma_{i+1}\partial_\varphi u$ after the change of coordinates. Since $\sigma\partial_\varphi u$ is Lipschitz on $\partial D(0,\varepsilon)$, we have that $\partial_\varphi(\sigma\partial_\varphi u)$ is bounded on $\partial D(0,\varepsilon)$ and hence in L^2 on $\partial D(0,\varepsilon)$. Therefore, $\partial_\varphi(\sigma\partial_\varphi f)$ makes sense as an L^2 function on the circle.

Recall that $\overline{P}$ is the operator defined in Eq. (3.37) and $\tilde{P}$ is the correction term which can be expressed in polar coordinates as in Eqs. (3.38) and (3.39). We can write the solution to the problem Eq. (3.41) as the sum of the solution $\overline{u}$ to the problem:

$$\begin{cases} \overline{P}\overline{u} = 0 & \text{in } D(0,\varepsilon) \\ \overline{u} = f & \text{on } \partial D(0,\varepsilon) \end{cases} \tag{3.42}$$

and a correction term $\tilde{u}$, *i.e.*,

$$u = \overline{u} + \tilde{u}. \tag{3.43}$$

In view of the divergence form of $\overline{P}$ defined in Eq. (3.36), we will refer to Eq. (3.42) along with the current matching condition as the "angularly matched Laplace equations".

Now, combining Eqs. (3.36) and (3.43) yields

$$Pu = (\overline{P} + \tilde{P})(\overline{u} + \tilde{u}). \tag{3.44}$$

Then we can rewrite Eq. (3.41) as

$$\begin{cases} (\overline{P} + \tilde{P})(\overline{u} + \tilde{u}) = 0 & \text{in } D(0,\varepsilon) \\ \overline{u} + \tilde{u} = f & \text{on } \partial D(0,\varepsilon). \end{cases} \tag{3.45}$$

By Eq. (3.42), $\overline{P}\overline{u} = 0$ in $D(0,\varepsilon)$ and $\overline{u} = f$ on $\partial D(0,\varepsilon)$, so we need to solve the problem:

$$\begin{cases} (\overline{P} + \tilde{P})\tilde{u} = -\tilde{P}\overline{u} & \text{in } D(0,\varepsilon) \\ \tilde{u} = 0 & \text{on } \partial D(0,\varepsilon) \end{cases}. \tag{3.46}$$

In Proposition 3.13, we will show that $\tilde{P} : \dot{H}^2_1(D(0,\varepsilon)) \to L^2(D(0,\varepsilon))$, and hence $\tilde{P}(\overline{u}) \in L^2(D(0,\varepsilon))$. For $g := -\tilde{P}(\overline{u}) \in L^2(D(0,\varepsilon))$, we can rewrite problem (3.46) in the form

$$\begin{cases} \left(\overline{P} + \tilde{P}\right)\tilde{u} = g & \text{in } D(0,\varepsilon) \\ \tilde{u} = 0 & \text{on } \partial D(0,\varepsilon) \end{cases}, \tag{3.47}$$

that is, $\tilde{u}$ satisfies the elliptic PDE $\nabla \cdot (\sigma(\boldsymbol{x})\nabla\tilde{u}(\boldsymbol{x})) = g(\boldsymbol{x})$ inside the disk $D(0,\varepsilon)$ with Dirichlet boundary condition.

In general, for a divergence type elliptic operator B on $D(0,\varepsilon)$ and a function $g \in L^2(D(0,\varepsilon))$, we define the function $v := B^{-1}g \in H^1(D(0,\varepsilon))$ to be the unique solution of the problem

$$\begin{cases} Bv = g & \text{in } D(0,\varepsilon) \\ v = 0 & \text{on } \partial D(0,\varepsilon) \end{cases}. \tag{3.48}$$

In our case, $B = \left(\overline{P} + \tilde{P}\right)$, so for $g \in L^2(D(0,\varepsilon))$, we are able to define $\left(\overline{P} + \tilde{P}\right)^{-1} g \in H^1(D(0,\varepsilon))$ to be the solution to Eq. (3.47). We will also

define $\overline{P}^{-1}$ as follows: Let $g \in L^2(D(0,\varepsilon))$. Then, define $v := \overline{P}^{-1}g$ to be the solution to the boundary value problem:

$$\begin{cases} \overline{P}v = g & \text{in } D(0,\varepsilon) \\ v = 0 & \text{on } \partial D(0,\varepsilon) \end{cases}. \tag{3.49}$$

Since $\sigma \in L^\infty$ and $\sigma > 0$, we *a priori* know that for $g \in L^2(D(0,\varepsilon))$ we have $v \in H^1(D(0,\varepsilon))$ [Eva10]. We will show further mapping properties of $\overline{P}^{-1}$ below. We now state bounds on the operator norms of $\tilde{P}$ and $\overline{P}^{-1}$:

Proposition 3.10. *For $\tilde{P}$ and $\overline{P}^{-1}$ as defined above we have the following bounds:*

$$\|\overline{P}^{-1}\|_{L^2(D(0,\varepsilon))\to\dot{H}^2_1(D(0,\varepsilon))} \leq C\varepsilon \tag{3.50}$$

$$\|\tilde{P}\|_{\dot{H}^2_1(D(0,\varepsilon))\to L^2(D(0,\varepsilon))} \leq c \tag{3.51}$$

for some $c, C > 0$.

We will prove these two bounds in Propositions 3.12 and 3.13, respectively. For a bounded linear operator T on a Banach space X, the Neumann series $\sum_{j=1}^{\infty} T^j$ will converge in the operator norm if the operator norm $\|T\| < 1$. In Lemma 3.14 we will show that $\|\overline{P}^{-1}\tilde{P}\|_{\dot{H}^2_1(D(0,\varepsilon))\to\dot{H}^2_1(D(0,\varepsilon))} < 1$.

3.2.2.1 $\overline{P}^{-1}$ *is a map from* $L^2(\mathbb{D})$ *to* $\dot{H}^2_1(\mathbb{D})$

Denote the unit disk centred at the origin by $\mathbb{D}$. We will show that $\overline{P}^{-1}$ is a bounded map from $L^2(\mathbb{D})$ to $\dot{H}^2_1(\mathbb{D})$.

Proposition 3.11. *Consider the following problem,*

$$\begin{cases} \overline{P}v = g & \text{in } \mathbb{D} \\ v = 0 & \text{on } \partial\mathbb{D} \end{cases} \tag{3.52}$$

in which $g \in L^2(\mathbb{D})$. Define $v := \overline{P}^{-1}g$. Then $\overline{P}^{-1}$ is a bounded map from $L^2(\mathbb{D})$ to $\dot{H}^2_1(\mathbb{D})$, i.e., there exists a constant $C > 0$ such that

$$\|v\|_{\dot{H}^2_1(\mathbb{D})} \leq C\|g\|_{L^2(\mathbb{D})}. \tag{3.53}$$

Proof. Since $\sigma \in L^\infty$, from general PDE theory we obtain that there exists a unique weak solution $v \in H^1(\mathbb{D})$ [Eva10]. We now want to establish the higher regularity that $v \in \dot{H}^2_1(\mathbb{D})$ for $g \in L^2(\mathbb{D})$. To derive $\dot{H}^2_1$-regularity we use a mollifier approach.

Since v is a weak solution of the PDE Eq. (3.52), we have for all $w \in H^1(\mathbb{D})$,

$$\int_{\mathbb{D}} \left[\partial_\rho v \partial_\rho w + \rho^{-2}\sigma(\varphi)\partial_\varphi v \partial_\varphi w\right] \ \rho d\rho d\varphi = -\int_{\mathbb{D}} gw \ dA. \tag{3.54}$$

We write the resulting expression as

$$A = B, \tag{3.55}$$

in which

$$A := \int_{\mathbb{D}} \left[\partial_\rho v \partial_\rho w + \rho^{-2}\sigma(\varphi)\partial_\varphi v \partial_\varphi w\right] \ \rho d\rho d\varphi \tag{3.56}$$

and

$$B := -\int_{\mathbb{D}} gw \ dA. \tag{3.57}$$

We can further write $A = A_1 + A_2$ for

$$A_1 = \int_{\mathbb{D}} \left[\partial_\rho v \partial_\rho w\right] \ \rho d\rho d\varphi \tag{3.58}$$

and

$$A_2 = \int_{\mathbb{D}} \left[\rho^{-2}\sigma(\varphi)\partial_\varphi v \partial_\varphi w\right] \ \rho d\rho d\varphi. \tag{3.59}$$

Let $\Psi(\varphi)$ be a symmetric mollifier in the angular coordinate φ defined by

$$\Psi(\varphi) = \begin{cases} e^{-1/(1-|\varphi|^2)}/K & \text{if } |\varphi| < 1 \\ 0 & \text{if } |\varphi| \geq 1 \end{cases}, \tag{3.60}$$

where the numerical constant K ensures the normalization $\int_{-\pi}^{\pi} |\Psi(\varphi)| \, d\varphi = 1$. Define $\Psi_\varepsilon(\varphi) := \varepsilon^{-1}\Psi(\frac{\varphi}{\varepsilon})$. Using the definition of convolution, Fubini's Theorem, and a change of variables we get the identity

$$\int_0^{2\pi} f(\varphi)(g * \Psi_\varepsilon)(\varphi) \ d\varphi = \int_0^{2\pi} f(\varphi) \int_0^{2\pi} g(\tilde{\varphi})\Psi_\varepsilon(\varphi - \tilde{\varphi}) \ d\tilde{\varphi} d\varphi \tag{3.61}$$

$$= \int_0^{2\pi} g(\tilde{\varphi}) \int_0^{2\pi} f(\varphi)\Psi_\varepsilon(\varphi - \tilde{\varphi}) \ d\varphi d\tilde{\varphi} \tag{3.62}$$

$$= -\int_0^{2\pi} g(\varphi)(f * \Psi_\varepsilon)(\varphi) \ d\varphi. \tag{3.63}$$

Introduce the notation $*_\varphi$ to denote the convolution taken in the φ variable, *i.e.*,

$$v(r, \varphi) *_\varphi f(\varphi) := \int_0^{2\pi} v(r, \tilde{\varphi}) f(\varphi - \tilde{\varphi}) \ d\tilde{\varphi}. \tag{3.64}$$

Using the definition and commutativity of convolution, we can show that

$$\partial_\varphi[v *_\varphi \Psi_\varepsilon] = \partial_\varphi[\Psi_\varepsilon *_\varphi v] \tag{3.65}$$
$$= \partial_\varphi \int_0^{2\pi} \Psi_\varepsilon(\tilde{\varphi}) v(r, \varphi - \tilde{\varphi})\, d\tilde{\varphi} \tag{3.66}$$
$$= \int_0^{2\pi} \Psi_\varepsilon(\tilde{\varphi}) \partial_\varphi v(r, \varphi - \tilde{\varphi})\, d\tilde{\varphi} \tag{3.67}$$
$$= \Psi_\varepsilon *_\varphi [\partial_\varphi v] \tag{3.68}$$
$$= [\partial_\varphi v] *_\varphi \Psi_\varepsilon. \tag{3.69}$$

We will choose the test function

$$w(\rho, \varphi) = \{[\partial_\varphi(\sigma(\varphi) \cdot \partial_\varphi v)] *_\varphi \Psi_\varepsilon\} *_\varphi \Psi_\varepsilon \tag{3.70}$$

in Eq. (3.54). We first verify that this function lies in $H^1(\mathbb{D})$, and then derive our $\dot{H}^2_1(\mathbb{D})$ estimates using it. To derive that this function is a valid test function, it suffices to show that $\rho^{-1}\partial_\varphi w$ and $\partial_\rho w$ lie in $L^2(\mathbb{D})$. By the properties of convolutions noted above, we observe that:

$$\rho^{-1}\partial_\varphi w = (\partial_\varphi \Psi_\varepsilon) *_\varphi (\partial_\varphi \Psi_\varepsilon) *_\varphi (\sigma(\varphi) \cdot \rho^{-1}\partial_\varphi v)). \tag{3.71}$$

Now, recall that since $v \in H^1(\mathbb{D})$, $(\sigma(\varphi) \cdot \rho^{-1}\partial_\varphi v)) \in L^2(\mathbb{D})$. Now note that by construction $(\partial_\varphi \Psi_\varepsilon)$ is a bounded function of φ only, (bounded by some constant $B_\varepsilon < \infty$) thus we obtain on each fixed radius $\rho \in (0, 1)$:

$$\int_0^{2\pi} |\rho^{-1}\partial_\varphi w|^2(\rho, \varphi) d\varphi \leq B_\varepsilon^2 \cdot \max(\sigma(\varphi)) \cdot \int_0^{2\pi} (\rho^{-1}\partial_\varphi v(\rho, \varphi))^2 d\varphi. \tag{3.72}$$

Integrating the above in ρ with respect to $\rho d\rho$ over $\rho \in (0, 1)$ yields that $\rho^{-1}\partial_\varphi w$ lies in $L^2(\mathbb{D})$. To show that $\partial_\rho w \in L^2(\mathbb{D})$ we write:

$$\partial_\rho w = \{[\partial_\varphi(\sigma(\varphi) \cdot \partial_\varphi \partial_\rho v)] *_\varphi \Psi_\varepsilon\} *_\varphi \Psi_\varepsilon \tag{3.73}$$
$$= (\partial_\varphi \Psi_\varepsilon) *_\varphi \{\Psi_\varepsilon *_\varphi (\sigma(\varphi) \cdot \partial_\varphi \partial_\rho v)\}. \tag{3.74}$$

To show this lies in $L^2(\mathbb{D})$ it suffices to show that $\{\sigma(\varphi) \cdot \partial_\varphi \Psi_\varepsilon\} *_\varphi (\partial_\rho v)$ lies in $L^2(\mathbb{D})$. This again follows by noting that $\{\sigma(\varphi) \cdot \partial_\varphi \Psi_\varepsilon\}$ is everywhere bounded, and $(\partial_\rho v) \in L^2(\mathbb{D})$. Thus repeating the Fubini-type argument from above confirms that $w \in L^2(\mathbb{D})$.

Using the above properties of convolutions,

$$A_1 = \int_{\mathbb{D}} \partial_\rho v \partial_\rho w \; \rho d\rho d\varphi \tag{3.75}$$

$$= \int_{\varphi=0}^{2\pi} \int_{\rho=0}^{1} \partial_\rho v \{[\partial_\varphi(\sigma(\varphi) \cdot \partial_\varphi \partial_\rho v)] *_\varphi \Psi_\varepsilon\} *_\varphi \Psi_\varepsilon \; \rho d\rho d\varphi \tag{3.76}$$

$$= -\int_{\rho=0}^{1} \int_{\varphi=0}^{2\pi} (\partial_\rho v *_\varphi \Psi_\varepsilon)([\partial_\varphi(\sigma(\varphi) \cdot \partial_\varphi \partial_\rho v)] *_\varphi \Psi_\varepsilon) \; d\varphi\rho d\rho \tag{3.77}$$

$$= \int_{\rho=0}^{1} \int_{\varphi=0}^{2\pi} (\partial_\varphi \partial_\rho v *_\varphi \Psi_\varepsilon)(\partial_\rho(\sigma(\varphi)\partial_\varphi v *_\varphi \Psi_\varepsilon)) \; d\varphi\rho d\rho \tag{3.78}$$

$$= \int_{\rho=0}^{1} \int_{\varphi=0}^{2\pi} \sigma(\varphi)[\partial_\rho(\partial_\varphi v *_\varphi \Psi_\varepsilon)]^2 \; d\varphi\rho d\rho \tag{3.79}$$

$$= \int_{\mathbb{D}} \sigma(\varphi)[\partial_\rho(\partial_\varphi v *_\varphi \Psi_\varepsilon)]^2 \; d\varphi\rho d\rho \tag{3.80}$$

is finite. Similarly,

$$A_2 = \int_{\mathbb{D}} \left[\rho^{-2}\sigma(\varphi)\partial_\varphi v \partial_\varphi w\right] \; \rho d\rho d\varphi \tag{3.81}$$

$$= \int_{\varphi=0}^{2\pi} \int_{\rho=0}^{1} \left[\rho^{-2}\sigma(\varphi)\partial_\varphi v\right] \partial_\varphi \left(\{[\partial_\varphi(\sigma(\varphi) \cdot \partial_\varphi v)] *_\varphi \Psi_\varepsilon\} *_\varphi \Psi_\varepsilon\right) \; \rho d\rho d\varphi \tag{3.82}$$

$$= -\int_{\varphi=0}^{2\pi} \int_{\rho=0}^{1} \partial_\varphi \left[\rho^{-2}\sigma(\varphi)\partial_\varphi v\right] \left(\{[\partial_\varphi(\sigma(\varphi) \cdot \partial_\varphi v)] *_\varphi \Psi_\varepsilon\} *_\varphi \Psi_\varepsilon\right) \; \rho d\rho d\varphi \tag{3.83}$$

$$= \int_{\varphi=0}^{2\pi} \int_{\rho=0}^{1} \rho^{-2} \left(\{[\partial_\varphi(\sigma(\varphi) \cdot \partial_\varphi v)] *_\varphi \Psi_\varepsilon\}\right) \left(\{[\partial_\varphi(\sigma(\varphi) \cdot \partial_\varphi v)] *_\varphi \Psi_\varepsilon\}\right) \; \rho d\rho d\varphi \tag{3.84}$$

$$= \int_{\mathbb{D}} \left|\frac{1}{\rho}[\partial_\varphi(\sigma(\varphi) \cdot \partial_\varphi v)] *_\varphi \Psi_\varepsilon\right|^2 \; d\varphi\rho d\rho \tag{3.85}$$

is finite. Using the Cauchy–Schwarz inequality we get the bound for all $\eta > 0$,

$$|B| \leq \frac{\eta}{2} \int_{\mathbb{D}} |w|^2 \; dA + \frac{1}{2\eta} \int_{\mathbb{D}} |g|^2 \; dA. \tag{3.86}$$

Since we chose $w = \{[\partial_\varphi(\sigma(\varphi) \cdot \partial_\varphi v)] *_\varphi \Psi_\varepsilon\} *_\varphi \Psi_\varepsilon$, we get the bound

$$|B| \leq \frac{\eta}{2} \int_{\mathbb{D}} |\{[\partial_\varphi(\sigma(\varphi) \cdot \partial_\varphi v)] *_\varphi \Psi_\varepsilon\} *_\varphi \Psi_\varepsilon|^2 \; dA + \frac{1}{2\eta} \int_{\mathbb{D}} |g|^2 \; dA. \tag{3.87}$$

Since $\|\Psi\|_{L^1(\mathbb{S}^1)} \leq 1$, we have that $\|\widehat{\Psi}\|_{L^\infty(\mathbb{S}^1)} \leq 1$. Using the Plancherel Theorem on $\mathbb{S}^1$, we show that our convolution decreases the L^2-norm:

$$\begin{aligned}
\|f *_\varphi \Psi\|^2_{L^2(\mathbb{D})} &= \int_{\rho=0}^{1}\int_{\varphi=0}^{2\pi} |f *_\varphi \Psi|^2 \, d\varphi\rho d\rho && (3.88)\\
&= \int_{\rho=0}^{1}\int_{\varphi=0}^{2\pi} |\widehat{f *_\varphi \Psi}|^2 \, d\varphi\rho d\rho && (3.89)\\
&= \int_{\rho=0}^{1}\int_{\varphi=0}^{2\pi} |\widehat{f} \cdot \widehat{\Psi}|^2 \, d\varphi\rho d\rho && (3.90)\\
&\leq \int_{\rho=0}^{1}\int_{\varphi=0}^{2\pi} |\widehat{f} \cdot \|\widehat{\Psi}\|_{L^\infty(\mathbb{S}^1)}|^2 \, d\varphi\rho d\rho && (3.91)\\
&\leq \int_{\rho=0}^{1}\int_{\varphi=0}^{2\pi} |\widehat{f}|^2 \, d\varphi\rho d\rho && (3.92)\\
&= \int_{\rho=0}^{1}\int_{\varphi=0}^{2\pi} |f|^2 \, d\varphi\rho d\rho && (3.93)\\
&= \|f\|^2_{L^2(\mathbb{D})}. && (3.94)
\end{aligned}$$

Since our convolution decreases the L^2-norm and $r \leq 1$ in $\mathbb{D}$,

$$\int_{\mathbb{D}} |\{[\partial_\varphi(\sigma(\varphi)\cdot\partial_\varphi v)] *_\varphi \Psi_\varepsilon\} *_\varphi \Psi_\varepsilon|^2 \, dA \leq \int_{\mathbb{D}} |[\partial_\varphi(\sigma(\varphi)\cdot\partial_\varphi v)] *_\varphi \Psi_\varepsilon|^2 \, dA \tag{3.95}$$

$$\leq \int_{\mathbb{D}} \left|\frac{1}{\rho}[\partial_\varphi(\sigma(\varphi)\cdot\partial_\varphi v)] *_\varphi \Psi_\varepsilon\right|^2 dA. \tag{3.96}$$

By Eqs. (3.87) and (3.96) we have the bound

$$|B| \leq \frac{\eta}{2}\int_{\mathbb{D}} \left|\frac{1}{\rho}[\partial_\varphi(\sigma(\varphi)\cdot\partial_\varphi v)] *_\varphi \Psi_\varepsilon\right|^2 dA + \frac{1}{2\eta}\int_{\mathbb{D}} |g|^2 \, dA \tag{3.97}$$

and thus we obtain a bound:

$$\begin{aligned}
&\int_{\mathbb{D}} \sigma(\varphi)[\partial_\rho(\partial_\varphi v *_\varphi \Psi_\varepsilon)]^2 \, d\varphi\rho d\rho \\
&\quad + \int_{\mathbb{D}} \left|\frac{1}{\rho}[\partial_\varphi(\sigma(\varphi)\cdot\partial_\varphi v)] *_\varphi \Psi_\varepsilon\right|^2 d\varphi\rho d\rho \\
\leq &\frac{\eta}{2}\int_{\mathbb{D}} \left|\frac{1}{\rho}[\partial_\varphi(\sigma(\varphi)\cdot\partial_\varphi v)] *_\varphi \Psi_\varepsilon\right|^2 dA + \frac{1}{2\eta}\int_{\mathbb{D}} |g|^2 \, dA. && (3.98)
\end{aligned}$$

Since $\int_{\mathbb{D}} \sigma(\varphi)[\partial_\rho(\partial_\varphi v *_\varphi \Psi_\varepsilon)]^2 \, d\varphi\rho d\rho \geq 0$, rearranging gives

$$\left(1 - \frac{\eta}{2}\right)\int_{\mathbb{D}} \left|\frac{1}{\rho}[\partial_\varphi(\sigma(\varphi)\cdot\partial_\varphi v)] *_\varphi \Psi_\varepsilon\right|^2 dA \leq \frac{1}{2\eta}\int_{\mathbb{D}} |g|^2 \, dA. \tag{3.99}$$

Taking $\eta = 1$ gives that $\frac{1}{\rho}[\partial_\varphi(\sigma(\varphi)\cdot\partial_\varphi v)] *_\varphi \Psi_\varepsilon$ is in $L^2(\mathbb{D})$ with the bound,

$$\left\|\frac{1}{\rho}[\partial_\varphi(\sigma(\varphi)\cdot\partial_\varphi v)] *_\varphi \Psi_\varepsilon\right\|_{L^2(\mathbb{D})} \leq \|g\|_{L^2(\mathbb{D})}. \tag{3.100}$$

Taking $\varepsilon \to 0$, we get the bound

$$\left\|\frac{1}{\rho}\partial_\varphi(\sigma(\varphi)\partial_\varphi v)\right\|_{L^2(\mathbb{D})} \leq \|g\|_{L^2(\mathbb{D})}. \tag{3.101}$$

From Eq. (3.98) we obtain the inequality

$$\begin{aligned}&\int_{\mathbb{D}} |\sigma(\varphi)\partial_\rho\partial_\varphi(v *_\varphi \Psi_\varepsilon)|^2\, dA + \int_{\mathbb{D}} \left|\frac{1}{\rho}[\partial_\varphi(\sigma(\varphi)\cdot\partial_\varphi v)] *_\varphi \Psi_\varepsilon\right|^2 dA \\ \leq &\frac{\eta}{2}\int_{\mathbb{D}} \left|\frac{1}{\rho}[\partial_\varphi(\sigma(\varphi)\cdot\partial_\varphi v)] *_\varphi \Psi_\varepsilon\right|^2 dA + \frac{1}{2\eta}\int_{\mathbb{D}} |g|^2\, dA.\end{aligned} \tag{3.102}$$

Taking $\eta = 2$ yields

$$\int_{\mathbb{D}} |\sigma(\varphi)\partial_\rho\partial_\varphi(v *_\varphi \Psi_\varepsilon)|^2\, dA \leq \frac{1}{4}\int_{\mathbb{D}} |g|^2\, dA. \tag{3.103}$$

Hence, $\sigma(\varphi)\partial_\rho\partial_\varphi(v *_\varphi \Psi_\varepsilon)$ is in $L^2(\mathbb{D})$ with the bound

$$\left\|\sigma(\varphi)\partial_\rho\partial_\varphi(v *_\varphi \Psi_\varepsilon)\right\|_{L^2(\mathbb{D})} \leq \frac{1}{2}\|g\|_{L^2(\mathbb{D})}. \tag{3.104}$$

Furthermore,

$$\left\|\partial_\rho\partial_\varphi(v *_\varphi \Psi_\varepsilon)\right\|_{L^2(\mathbb{D})} \leq \frac{1}{2\min_{\mathbb{D}}(\sigma)}\|g\|_{L^2(\mathbb{D})}. \tag{3.105}$$

By Eq. (3.69),

$$\left\|\partial_\rho\partial_\varphi(v *_\varphi \Psi_\varepsilon)\right\|_{L^2(\mathbb{D})} = \left\|(\partial_\rho\partial_\varphi v) *_\varphi \Psi_\varepsilon\right\|_{L^2(\mathbb{D})} \tag{3.106}$$

so

$$\left\|(\partial_\rho\partial_\varphi v) *_\varphi \Psi_\varepsilon\right\|_{L^2(\mathbb{D})} \leq \frac{1}{2\min_{\mathbb{D}}(\sigma)}\|g\|_{L^2(\mathbb{D})}. \tag{3.107}$$

Taking $\varepsilon \to 0$, we get

$$\left\|\partial_\rho\partial_\varphi v\right\|_{L^2(\mathbb{D})} \leq \frac{1}{2\min_{\mathbb{D}}(\sigma)}\|g\|_{L^2(\mathbb{D})}. \tag{3.108}$$

Hence, we have the bound

$$\left\|\sigma(\varphi)\partial_\rho\partial_\varphi v\right\|_{L^2(\mathbb{D})} \leq \max_{\mathbb{D}}(\sigma)\left\|\partial_\rho\partial_\varphi v\right\|_{L^2(\mathbb{D})} \tag{3.109}$$

$$\leq \frac{\max_{\mathbb{D}}(\sigma)}{2\min_{\mathbb{D}}(\sigma)}\|g\|_{L^2(\mathbb{D})}. \tag{3.110}$$

We can bound $\sigma(\varphi)\rho\partial_\rho\partial_\rho v$ in $L^2(\mathbb{D})$ by using the partial differential equation Eq. (3.52), the triangle inequality, and Eq. (3.101):

$$\left\|\sigma(\varphi)\rho\partial_\rho\partial_\rho v\right\|_{L^2(\mathbb{D})} = \left\|\rho g - \sigma(\varphi)\partial_\rho v - \frac{1}{\rho}\partial_\varphi(\sigma(\varphi)\partial_\varphi v)\right\|_{L^2(\mathbb{D})} \tag{3.111}$$

$$= \left\|\rho g\right\|_{L^2(\mathbb{D})} + \left\|\sigma(\varphi)\partial_\rho v\right\|_{L^2(\mathbb{D})} + \left\|\frac{1}{\rho}\partial_\varphi(\sigma(\varphi)\partial_\varphi v)\right\|_{L^2(\mathbb{D})} \tag{3.112}$$

$$\leq \left\|g\right\|_{L^2(\mathbb{D})} + \left\|g\right\|_{L^2(\mathbb{D})} + \left\|g\right\|_{L^2(\mathbb{D})} \tag{3.113}$$

$$\leq 3\left\|g\right\|_{L^2(\mathbb{D})}. \tag{3.114}$$

Since $v \in H^1(\mathbb{D})$ with the bound $\|v\|_{H^1(\mathbb{D})} \leq \|g\|_{L^2(\mathbb{D})}$ from standard PDE theory [Eva10], we can bound v in $\dot{H}^2_1(\mathbb{D})$ using Eqs. (3.101), (3.110), and (3.114):

$$\|v\|_{\dot{H}^2_1(\mathbb{D})} \leq \|v\|_{H^1(\mathbb{D})} + \|\sigma(\varphi)\rho\partial_\rho\partial_\rho v\|_{L^2(\mathbb{D})} \tag{3.115}$$

$$+ \|\sigma(\varphi)\partial_\rho\partial_\varphi v\|_{L^2(\mathbb{D})} + \|\rho^{-1}\partial_\varphi(\sigma(\varphi)\partial_\varphi v)\|_{L^2(\mathbb{D})}$$

$$\leq \|g\|_{L^2(\mathbb{D})} + 3\|g\|_{L^2(\mathbb{D})} + \frac{\max_{\mathbb{D}}(\sigma)}{2\min_{\mathbb{D}}(\sigma)}\|g\|_{L^2(\mathbb{D})} + \|g\|_{L^2(\mathbb{D})} \tag{3.116}$$

$$= C\|g\|_{L^2(\mathbb{D})} \tag{3.117}$$

in which $C = 5 + \frac{\max_{\mathbb{D}}(\sigma)}{2\min_{\mathbb{D}}(\sigma)}$. Hence $\overline{P}^{-1}$ is a bounded map from $L^2(\mathbb{D})$ to $\dot{H}^2_1(\mathbb{D})$.

□

Recall the space $\dot{H}^2_1(D(0,\varepsilon))$ defined in Eq. (3.8) and the solution $\overline{u}$ to the angularly matched Laplace equations Eq. (3.42):

$$\begin{cases} \overline{P}\overline{u} = 0 & \text{in } D(0,\varepsilon) \\ \overline{u} = f & \text{on } \partial D(0,\varepsilon) \end{cases}$$

We define a C^∞-smooth radially symmetric cutoff function $\chi(r)$ which is identically 1 at $\rho = \varepsilon$ and equals 0 for $\rho < \frac{\varepsilon}{2}$. Then we define the extension

$u^{\#}(\rho,\varphi) := f(\varphi)\chi(\rho)$. The extension $u^{\#}$ will be C^∞ in ρ. Then the function $v := \overline{u} - u^{\#}$ satisfies

$$\begin{cases} \overline{P}v = -\overline{P}u^{\#} & \text{in } D(0,\varepsilon) \\ v = 0 & \text{on } \partial D(0,\varepsilon) \end{cases}. \tag{3.118}$$

Since $u^{\#}$ satisfies the current continuity matching conditions across each interface, $\tilde{\sigma}(\varphi)\partial_\varphi u^{\#}$ is Lipschitz in φ in $D(0,\varepsilon)$. Invoking the piecewise C^1 property of $\tilde{\sigma}\partial_\varphi u^{\#}$ we have derived in Chapter 2, we derive $\partial_\varphi(\tilde{\sigma}(\varphi)\partial_\varphi u^{\#})$ is a bounded function in $D(0,\varepsilon)$. Thus, $\overline{P}u^{\#}$ is in L^2 in $D(0,\varepsilon)$. In Proposition 3.12 we will show that $\overline{P}^{-1} : L^2(D(0,\varepsilon)) \to \dot{H}^2_1(D(0,\varepsilon))$, so $v \in \dot{H}^2_1(D(0,\varepsilon))$.

Because of the current continuity matching conditions across each interface and that $u^{\#}$ is C^∞ in ρ, all first derivatives and all second derivatives with a weight ρ (except $\partial_{\varphi\varphi}$) of $u^{\#}$ are bounded and hence will be in $L^2(D(0,\varepsilon))$, *i.e.*, $\partial_\rho u^{\#}, \tilde{\sigma}\partial_\varphi u^{\#}, \rho\partial_\varphi\left(\partial_\rho u^{\#}\right), \rho\partial_\rho\left(\partial_\rho u^{\#}\right) \in L^2(D(0,\varepsilon))$. Additionally, since $u^{\#}$ satisfies the Laplacian in each sector, $\partial_{\rho\rho}u^{\#} + \frac{1}{\rho}\partial_\rho u^{\#} + \frac{1}{\rho^2}\partial_{\varphi\varphi}u^{\#} = 0$. Rearranging and multiplying by ρ yields $\rho^{-1}\partial_{\varphi\varphi}u^{\#} = -\rho\partial_{\rho\rho}u^{\#} - \partial_\rho u^{\#}$. Since both $\rho\partial_{\rho\rho}u^{\#}$ and $\partial_\rho u^{\#}$ are in $L^2(D(0,\varepsilon))$, we also get $\rho^{-1}\partial_{\varphi\varphi}u^{\#} \in L^2(D(0,\varepsilon))$. Hence, $u^{\#}$ is also in $\dot{H}^2_1(D(0,\varepsilon))$ as defined in Definition 3.4. Since both v and $u^{\#}$ are in $\dot{H}^2_1(D(0,\varepsilon))$ and $\overline{u} = v + u^{\#}$, we conclude that $\overline{u} \in \dot{H}^2_1(D(0,\varepsilon))$.

3.2.2.2 *Norm of $\overline{P}^{-1}$ as an operator from $L^2(D(0,\varepsilon))$ to $\dot{H}^2_1(D(0,\varepsilon))$*

We will show that $\overline{P}^{-1}$ as an operator from $L^2(D(0,\varepsilon))$ to $\dot{H}^2_1(D(0,\varepsilon))$ has norm proportional to the radius of the disk, ε.

Proposition 3.12. *Let $\varepsilon \in (0,1)$ and let $g \in L^2(D(0,\varepsilon))$. Consider the unique solution, $v := \overline{P}^{-1}g$, to the problem*

$$\begin{cases} \overline{P}v = g & \text{in } D(0,\varepsilon) \\ v = 0 & \text{on } \partial D(0,\varepsilon) \end{cases}. \tag{3.119}$$

Then $\overline{P}^{-1}$ as an operator from $L^2(D(0,\varepsilon))$ to $\dot{H}^2_1(D(0,\varepsilon))$ has norm proportional to the radius of the disk, ε, i.e.,

$$\|\overline{P}^{-1}\|_{L^2(D(0,\varepsilon))\to\dot{H}^2_1(D(0,\varepsilon))} \leq C\varepsilon, \tag{3.120}$$

in which C is a constant that may depend on the conductivities (σ_i's) and the angles (ω_i's) but not on ε.

Proof. Since v is a weak solution of the PDE Eq. (3.119), we have for all $w \in H^1(D(0,\varepsilon))$,

$$\sum_{i=1}^{N} \sigma_i \int_{\varphi=\omega_{i-1}}^{\omega_i} \int_{\rho=0}^{\varepsilon} \left[\partial_\rho v \partial_\rho w + \rho^{-2} \partial_\varphi v \partial_\varphi w\right] \ \rho d\rho d\varphi = -\int_{D(0,\varepsilon)} gw \ dA. \tag{3.121}$$

Define a new function V over the unit disk via the formula $V(\tilde{\rho}, \varphi) = v(\varepsilon\tilde{\rho}, \varphi)$. For all $w \in H^1(D(0,\varepsilon))$, define a new H^1 function on the unit disk via $W(\tilde{\rho}, \varphi) = w(\varepsilon\tilde{\rho}, \varphi)$. Now, via Eq. (3.121) and a change of variables, $\rho = \varepsilon\tilde{\rho}$,

$$\sum_{i=1}^{N} \sigma_i \int_{\varphi=\omega_{i-1}}^{\omega_i} \int_{\tilde{\rho}=0}^{1} \left[\partial_{\tilde{\rho}} V(\tilde{\rho}, \varphi) \partial_{\tilde{\rho}} W(\tilde{\rho}, \varphi) + \tilde{\rho}^{-2} \partial_\varphi V(\tilde{\rho}, \varphi) \partial_\varphi W(\tilde{\rho}, \varphi)\right] \ \tilde{\rho} d\tilde{\rho} d\varphi \tag{3.122}$$

$$= \sum_{i=1}^{N} \sigma_i \int_{\varphi=\omega_{i-1}}^{\omega_i} \int_{\tilde{\rho}=0}^{1} \left[\partial_{\tilde{\rho}} v(\varepsilon\tilde{\rho}, \varphi) \partial_{\tilde{\rho}} w(\varepsilon\tilde{\rho}, \varphi) + \tilde{\rho}^{-2} \partial_\varphi v(\varepsilon\tilde{\rho}, \varphi) \partial_\varphi w(\varepsilon\tilde{\rho}, \varphi)\right] \ \tilde{\rho} d\tilde{\rho} d\varphi \tag{3.123}$$

$$= \sum_{i=1}^{N} \sigma_i \int_{\varphi=\omega_{i-1}}^{\omega_i} \int_{\rho=0}^{\varepsilon} \left[\varepsilon \partial_\rho v(\rho, \varphi) \varepsilon \partial_\rho w(\rho, \varphi) + \varepsilon^2 \rho^{-2} \partial_\varphi v(\rho, \varphi) \partial_\varphi w(\rho, \varphi)\right] \ \frac{1}{\varepsilon}\rho \ \frac{1}{\varepsilon} d\rho d\varphi \tag{3.124}$$

$$= -\int_{D(0,\varepsilon)} g(\rho, \varphi) w(\rho, \varphi) \rho \ d\rho d\varphi \tag{3.125}$$

$$= -\int_{D(0,\varepsilon)} g(\varepsilon\tilde{\rho}, \varphi) w(\varepsilon\tilde{\rho}, \varphi) \varepsilon\tilde{\rho} \ \varepsilon d\tilde{\rho} d\varphi \tag{3.126}$$

$$= -\int_{\mathbb{D}} \varepsilon^2 g(\varepsilon\tilde{\rho}, \varphi) W(\tilde{\rho}, \varphi) \ dA. \tag{3.127}$$

Hence V is a weak solution to the problem

$$\begin{cases} \overline{P} V = G & \text{in } \mathbb{D} \\ V = 0 & \text{on } \partial\mathbb{D} \end{cases}, \tag{3.128}$$

in which $G(\tilde{\rho}, \varphi) = \varepsilon^2 g(\varepsilon\tilde{\rho}, \varphi)$. From Proposition 3.11, there exists some $C > 0$ such that

$$\|V\|_{\dot{H}^2_1(\mathbb{D})} \leq C \|G\|_{L^2(\mathbb{D})}. \tag{3.129}$$

We consider the change of variables, $\rho = \varepsilon\tilde{\rho}$, represented by the dilation map $(\rho, \varphi) \xrightarrow{M} (\frac{\rho}{\varepsilon}, \varphi)$. The Euclidean metric changes by

$$M_* g_{D(0,\varepsilon)} = \varepsilon^2 g_{\mathbb{D}} \tag{3.130}$$
$$M_* v = V \tag{3.131}$$
$$M_* g = \tilde{G}. \tag{3.132}$$

So,

$$\Delta_{g_{D(0,\varepsilon)}} v = \varepsilon^{-2} \Delta_{g_{\mathbb{D}}} V \tag{3.133}$$

and hence,

$$\Delta_{g_{\mathbb{D}}} V = \varepsilon^2 \tilde{G} = G. \tag{3.134}$$

From Eq. (3.131), we get

$$\|v\|_{\dot{H}^2_1(D(0,\varepsilon))} = \|V\|_{\dot{H}^2_1(\mathbb{D})}. \tag{3.135}$$

From Eqs. (3.132) and (3.134), we get

$$\|G\|_{L^2(\mathbb{D})} = \varepsilon \|g\|_{L^2(D(0,\varepsilon))}. \tag{3.136}$$

Hence, combining Eqs. (3.129), (3.135), and (3.136), we get the bound

$$\|v\|_{\dot{H}^2_1(D(0,\varepsilon))} = \|V\|_{\dot{H}^2_1(\mathbb{D})} \tag{3.137}$$
$$\leq C \|G\|_{L^2(\mathbb{D})} \tag{3.138}$$
$$= C\varepsilon \|g\|_{L^2(D(0,\varepsilon))}. \tag{3.139}$$

Thus, $\overline{P}^{-1}$ is an operator from $L^2(D(0,\varepsilon))$ to $\dot{H}^2_1(D(0,\varepsilon))$ with norm proportional to the radius of the disk, *i.e.*, there exists some $C > 0$ such that

$$\|\overline{P}^{-1}\|_{L^2(D(0,\varepsilon)) \to \dot{H}^2_1(D(0,\varepsilon))} \leq C\varepsilon. \tag{3.140}$$

□

3.2.2.3 *Regularity of the Operator $\tilde{P}$*

We will show that $\tilde{P}$ is a bounded map from $\dot{H}^2_1(D(0,\varepsilon))$ to $L^2(D(0,\varepsilon))$.

Proposition 3.13. *The operator $P(f) = \partial^i(\tilde{\sigma}(r,\theta)\partial_i f)$, after the change of coordinates transformation from $(r,\theta) \to (\rho,\varphi)$ defined by Eq. (3.32) is given by*

$$P = \overline{P} + \tilde{P},$$

in which $\overline{P}$ is the operator defined in Eq. (3.37) and $\tilde{P}$ is the correction term which can be expressed in polar coordinates as in Eqs. (3.38) and (3.39). Furthermore, on $D(0,\varepsilon)$, we have the bound

$$\|\tilde{P}f\|_{L^2(D(0,\varepsilon))} \leq c\|f\|_{\dot{H}^2_1(D(0,\varepsilon))} \tag{3.141}$$

for some $c > 0$ and hence $\tilde{P}$ is a bounded map from $\dot{H}^2_1(D(0,\varepsilon))$ to $L^2(D(0,\varepsilon))$.

Proof. We seek to write down the operator in the new coordinates.

The Jacobian determinant for the change of coordinates transformation Eq. (3.32) from $(r,\theta) \to (\rho,\varphi)$ is

$$J = \begin{vmatrix} \frac{\partial\rho}{\partial r} & \frac{\partial\rho}{\partial\theta} \\ \frac{\partial\varphi}{\partial r} & \frac{\partial\varphi}{\partial\theta} \end{vmatrix} \tag{3.142}$$

$$= \begin{vmatrix} \frac{\partial\rho}{\partial r} & r^2\theta_i'(r)\frac{\partial\rho}{\partial r} \\ -\chi(\theta)\theta_i'(r) & \chi'(\theta)[-\theta_i(r)+\omega_i]+1 \end{vmatrix} \tag{3.143}$$

$$= \left(\chi'(\theta)[-\theta_i(r)+\omega_i]+1\right)\frac{\partial\rho}{\partial r} + \chi(\theta)\theta_i'(r)\frac{\partial\rho}{\partial r} \tag{3.144}$$

for $\theta \in [M_{i-1}, M_i]$ in which $\chi(\theta)$ is a $\mathcal{C}^\infty$-smooth 2π-periodic function defined in Definition 3.8, $0 \leq \chi(\theta) \leq 1$ which equals 1 in open neighbourhoods around the values $\omega_i, i \in \{1,\dots,N\}$, and 0 in open neighbourhoods around the mid-point values $M_1 = \frac{1}{2}[\omega_1+\omega_2], \dots, M_N = \frac{1}{2}[\omega_N+\omega_1]$.

The operator P accounting for the conductivity in our original coordinates (r,θ) is

$$P(f) = \partial_r(\tilde{\sigma}\partial_r f) + \frac{\tilde{\sigma}}{r}\partial_r f + r^{-2}\partial_\theta(\tilde{\sigma}\partial_\theta f) \tag{3.145}$$

We compute the first derivatives of f. Since $\frac{\partial\varphi}{\partial r} = -\chi(\theta)\theta_i'(r)$,

$$\frac{\partial f}{\partial r} = \frac{\partial\rho}{\partial r}\frac{\partial f}{\partial\rho} + \frac{\partial\varphi}{\partial r}\frac{\partial f}{\partial\varphi} \tag{3.146}$$

$$= \frac{\partial\rho}{\partial r}\frac{\partial f}{\partial\rho} - \chi(\theta)\theta_i'(r)\frac{\partial f}{\partial\varphi}. \tag{3.147}$$

Since $\frac{\partial\rho}{\partial\theta} = r^2\theta_i'(r)\frac{\partial\rho}{\partial r}$ and $\frac{\partial\varphi}{\partial\theta} = \chi'(\theta)[-\theta_i(r)+\omega_i]+1$,

$$\frac{\partial f}{\partial\theta} = \frac{\partial\rho}{\partial\theta}\frac{\partial f}{\partial\rho} + \frac{\partial\varphi}{\partial\theta}\frac{\partial f}{\partial\varphi} \tag{3.148}$$

$$= r^2\theta_i'(r)\frac{\partial\rho}{\partial r}\frac{\partial f}{\partial\rho} + \left(\chi'(\theta)[-\theta_i(r)+\omega_i]+1\right)\frac{\partial f}{\partial\varphi}. \tag{3.149}$$

We can express ∂_ρ and ∂_φ in terms of ∂_r and ∂_θ,

$$\begin{cases} \frac{\partial f}{\partial \rho} &= \frac{(\chi'(\theta)[-\theta_i(r)+\omega_i]+1)}{\frac{\partial \rho}{\partial r}(\chi'(\theta)[-\theta_i(r)+\omega_i]+1)+\chi(\theta)\theta_i'(r)r^2\theta_i'(r)\frac{\partial \rho}{\partial r}}\frac{\partial f}{\partial r} \\ &\quad + \frac{\chi(\theta)\theta_i'(r)}{\frac{\partial \rho}{\partial r}(\chi'(\theta)[-\theta_i(r)+\omega_i]+1)+\chi(\theta)\theta_i'(r)r^2\theta_i'(r)\frac{\partial \rho}{\partial r}}\frac{\partial f}{\partial \theta} \\ \frac{\partial f}{\partial \varphi} &= \frac{-r^2\theta_i'(r)}{(\chi'(\theta)[-\theta_i(r)+\omega_i]+1)+\chi(\theta)\theta_i'(r)r^2\theta_i'(r)}\frac{\partial f}{\partial r}+ \\ &\quad \frac{1}{(\chi'(\theta)[-\theta_i(r)+\omega_i]+1)+\chi(\theta)\theta_i'(r)r^2\theta_i'(r)}\frac{\partial f}{\partial \theta} \end{cases}. \tag{3.150}$$

Next, we compute the second unmixed derivatives of f. We compute

$$\frac{\partial}{\partial r}\left(\tilde{\sigma}(r,\theta)\frac{\partial f}{\partial r}\right) = \frac{\partial}{\partial r}\left(\tilde{\sigma}(r,\theta)\left[\frac{\partial \rho}{\partial r}\frac{\partial f}{\partial \rho}-\chi(\theta)\theta_i'(r)\frac{\partial f}{\partial \varphi}\right]\right) \tag{3.151}$$

$$= \frac{\partial \rho}{\partial r}\frac{\partial}{\partial \rho}\left(\tilde{\sigma}(r,\theta)\left[\frac{\partial \rho}{\partial r}\frac{\partial f}{\partial \rho}-\chi(\theta)\theta_i'(r)\frac{\partial f}{\partial \varphi}\right]\right) \tag{3.152}$$

$$- \chi(\theta)\theta_i'(r)\frac{\partial}{\partial \varphi}\left(\tilde{\sigma}(r,\theta)\left[\frac{\partial \rho}{\partial r}\frac{\partial f}{\partial \rho}-\chi(\theta)\theta_i'(r)\frac{\partial f}{\partial \varphi}\right]\right)$$

$$= \tilde{\sigma}(\varphi)\frac{\partial \rho}{\partial r}\frac{\partial}{\partial \rho}\frac{\partial \rho}{\partial r}\frac{\partial f}{\partial \rho}-\frac{\partial \rho}{\partial r}\tilde{\sigma}(\varphi)\left(\frac{\partial}{\partial \rho}\chi(\theta)\right)\theta_i'(r)\frac{\partial f}{\partial \varphi} \tag{3.153}$$

$$- \frac{\partial \rho}{\partial r}\tilde{\sigma}(\varphi)\chi(\theta)\left(\frac{\partial}{\partial \rho}\theta_i'(r)\right)\frac{\partial f}{\partial \varphi}-\frac{\partial \rho}{\partial r}\chi(\theta)\theta_i'(r)\frac{\partial}{\partial \rho}\left(\tilde{\sigma}(\varphi)\frac{\partial f}{\partial \varphi}\right)$$

$$- \chi(\theta)\theta_i'(r)\left[\frac{\partial}{\partial \varphi}\left(\tilde{\sigma}(\varphi)\frac{\partial \rho}{\partial r}\frac{\partial f}{\partial \rho}\right)-\tilde{\sigma}(\varphi)\left(\frac{\partial}{\partial \varphi}\chi(\theta)\right)\theta_i'(r)\frac{\partial f}{\partial \varphi}\right.$$

$$- \tilde{\sigma}(\varphi)\chi(\theta)\left(\frac{\partial}{\partial \varphi}\theta_i'(r)\right)\frac{\partial f}{\partial \varphi}$$

$$\left.- \chi(\theta)\theta_i'(r)\frac{\partial}{\partial \varphi}\left(\tilde{\sigma}(\varphi)\frac{\partial f}{\partial \varphi}\right)\right].$$

Now, we compute the derivatives

$$\frac{\partial}{\partial \rho}\chi(\theta) = \frac{\chi(\theta)\theta_i'(r)\chi'(\theta)}{\frac{\partial \rho}{\partial r}(\chi'(\theta)[-\theta_i(r)+\omega_i]+1)+\chi(\theta)\theta_i'(r)r^2\theta_i'(r)\frac{\partial \rho}{\partial r}} \tag{3.154}$$

$$\frac{\partial}{\partial \rho}\theta_i'(r) = \frac{(\chi'(\theta)[-\theta_i(r)+\omega_i]+1)\,\theta_i''(r)}{\frac{\partial \rho}{\partial r}(\chi'(\theta)[-\theta_i(r)+\omega_i]+1)+\chi(\theta)\theta_i'(r)r^2\theta_i'(r)\frac{\partial \rho}{\partial r}} \tag{3.155}$$

$$\frac{\partial}{\partial \varphi}\chi(\theta) = \frac{\chi'(\theta)}{(\chi'(\theta)[-\theta_i(r)+\omega_i]+1)+\chi(\theta)\theta_i'(r)r^2\theta_i'(r)} \tag{3.156}$$

$$\frac{\partial}{\partial \varphi}\theta_i'(r) = \frac{-r^2\theta_i'(r)\theta_i''(r)}{(\chi'(\theta)[-\theta_i(r)+\omega_i]+1)+\chi(\theta)\theta_i'(r)r^2\theta_i'(r)}. \tag{3.157}$$

Thus,

$$
\begin{aligned}
&\frac{\partial}{\partial r}\left(\tilde{\sigma}(r,\theta)\frac{\partial f}{\partial r}\right)\\
&=\tilde{\sigma}(\varphi)\frac{\partial \rho}{\partial r}\frac{\partial}{\partial \rho}\left(\frac{\partial \rho}{\partial r}\frac{\partial f}{\partial \rho}\right) \qquad (3.158)\\
&\quad-\frac{\partial \rho}{\partial r}\tilde{\sigma}(\varphi)\left(\frac{\chi(\theta)\theta_i'(r)\chi'(\theta)}{\frac{\partial \rho}{\partial r}(\chi'(\theta)[-\theta_i(r)+\omega_i]+1)+\chi(\theta)\theta_i'(r)r^2\theta_i'(r)\frac{\partial \rho}{\partial r}}\right)\theta_i'(r)\frac{\partial f}{\partial \varphi}\\
&\quad-\frac{\partial \rho}{\partial r}\tilde{\sigma}(\varphi)\chi(\theta)\left(\frac{(\chi'(\theta)[-\theta_i(r)+\omega_i]+1)\,\theta_i''(r)}{\frac{\partial \rho}{\partial r}(\chi'(\theta)[-\theta_i(r)+\omega_i]+1)+\chi(\theta)\theta_i'(r)r^2\theta_i'(r)\frac{\partial \rho}{\partial r}}\right)\frac{\partial f}{\partial \varphi}\\
&\quad-\frac{\partial \rho}{\partial r}\chi(\theta)\theta_i'(r)\frac{\partial}{\partial \rho}\left(\tilde{\sigma}(\varphi)\frac{\partial f}{\partial \varphi}\right)\\
&\quad-\chi(\theta)\theta_i'(r)\left[\frac{\partial}{\partial \varphi}\left(\tilde{\sigma}(\varphi)\frac{\partial \rho}{\partial r}\frac{\partial f}{\partial \rho}\right)\right.\\
&\qquad\qquad-\tilde{\sigma}(\varphi)\left(\frac{\chi'(\theta)}{(\chi'(\theta)[-\theta_i(r)+\omega_i]+1)+\chi(\theta)\theta_i'(r)r^2\theta_i'(r)}\right)\theta_i'(r)\frac{\partial f}{\partial \varphi}\\
&\qquad\qquad-\tilde{\sigma}(\varphi)\chi(\theta)\left(\frac{-r^2\theta_i'(r)\theta_i''(r)}{(\chi'(\theta)[-\theta_i(r)+\omega_i]+1)+\chi(\theta)\theta_i'(r)r^2\theta_i'(r)}\right)\frac{\partial f}{\partial \varphi}\\
&\qquad\qquad\left.-\chi(\theta)\theta_i'(r)\frac{\partial}{\partial \varphi}\left(\tilde{\sigma}(\varphi)\frac{\partial f}{\partial \varphi}\right)\right].
\end{aligned}
$$

And we compute

$$\frac{\partial}{\partial\theta}\left(\tilde{\sigma}(r,\theta)\frac{\partial f}{\partial\theta}\right)$$

$$= \frac{\partial}{\partial\theta}\left(\tilde{\sigma}(r,\theta)r^2\theta_i'(r)\frac{\partial\rho}{\partial r}\frac{\partial f}{\partial\rho} + \tilde{\sigma}(r,\theta)\left(\chi'(\theta)[-\theta_i(r)+\omega_i]+1\right)\frac{\partial f}{\partial\varphi}\right) \tag{3.159}$$

$$= r^2\theta_i'(r)\frac{\partial\rho}{\partial r}\frac{\partial}{\partial\rho}\left(\tilde{\sigma}(r,\theta)r^2\theta_i'(r)\frac{\partial\rho}{\partial r}\frac{\partial f}{\partial\rho} + \tilde{\sigma}(r,\theta)\left(\chi'(\theta)[-\theta_i(r)+\omega_i]+1\right)\frac{\partial f}{\partial\varphi}\right) \tag{3.160}$$

$$+ \left(\chi'(\theta)[-\theta_i(r)+\omega_i]+1\right)\frac{\partial}{\partial\varphi}\left(\tilde{\sigma}(r,\theta)r^2\theta_i'(r)\frac{\partial\rho}{\partial r}\frac{\partial f}{\partial\rho} + \tilde{\sigma}(r,\theta)\left(\chi'(\theta)[-\theta_i(r)+\omega_i]+1\right)\frac{\partial f}{\partial\varphi}\right)$$

$$= r^2\theta_i'(r)\frac{\partial\rho}{\partial r}\frac{\partial}{\partial\rho}\left(r^2\theta_i'(r)\frac{\partial\rho}{\partial r}\tilde{\sigma}(\varphi)\frac{\partial f}{\partial\rho}\right) \tag{3.161}$$

$$+ r^2\theta_i'(r)\frac{\partial\rho}{\partial r}\frac{\partial}{\partial\rho}\left(\left(\chi'(\theta)[-\theta_i(r)+\omega_i]+1\right)\tilde{\sigma}(\varphi)\frac{\partial f}{\partial\varphi}\right)$$

$$+ \left(\chi'(\theta)[-\theta_i(r)+\omega_i]+1\right)\frac{\partial}{\partial\varphi}\left(r^2\theta_i'(r)\frac{\partial\rho}{\partial r}\tilde{\sigma}(\varphi)\frac{\partial f}{\partial\rho}\right)$$

$$+ \left(\chi'(\theta)[-\theta_i(r)+\omega_i]+1\right)\frac{\partial}{\partial\varphi}\left(\left(\chi'(\theta)[-\theta_i(r)+\omega_i]+1\right)\tilde{\sigma}(\varphi)\frac{\partial f}{\partial\varphi}\right)$$

Further computation gives

$$
\begin{aligned}
&\frac{\partial}{\partial\theta}\left(\tilde{\sigma}(r,\theta)\frac{\partial f}{\partial\theta}\right)\\
&= r^2\theta_i'(r)\frac{\partial\rho}{\partial r}\Bigg[\left(\frac{\partial}{\partial\rho}\left(r^2\theta_i'(r)\right)\right)\frac{\partial\rho}{\partial r}\tilde{\sigma}(\varphi)\frac{\partial f}{\partial\rho}\\
&\qquad\qquad + r^2\theta_i'(r)\left(\frac{\partial}{\partial\rho}\left(\frac{\partial\rho}{\partial r}\right)\right)\tilde{\sigma}(\varphi)\frac{\partial f}{\partial\rho}\\
&\qquad\qquad + r^2\theta_i'(r)\frac{\partial\rho}{\partial r}\left(\frac{\partial}{\partial\rho}\left(\tilde{\sigma}(\varphi)\frac{\partial f}{\partial\rho}\right)\right)\Bigg]\\
&\quad + r^2\theta_i'(r)\frac{\partial\rho}{\partial r}\Bigg[\left(\chi'(\theta)[-\theta_i(r)+\omega_i]+1\right)\frac{\partial}{\partial\rho}\left(\tilde{\sigma}(\varphi)\frac{\partial f}{\partial\varphi}\right)\\
&\qquad\qquad + \tilde{\sigma}(\varphi)\left(\frac{\partial}{\partial\rho}\chi'(\theta)\right)[-\theta_i(r)+\omega_i]\frac{\partial f}{\partial\varphi}\\
&\qquad\qquad + \tilde{\sigma}(\varphi)\chi'(\theta)\left(-\frac{\partial}{\partial\rho}\theta_i(r)\right)\frac{\partial f}{\partial\varphi}\Bigg]\\
&\quad + \left(\chi'(\theta)[-\theta_i(r)+\omega_i]+1\right)\Bigg[\left(\frac{\partial}{\partial\varphi}\left(r^2\theta_i'(r)\right)\right)\frac{\partial\rho}{\partial r}\tilde{\sigma}(\varphi)\frac{\partial f}{\partial\rho}\\
&\qquad\qquad + r^2\theta_i'(r)\left(\frac{\partial}{\partial\varphi}\left(\frac{\partial\rho}{\partial r}\right)\right)\tilde{\sigma}(\varphi)\frac{\partial f}{\partial\rho}\\
&\qquad\qquad + r^2\theta_i'(r)\frac{\partial\rho}{\partial r}\left(\frac{\partial}{\partial\varphi}\left(\tilde{\sigma}(\varphi)\frac{\partial f}{\partial\rho}\right)\right)\Bigg]\\
&\quad + \left(\chi'(\theta)[-\theta_i(r)+\omega_i]+1\right)\Bigg[\left(\chi'(\theta)[-\theta_i(r)+\omega_i]+1\right)\frac{\partial}{\partial\varphi}\left(\tilde{\sigma}(\varphi)\frac{\partial f}{\partial\varphi}\right)\\
&\qquad\qquad + \tilde{\sigma}(\varphi)\left(\frac{\partial}{\partial\varphi}\chi'(\theta)\right)[-\theta_i(r)+\omega_i]\frac{\partial f}{\partial\varphi}\\
&\qquad\qquad + \tilde{\sigma}(\varphi)\chi'(\theta)\left(-\frac{\partial}{\partial\varphi}\theta_i(r)\right)\frac{\partial f}{\partial\varphi}\Bigg]
\end{aligned}
\tag{3.162}
$$

Now, we compute the derivatives

$$\frac{\partial}{\partial\varphi}\chi'(\theta) = \frac{\chi''(\theta)}{(\chi'(\theta)[-\theta_i(r)+\omega_i]+1)+\chi(\theta)\theta_i'(r)r^2\theta_i'(r)} \tag{3.163}$$

$$\frac{\partial}{\partial\varphi}\theta_i(r) = \frac{-r^2\theta_i'(r)\theta_i'(r)}{(\chi'(\theta)[-\theta_i(r)+\omega_i]+1)+\chi(\theta)\theta_i'(r)r^2\theta_i'(r)} \tag{3.164}$$

$$\frac{\partial}{\partial\varphi}\left(r^2\theta_i'(r)\right) = \frac{-r^2\theta_i'(r)\left(2r\theta_i'(r)+r^2\theta_i''(r)\right)}{(\chi'(\theta)[-\theta_i(r)+\omega_i]+1)+\chi(\theta)\theta_i'(r)r^2\theta_i'(r)} \tag{3.165}$$

$$\frac{\partial}{\partial\rho}\chi'(\theta) = \frac{\chi(\theta)\theta_i'(r)\chi''(\theta)}{\frac{\partial\rho}{\partial r}(\chi'(\theta)[-\theta_i(r)+\omega_i]+1)+\chi(\theta)\theta_i'(r)r^2\theta_i'(r)\frac{\partial\rho}{\partial r}} \tag{3.166}$$

$$\frac{\partial}{\partial\rho}\theta_i(r) = \frac{(\chi'(\theta)[-\theta_i(r)+\omega_i]+1)\,\theta_i'(r)}{\frac{\partial\rho}{\partial r}(\chi'(\theta)[-\theta_i(r)+\omega_i]+1)+\chi(\theta)\theta_i'(r)r^2\theta_i'(r)\frac{\partial\rho}{\partial r}} \tag{3.167}$$

$$\frac{\partial}{\partial\rho}\left(r^2\theta_i'(r)\right) = \frac{(\chi'(\theta)[-\theta_i(r)+\omega_i]+1)\left(2r\theta_i'(r)+r^2\theta_i''(r)\right)}{\frac{\partial\rho}{\partial r}(\chi'(\theta)[-\theta_i(r)+\omega_i]+1)+\chi(\theta)\theta_i'(r)r^2\theta_i'(r)\frac{\partial\rho}{\partial r}}. \tag{3.168}$$

Thus,

$$
\begin{aligned}
&\frac{\partial}{\partial\theta}\left(\tilde{\sigma}(r,\theta)\frac{\partial f}{\partial\theta}\right)\\
&= r^2\theta_i'(r)\frac{\partial\rho}{\partial r}\Bigg[\left(\frac{(\chi'(\theta)[-\theta_i(r)+\omega_i]+1)\left(2r\theta_i'(r)+r^2\theta_i''(r)\right)}{\frac{\partial\rho}{\partial r}(\chi'(\theta)[-\theta_i(r)+\omega_i]+1)+\chi(\theta)\theta_i'(r)r^2\theta_i'(r)\frac{\partial\rho}{\partial r}}\right)\frac{\partial\rho}{\partial r}\tilde{\sigma}(\varphi)\frac{\partial f}{\partial\rho}\\
&\qquad + r^2\theta_i'(r)\left(\frac{\partial}{\partial\rho}\left(\frac{\partial\rho}{\partial r}\right)\right)\tilde{\sigma}(\varphi)\frac{\partial f}{\partial\rho}\\
&\qquad + r^2\theta_i'(r)\frac{\partial\rho}{\partial r}\left(\frac{\partial}{\partial\rho}\left(\tilde{\sigma}(\varphi)\frac{\partial f}{\partial\rho}\right)\right)\Bigg]\\
&\quad + r^2\theta_i'(r)\frac{\partial\rho}{\partial r}\Bigg[(\chi'(\theta)[-\theta_i(r)+\omega_i]+1)\frac{\partial}{\partial\rho}\left(\tilde{\sigma}(\varphi)\frac{\partial f}{\partial\varphi}\right)\\
&\qquad + \tilde{\sigma}(\varphi)\left(\frac{\chi(\theta)\theta_i'(r)\chi''(\theta)[-\theta_i(r)+\omega_i]}{\frac{\partial\rho}{\partial r}(\chi'(\theta)[-\theta_i(r)+\omega_i]+1)+\chi(\theta)\theta_i'(r)r^2\theta_i'(r)\frac{\partial\rho}{\partial r}}\right)\frac{\partial f}{\partial\varphi}\\
&\qquad + \tilde{\sigma}(\varphi)\chi'(\theta)\left(-\frac{(\chi'(\theta)[-\theta_i(r)+\omega_i]+1)\,\theta_i'(r)}{\frac{\partial\rho}{\partial r}(\chi'(\theta)[-\theta_i(r)+\omega_i]+1)+\chi(\theta)\theta_i'(r)r^2\theta_i'(r)\frac{\partial\rho}{\partial r}}\right)\frac{\partial f}{\partial\varphi}\Bigg]\\
&\quad + (\chi'(\theta)[-\theta_i(r)+\omega_i]+1)\Bigg[\\
&\qquad \left(\frac{-r^2\theta_i'(r)\left(2r\theta_i'(r)+r^2\theta_i''(r)\right)}{(\chi'(\theta)[-\theta_i(r)+\omega_i]+1)+\chi(\theta)\theta_i'(r)r^2\theta_i'(r)}\right)\frac{\partial\rho}{\partial r}\tilde{\sigma}(\varphi)\frac{\partial f}{\partial\rho}\\
&\qquad + r^2\theta_i'(r)\left(\frac{\partial}{\partial\varphi}\left(\frac{\partial\rho}{\partial r}\right)\right)\tilde{\sigma}(\varphi)\frac{\partial f}{\partial\rho}\\
&\qquad + r^2\theta_i'(r)\frac{\partial\rho}{\partial r}\left(\frac{\partial}{\partial\varphi}\left(\tilde{\sigma}(\varphi)\frac{\partial f}{\partial\rho}\right)\right)\Bigg]\\
&\quad + (\chi'(\theta)[-\theta_i(r)+\omega_i]+1)\Bigg[(\chi'(\theta)[-\theta_i(r)+\omega_i]+1)\frac{\partial}{\partial\varphi}\left(\tilde{\sigma}(\varphi)\frac{\partial f}{\partial\varphi}\right)\\
&\qquad + \tilde{\sigma}(\varphi)\left(\frac{\chi''(\theta)[-\theta_i(r)+\omega_i]}{(\chi'(\theta)[-\theta_i(r)+\omega_i]+1)+\chi(\theta)\theta_i'(r)r^2\theta_i'(r)}\right)\frac{\partial f}{\partial\varphi}\\
&\qquad + \tilde{\sigma}(\varphi)\chi'(\theta)\left(-\frac{-r^2\theta_i'(r)\theta_i'(r)}{(\chi'(\theta)[-\theta_i(r)+\omega_i]+1)+\chi(\theta)\theta_i'(r)r^2\theta_i'(r)}\right)\frac{\partial f}{\partial\varphi}\Bigg]
\end{aligned}
\tag{3.169}
$$

The operator P accounting for the conductivity can now be expressed in terms of the new coordinates

$$
\begin{aligned}
&P(f)\\
&= \partial_r(\tilde{\sigma}\partial_r f)+\frac{\tilde{\sigma}}{r}\partial_r f + r^{-2}\partial_\theta(\tilde{\sigma}\partial_\theta f)
\end{aligned}
\tag{3.170}
$$

$$
\begin{aligned}
&= \tilde{\sigma}(\varphi)\frac{\partial\rho}{\partial r}\frac{\partial}{\partial\rho}\left(\frac{\partial\rho}{\partial r}\frac{\partial f}{\partial\rho}\right) \qquad (3.171)\\
&\quad - \frac{\partial\rho}{\partial r}\tilde{\sigma}(\varphi)\left(\frac{\chi(\theta)\theta_i'(r)\chi'(\theta)}{\frac{\partial\rho}{\partial r}(\chi'(\theta)[-\theta_i(r)+\omega_i]+1)+\chi(\theta)\theta_i'(r)r^2\theta_i'(r)\frac{\partial\rho}{\partial r}}\right)\theta_i'(r)\frac{\partial f}{\partial\varphi}\\
&\quad - \frac{\partial\rho}{\partial r}\tilde{\sigma}(\varphi)\chi(\theta)\left(\frac{(\chi'(\theta)[-\theta_i(r)+\omega_i]+1)\,\theta_i''(r)}{\frac{\partial\rho}{\partial r}(\chi'(\theta)[-\theta_i(r)+\omega_i]+1)+\chi(\theta)\theta_i'(r)r^2\theta_i'(r)\frac{\partial\rho}{\partial r}}\right)\frac{\partial f}{\partial\varphi}\\
&\quad - \frac{\partial\rho}{\partial r}\chi(\theta)\theta_i'(r)\frac{\partial}{\partial\rho}\left(\tilde{\sigma}(\varphi)\frac{\partial f}{\partial\varphi}\right)\\
&\quad - \chi(\theta)\theta_i'(r)\left[\frac{\partial}{\partial\varphi}\left(\tilde{\sigma}(\varphi)\frac{\partial\rho}{\partial r}\frac{\partial f}{\partial\rho}\right)\right.\\
&\qquad\qquad - \tilde{\sigma}(\varphi)\left(\frac{\chi'(\theta)}{(\chi'(\theta)[-\theta_i(r)+\omega_i]+1)+\chi(\theta)\theta_i'(r)r^2\theta_i'(r)}\right)\theta_i'(r)\frac{\partial f}{\partial\varphi}\\
&\qquad\qquad - \tilde{\sigma}(\varphi)\chi(\theta)\left(\frac{-r^2\theta_i'(r)\theta_i''(r)}{(\chi'(\theta)[-\theta_i(r)+\omega_i]+1)+\chi(\theta)\theta_i'(r)r^2\theta_i'(r)}\right)\frac{\partial f}{\partial\varphi}\\
&\qquad\qquad \left. - \chi(\theta)\theta_i'(r)\frac{\partial}{\partial\varphi}\left(\tilde{\sigma}(\varphi)\frac{\partial f}{\partial\varphi}\right)\right]\\
&\quad + \tilde{\sigma}(\varphi)\frac{1}{r}\left[\frac{\partial\rho}{\partial r}\frac{\partial f}{\partial\rho} - \chi(\theta)\theta_i'(r)\frac{\partial f}{\partial\varphi}\right]\\
&\quad + \frac{1}{r^2}\left[r^2\theta_i'(r)\frac{\partial\rho}{\partial r}\left[\left(\frac{(\chi'(\theta)[-\theta_i(r)+\omega_i]+1)\left(2r\theta_i'(r)+r^2\theta_i''(r)\right)}{\frac{\partial\rho}{\partial r}(\chi'(\theta)[-\theta_i(r)+\omega_i]+1)+\chi(\theta)\theta_i'(r)r^2\theta_i'(r)\frac{\partial\rho}{\partial r}}\right)\frac{\partial\rho}{\partial r}\tilde{\sigma}(\varphi)\frac{\partial f}{\partial\rho}\right.\right.\\
&\qquad\qquad + r^2\theta_i'(r)\left(\frac{\partial}{\partial\rho}\left(\frac{\partial\rho}{\partial r}\right)\right)\tilde{\sigma}(\varphi)\frac{\partial f}{\partial\rho}\\
&\qquad\qquad \left.\left. + r^2\theta_i'(r)\frac{\partial\rho}{\partial r}\left(\frac{\partial}{\partial\rho}\left(\tilde{\sigma}(\varphi)\frac{\partial f}{\partial\rho}\right)\right)\right]\right.\\
&\qquad + r^2\theta_i'(r)\frac{\partial\rho}{\partial r}\left[\left(\chi'(\theta)[-\theta_i(r)+\omega_i]+1\right)\frac{\partial}{\partial\rho}\left(\tilde{\sigma}(\varphi)\frac{\partial f}{\partial\varphi}\right)\right.\\
&\qquad\qquad + \tilde{\sigma}(\varphi)\left(\frac{\chi(\theta)\theta_i'(r)\chi''(\theta)[-\theta_i(r)+\omega_i]}{\frac{\partial\rho}{\partial r}(\chi'(\theta)[-\theta_i(r)+\omega_i]+1)+\chi(\theta)\theta_i'(r)r^2\theta_i'(r)\frac{\partial\rho}{\partial r}}\right)\frac{\partial f}{\partial\varphi}\\
&\qquad\qquad \left. + \tilde{\sigma}(\varphi)\chi'(\theta)\left(-\frac{(\chi'(\theta)[-\theta_i(r)+\omega_i]+1)\,\theta_i'(r)}{\frac{\partial\rho}{\partial r}(\chi'(\theta)[-\theta_i(r)+\omega_i]+1)+\chi(\theta)\theta_i'(r)r^2\theta_i'(r)\frac{\partial\rho}{\partial r}}\right)\frac{\partial f}{\partial\varphi}\right]\\
&\qquad + \left(\chi'(\theta)[-\theta_i(r)+\omega_i]+1\right)\left[\right.\\
&\qquad\qquad \left(\frac{-r^2\theta_i'(r)\left(2r\theta_i'(r)+r^2\theta_i''(r)\right)}{(\chi'(\theta)[-\theta_i(r)+\omega_i]+1)+\chi(\theta)\theta_i'(r)r^2\theta_i'(r)}\right)\frac{\partial\rho}{\partial r}\tilde{\sigma}(\varphi)\frac{\partial f}{\partial\rho}\\
&\qquad\qquad + r^2\theta_i'(r)\left(\frac{\partial}{\partial\varphi}\left(\frac{\partial\rho}{\partial r}\right)\right)\tilde{\sigma}(\varphi)\frac{\partial f}{\partial\rho}
\end{aligned}
$$

$$
\begin{aligned}
&+ r^2\theta_i'(r)\frac{\partial\rho}{\partial r}\left(\frac{\partial}{\partial\varphi}\left(\tilde{\sigma}(\varphi)\frac{\partial f}{\partial\rho}\right)\right)\Bigg] \\
&+ \left(\chi'(\theta)[-\theta_i(r)+\omega_i]+1\right)\Bigg[\left(\chi'(\theta)[-\theta_i(r)+\omega_i]+1\right)\frac{\partial}{\partial\varphi}\left(\tilde{\sigma}(\varphi)\frac{\partial f}{\partial\varphi}\right) \\
&\quad + \tilde{\sigma}(\varphi)\left(\frac{\chi''(\theta)[-\theta_i(r)+\omega_i]}{\left(\chi'(\theta)[-\theta_i(r)+\omega_i]+1\right)+\chi(\theta)\theta_i'(r)r^2\theta_i'(r)}\right)\frac{\partial f}{\partial\varphi} \\
&\quad + \tilde{\sigma}(\varphi)\chi'(\theta)\left(-\frac{-r^2\theta_i'(r)\theta_i'(r)}{\left(\chi'(\theta)[-\theta_i(r)+\omega_i]+1\right)+\chi(\theta)\theta_i'(r)r^2\theta_i'(r)}\right)\frac{\partial f}{\partial\varphi}\Bigg]\Bigg] \\
&= \overline{P}f + \tilde{P}f, \qquad (3.172)
\end{aligned}
$$

in which we define the operator $\overline{P}$

$$
\overline{P}(f) := \tilde{\sigma}(\varphi)\left(\frac{\partial^2}{\partial\rho^2}+\frac{1}{\rho}\frac{\partial}{\partial\rho}\right)f + \frac{1}{\rho^2}\frac{\partial}{\partial\varphi}\left(\tilde{\sigma}(\varphi)\frac{\partial f}{\partial\varphi}\right) \qquad (3.173)
$$

and we define the operator $\tilde{P} := P - \overline{P}$. We can explicitly denote the operator $\tilde{P}$ by

$$
\tilde{P}(f) = \left(A_{\rho\rho} + A_{\varphi\rho} + A_{\rho\varphi} + A_{\varphi\varphi} + A_{\varphi} + A_{\rho}\right) f \qquad (3.174)
$$

in which the second order terms are

$$
A_{\rho\rho}f = \tilde{\sigma}(\varphi)\frac{\partial\rho}{\partial r}\frac{\partial}{\partial\rho}\left(\frac{\partial\rho}{\partial r}\frac{\partial f}{\partial\rho}\right) - \tilde{\sigma}(\varphi)\frac{\partial^2 f}{\partial\rho^2} + \left(\theta_i'(r)\frac{\partial\rho}{\partial r}\right)^2\left(\frac{\partial}{\partial\rho}\left(\tilde{\sigma}(\varphi)\frac{\partial f}{\partial\rho}\right)\right) \qquad (3.175)
$$

$$
\begin{aligned}
A_{\varphi\rho}f = &\left(\chi'(\theta)[-\theta_i(r)+\omega_i]+1\right)\theta_i'(r)\frac{\partial\rho}{\partial r}\left[\frac{\partial}{\partial\varphi}\left(\tilde{\sigma}(\varphi)\frac{\partial f}{\partial\rho}\right)\right] \qquad (3.176)\\
&- \chi(\theta)\theta_i'(r)\left[\frac{\partial}{\partial\varphi}\left(\tilde{\sigma}(\varphi)\frac{\partial\rho}{\partial r}\frac{\partial f}{\partial\rho}\right)\right]
\end{aligned}
$$

$$
\begin{aligned}
A_{\rho\varphi}f = &\,\theta_i'(r)\frac{\partial\rho}{\partial r}\left[\left(\chi'(\theta)[-\theta_i(r)+\omega_i]+1\right)\frac{\partial}{\partial\rho}\left(\tilde{\sigma}(\varphi)\frac{\partial f}{\partial\varphi}\right)\right] \qquad (3.177)\\
&- \frac{\partial\rho}{\partial r}\chi(\theta)\theta_i'(r)\frac{\partial}{\partial\rho}\left(\tilde{\sigma}(\varphi)\frac{\partial f}{\partial\varphi}\right)
\end{aligned}
$$

$$
\begin{aligned}
A_{\varphi\varphi}f = &\left(\chi(\theta)\theta_i'(r)\right)^2\frac{\partial}{\partial\varphi}\left(\tilde{\sigma}(\varphi)\frac{\partial f}{\partial\varphi}\right) \\
&+ \frac{1}{r^2}\left(\chi'(\theta)[-\theta_i(r)+\omega_i]+1\right)^2\frac{\partial}{\partial\varphi}\left(\tilde{\sigma}(\varphi)\frac{\partial f}{\partial\varphi}\right) \qquad (3.178)\\
&- \frac{1}{\rho^2}\frac{\partial}{\partial\varphi}\left(\tilde{\sigma}(\varphi)\frac{\partial f}{\partial\varphi}\right)
\end{aligned}
$$

and the first order terms are

$$A_\varphi f = -\tilde{\sigma}(\varphi)\left(\frac{\chi(\theta)\theta_i'(r)\chi'(\theta)}{(\chi'(\theta)[-\theta_i(r)+\omega_i]+1)+\chi(\theta)\theta_i'(r)r^2\theta_i'(r)}\right)\theta_i'(r)\frac{\partial f}{\partial\varphi} \tag{3.179}$$
$$-\tilde{\sigma}(\varphi)\chi(\theta)\left(\frac{(\chi'(\theta)[-\theta_i(r)+\omega_i]+1)\,\theta_i''(r)}{(\chi'(\theta)[-\theta_i(r)+\omega_i]+1)+\chi(\theta)\theta_i'(r)r^2\theta_i'(r)}\right)\frac{\partial f}{\partial\varphi}$$
$$+\chi(\theta)\theta_i'(r)\tilde{\sigma}(\varphi)\left(\frac{\chi'(\theta)}{(\chi'(\theta)[-\theta_i(r)+\omega_i]+1)+\chi(\theta)\theta_i'(r)r^2\theta_i'(r)}\right)\theta_i'(r)\frac{\partial f}{\partial\varphi}$$
$$+\chi(\theta)\theta_i'(r)\tilde{\sigma}(\varphi)\chi(\theta)\left(\frac{-r^2\theta_i'(r)\theta_i''(r)}{(\chi'(\theta)[-\theta_i(r)+\omega_i]+1)+\chi(\theta)\theta_i'(r)r^2\theta_i'(r)}\right)\frac{\partial f}{\partial\varphi}$$
$$+\tilde{\sigma}(\varphi)\frac{1}{r}\left[-\chi(\theta)\theta_i'(r)\frac{\partial f}{\partial\varphi}\right]$$
$$+\theta_i'(r)\tilde{\sigma}(\varphi)\left(\frac{\chi(\theta)\theta_i'(r)\chi''(\theta)}{(\chi'(\theta)[-\theta_i(r)+\omega_i]+1)+\chi(\theta)\theta_i'(r)r^2\theta_i'(r)}\right)[-\theta_i(r)+\omega_i]\frac{\partial f}{\partial\varphi}$$
$$+\theta_i'(r)\tilde{\sigma}(\varphi)\chi'(\theta)\left(-\frac{(\chi'(\theta)[-\theta_i(r)+\omega_i]+1)\,\theta_i'(r)}{(\chi'(\theta)[-\theta_i(r)+\omega_i]+1)+\chi(\theta)\theta_i'(r)r^2\theta_i'(r)}\right)\frac{\partial f}{\partial\varphi}$$
$$+\frac{1}{r^2}\tilde{\sigma}(\varphi)\left(\frac{(\chi'(\theta)[-\theta_i(r)+\omega_i]+1)\,\chi''(\theta)}{(\chi'(\theta)[-\theta_i(r)+\omega_i]+1)+\chi(\theta)\theta_i'(r)r^2\theta_i'(r)}\right)[-\theta_i(r)+\omega_i]\frac{\partial f}{\partial\varphi}$$
$$+\tilde{\sigma}(\varphi)\chi'(\theta)\left(\frac{(\chi'(\theta)[-\theta_i(r)+\omega_i]+1)\,\theta_i'(r)\theta_i'(r)}{(\chi'(\theta)[-\theta_i(r)+\omega_i]+1)+\chi(\theta)\theta_i'(r)r^2\theta_i'(r)}\right)\frac{\partial f}{\partial\varphi}$$

$$A_\rho f = \tilde{\sigma}(\varphi)\frac{1}{r}\frac{\partial\rho}{\partial r}\frac{\partial f}{\partial\rho}-\tilde{\sigma}(\varphi)\frac{1}{\rho}\frac{\partial f}{\partial\rho} \tag{3.180}$$
$$+\theta_i'(r)\left(\frac{(\chi'(\theta)[-\theta_i(r)+\omega_i]+1)\,\left(2r\theta_i'(r)+r^2\theta_i''(r)\right)}{(\chi'(\theta)[-\theta_i(r)+\omega_i]+1)+\chi(\theta)\theta_i'(r)r^2\theta_i'(r)}\right)\frac{\partial\rho}{\partial r}\tilde{\sigma}(\varphi)\frac{\partial f}{\partial\rho}$$
$$+\theta_i'(r)\frac{\partial\rho}{\partial r}\theta_i'(r)\left(\frac{\partial}{\partial\rho}\left(\frac{\partial\rho}{\partial r}\right)\right)\tilde{\sigma}(\varphi)\frac{\partial f}{\partial\rho}$$
$$+\left(\frac{-\left(\chi'(\theta)[-\theta_i(r)+\omega_i]+1\right)\theta_i'(r)\left(2r\theta_i'(r)+\theta_i''(r)\right)}{(\chi'(\theta)[-\theta_i(r)+\omega_i]+1)+\chi(\theta)\theta_i'(r)r^2\theta_i'(r)}\right)\frac{\partial\rho}{\partial r}\tilde{\sigma}(\varphi)\frac{\partial f}{\partial\rho}$$
$$+\left(\chi'(\theta)[-\theta_i(r)+\omega_i]+1\right)\theta_i'(r)\left(\frac{\partial}{\partial\varphi}\left(\frac{\partial\rho}{\partial r}\right)\right)\tilde{\sigma}(\varphi)\frac{\partial f}{\partial\rho}$$

Recall that from Eq. (3.18), for a general C^2 curve,

$$\theta_i(r) = \omega_i + \kappa_i r^2 + o(r^2).$$

The first and second derivatives of $\theta_i(r)$ are

$$\theta_i'(r) = 2\kappa_i r + o(r) \tag{3.181}$$

and

$$\theta_i''(r) = 2\kappa_i + o(1), \tag{3.182}$$

respectively. We consider neighbourhoods $\{\varphi \in (\omega_i - \delta, \omega_i + \delta), \rho \in (0, \varepsilon)\}$ of the curves. In these neighbourhoods $\chi(\theta) = 1$ and $\chi'(\theta) = 0$ and from Lemma 3.9 we have the bounds $\rho(r,\theta) - r = \mathcal{O}(r^3), \partial_r\rho(r,\theta) - 1 = \mathcal{O}(r^2), \partial_\theta\rho(r,\theta) = \mathcal{O}(r^3)$. In these neighbourhoods, we can explicitly denote the operator $\tilde{P}$ in terms of its coefficients

$$\begin{aligned}\tilde{P} = a_{\rho\rho}\partial_{\rho\rho} + a_{\rho\varphi}\partial_\rho[\tilde{\sigma}(\varphi)\partial_\varphi] + a_{\varphi\rho}\partial_\varphi[\tilde{\sigma}(\varphi)\partial_\rho] + a_{\varphi\varphi}\partial_\varphi[\tilde{\sigma}(\varphi)\partial_\varphi] \\ + a_\rho\partial_\rho + \tilde{\sigma}(\varphi)a_\varphi\partial_\varphi,\end{aligned} \tag{3.183}$$

in which the second order coefficients are

$$a_{\rho\rho} := \mathcal{O}(\rho) \tag{3.184}$$

$$a_{\varphi\rho} := 0 \tag{3.185}$$

$$a_{\rho\varphi} := 0 \tag{3.186}$$

$$a_{\varphi\varphi} := \mathcal{O}(\rho^{-1}) \tag{3.187}$$

and the first order coefficients are

$$\begin{aligned} a_\varphi :&= -\tilde{\sigma}(\varphi)\left(\frac{\theta_i''(r)}{1+\theta_i'(r)r^2\theta_i'(r)}\right) \\ &\quad + \theta_i'(r)\tilde{\sigma}(\varphi)\left(\frac{-r^2\theta_i'(r)\theta_i''(r)}{1+\theta_i'(r)r^2\theta_i'(r)}\right) \\ &\quad - \tilde{\sigma}(\varphi)\frac{1}{r}\theta_i'(r) \end{aligned} \tag{3.188}$$

$$= \mathcal{O}(1), \tag{3.189}$$

$$\begin{aligned} a_\rho &= \tilde{\sigma}(\varphi)\frac{1}{r}\frac{\partial\rho}{\partial r} - \tilde{\sigma}(\varphi)\frac{1}{\rho} \\ &\quad + \theta_i'(r)\frac{\partial\rho}{\partial r}\theta_i'(r)\left(\frac{\partial}{\partial\rho}\left(\frac{\partial\rho}{\partial r}\right)\right)\tilde{\sigma}(\varphi) \\ &\quad + \theta_i'(r)\left(\frac{\partial}{\partial\varphi}\left(\frac{\partial\rho}{\partial r}\right)\right)\tilde{\sigma}(\varphi) \end{aligned} \tag{3.190}$$

$$= \mathcal{O}(\rho). \tag{3.191}$$

Note in particular that the coefficient $a_{\varphi\rho}$ vanishes in neighbourhoods $\{(\rho,\varphi)|\varphi \in (\omega_i - \delta, \omega_i + \delta), \rho \in (0,\varepsilon)\}$ where $\chi'(\varphi) = 0$. This will prove important further down. This is one key feature of the change of coordinates $(r,\theta) \to (\rho,\varphi)$ that we performed.

Thus, in these corner-like neighbourhoods $\{(\rho,\varphi)|\varphi \in (\omega_i-\delta,\omega_i+\delta),\rho\in(0,\varepsilon)\}$ around the angles $\varphi=\omega_i$ the operator $\tilde{P}$ can be expressed:

$$\begin{aligned}\tilde{P}f &= \big(a_{\rho\rho}\partial_{\rho\rho}+a_{\rho\varphi}\partial_\rho[\tilde{\sigma}(\varphi)\partial_\varphi]+a_{\varphi\rho}\partial_\varphi[\tilde{\sigma}(\varphi)\partial_\rho]+a_{\varphi\varphi}\partial_\varphi[\tilde{\sigma}(\varphi)\partial_\varphi] \\ &\quad +a_\rho\partial_\rho+\tilde{\sigma}(\varphi)a_\varphi\partial_\varphi\big)f \qquad (3.192)\\ &= \mathcal{O}(\rho)\partial_\rho[\tilde{\sigma}(\varphi)\partial_\rho]f+\mathcal{O}(\rho^{-1})\partial_\varphi[\tilde{\sigma}(\varphi)\partial_\varphi]f \qquad (3.193)\\ &\quad +\mathcal{O}(1)\partial_\varphi f+\mathcal{O}(\rho)\partial_\rho f.\end{aligned}$$

On the other hand, *away* from the corner-like neighbourhoods around $\varphi=\omega_i$, $\tilde{\sigma}(\varphi)$ is just a constant function. Invoking the calculations on the coefficients $a_{\rho\rho},a_{\rho\varphi},a_{\varphi\rho},a_{\varphi\varphi},a_\rho,a_\varphi$, we derive that there, the operator $\tilde{P}$ can be expressed as:

$$\begin{aligned}\tilde{P}f &= \big(a_{\rho\rho}\partial_{\rho\rho}+a_{\rho\varphi}\partial_\rho[\tilde{\sigma}(\varphi)\partial_\varphi]+a_{\varphi\rho}\partial_\varphi[\tilde{\sigma}(\varphi)\partial_\rho]+a_{\varphi\varphi}\partial_\varphi[\tilde{\sigma}(\varphi)\partial_\varphi] \\ &\quad +a_\rho\partial_\rho+\tilde{\sigma}(\varphi)a_\varphi\partial_\varphi\big)f \qquad (3.194)\\ &= \mathcal{O}(\rho^2)\partial_\rho\partial_\rho f+\mathcal{O}(\rho)\partial_\varphi\partial_\rho f+\mathcal{O}(\rho^{-2})\partial_\varphi\partial_\varphi f \qquad (3.195)\\ &\quad +\mathcal{O}(1)\partial_\varphi f+\mathcal{O}(\rho)\partial_\rho f.\end{aligned}$$

In particular, dividing the domain $\varphi\in[0,2\pi),\rho\in(0,\varepsilon)$ into the corner domains around the angles ω_i and the rest, and applying the above two formulas in the resulting domains and adding, we obtain the bound $D(0,\varepsilon)$,

$$\|\tilde{P}f\|_{L^2(D(0,\varepsilon))}\leq C_2\|f\|_{\dot{H}^2_1(D(0,\varepsilon))} \qquad (3.196)$$

for some constant $C_2>0$. □

3.2.2.4 *The Composition* $\overline{P}^{-1}\tilde{P}$

Lemma 3.14. *Let $\varepsilon>0$. On $D(0,\varepsilon)$, the composition $\overline{P}^{-1}\tilde{P}$ has operator norm from $\dot{H}^2_1(D(0,\varepsilon))\to\dot{H}^2_1(D(0,\varepsilon))$ less than 1, i.e.,*

$$\|\overline{P}^{-1}\tilde{P}\|_{\dot{H}^2_1(D(0,\varepsilon))\to\dot{H}^2_1(D(0,\varepsilon))}<1. \qquad (3.197)$$

Proof. From Proposition 3.12, we have that $\|\overline{P}^{-1}g\|_{\dot{H}^2_1(D(0,\varepsilon))}\leq C_1\varepsilon\|g\|_{L^2(D(0,\varepsilon))}$ for some $C_1>0$. Thus, the operator norm $\|\overline{P}^{-1}\|_{L^2(D(0,\varepsilon))\to\dot{H}^2_1(D(0,\varepsilon))}\leq C_1\varepsilon$.

From Proposition 3.13, $\|\tilde{P}v\|_{L^2(D(0,\varepsilon))}$ is bounded, so we have that on $D(0,\varepsilon)$,

$$\|\tilde{P}v\|_{L^2(D(0,\varepsilon))}\leq C_2\|v\|_{\dot{H}^2_1(D(0,\varepsilon))}. \qquad (3.198)$$

Hence $\|\tilde{P}\|_{\dot{H}^2_1(D(0,\varepsilon))\to L^2(D(0,\varepsilon))} \leq C_2$. Taking $\varepsilon = \frac{1}{2C_1C_2}$ yields

$$\|\overline{P}^{-1}\tilde{P}v\|_{\dot{H}^2_1(D(0,\varepsilon))} \leq \|\overline{P}^{-1}\|_{L^2\to\dot{H}^2_1(D(0,\varepsilon))}\|\tilde{P}\|_{\dot{H}^2_1\to L^2}\|v\|_{\dot{H}^2_1(D(0,\varepsilon))} \tag{3.199}$$

$$\leq C_1\varepsilon C_2\|v\|_{\dot{H}^2_1(D(0,\varepsilon))} \tag{3.200}$$

$$= \frac{1}{2}\|v\|_{\dot{H}^2_1(D(0,\varepsilon))}. \tag{3.201}$$

Thus, $\|\overline{P}^{-1}\tilde{P}\|_{\dot{H}^2_1(D(0,\varepsilon))\to\dot{H}^2_1(D(0,\varepsilon))} \leq \frac{1}{2} < 1$. □

Since $\|\overline{P}^{-1}\tilde{P}\|_{\dot{H}^2_1(D(0,\varepsilon))\to\dot{H}^2_1(D(0,\varepsilon))} < 1$, the series representation for $\tilde{u}$ given in Eq. (3.202) converges.

Lemma 3.15. *Let $\tilde{u}$ be the solution to Eq. (3.47). Let $g = -\tilde{P}(\overline{u}) \in L^2(D(0,\varepsilon))$. Assume $\|\overline{P}^{-1}\tilde{P}\|_{\dot{H}^2_1(D(0,\varepsilon))\to\dot{H}^2_1(D(0,\varepsilon))} < 1$. Then we can write $\tilde{u}$ as a Neumann series:*

$$\tilde{u} = -\left[I + \sum_{j=1}^{\infty}(-1)^j(\overline{P}^{-1}\tilde{P})^j\right]\overline{P}^{-1}\tilde{P}(\overline{u}). \tag{3.202}$$

Proof. Let $\tilde{u}$ be defined as in Eq. (3.47). Then we can write $\tilde{u}$ as a Neumann series,

$$\tilde{u} = (\overline{P}+\tilde{P})^{-1}g \tag{3.203}$$

$$= \left[\overline{P}(I+\overline{P}^{-1}\tilde{P})\right]^{-1}g \tag{3.204}$$

$$= (I+\overline{P}^{-1}\tilde{P})^{-1}\overline{P}^{-1}g \tag{3.205}$$

$$= \left[I - (\overline{P}^{-1}\tilde{P}) + (\overline{P}^{-1}\tilde{P})^2 - (\overline{P}^{-1}\tilde{P})^3 + \cdots\right]\overline{P}^{-1}g \tag{3.206}$$

$$= \left[I + \sum_{j=1}^{\infty}(-1)^j(\overline{P}^{-1}\tilde{P})^j\right]\overline{P}^{-1}g \tag{3.207}$$

$$= -\left[I + \sum_{j=1}^{\infty}(-1)^j(\overline{P}^{-1}\tilde{P})^j\right]\overline{P}^{-1}\tilde{P}(\overline{u}). \tag{3.208}$$

□

Next, we will control the asymptotics of $\tilde{u}$ as defined in Eq. (3.202) as $\rho \to 0^+$.

Lemma 3.16. *Let $g \in L^2(D(0,\varepsilon))$. Consider the solution, $v := \overline{P}^{-1}g$, to the boundary value problem,*

$$\begin{cases} \overline{P}v = g & \text{in } D(0,\varepsilon) \\ v = 0 & \text{on } \partial D(0,\varepsilon) \end{cases}. \tag{3.209}$$

Then the solution admits the representation

$$v(\rho,\varphi)=\sum_{k=0}^{\infty} l_k(\rho)e_k(\varphi), \tag{3.210}$$

in which $e_0(\varphi), e_1(\varphi), \dots$ *are the orthonormal eigenfunctions of* L *defined in Definition 3.3 normalized such that* $\int_0^{2\pi} \tilde{\sigma}(\varphi)|e_k(\varphi)|^2\, d\varphi = 1$.

Proof. By expanding out the operator $\overline{P}$ defined in Eq. (3.173):

$$\overline{P}v = \tilde{\sigma}(\varphi)\left(\frac{\partial^2}{\partial\rho^2}+\frac{1}{\rho}\frac{\partial}{\partial\rho}\right)v+\frac{1}{\rho^2}\frac{\partial}{\partial\varphi}\left(\tilde{\sigma}(\varphi)\frac{\partial v}{\partial\varphi}\right) \tag{3.211}$$

and dividing by $\tilde{\sigma}(\varphi)$ we obtain the boundary value problem

$$\begin{cases}\left(\frac{\partial^2}{\partial\rho^2}+\frac{1}{\rho}\frac{\partial}{\partial\rho}\right)v-\frac{1}{\rho^2}Lv=\frac{g}{\tilde{\sigma}} & \text{in } D(0,\varepsilon)\\ v=0 & \text{on } \partial D(0,\varepsilon)\end{cases} \tag{3.212}$$

in which $L := -[\tilde{\sigma}(\varphi)]^{-1}\partial_\varphi(\tilde{\sigma}(\varphi)\partial_\varphi)$ defined in Definition 3.2. For fixed $\rho > 0$, we have an orthonormal basis of $L^2(\tilde{\sigma}(\varphi)d\varphi)$ consisting of the eigenfunctions $\{e_k\}_{k\in\mathbb{N}}$ of L on the circle of radius ρ normalized such that $\int_0^{2\pi}\tilde{\sigma}(\varphi)|e_k(\varphi)|^2\, d\varphi = 1$ for all $k\in\mathbb{N}$ as defined in Definition 3.3. Note that this basis is independent of ρ. For any $c\in(0,\varepsilon)$, we can express $\frac{g(\rho,\varphi)}{\tilde{\sigma}(\varphi)}|_{\rho=c} \in L^2(\tilde{\sigma}(\varphi)d\varphi)$ in this basis $\{e_k\}_{k\in\mathbb{N}}$. For almost every $\rho>0$, we can write $\frac{g(\rho,\varphi)}{\tilde{\sigma}(\varphi)} = \sum_{k=0}^{\infty} h_k(\rho)e_k(\varphi)$. Define

$$l_k(\rho) := \int_0^{2\pi}\tilde{\sigma}(\varphi)v(\rho,\varphi)e_k(\varphi)\, d\varphi. \tag{3.213}$$

Then $v(\rho,\varphi)=\sum_{k=0}^{\infty} l_k(\rho)e_k(\varphi)$. □

We will determine the asymptotic behaviour of $l_k(\rho)$ as $\rho\to 0^+$ below.

It is useful to note the equivalence of L^2-norms over the circle and over the disc when we use norms $L^2(d\varphi)$, $L^2(\tilde{\sigma}(\varphi)d\varphi)$ and $L^2(\rho\cdot\tilde{\sigma}(\varphi)d\rho d\varphi)$, $L^2(\rho\cdot\tilde{\sigma}(\varphi)d\rho d\varphi)$. In particular,

$$(min_{i\in\{1,\dots,N\}}\sigma_i)\|\cdot\|_{L^2(d\varphi)} \le \|\cdot\|_{L^2(\tilde{\sigma}(\varphi)\cdot d\varphi)} \le (max_{i\in\{1,\dots,N\}}\sigma_i)\|\cdot\|_{L^2(d\varphi)}.$$

We will then use the convention $\|\cdot\|_1 \simeq \|\cdot\|_2$ to mean that there exists a universal C (depending only on $\sigma_i, i\in\{1,\dots,N\}$) so that $C^{-1}\cdot\|\cdot\|_2 \le \|\cdot\|_1 \le C\cdot\|\cdot\|_2$.

We state a short lemma.

Lemma 3.17. *Let* $\frac{g(\rho,\varphi)}{\tilde{\sigma}(\varphi)} = \sum_{k=0}^{\infty} h_k(\rho)e_k(\varphi) \in L^2(D(0,\varepsilon))$. *Then*

$$\left\| \frac{g(\rho,\varphi)}{\tilde{\sigma}(\varphi)} \right\|^2_{L^2(D(0,\varepsilon),\tilde{\sigma}(\varphi)\rho d\rho d\varphi)} = \sum_{k=0}^{\infty} \int_0^{\varepsilon} \rho |h_k(\rho)|^2 \, d\rho. \tag{3.214}$$

Proof. First, by the orthonormality of the e_k's,

$$\int_0^{2\pi} \left| \frac{g(\rho,\varphi)}{\tilde{\sigma}(\varphi)} \right|^2 \tilde{\sigma}(\varphi) \, d\varphi = \int_0^{2\pi} \left| \sum_{k=0}^{\infty} h_k(\rho)e_k(\varphi) \right|^2 \tilde{\sigma}(\varphi) \, d\varphi \tag{3.215}$$

$$= \sum_{k=0}^{\infty} |h_k(\rho)|^2 \int_0^{2\pi} |e_k(\varphi)|^2 \tilde{\sigma}(\varphi) \, d\varphi \tag{3.216}$$

$$= \sum_{k=0}^{\infty} |h_k(\rho)|^2. \tag{3.217}$$

Then by Eq. (3.217), we compute

$$\left\| \frac{g(\rho,\varphi)}{\tilde{\sigma}(\varphi)} \right\|^2_{L^2(D(0,\varepsilon),\tilde{\sigma}(\varphi)\rho d\rho d\varphi)} = \int_{\rho=0}^{\varepsilon} \int_{\varphi=0}^{2\pi} \left| \frac{g(\rho,\varphi)}{\tilde{\sigma}(\varphi)} \right|^2 \tilde{\sigma}(\varphi) \, d\varphi \rho d\rho \tag{3.218}$$

$$= \int_{\rho=0}^{\varepsilon} \sum_{k=0}^{\infty} |h_k(\rho)|^2 \rho d\rho \tag{3.219}$$

$$= \sum_{k=0}^{\infty} \int_0^{\varepsilon} \rho |h_k(\rho)|^2 \, d\rho. \tag{3.220}$$

□

Proposition 3.18. *Let* $g \in L^2(D(0,\varepsilon))$. *Let* v *be a solution to the boundary value problem Eq. (3.49) in which for almost every* $\rho > 0$, *we can write* $\frac{g(\rho,\varphi)}{\tilde{\sigma}(\varphi)} = \sum_{k=0}^{\infty} h_k(\rho)e_k(\varphi)$ *where the* e_k*'s are orthogonal eigenfunctions of the model operator* $L = -[\tilde{\sigma}(\varphi)]^{-1}\partial_\varphi(\tilde{\sigma}(\varphi)\partial_\varphi)$ *with associated eigenvalues* λ_{e_k}*'s.*

Then we can express v *in the following form:*

$$v(\rho,\varphi) = -\int_\rho^{\varepsilon} s^{-1} \int_0^s t h_0(t) dt ds + \sum_{k=1}^{\infty} \left[\frac{1}{2\sqrt{\lambda_{e_k}}} \rho^{\sqrt{\lambda_{e_k}}} \varepsilon^{-2\sqrt{\lambda_{e_k}}} \int_0^{\varepsilon} t^{1+\sqrt{\lambda_{e_k}}} h_k(t) \, dt \right. \tag{3.221}$$

$$+ \frac{1}{2\sqrt{\lambda_{e_k}}} \rho^{\sqrt{\lambda_{e_k}}} \int_\varepsilon^{\rho} t^{1-\sqrt{\lambda_{e_k}}} h_k(t) dt$$

$$\left. - \frac{1}{2\sqrt{\lambda_{e_k}}} \rho^{-\sqrt{\lambda_{e_k}}} \int_0^{\rho} t^{1+\sqrt{\lambda_{e_k}}} h_k(t) dt \right] e_k(\varphi) \tag{3.222}$$

Proof. By dividing the equation $\overline{P}v = g$ in Eq. (3.49) by $\tilde{\sigma}(\varphi)$, we get an equation for each k:

$$\left[\partial_\rho^2 + \frac{1}{\rho}\partial_\rho - \frac{1}{\rho^2}\lambda_{e_k}\right] l_k(\rho)e_k(\varphi) = h_k(\rho)e_k(\varphi). \tag{3.223}$$

The first summand in the right hand side of (3.221) is the the term corresponding to $k = 0$, (in which case $\lambda_{e_0} = 0$) and is obtained by explicit integration. For all $k \geq 1$ we seek to find an explicit solution to Eq. (3.223) using variation of parameters and invoking that $v \in H^1(D(0,\varepsilon))$. To solve the inhomogeneous ODE

$$\left[\partial_\rho^2 + \frac{1}{\rho}\partial_\rho - \frac{1}{\rho^2}\lambda_{e_k}\right] l_k(\rho) = h_k(\rho), \tag{3.224}$$

we first find the complimentary solution $\ell_{k,\mathrm{comp}}(\rho)$, *i.e.*, the general solution to the corresponding homogeneous ODE

$$\left[\partial_\rho^2 + \frac{1}{\rho}\partial_\rho - \frac{1}{\rho^2}\lambda_{e_k}\right] \ell_{k,\mathrm{comp}}(\rho) = 0. \tag{3.225}$$

These types of second order linear homogeneous ODEs are called Euler Equations (or Cauchy–Euler equations). The solution to this Euler Equation for $k \geq 1$ is

$$\ell_{k,\mathrm{comp}}(\rho) = c_1\ell_{k,1}(\rho) + c_2\ell_{k,2}(\rho). \tag{3.226}$$

in which the two fundamental solutions are

$$\ell_{k,1}(\rho) = \rho^{\sqrt{\lambda_{e_k}}}, \quad \ell_{k,2}(\rho) = \rho^{-\sqrt{\lambda_{e_k}}}. \tag{3.227}$$

We will now use variation of parameters to find a particular solution to the inhomogeneous ODE Eq. (3.224). A particular solution is

$$\ell_{k,\mathrm{P}}(\rho) = \ell_{k,1}(\rho)v_1(\rho) + \ell_{k,2}(\rho)v_2(\rho) \tag{3.228}$$

in which

$$v_1(\rho) = -\int \frac{\ell_{k,2}(\rho)h_k(\rho)}{W(\ell_{k,1},\ell_{k,2})}d\rho, \quad v_2(\rho) = \int \frac{\ell_{k,1}(\rho)h_k(\rho)}{W(\ell_{k,1},\ell_{k,2})}d\rho \tag{3.229}$$

and W denotes the Wronskian

$$W(\ell_{k,1},\ell_{k,2}) = \ell_{k,1}\ell'_{k,2} - \ell_{k,2}\ell'_{k,1}. \tag{3.230}$$

The derivatives of the fundamental solutions are

$$\ell'_{k,1}(\rho) = \sqrt{\lambda_{e_k}}\rho^{\sqrt{\lambda_{e_k}}-1}, \quad \ell'_{k,2}(\rho) = -\sqrt{\lambda_{e_k}}\rho^{-\sqrt{\lambda_{e_k}}-1} \tag{3.231}$$

and hence, the Wronskian is

$$\begin{aligned} W(\ell_{k,1}, \ell_{k,2}) &= \ell_{k,1}\ell'_{k,2} - \ell_{k,2}\ell'_{k,1} && (3.232)\\ &= -\rho^{\sqrt{\lambda_{e_k}}}\sqrt{\lambda_{e_k}}\rho^{-\sqrt{\lambda_{e_k}}-1} - \rho^{-\sqrt{\lambda_{e_k}}}\sqrt{\lambda_{e_k}}\rho^{\sqrt{\lambda_{e_k}}-1} && (3.233)\\ &= -2\sqrt{\lambda_{e_k}}\rho^{-1}. && (3.234)\end{aligned}$$

Thus,

$$v_1(\rho) = \int_\varepsilon^\rho \frac{t^{-\sqrt{\lambda_{e_k}}}h_k(t)}{2\sqrt{\lambda_{e_k}}t^{-1}}dt, \quad v_2(\rho) = \int_0^\rho \frac{t^{\sqrt{\lambda_{e_k}}}h_k(t)}{-2\sqrt{\lambda_{e_k}}t^{-1}}dt \tag{3.235}$$

and a particular solution is

$$\ell_{k,\mathrm{P}}(\rho) = \rho^{\sqrt{\lambda_{e_k}}}\int_\varepsilon^\rho \frac{t^{-\sqrt{\lambda_{e_k}}}h_k(t)}{2\sqrt{\lambda_{e_k}}t^{-1}}dt + \rho^{-\sqrt{\lambda_{e_k}}}\int_0^\rho \frac{t^{\sqrt{\lambda_{e_k}}}h_k(t)}{-2\sqrt{\lambda_{e_k}}t^{-1}}dt. \tag{3.236}$$

The general solution to the inhomogeneous differential equation Eq. (3.224) is

$$\begin{aligned} l_k(\rho) &= \ell_{k,\mathrm{comp}}(\rho) + \ell_{k,\mathrm{P}}(\rho) && (3.237)\\ &= A_k\rho^{\sqrt{\lambda_{e_k}}} + B_k\rho^{-\sqrt{\lambda_{e_k}}} + \rho^{\sqrt{\lambda_{e_k}}}\int_\varepsilon^\rho \frac{t^{-\sqrt{\lambda_{e_k}}}h_k(t)}{2\sqrt{\lambda_{e_k}}t^{-1}}dt + \rho^{-\sqrt{\lambda_{e_k}}}\int_0^\rho \frac{t^{\sqrt{\lambda_{e_k}}}h_k(t)}{-2\sqrt{\lambda_{e_k}}t^{-1}}dt && (3.238)\\ &= A_k\rho^{\sqrt{\lambda_{e_k}}} + B_k\rho^{-\sqrt{\lambda_{e_k}}} + \frac{1}{2\sqrt{\lambda_{e_k}}}\rho^{\sqrt{\lambda_{e_k}}}\int_\varepsilon^\rho t^{1-\sqrt{\lambda_{e_k}}}h_k(t)dt && (3.239)\\ &\quad - \frac{1}{2\sqrt{\lambda_{e_k}}}\rho^{-\sqrt{\lambda_{e_k}}}\int_0^\rho t^{1+\sqrt{\lambda_{e_k}}}h_k(t)dt.\end{aligned}$$

Since our solution v is in $H^1(D(0,\varepsilon))$, this forces $B_k = 0$. Hence,

$$l_k(\rho) = A_k\rho^{\sqrt{\lambda_{e_k}}} + \frac{1}{2\sqrt{\lambda_{e_k}}}\rho^{\sqrt{\lambda_{e_k}}}\int_\varepsilon^\rho t^{1-\sqrt{\lambda_{e_k}}}h_k(t)dt - \frac{1}{2\sqrt{\lambda_{e_k}}}\rho^{-\sqrt{\lambda_{e_k}}}\int_0^\rho t^{1+\sqrt{\lambda_{e_k}}}h_k(t)dt. \tag{3.240}$$

The condition that $l_k(\varepsilon) = 0$ implies that

$$A_k = \frac{1}{2\sqrt{\lambda_{e_k}}}\varepsilon^{-2\sqrt{\lambda_{e_k}}}\int_0^\varepsilon t^{1+\sqrt{\lambda_{e_k}}}h_k(t)\,dt. \tag{3.241}$$

Thus, the solution to the boundary value problem Eq. (3.49) is

$$v(\rho,\varphi) = \sum_{k=1}^{\infty} l_k(\rho)e_k(\varphi) - \int_\rho^\varepsilon \int_0^s t h_0(t)dtds \tag{3.242}$$

$$= \sum_{k=1}^{\infty} \left[\frac{1}{2\sqrt{\lambda_{e_k}}} \rho^{\sqrt{\lambda_{e_k}}} \varepsilon^{-2\sqrt{\lambda_{e_k}}} \int_0^\varepsilon t^{1+\sqrt{\lambda_{e_k}}} h_k(t)\, dt + \frac{1}{2\sqrt{\lambda_{e_k}}} \rho^{\sqrt{\lambda_{e_k}}} \int_\varepsilon^\rho t^{1-\sqrt{\lambda_{e_k}}} h_k(t)dt \right. \tag{3.243}$$

$$\left. - \frac{1}{2\sqrt{\lambda_{e_k}}} \rho^{-\sqrt{\lambda_{e_k}}} \int_0^\rho t^{1+\sqrt{\lambda_{e_k}}} h_k(t)dt \right] e_k(\varphi) - \int_\rho^\varepsilon \int_0^s t h_0(t)dtds.$$

which concludes the proof of Proposition 3.18. □

Note that $-\int_0^\varepsilon s^{-1} \int_0^s t h_0(t)\, dtds$ equals $v(0,\varphi)$, which is the origin in polar coordinates; we now denote this by $v(0)$; sometimes to stress the dependence on $h_0(t)$ we write: $v[h_0](0)$. We note that applying Cauchy-Schwarz, then Hardy inequality and the Cauchy-Schwarz again, yields:

$$|v[h_0](0)| \le \sqrt{\varepsilon} \cdot \left\| s^{-1} \int_0^s t h_0(t)dt \right\|_{L^2\left((0,\varepsilon),ds\right)} \tag{3.244}$$

$$\le 4\sqrt{\varepsilon} \cdot \|t \cdot h_0(t)\|_{L^2\left((0,\varepsilon),dt\right)} \tag{3.245}$$

$$\le 4\varepsilon \cdot \sqrt{\int_0^\varepsilon t \cdot |h_0(t)|^2 dt} \tag{3.246}$$

$$\le \varepsilon \cdot C\|g\|_{L^2\left(D(0,\varepsilon)\right)}. \tag{3.247}$$

Our main remaining task is to show that $\lim_{\rho\to 0^+} \frac{l_k(\rho)}{\rho^{\sqrt{\lambda_1}}}$ has a limit as $\rho \to 0^+$ for $k = 1,\dots,M$. (Recall that M is the multiplicity of the eigenvalue λ_1).

Recall that Lemma 3.17 provides an expression for computing the $L^2(D(0,\varepsilon),\tilde{\sigma}(\varphi\rho d\rho d\varphi))$-norm of the function g and due to the equivalence of the $L^2(D(0,\varepsilon))$ and $L^2(D(0,\varepsilon),\tilde{\sigma}(\varphi\rho d\rho d\varphi))$ norms:

$$\|g\|_{L^2(D(0,\varepsilon))} \simeq \sqrt{\sum_{k=0}^{\infty} \int_0^\varepsilon \rho |h_k(\rho)|^2\, d\rho}. \tag{3.248}$$

For functions that depend on the polar coordinates (ρ,φ), we define a new function of ρ alone by taking the $L^2(\tilde{\sigma}(\varphi)d\varphi)$-norm as

$$\|f\|_{L^2(\tilde{\sigma}(\varphi)d\varphi)}(\rho) := \sqrt{\int_0^{2\pi} |f(\rho,\varphi)|^2\, \tilde{\sigma}(\varphi)d\varphi}. \tag{3.249}$$

Let $g \in L^2(D(0,\varepsilon))$. Then we seek to obtain a strong understanding of the asymptotic behaviour as $\rho \to 0^+$ of the solution v to the system

$$\begin{cases} \overline{P}v = g & \text{in } D(0,\varepsilon) \\ v = 0 & \text{on } \partial D(0,\varepsilon) \end{cases}. \tag{3.250}$$

In Proposition 3.18 we derived that the solution to Eq. (3.250) can be written in the form

$$v(\rho,\varphi) + \int_\rho^\varepsilon s^{-1} \int_0^s t h_0(t) dt ds = \sum_{k=1}^\infty l_k(\rho) e_k(\varphi), \tag{3.251}$$

in which

$$\begin{aligned} l_k(\rho) := A_k \rho^{\sqrt{\lambda_{e_k}}} + \frac{1}{2\sqrt{\lambda_{e_k}}} \rho^{\sqrt{\lambda_{e_k}}} \int_\varepsilon^\rho t^{1-\sqrt{\lambda_{e_k}}} h_k(t) dt \\ - \frac{1}{2\sqrt{\lambda_{e_k}}} \rho^{-\sqrt{\lambda_{e_k}}} \int_0^\rho t^{1+\sqrt{\lambda_{e_k}}} h_k(t) dt \end{aligned} \tag{3.252}$$

and

$$A_k := \frac{1}{2\sqrt{\lambda_{e_k}}} \varepsilon^{-2\sqrt{\lambda_{e_k}}} \int_0^\varepsilon t^{1+\sqrt{\lambda_{e_k}}} h_k(t)\, dt. \tag{3.253}$$

Lemma 3.19. *Let $l_1(\rho), \dots, l_M(\rho)$ be defined by Eq. (3.252). Then $\lim_{\rho\to 0^+} \frac{l_k(\rho)}{\rho^{\sqrt{\lambda_1}}}$ exists for $k = 1, \dots, M$. Furthermore,*

$$\lim_{\rho\to 0^+} \frac{l_k(\rho)}{\rho^{\sqrt{\lambda_1}}} = \frac{1}{2\sqrt{\lambda_1}} \varepsilon^{-2\sqrt{\lambda_1}} \int_0^\varepsilon t^{1+\sqrt{\lambda_1}} h_k(t)\, dt - \frac{1}{2\sqrt{\lambda_1}} \int_0^\varepsilon t^{1-\sqrt{\lambda_1}} h_k(t)\, dt \tag{3.254}$$

and there exists a $C > 0$ such that

$$\lim_{\rho\to 0^+} \frac{l_k(\rho)}{\rho^{\sqrt{\lambda_1}}} \leq C \|g\|_{L^2(D(0,\varepsilon))}. \tag{3.255}$$

Proof. We will show that $\lim_{\rho\to 0^+} \frac{l_k(\rho)}{\rho^{\sqrt{\lambda_1}}}$ exists for $k = 1, \dots, M$. Once this is proven we will define

$$\alpha_k := \lim_{\rho\to 0^+} \frac{l_k(\rho)}{\rho^{\sqrt{\lambda_1}}}. \tag{3.256}$$

Now, we need to show that $\frac{l_k(\rho)}{\rho^{\sqrt{\lambda_1}}}$ has a limit as $\rho \to 0^+$ for $k = 1, \dots, M$. It suffices to show that for any sequence $\{\rho_n\}_{n=1}^\infty$ with $\rho_n \to 0$,

$$\lim_{n\to\infty} \left| \frac{l_k(\rho_n)}{\rho_n^{\sqrt{\lambda_1}}} - \frac{l_k(\rho_{n+1})}{\rho_{n+1}^{\sqrt{\lambda_1}}} \right| = 0. \tag{3.257}$$

Recall that

$$\frac{l_k(\rho)}{\rho^{\sqrt{\lambda_1}}} = A_k + \frac{1}{2\sqrt{\lambda_1}} \int_\varepsilon^\rho t^{1-\sqrt{\lambda_1}} h_k(t)\, dt - \frac{1}{2\sqrt{\lambda_1}} \rho^{-2\sqrt{\lambda_1}} \int_0^\rho t^{1+\sqrt{\lambda_1}} h_k(t)\, dt \tag{3.258}$$

and

$$A_k := \frac{1}{2\sqrt{\lambda_1}} \varepsilon^{-2\sqrt{\lambda_1}} \int_0^\varepsilon t^{1+\sqrt{\lambda_1}} h_k(t)\, dt. \tag{3.259}$$

Using the triangle inequality, we compute

$$\begin{aligned} \left| \frac{l_k(\rho_n)}{\rho_n^{\sqrt{\lambda_1}}} - \frac{l_k(\rho_{n+1})}{\rho_{n+1}^{\sqrt{\lambda_1}}} \right| \leq \Big| A_k - A_k \Big| \\ + \Big| B_k(\rho_n) - B_k(\rho_{n+1}) \Big| \\ + \Big| C_k(\rho_n) - C_k(\rho_{n+1}) \Big|, \end{aligned} \tag{3.260}$$

in which

$$B_k(\rho) := \frac{1}{2\sqrt{\lambda_1}} \int_\varepsilon^\rho t^{1-\sqrt{\lambda_1}} h_k(t)\, dt \tag{3.261}$$

and

$$C_k(\rho) := -\frac{1}{2\sqrt{\lambda_1}} \rho^{-2\sqrt{\lambda_1}} \int_0^\rho t^{1+\sqrt{\lambda_1}} h_k(t)\, dt. \tag{3.262}$$

Clearly, $|A_k - A_k| = 0$. By the Cauchy–Schwarz inequality,

$$
\begin{aligned}
&\left|B_k(\rho_n) - B_k(\rho_{n+1})\right| \\
&= \left|\frac{1}{2\sqrt{\lambda_1}} \int_\varepsilon^{\rho_n} t^{1-\sqrt{\lambda_1}} h_k(t)\, dt - \frac{1}{2\sqrt{\lambda_1}} \int_\varepsilon^{\rho_{n+1}} t^{1-\sqrt{\lambda_1}} h_k(t)\, dt\right| && (3.263)\\
&= \left|\frac{1}{2\sqrt{\lambda_1}} \int_{\rho_{n+1}}^{\rho_n} t^{1-\sqrt{\lambda_1}} h_k(t)\, dt\right| && (3.264)\\
&\leq \frac{1}{2\sqrt{\lambda_1}} \int_{\rho_{n+1}}^{\rho_n} \left|t^{1-\sqrt{\lambda_1}} h_k(t)\right| dt && (3.265)\\
&\leq \frac{1}{2\sqrt{\lambda_1}} \sqrt{\int_{\rho_{n+1}}^{\rho_n} \left|t^{\frac{1}{2}-\sqrt{\lambda_1}}\right|^2 dt} \sqrt{\int_{\rho_{n+1}}^{\rho_n} \left|t^{\frac{1}{2}} h_k(t)\right|^2 dt} && (3.266)\\
&= \frac{1}{2\sqrt{\lambda_1}} \sqrt{\int_{\rho_{n+1}}^{\rho_n} t^{1-2\sqrt{\lambda_1}}\, dt} \sqrt{\int_{\rho_{n+1}}^{\rho_n} t\left|h_k(t)\right|^2 dt} && (3.267)\\
&= \frac{1}{2\sqrt{\lambda_1}} \sqrt{\frac{t^{2-2\sqrt{\lambda_1}}}{2-2\sqrt{\lambda_1}}\Big|_{\rho_{n+1}}^{\rho_n}} \sqrt{\int_{\rho_{n+1}}^{\rho_n} t\left|h_k(t)\right|^2 dt} && (3.268)\\
&\leq \frac{(max_{i\in\{1,\dots,N\}}\sigma_i)}{2\sqrt{\lambda_1}} \sqrt{\frac{(\rho_n)^{2-2\sqrt{\lambda_1}} - (\rho_{n+1})^{2-2\sqrt{\lambda_1}}}{2-2\sqrt{\lambda_1}}} \|g\|_{L^2(D(0,\varepsilon))} && (3.269)\\
&\xrightarrow[n\to\infty]{} 0. && (3.270)
\end{aligned}
$$

For the third term, using the triangle and Cauchy-Schwarz inequalities,

$$\begin{aligned}
&\left|C_k(\rho_n) - C_k(\rho_{n+1})\right| \\
&= \Big| - \frac{1}{2\sqrt{\lambda_1}}\rho_n^{-2\sqrt{\lambda_1}} \int_0^{\rho_n} t^{1+\sqrt{\lambda_1}} h_k(t)\, dt + \frac{1}{2\sqrt{\lambda_1}}\rho_{n+1}^{-2\sqrt{\lambda_1}} \int_0^{\rho_{n+1}} t^{1+\sqrt{\lambda_1}} h_k(t)\, dt \Big| && (3.271)\\
&= \frac{1}{2\sqrt{\lambda_1}} \Big| \rho_n^{-2\sqrt{\lambda_1}} \int_0^{\rho_n} t^{1+\sqrt{\lambda_1}} h_k(t)\, dt - \rho_{n+1}^{-2\sqrt{\lambda_1}} \int_0^{\rho_{n+1}} t^{1+\sqrt{\lambda_1}} h_k(t)\, dt \Big| && (3.272)\\
&\leq \frac{1}{2\sqrt{\lambda_1}}\rho_n^{-2\sqrt{\lambda_1}} \int_0^{\rho_n} \left| t^{1+\sqrt{\lambda_1}} h_k(t) \right| dt + \frac{1}{2\sqrt{\lambda_1}}\rho_{n+1}^{-2\sqrt{\lambda_1}} \int_0^{\rho_{n+1}} \left| t^{1+\sqrt{\lambda_1}} h_k(t) \right| dt && (3.273)\\
&\leq \frac{1}{2\sqrt{\lambda_1}}\rho_n^{-2\sqrt{\lambda_1}} \sqrt{\int_0^{\rho_n} |t^{\frac{1}{2}+\sqrt{\lambda_1}}|^2\, dt} \sqrt{\int_0^{\rho_n} \left| t^{\frac{1}{2}} h_k(t) \right|^2 dt} && (3.274)\\
&\quad + \frac{1}{2\sqrt{\lambda_1}}\rho_{n+1}^{-2\sqrt{\lambda_1}} \sqrt{\int_0^{\rho_{n+1}} |t^{\frac{1}{2}+\sqrt{\lambda_1}}|^2\, dt} \sqrt{\int_0^{\rho_{n+1}} \left| t^{\frac{1}{2}} h_k(t) \right|^2 dt} \\
&= \frac{1}{2\sqrt{\lambda_1}}\rho_n^{-2\sqrt{\lambda_1}} \sqrt{\frac{t^{2+2\sqrt{\lambda_1}}}{2+2\sqrt{\lambda_1}}\Big|_0^{\rho_n}} \sqrt{\int_0^{\rho_n} t \left| h_k(t) \right|^2 dt} && (3.275)\\
&\quad + \frac{1}{2\sqrt{\lambda_1}}\rho_{n+1}^{-2\sqrt{\lambda_1}} \sqrt{\frac{t^{2+2\sqrt{\lambda_1}}}{2+2\sqrt{\lambda_1}}\Big|_0^{\rho_{n+1}}} \sqrt{\int_0^{\rho_{n+1}} t \left| h_k(t) \right|^2 t dt} \\
&\leq \frac{(max_{i\in\{1,\ldots,N\}}\sigma_i)}{2\sqrt{\lambda_1}} \frac{(\rho_n)^{1-\sqrt{\lambda_1}} + (\rho_{n+1})^{1-\sqrt{\lambda_1}}}{\sqrt{2+2\sqrt{\lambda_1}}} \|g\|_{L^2(D(0,\varepsilon))}, && (3.276)
\end{aligned}$$

which converges to 0 as $n \to \infty$ because $1 - \sqrt{\lambda_1} > 0$. Thus,

$$\lim_{n\to\infty} \left| \frac{l_k(\rho_n)}{\rho_n^{\sqrt{\lambda_1}}} - \frac{l_k(\rho_{n+1})}{\rho_{n+1}^{\sqrt{\lambda_1}}} \right| = 0. \tag{3.277}$$

Hence, $\frac{l_k(\rho)}{\rho^{\sqrt{\lambda_1}}}$ has a limit as $\rho \to 0^+$ for $k = 1, \ldots, M$.

Our argument shows that

$$\alpha_k := \lim_{\rho\to 0^+} \frac{l_k(\rho)}{\rho^{\sqrt{\lambda_1}}} \tag{3.278}$$

$$= \lim_{\rho\to 0^+} \left[\frac{1}{2\sqrt{\lambda_1}}\varepsilon^{-2\sqrt{\lambda_1}} \int_0^\varepsilon t^{1+\sqrt{\lambda_1}} h_k(t)\, dt + \frac{1}{2\sqrt{\lambda_1}} \int_\varepsilon^\rho t^{1-\sqrt{\lambda_1}} h_k(t)\, dt \right. \tag{3.279}$$

$$\left. -\frac{1}{2\sqrt{\lambda_1}}\rho^{-2\sqrt{\lambda_1}} \int_0^\rho t^{1+\sqrt{\lambda_1}} h_k(t)\, dt\right]$$

$$= \frac{1}{2\sqrt{\lambda_1}}\varepsilon^{-2\sqrt{\lambda_1}} \int_0^\varepsilon t^{1+\sqrt{\lambda_1}} h_k(t)\, dt - \frac{1}{2\sqrt{\lambda_1}} \int_0^\varepsilon t^{1-\sqrt{\lambda_1}} h_k(t)\, dt. \tag{3.280}$$

By the Cauchy–Schwarz inequality,

$$\int_0^\varepsilon t^{1+\sqrt{\lambda_1}} h_k(t)\, dt \le \sqrt{\int_0^\varepsilon |t^{\frac{1}{2}+\sqrt{\lambda_1}}|^2\, dt}\sqrt{\int_0^\varepsilon |t^{\frac{1}{2}} h_k(t)|^2\, dt} \tag{3.281}$$

$$= \sqrt{\int_0^\varepsilon t^{1+2\sqrt{\lambda_1}}\, dt}\sqrt{\int_0^\varepsilon t|h_k(t)|^2\, dt} \tag{3.282}$$

$$= \sqrt{\frac{\varepsilon^{2+2\sqrt{\lambda_1}}}{2+2\sqrt{\lambda_1}}}\sqrt{\int_0^\varepsilon t|h_k(t)|^2\, dt} \tag{3.283}$$

and

$$\int_0^\varepsilon t^{1-\sqrt{\lambda_1}} h_k(t)\, dt \le \sqrt{\int_0^\varepsilon |t^{\frac{1}{2}-\sqrt{\lambda_1}}|^2\, dt}\sqrt{\int_0^\varepsilon |t^{\frac{1}{2}} h_k(t)|^2\, dt} \tag{3.284}$$

$$= \sqrt{\int_0^\varepsilon t^{1-2\sqrt{\lambda_1}}\, dt}\sqrt{\int_0^\varepsilon t|h_k(t)|^2\, dt} \tag{3.285}$$

$$= \sqrt{\frac{\varepsilon^{2-2\sqrt{\lambda_1}}}{2-2\sqrt{\lambda_1}}}\sqrt{\int_0^\varepsilon t|h_k(t)|^2\, dt}. \tag{3.286}$$

Hence, $\alpha_k \le \frac{(max_{i\in\{1,\dots,N\}}\sigma_i)}{2\sqrt{\lambda_1}}\left(\frac{1}{\sqrt{2+2\sqrt{\lambda_1}}} + \frac{1}{\sqrt{2-2\sqrt{\lambda_1}}}\right)\|g\|_{L^2(D(0,\varepsilon))}$.
Taking $C = \frac{(max_{i\in\{1,\dots,N\}}\sigma_i)}{2\sqrt{\lambda_1}}\left(\frac{1}{\sqrt{2+2\sqrt{\lambda_1}}} + \frac{1}{\sqrt{2-2\sqrt{\lambda_1}}}\right)$ completes the proof of Lemma 3.19. □

Proposition 3.20. *Let v be the solution to Eq. (3.250) where $g \in L^2(D(0,\varepsilon))$ and α_k be defined by Eq. (3.280). Let $\delta = \min(\sqrt{\lambda_2} - \sqrt{\lambda_1}, \frac{1}{3}(1-\sqrt{\lambda_1}))$ and*

$$D = (max_{i\in\{1,\dots,N\}}\sigma_i)\max\left(\frac{M}{\sqrt{\lambda_1}}\left(\frac{1}{\sqrt{2-2\sqrt{\lambda_1}}}+\frac{1}{\sqrt{2+2\sqrt{\lambda_1}}}\right),\right.$$
$$\left.\sqrt{\frac{5}{\lambda_2}\left(\frac{1+\frac{1}{2}\varepsilon^{2\sqrt{\lambda_2}-2}}{1+\sqrt{\lambda_2}}+\frac{9}{1-\sqrt{\lambda_1}}\right)}\right)\|g\|_{L^2(D(0,\varepsilon))}.$$

Consider the function

$$\mathcal{M}(\rho,\varphi) := \frac{v(\rho,\varphi)-v(0)}{\rho^{\sqrt{\lambda_1}}} - \sum_{k=1}^{M}\alpha_k e_k(\varphi). \tag{3.287}$$

Then for every $\rho \in (0,\varepsilon)$:

$$\left\|\mathcal{M}(\rho,\varphi)\right\|_{L^2(d\varphi)} \le \rho^{\delta} D. \tag{3.288}$$

Proof. Note that by the triangle inequality and the Plancherel theorem

$$\left\|\mathcal{M}(\rho,\varphi)\right\|_{L^2(d\varphi)} = \left\|\frac{v(\rho,\varphi)-v(0)}{\rho^{\sqrt{\lambda_1}}} - \sum_{k=1}^{M}\alpha_k e_k(\varphi)\right\|_{L^2(d\varphi)} \tag{3.289}$$

$$= \left\|\sum_{k=1}^{\infty}\frac{l_k(\rho)}{\rho^{\sqrt{\lambda_1}}}e_k(\varphi) - \sum_{k=1}^{M}\alpha_k e_k(\varphi)\right\|_{L^2(d\varphi)} \tag{3.290}$$

$$\le \left\|\sum_{k=1}^{M}\frac{l_k(\rho)}{\rho^{\sqrt{\lambda_1}}}e_k(\varphi) - \sum_{k=1}^{M}\alpha_k e_k(\varphi)\right\|_{L^2(d\varphi)} + \left\|\sum_{k=M+1}^{\infty}\frac{l_k(\rho)}{\rho^{\sqrt{\lambda_1}}}e_k(\varphi)\right\|_{L^2(d\varphi)} \tag{3.291}$$

$$\le \sum_{k=1}^{M}\left\|\frac{l_k(\rho)}{\rho^{\sqrt{\lambda_1}}}e_k(\varphi) - \alpha_k e_k(\varphi)\right\|_{L^2(d\varphi)} + \sqrt{\sum_{k=M+1}^{\infty}\frac{l_k^2(\rho)}{\rho^{2\sqrt{\lambda_1}}}}. \tag{3.292}$$

We seek to show that $\left\|\mathcal{M}(\rho,\varphi)\right\|_{L^2(d\varphi)} < \rho^{\delta}\cdot D$, for which by Eqs. (3.289) to (3.292) it suffices to show that for $k = 1\dots,M$

$$\left\|\frac{l_k(\rho)}{\rho^{\sqrt{\lambda_1}}}e_k(\varphi) - \alpha_k e_k(\varphi)\right\|_{L^2(d\varphi)} \le \frac{1}{2M}\rho^{\delta}\cdot D \tag{3.293}$$

and that

$$\sum_{k=M+1}^{\infty}\frac{l_k^2(\rho)}{\rho^{2\sqrt{\lambda_1}}} \le \frac{1}{4}\rho^{2\delta}\cdot D^2. \tag{3.294}$$

We first seek to show Eq. (3.293). By the triangle inequality, we have that

$$
\begin{aligned}
&\left\| \frac{l_k(\rho)}{\rho^{\sqrt{\lambda_1}}} e_k(\varphi) - \alpha_k e_k(\varphi) \right\|_{L^2(d\varphi)} \\
&= \sqrt{\int_0^{2\pi} \left| \frac{l_k(\rho)}{\rho^{\sqrt{\lambda_1}}} e_k(\varphi) - \alpha_k e_k(\varphi) \right|^2 d\varphi} && (3.295) \\
&= \sqrt{\left| \frac{l_k(\rho)}{\rho^{\sqrt{\lambda_1}}} - \alpha_k \right|^2 \int_0^{2\pi} |e_k(\varphi)|^2 \, d\varphi} && (3.296) \\
&= \left| \frac{l_k(\rho)}{\rho^{\sqrt{\lambda_1}}} - \alpha_k \right| && (3.297) \\
&= \Bigg| \frac{1}{2\sqrt{\lambda_1}} \varepsilon^{-2\sqrt{\lambda_1}} \int_0^{\varepsilon} t^{1+\sqrt{\lambda_1}} h_k(t) \, dt + \frac{1}{2\sqrt{\lambda_1}} \int_{\varepsilon}^{\rho} t^{1-\sqrt{\lambda_1}} h_k(t) \, dt && (3.298) \\
&\quad - \frac{1}{2\sqrt{\lambda_1}} \rho^{-2\sqrt{\lambda_1}} \int_0^{\rho} t^{1+\sqrt{\lambda_1}} h_k(t) \, dt - \alpha_k \Bigg| && (3.299) \\
&= \Bigg| \frac{1}{2\sqrt{\lambda_1}} \varepsilon^{-2\sqrt{\lambda_1}} \int_0^{\varepsilon} t^{1+\sqrt{\lambda_1}} h_k(t) \, dt - \frac{1}{2\sqrt{\lambda_1}} \int_0^{\varepsilon} t^{1-\sqrt{\lambda_1}} h_k(t) \, dt && (3.300) \\
&\quad + \frac{1}{2\sqrt{\lambda_1}} \int_0^{\rho} t^{1-\sqrt{\lambda_1}} h_k(t) \, dt \\
&\quad - \frac{1}{2\sqrt{\lambda_1}} \rho^{-2\sqrt{\lambda_1}} \int_0^{\rho} t^{1+\sqrt{\lambda_1}} h_k(t) \, dt - \alpha_k \Bigg| \\
&= \Bigg| \frac{1}{2\sqrt{\lambda_1}} \int_0^{\rho} t^{1-\sqrt{\lambda_1}} h_k(t) \, dt - \frac{1}{2\sqrt{\lambda_1}} \rho^{-2\sqrt{\lambda_1}} \int_0^{\rho} t^{1+\sqrt{\lambda_1}} h_k(t) \, dt \Bigg| && (3.301) \\
&\leq \frac{1}{2\sqrt{\lambda_1}} \int_0^{\rho} \left| t^{1-\sqrt{\lambda_1}} h_k(t) \right| dt + \frac{1}{2\sqrt{\lambda_1}} \rho^{-2\sqrt{\lambda_1}} \int_0^{\rho} \left| t^{1+\sqrt{\lambda_1}} h_k(t) \right| dt && (3.302)
\end{aligned}
$$

By the Cauchy–Schwarz inequality, we have that

$$\begin{aligned}
&\left\| \frac{l_k(\rho)}{\rho^{\sqrt{\lambda_1}}} e_k(\varphi) - \alpha_k e_k(\varphi) \right\|_{L^2(d\varphi)} \\
&\leq \frac{1}{2\sqrt{\lambda_1}} \sqrt{\int_0^\rho |t^{\frac{1}{2}-\sqrt{\lambda_1}}|^2 \, dt} \sqrt{\int_0^\rho |t^{\frac{1}{2}} h_k(t)|^2 \, dt} && (3.303) \\
&\quad + \frac{1}{2\sqrt{\lambda_1}} \rho^{-2\sqrt{\lambda_1}} \sqrt{\int_0^\rho |t^{\frac{1}{2}+\sqrt{\lambda_1}}|^2 \, dt} \sqrt{\int_0^\rho |t^{\frac{1}{2}} h_k(t)|^2 \, dt} \\
&= \frac{1}{2\sqrt{\lambda_1}} \sqrt{\int_0^\rho t^{1-2\sqrt{\lambda_1}} \, dt} \sqrt{\int_0^\rho t |h_k(t)|^2 \, dt} && (3.304) \\
&\quad + \frac{1}{2\sqrt{\lambda_1}} \rho^{-2\sqrt{\lambda_1}} \sqrt{\int_0^\rho t^{1+2\sqrt{\lambda_1}} \, dt} \sqrt{\int_0^\rho t |h_k(t)|^2 \, dt} \\
&= \frac{1}{2\sqrt{\lambda_1}} \sqrt{\frac{1}{2-2\sqrt{\lambda_1}} \rho^{2-2\sqrt{\lambda_1}}} \sqrt{\int_0^\rho t |h_k(t)|^2 \, dt} && (3.305) \\
&\quad + \frac{1}{2\sqrt{\lambda_1}} \rho^{-2\sqrt{\lambda_1}} \sqrt{\frac{1}{2+2\sqrt{\lambda_1}} \rho^{2+2\sqrt{\lambda_1}}} \sqrt{\int_0^\rho t |h_k(t)|^2 \, dt} \\
&\leq \frac{1}{2} \rho^{1-\sqrt{\lambda_1}} \frac{(max_{i\in\{1,\dots,N\}}\sigma_i)}{\sqrt{\lambda_1}} \left(\frac{1}{\sqrt{2-2\sqrt{\lambda_1}}} + \frac{1}{\sqrt{2+2\sqrt{\lambda_1}}} \right) \|g\|_{L^2(D(0,\varepsilon))} && (3.306) \\
&\leq \frac{1}{2M} \rho^\delta \cdot D, && (3.307)
\end{aligned}$$

in which $\delta = \min(\sqrt{\lambda_2} - \sqrt{\lambda_1}, \frac{1}{3}(1 - \sqrt{\lambda_1}))$ and

$$\begin{aligned}
D = (max_{i\in\{1,\dots,N\}}\sigma_i) \max \Bigg(&\frac{M}{\sqrt{\lambda_1}} \left(\frac{1}{\sqrt{2-2\sqrt{\lambda_1}}} + \frac{1}{\sqrt{2+2\sqrt{\lambda_1}}} \right), \\
&\sqrt{\frac{5}{\lambda_2} \left(\frac{1}{1+\sqrt{\lambda_2}} + \frac{9}{1-\sqrt{\lambda_1}} \right)} \Bigg) \|g\|_{L^2(D(0,\varepsilon))}.
\end{aligned}$$

Hence, $\left\| \frac{l_k(\rho)}{\rho^{\sqrt{\lambda_1}}} e_k(\varphi) - \alpha_k e_k(\varphi) \right\|_{L^2(d\varphi)} \leq \frac{1}{2M} \rho^\delta \cdot D$, proving Eq. (3.293).

We now turn our attention to showing Eq. (3.294). By Eq. (3.252), we seek to show that

$$\begin{aligned}
\sum_{k=M+1}^{\infty} \Bigg(&A_k \rho^{\sqrt{\lambda_{e_k}}-\sqrt{\lambda_1}} + \frac{1}{2\sqrt{\lambda_{e_k}}} \rho^{\sqrt{\lambda_{e_k}}-\sqrt{\lambda_1}} \int_\varepsilon^\rho t^{1-\sqrt{\lambda_{e_k}}} h_k(t) dt \qquad (3.308) \\
&- \frac{1}{2\sqrt{\lambda_{e_k}}} \rho^{-\sqrt{\lambda_{e_k}}-\sqrt{\lambda_1}} \int_0^\rho t^{1+\sqrt{\lambda_{e_k}}} h_k(t) dt \Bigg)^2 \leq \frac{1}{4} \rho^{2\delta} \cdot D^2.
\end{aligned}$$

We define

$$A(\rho) := \sum_{k=M+1}^{\infty} A_k^2 \rho^{2\sqrt{\lambda_{e_k}}-2\sqrt{\lambda_1}}, \tag{3.309}$$

$$B(\rho) := \sum_{k=M+1}^{\infty} \frac{1}{4\lambda_{e_k}} \rho^{2\sqrt{\lambda_{e_k}}-2\sqrt{\lambda_1}} \left(\int_{\varepsilon}^{\rho} t^{1-\sqrt{\lambda_{e_k}}} h_k(t) dt \right)^2, \tag{3.310}$$

$$C(\rho) := \sum_{k=M+1}^{\infty} \frac{1}{4\lambda_{e_k}} \rho^{-2\sqrt{\lambda_{e_k}}-2\sqrt{\lambda_1}} \left(\int_{0}^{\rho} t^{1+\sqrt{\lambda_{e_k}}} h_k(t) dt \right)^2. \tag{3.311}$$

It suffices to show that $|A(\rho)| + |B(\rho)| + |C(\rho)| \leq \frac{1}{5}\frac{1}{4}\rho^{2\delta} \cdot D^2$. Using Eq. (3.253) and the Cauchy–Schwarz inequality

$$|A(\rho)| = \sum_{k=M+1}^{\infty} \left(\frac{1}{2\sqrt{\lambda_{e_k}}} \varepsilon^{-2\sqrt{\lambda_{e_k}}} \int_0^{\varepsilon} t^{1+\sqrt{\lambda_{e_k}}} h_k(t)\, dt \right)^2 \rho^{2\sqrt{\lambda_{e_k}}-2\sqrt{\lambda_1}} \tag{3.312}$$

$$= \sum_{k=M+1}^{\infty} \frac{1}{4\lambda_{e_k}} \rho^{2\sqrt{\lambda_{e_k}}-2\sqrt{\lambda_1}} \varepsilon^{-4\sqrt{\lambda_{e_k}}} \int_0^{\varepsilon} |t^{\frac{1}{2}+\sqrt{\lambda_{e_k}}}|^2\, dt \int_0^{\varepsilon} |t^{\frac{1}{2}} h_k(t)|^2\, dt \tag{3.313}$$

$$= \sum_{k=M+1}^{\infty} \frac{1}{4\lambda_{e_k}} \rho^{2\sqrt{\lambda_{e_k}}-2\sqrt{\lambda_1}} \varepsilon^{-4\sqrt{\lambda_{e_k}}} \int_0^{\varepsilon} t^{1+2\sqrt{\lambda_{e_k}}}\, dt \int_0^{\varepsilon} t|h_k(t)|^2\, dt \tag{3.314}$$

$$= \sum_{k=M+1}^{\infty} \frac{1}{4\lambda_{e_k}} \rho^{2\sqrt{\lambda_{e_k}}-2\sqrt{\lambda_1}} \varepsilon^{-4\sqrt{\lambda_{e_k}}} \frac{\varepsilon^{2+2\sqrt{\lambda_{e_k}}}}{2+2\sqrt{\lambda_{e_k}}} \int_0^{\varepsilon} t|h_k(t)|^2\, dt \tag{3.315}$$

$$= \sum_{k=M+1}^{\infty} \frac{1}{4\lambda_{e_k}} \left(\frac{\rho}{\varepsilon}\right)^{2\sqrt{\lambda_{e_k}}-2} \frac{\rho^{2-2\sqrt{\lambda_1}}}{2+2\sqrt{\lambda_{e_k}}} \int_0^{\varepsilon} t|h_k(t)|^2\, dt. \tag{3.316}$$

We know that $\lambda_{e_k} \to \infty$ as $k \to \infty$. So there is only a finite number of k's for which $\lambda_{e_k} < 1$. Let that maximum k such that $\lambda_{e_k} < 1$ be K. Then considering the terms where $\lambda_{e_k} \geq 1$,

$$\sum_{k=K+1}^{\infty} \frac{1}{4\lambda_{e_k}} \left(\frac{\rho}{\varepsilon}\right)^{2\sqrt{\lambda_{e_k}}-2} \frac{\rho^{2-2\sqrt{\lambda_1}}}{2+2\sqrt{\lambda_{e_k}}} \int_0^{\varepsilon} t|h_k(t)|^2\, dt \tag{3.317}$$

$$\leq \rho^{2-2\sqrt{\lambda_1}} \frac{1}{4\lambda_2} \frac{1}{2+2\sqrt{\lambda_2}} \sum_{k=K+1}^{\infty} \int_0^{\varepsilon} t|h_k(t)|^2\, dt \tag{3.318}$$

$$\leq \rho^{2\delta_{A_1}} \cdot D_{A_1}^2, \tag{3.319}$$

in which $\delta_{A_1} = 1 - \sqrt{\lambda_1}$ and $D_{A_1} = \frac{(max_{i\in\{1,\dots,N\}}\sigma_i)}{2\sqrt{\lambda_2}} \frac{1}{\sqrt{2+2\sqrt{\lambda_2}}} \|g\|_{L^2(D(0,\varepsilon))}$. And considering the terms where $\lambda_{e_k} < 1$,

$$\sum_{k=M+1}^{K} \frac{1}{4\lambda_{e_k}} \left(\frac{\rho}{\varepsilon}\right)^{2\sqrt{\lambda_{e_k}}-2} \frac{\rho^{2-2\sqrt{\lambda_1}}}{2+2\sqrt{\lambda_{e_k}}} \int_0^{\varepsilon} t|h_k(t)|^2\, dt \tag{3.320}$$

$$\leq \frac{1}{4\lambda_2} \frac{1}{2+2\sqrt{\lambda_2}} \sum_{k=M+1}^{K} \rho^{2\sqrt{\lambda_{e_k}}-2\sqrt{\lambda_1}} \varepsilon^{2-2\sqrt{\lambda_{e_k}}} \int_0^{\varepsilon} t|h_k(t)|^2\, dt \tag{3.321}$$

$$\leq \rho^{2\sqrt{\lambda_2}-2\sqrt{\lambda_1}} \varepsilon^{2\sqrt{\lambda_2}-2} \frac{1}{4\lambda_2} \frac{1}{2+2\sqrt{\lambda_2}} \sum_{k=M+1}^{K} \int_0^{\varepsilon} t|h_k(t)|^2\, dt \tag{3.322}$$

$$\leq \rho^{2\delta_{A_2}} \cdot D_{A_2}^2, \tag{3.323}$$

in which $\delta_{A_2} = \sqrt{\lambda_2} - \sqrt{\lambda_1}$ and $D_{A_2} = \frac{(max_{i\in\{1,\dots,N\}}\sigma_i)}{2\sqrt{\lambda_2}} \frac{\varepsilon^{\sqrt{\lambda_2}-1}}{\sqrt{2+2\sqrt{\lambda_2}}} \|g\|_{L^2(D(0,\varepsilon))}$. Hence,

$$|A(\rho)| = \sum_{k=M+1}^{\infty} \frac{1}{4\lambda_{e_k}} \left(\frac{\rho}{\varepsilon}\right)^{2\sqrt{\lambda_{e_k}}-2} \frac{\rho^{2-2\sqrt{\lambda_1}}}{2+2\sqrt{\lambda_{e_k}}} \int_0^{\varepsilon} t|h_k(t)|^2\, dt \tag{3.324}$$

$$\leq \rho^{2\delta_A} \cdot D_A^2, \tag{3.325}$$

in which $\delta_A = \min\{\delta_{A_1}, \delta_{A_2}\} = \min\{\sqrt{\lambda_2} - \sqrt{\lambda_1}, 1 - \sqrt{\lambda_1}\} > 0$ and $D_A = \sqrt{D_{A_1}^2 + D_{A_2}^2} = \frac{(max_{i\in\{1,\dots,N\}}\sigma_i)}{2\sqrt{\lambda_2}} \frac{\sqrt{1+\varepsilon^{2\sqrt{\lambda_2}-2}}}{\sqrt{2+2\sqrt{\lambda_2}}} \|g\|_{L^2(D(0,\varepsilon))} > 0$.

Using the Cauchy–Schwarz inequality and noting that all the terms in the sum in Eq. (3.310) are positive,

$$|B(\rho)| = \sum_{k=M+1}^{\infty} \left| \frac{1}{4\lambda_{e_k}} \rho^{2\sqrt{\lambda_{e_k}}-2\sqrt{\lambda_1}} \left(\int_{\varepsilon}^{\rho} t^{1-\sqrt{\lambda_{e_k}}} h_k(t) dt \right)^2 \right| \tag{3.326}$$

$$\leq \sum_{k=M+1}^{\infty} \frac{1}{4\lambda_{e_k}} \left| \rho^{2\sqrt{\lambda_{e_k}}-2\sqrt{\lambda_1}} \right| \cdot \left| \int_{\rho}^{\varepsilon} |t^{\frac{1}{2}-\sqrt{\lambda_{e_k}}}|^2 dt \right| \cdot \left| \int_{\rho}^{\varepsilon} |t^{\frac{1}{2}} h_k(t)|^2 dt \right| \tag{3.327}$$

$$= \sum_{k=M+1}^{\infty} \frac{1}{4\lambda_{e_k}} \rho^{2\sqrt{\lambda_{e_k}}-2\sqrt{\lambda_1}} \left| \int_{\rho}^{\varepsilon} t^{1-2\sqrt{\lambda_{e_k}}} dt \right| \int_{\rho}^{\varepsilon} t|h_k(t)|^2 dt. \tag{3.328}$$

Let $\eta = 1 - \sqrt{\lambda_1} > 0$. We split the sum into two parts: one part containing the terms where $|\sqrt{\lambda_{e_k}} - 1| \geq \frac{\eta}{3}$ and one part containing the terms where $|\sqrt{\lambda_{e_k}} - 1| < \frac{\eta}{3}$:

$$|B(\rho)| \leq \sum_{\substack{k \geq M+1 \\ |\sqrt{\lambda_{e_k}}-1| \geq \frac{\eta}{3}}} \frac{1}{4\lambda_{e_k}} \rho^{2\sqrt{\lambda_{e_k}}-2\sqrt{\lambda_1}} \Big| \int_\rho^\varepsilon t^{1-2\sqrt{\lambda_{e_k}}} dt \Big| \int_\rho^\varepsilon t |h_k(t)|^2 dt \tag{3.329}$$

$$+ \sum_{\substack{k \geq M+1 \\ |\sqrt{\lambda_{e_k}}-1| < \frac{\eta}{3}}} \frac{1}{4\lambda_{e_k}} \rho^{2\sqrt{\lambda_{e_k}}-2\sqrt{\lambda_1}} \Big| \int_\rho^\varepsilon t^{1-2\sqrt{\lambda_{e_k}}} dt \Big| \int_\rho^\varepsilon t |h_k(t)|^2 dt.$$

Firstly, we consider the terms where $|\sqrt{\lambda_{e_k}} - 1| \geq \frac{\eta}{3}$ (which implies $\frac{1}{|2-2\sqrt{\lambda_{e_k}}|} \leq \frac{3}{2\eta}$):

$$\sum_{\substack{k \geq M+1 \\ |\sqrt{\lambda_{e_k}}-1| \geq \frac{\eta}{3}}} \frac{1}{4\lambda_{e_k}} \rho^{2\sqrt{\lambda_{e_k}}-2\sqrt{\lambda_1}} \Big| \frac{\varepsilon^{2-2\sqrt{\lambda_{e_k}}} - \rho^{2-2\sqrt{\lambda_{e_k}}}}{2-2\sqrt{\lambda_{e_k}}} \Big| \int_\rho^\varepsilon t |h_k(t)|^2 dt$$

$$\leq \sum_{\substack{k \geq M+1 \\ |\sqrt{\lambda_{e_k}}-1| \geq \frac{\eta}{3}}} \frac{3}{8\lambda_{e_k}\eta} \rho^{2\sqrt{\lambda_{e_k}}-2\sqrt{\lambda_1}} \Big| \varepsilon^{2-2\sqrt{\lambda_{e_k}}} - \rho^{2-2\sqrt{\lambda_{e_k}}} \Big| \int_\rho^\varepsilon t |h_k(t)|^2 dt \tag{3.330}$$

$$\leq \sum_{\substack{k \geq M+1 \\ |\sqrt{\lambda_{e_k}}-1| \geq \frac{\eta}{3}}} \frac{3}{8\lambda_{e_k}\eta} \rho^{2\sqrt{\lambda_{e_k}}-2\sqrt{\lambda_1}} \left(\left| \varepsilon^{2-2\sqrt{\lambda_{e_k}}} \right| + \left| \rho^{2-2\sqrt{\lambda_{e_k}}} \right| \right) \int_\rho^\varepsilon t |h_k(t)|^2 dt \tag{3.331}$$

$$\leq \sum_{\substack{k \geq M+1 \\ |\sqrt{\lambda_{e_k}}-1| \geq \frac{\eta}{3}}} \frac{3}{8\lambda_{e_k}\eta} \rho^{2\sqrt{\lambda_{e_k}}-2\sqrt{\lambda_1}} \left(2 + 2\rho^{2-2\sqrt{\lambda_{e_k}}} \right) \int_\rho^\varepsilon t |h_k(t)|^2 dt \tag{3.332}$$

$$= \sum_{\substack{k \geq M+1 \\ |\sqrt{\lambda_{e_k}}-1| \geq \frac{\eta}{3}}} \frac{3}{4\lambda_{e_k}\eta} \left(\rho^{2\sqrt{\lambda_{e_k}}-2\sqrt{\lambda_1}} + \rho^{2-2\sqrt{\lambda_1}} \right) \int_\rho^\varepsilon t |h_k(t)|^2 dt \tag{3.333}$$

$$\leq \rho^{2\min(\sqrt{\lambda_2}-\sqrt{\lambda_1}, 1-\sqrt{\lambda_1})} \frac{3}{2\lambda_2\eta} \sum_{\substack{k \geq M+1 \\ |\sqrt{\lambda_{e_k}}-1| \geq \frac{\eta}{3}}} \int_\rho^\varepsilon t |h_k(t)|^2 dt \tag{3.334}$$

$$\leq \rho^{2\min(\sqrt{\lambda_2}-\sqrt{\lambda_1}, 1-\sqrt{\lambda_1})} \frac{3}{2\lambda_2\eta} \sum_{\substack{k \geq M+1 \\ |\sqrt{\lambda_{e_k}}-1| \geq \frac{\eta}{3}}} \int_\rho^\varepsilon t |h_k(t)|^2 dt \tag{3.335}$$

$$\leq \rho^{2\delta_{B_1}} D_{B_1}^2, \tag{3.336}$$

in which $\delta_{B_1} = \min(\sqrt{\lambda_2} - \sqrt{\lambda_1}, 1 - \sqrt{\lambda_1}) > 0$ and
$D_{B_1} = (max_{i\in\{1,\dots,N\}}\sigma_i)\sqrt{\frac{3}{2\lambda_2\eta}}\|g\|_{L^2(D(0,\varepsilon))} > 0$.

Secondly, we consider the terms where $|\sqrt{\lambda_{e_k}} - 1| < \frac{\eta}{3}$, *i.e.*, $1 - \frac{\eta}{3} < \sqrt{\lambda_{e_k}} < 1 + \frac{\eta}{3}$. Then since $\rho \in (0,1)$ and $\sqrt{\lambda_{e_k}} > 1 - \frac{\eta}{3}$,

$$\rho^{2\sqrt{\lambda_{e_k}}-2} < \rho^{2(1-\frac{\eta}{3})-2} \tag{3.337}$$

$$= \rho^{-\frac{2\eta}{3}}. \tag{3.338}$$

Since $\rho \in (0,1)$ and $\sqrt{\lambda_{e_k}} < 1 + \frac{\eta}{3}$,

$$\Big|\int_\rho^\varepsilon t^{1-2\sqrt{\lambda_{e_k}}}dt\Big| < \Big|\int_\rho^\varepsilon t^{1-2(1+\frac{\eta}{3})}dt\Big| \tag{3.339}$$

$$= \Big|\int_\rho^\varepsilon t^{(-1-\frac{2\eta}{3})}dt\Big| \tag{3.340}$$

$$= \Big|\frac{t^{-\frac{2\eta}{3}}}{-\frac{2\eta}{3}}\Big|_\rho^\varepsilon \tag{3.341}$$

$$= \Big|\frac{\varepsilon^{-\frac{2\eta}{3}}}{-\frac{2\eta}{3}} + \frac{\rho^{-\frac{2\eta}{3}}}{\frac{2\eta}{3}}\Big| \tag{3.342}$$

$$\leq \Big|\frac{\varepsilon^{-\frac{2\eta}{3}}}{-\frac{2\eta}{3}}\Big| + \Big|\frac{\rho^{-\frac{2\eta}{3}}}{\frac{2\eta}{3}}\Big| \tag{3.343}$$

$$\leq \frac{3\rho^{-\frac{2\eta}{3}}}{\eta}. \tag{3.344}$$

By combining Eqs. (3.338) and (3.344) we get the bound

$$\sum_{\substack{k\geq M+1\\ |\sqrt{\lambda_{e_k}}-1|<\frac{\eta}{3}}} \frac{1}{4\lambda_{e_k}}\rho^{2\sqrt{\lambda_{e_k}}-2\sqrt{\lambda_1}}\Big|\int_\rho^\varepsilon t^{1-2\sqrt{\lambda_{e_k}}}dt\Big|\int_\rho^\varepsilon t|h_k(t)|^2dt$$

$$\leq \sum_{\substack{k\geq M+1\\ |\sqrt{\lambda_{e_k}}-1|<\frac{\eta}{3}}} \frac{1}{4\lambda_{e_k}}\rho^{-\frac{2\eta}{3}}\cdot\rho^{2-2\sqrt{\lambda_1}}\cdot\frac{3\rho^{-\frac{2\eta}{3}}}{\eta}\int_\rho^\varepsilon t|h_k(t)|^2dt \tag{3.345}$$

$$\leq \rho^{2-2\sqrt{\lambda_1}-\frac{4\eta}{3}}\frac{3}{4\lambda_2\eta}\sum_{\substack{k\geq M+1\\ |\sqrt{\lambda_{e_k}}-1|<\frac{\eta}{3}}}\int_\rho^\varepsilon t|h_k(t)|^2dt \tag{3.346}$$

$$\leq \rho^{2\delta_{B_2}}D_{B_2}^2, \tag{3.347}$$

in which $\delta_{B_2} = 1 - \sqrt{\lambda_1} - \frac{2\eta}{3} = \frac{1}{3}\left(1 - \sqrt{\lambda_1}\right) > 0$ and
$D_{B_2} = (max_{i\in\{1,\dots,N\}}\sigma_i)\sqrt{\frac{3}{4\lambda_2\eta}}\|g\|_{L^2(D(0,\varepsilon))} > 0$.

Combining Eqs. (3.329), (3.336), and (3.347) yields the bound

$$|B(\rho)| \leq \rho^{2\delta_{B_1}} D_{B_1}^2 + \rho^{2\delta_{B_2}} D_{B_2}^2 \tag{3.348}$$

$$\leq \rho^{2\delta_B} D_B^2, \tag{3.349}$$

in which $\delta_B = \min\{\delta_{B_1}, \delta_{B_2}\} = \min\{\sqrt{\lambda_2} - \sqrt{\lambda_1}, \frac{1}{3}\left(1 - \sqrt{\lambda_1}\right)\} > 0$ and $D_B = \sqrt{D_{B_1}^2 + D_{B_2}^2} = (max_{i\in\{1,\dots,N\}}\sigma_i)\frac{3}{2\sqrt{\lambda_2\eta}}\|g\|_{L^2(D(0,\varepsilon))} > 0$.

Using the Cauchy–Schwarz inequality

$$|C(\rho)| = \sum_{k=M+1}^{\infty} \frac{1}{4\lambda_{e_k}} \rho^{-2\sqrt{\lambda_{e_k}}-2\sqrt{\lambda_1}} \left(\int_0^\rho t^{1+\sqrt{\lambda_{e_k}}} h_k(t)dt\right)^2 \tag{3.350}$$

$$\leq \sum_{k=M+1}^{\infty} \frac{1}{4\lambda_{e_k}} \rho^{-2\sqrt{\lambda_{e_k}}-2\sqrt{\lambda_1}} \int_0^\rho |t^{\frac{1}{2}+\sqrt{\lambda_{e_k}}}|^2 dt \int_0^\rho t|h_k(t)|^2 dt \tag{3.351}$$

$$= \sum_{k=M+1}^{\infty} \frac{1}{4\lambda_{e_k}} \rho^{-2\sqrt{\lambda_{e_k}}-2\sqrt{\lambda_1}} \int_0^\rho t^{1+2\sqrt{\lambda_{e_k}}} dt \int_0^\rho t|h_k(t)|^2 dt \tag{3.352}$$

$$= \sum_{k=M+1}^{\infty} \frac{1}{4\lambda_{e_k}} \rho^{-2\sqrt{\lambda_{e_k}}-2\sqrt{\lambda_1}} \frac{1}{2+2\sqrt{\lambda_{e_k}}} \rho^{2+2\sqrt{\lambda_{e_k}}} \int_0^\rho t|h_k(t)|^2 dt \tag{3.353}$$

$$= \rho^{2-2\sqrt{\lambda_1}} \sum_{k=M+1}^{\infty} \frac{1}{4\lambda_{e_k}} \frac{1}{2+2\sqrt{\lambda_{e_k}}} \int_0^\rho t|h_k(t)|^2 dt \tag{3.354}$$

$$\leq \rho^{2-2\sqrt{\lambda_1}} \frac{1}{4\lambda_2} \frac{1}{2+2\sqrt{\lambda_2}} \sum_{k=M+1}^{\infty} \int_0^\varepsilon t|h_k(t)|^2 dt \tag{3.355}$$

$$\leq \rho^{2\delta_C} \cdot D_C^2, \tag{3.356}$$

in which $\delta_C = 1 - \sqrt{\lambda_1}$ and $D_C = \frac{1}{2\sqrt{\lambda_2}} \frac{(max_{i\in\{1,\dots,N\}}\sigma_i)}{\sqrt{2+2\sqrt{\lambda_2}}} \|g\|_{L^2(D(0,\varepsilon))}$.

Note that

$$= \sqrt{5 \cdot 4\left(D_A^2 + D_B^2 + D_C^2\right)} \tag{3.357}$$

$$= (max_{i\in\{1,\dots,N\}}\sigma_i)\sqrt{5 \cdot 4\left(\frac{1}{4\lambda_2}\frac{1+\varepsilon^{2\sqrt{\lambda_2}-2}}{2+2\sqrt{\lambda_2}} + \frac{9}{4\lambda_2\eta} + \frac{1}{4\lambda_2}\frac{1}{2+2\sqrt{\lambda_2}}\right)} \tag{3.358}$$

$$= (max_{i\in\{1,\dots,N\}}\sigma_i)\sqrt{\frac{5}{\lambda_2}\left(\frac{1+\frac{1}{2}\varepsilon^{2\sqrt{\lambda_2}-2}}{1+\sqrt{\lambda_2}} + \frac{9}{1-\sqrt{\lambda_1}}\right)}. \tag{3.359}$$

Now, choosing

$$\delta = \min\{\delta_A, \delta_B, \delta_C\} \tag{3.360}$$

$$= \min\left\{\sqrt{\lambda_2} - \sqrt{\lambda_1}, \frac{1}{3}\left(1 - \sqrt{\lambda_1}\right)\right\} \tag{3.361}$$

and

$$D = (max_{i\in\{1,\dots,N\}}\sigma_i)\max\left\{\frac{M}{\sqrt{\lambda_1}}\left(\frac{1}{\sqrt{2-2\sqrt{\lambda_1}}} + \frac{1}{\sqrt{2+2\sqrt{\lambda_1}}}\right),\right.$$
$$\left.\sqrt{5\cdot 4\left(D_A^2 + D_B^2 + D_C^2\right)}\right\}\|g\|_{L^2(D(0,\varepsilon))} \tag{3.362}$$

$$= (max_{i\in\{1,\dots,N\}}\sigma_i)\max\left\{\frac{M}{\sqrt{\lambda_1}}\left(\frac{1}{\sqrt{2-2\sqrt{\lambda_1}}} + \frac{1}{\sqrt{2+2\sqrt{\lambda_1}}}\right),\right.$$
$$\left.\sqrt{\frac{5}{\lambda_2}\left(\frac{1+\frac{1}{2}\varepsilon^{2\sqrt{\lambda_2}-2}}{1+\sqrt{\lambda_2}} + \frac{9}{1-\sqrt{\lambda_1}}\right)}\right\}\|g\|_{L^2(D(0,\varepsilon))} \tag{3.363}$$

allows us to show Eq. (3.294), completing our proof of Proposition 3.20. □

We will use Proposition 3.20 to prove the corollary that $\tilde{u}$ as defined by the Neumann series in Eq. (3.208) has the same decomposition.

Corollary 3.21. *Let $\tilde{u}$ be as defined as in Eq. (3.208). Assume the following:*

$$\overline{P}^{-1} : L^2(D(0,\varepsilon)) \to \dot{H}_1^2(D(0,\varepsilon))$$
$$\tilde{P} : \dot{H}_1^2(D(0,\varepsilon)) \to L^2(D(0,\varepsilon))$$
$$\|\overline{P}^{-1}\tilde{P}\|_{\dot{H}_1^2(D(0,\varepsilon))\to\dot{H}_1^2(D(0,\varepsilon))} < 1.$$

Let $\delta = \min(\sqrt{\lambda_2} - \sqrt{\lambda_1}, \frac{1}{3}\left(1 - \sqrt{\lambda_1}\right))$. Then there exist $(\alpha_1^*, \dots, \alpha_M^*) \in \mathbb{R}^M$ such that

$$\|(\tilde{u}(\rho,\varphi) - \tilde{u}(0))\rho^{-\sqrt{\lambda_1}} - \sum_{i=1}^{M}\alpha_i^* e_i(\theta)\|_{L^2(d\varphi)} \leq \rho^{\delta}\cdot D_* \tag{3.364}$$

for some $D_* > 0$. Furthermore, $\alpha_1^*, \ldots, \alpha_M^*$, and D_* are bounded by $C\frac{1}{1-\varepsilon}\|\tilde{P}\overline{u}\|_{L^2(D(0,\varepsilon))}$ for

$$C = (max_{i\in\{1,\ldots,N\}}\sigma_i)\max\left(\frac{M}{\sqrt{\lambda_1}}\left(\frac{1}{\sqrt{2-2\sqrt{\lambda_1}}}+\frac{1}{\sqrt{2+2\sqrt{\lambda_1}}}\right),\right.$$
$$\left.\sqrt{\frac{5}{\lambda_2}\left(\frac{1+\frac{1}{2}\varepsilon^{2\sqrt{\lambda_2}-2}}{1+\sqrt{\lambda_2}}+\frac{9}{1-\sqrt{\lambda_1}}\right)}\right).$$

Proof. From Lemma 3.15, we can write $\tilde{u}$ as a Neumann series

$$\tilde{u} = -\left[I+\sum_{j=1}^{\infty}(-1)^j(\overline{P}^{-1}\tilde{P})^j\right]\overline{P}^{-1}\tilde{P}(\overline{u}). \tag{3.365}$$

From this series representation of $\tilde{u}$, we can write $\tilde{u} = \sum_{k=0}^{\infty}\tilde{u}_k$ in which

$$\tilde{u}_k = (-1)^{k+1}\left(\overline{P}^{-1}\tilde{P}\right)^k\overline{P}^{-1}\tilde{P}\overline{u}. \tag{3.366}$$

We note that

$$\overline{P}\tilde{u}_k = \overline{P}(-1)^{k+1}\left(\overline{P}^{-1}\tilde{P}\right)^k\overline{P}^{-1}\tilde{P}\overline{u} \tag{3.367}$$
$$= (-1)^{k+1}\tilde{P}\left(\overline{P}^{-1}\tilde{P}\right)^{k-1}\overline{P}^{-1}\tilde{P}\overline{u} \tag{3.368}$$
$$= (-1)^{k+1}\left(\tilde{P}\overline{P}^{-1}\right)^k\tilde{P}\overline{u}. \tag{3.369}$$

By defining $g_k := (-1)^{k+1}\left(\tilde{P}\overline{P}^{-1}\right)^k\tilde{P}\overline{u}$, we have the system

$$\begin{cases}\overline{P}\tilde{u}_k = g_k & \text{in } D(0,\varepsilon)\\ \tilde{u}_k = 0 & \text{on } \partial D(0,\varepsilon)\end{cases} \tag{3.370}$$

for each $k \geq 0$.

We can bound the L^2-norm of g_k on $D(0,\varepsilon)$ as follows

$$\|g_k\|_{L^2(D(0,\varepsilon))} = \|\left(\tilde{P}\overline{P}^{-1}\right)^k g_0\|_{L^2(D(0,\varepsilon))} \tag{3.371}$$
$$\leq \|\left(\tilde{P}\overline{P}^{-1}\right)\|^k_{L^2(D(0,\varepsilon))\to L^2(D(0,\varepsilon))}\|g_0\|_{L^2(D(0,\varepsilon))} \tag{3.372}$$
$$\leq \varepsilon^k\|g_0\|_{L^2(D(0,\varepsilon))} \tag{3.373}$$
$$= \varepsilon^k\|\tilde{P}\overline{u}\|_{L^2(D(0,\varepsilon))}. \tag{3.374}$$

Then by invoking Proposition 3.20 as well as (3.247) we get that for each $k \geq 0$, there exist $(\alpha_{1,k}, \ldots, \alpha_{M,k}) \in \mathbb{R}^M$ such that $\|(\tilde{u}_k(\rho,\varphi) - \tilde{u}_k(0))\rho^{-\sqrt{\lambda_1}} - \sum_{i=1}^{M} \alpha_{i,k} e_i(\theta)\|_{L^2(d\varphi)} \leq \rho^{\delta} \cdot D_k$ for $\delta = \min(\sqrt{\lambda_2} - \sqrt{\lambda_1}, \frac{1}{3}(1 - \sqrt{\lambda_1}))$ and $\alpha_{1,k}, \ldots, \alpha_{M,k}$, and D_k are bounded by $C\|g_k\|_{L^2(D(0,\varepsilon))}$ for

$$C = (max_{i\in\{1,\ldots,N\}}\sigma_i) \max\left(\frac{M}{\sqrt{\lambda_1}}\left(\frac{1}{\sqrt{2-2\sqrt{\lambda_1}}} + \frac{1}{\sqrt{2+2\sqrt{\lambda_1}}}\right), \sqrt{\frac{5}{\lambda_2}\left(\frac{1+\frac{1}{2}\varepsilon^{2\sqrt{\lambda_2}-2}}{1+\sqrt{\lambda_2}} + \frac{9}{1-\sqrt{\lambda_1}}\right)}\right).$$

First note that $\tilde{u}(0) = \sum_{k\geq 0} \tilde{u}_k(0)$, and the latter series converges, in view of bound (3.247) and the fact that $\sum_{k\geq 0} \|g_k\|_{L^2(D(0,\epsilon))} < \infty$.

We choose

$$\alpha_i^* = \sum_{k\geq 0} \alpha_{i,k} \tag{3.375}$$

whose sum converges because of Eq. (3.374)

$$\sum_{k\geq 0} \alpha_{i,k} \leq \sum_{k\geq 0} C\|g_k\|_{L^2(D(0,\varepsilon))} \tag{3.376}$$

$$\leq \sum_{k\geq 0} C\varepsilon^k \|\tilde{P}\overline{u}\|_{L^2(D(0,\varepsilon))} \tag{3.377}$$

$$= C\frac{1}{1-\varepsilon}\|\tilde{P}\overline{u}\|_{L^2(D(0,\varepsilon))}. \tag{3.378}$$

We compute using Eq. (3.374)

$$\begin{aligned}
&\|(\tilde{u}(\rho,\varphi)-\tilde{u}(0))\rho^{-\sqrt{\lambda_1}}-\sum_{i=1}^{M}\alpha_i^* e_i(\theta)\|_{L^2(d\varphi)} \\
&= \left\| \sum_{k\geq 0}\left((\tilde{u}_k(\rho,\varphi)-\tilde{u}_k(0))\rho^{-\sqrt{\lambda_1}}-\sum_{i=1}^{M}\alpha_{i,k}e_i(\theta)\right)\right\|_{L^2(d\varphi)} && (3.379)\\
&\leq \sum_{k\geq 0}\left\|(\tilde{u}_k(\rho,\varphi)-\tilde{u}_k(0))\rho^{-\sqrt{\lambda_1}}-\sum_{i=1}^{M}\alpha_{i,k}e_i(\theta)\right\|_{L^2(d\varphi)} && (3.380)\\
&\leq \sum_{k\geq 0}\rho^{\delta}\cdot D_k && (3.381)\\
&\leq \sum_{k\geq 0}\rho^{\delta}\cdot C\|g_k\|_{L^2(D(0,\varepsilon))} && (3.382)\\
&\leq \sum_{k\geq 0}\rho^{\delta}\cdot C\varepsilon^k\|\tilde{P}\overline{u}\|_{L^2(D(0,\varepsilon))} && (3.383)\\
&= \rho^{\delta}\cdot C\frac{1}{1-\varepsilon}\|\tilde{P}\overline{u}\|_{L^2(D(0,\varepsilon))} && (3.384)\\
&= \rho^{\delta}\cdot D_* && (3.385)
\end{aligned}$$

in which $D_* = C\frac{1}{1-\varepsilon}\|\tilde{P}\overline{u}\|_{L^2(D(0,\varepsilon))}$. Thus, for ε fixed, the Neumann series for $\tilde{u}$ divided by $\rho^{\sqrt{\lambda_1}}$ and measured in $L^2(d\varphi)$ converges as $\rho \to 0^+$. □

3.3 NUMERICAL RESULTS FOR GENERAL OVERLAPPING REGIONS

We consider general overlapping regions of constant conductivity. Figures 3.4 and 3.5 show the conductivity σ_{in} for the problem and potential u computed using our solver for several test cases. Figure 3.6 shows the automatically selected adaptive grid (black dots are the quadrature nodes, red lines are the panel boundaries, black curves are interfaces) for a test case.

3.3.1 *Data Structure for Conductivities*

In the case of non-overlapping regions of constant conductivity, we used a tree structure for the regions of constant conductivity, where each region i of conductivity σ_i had a unique parent region p_i of conductivity σ_{p_i}. Now, in the overlapping region case, every grid point on an interface has a corresponding inner conductivity σ_{in} and outer conductivity σ_{out}.

We give every curve a positive counterclockwise orientation. For each interface $\partial\Omega_i$, we compute $\sigma_{\text{out,background}}$ which is defined to be the contribution to σ_{out} from any interface that does not intersect our chosen

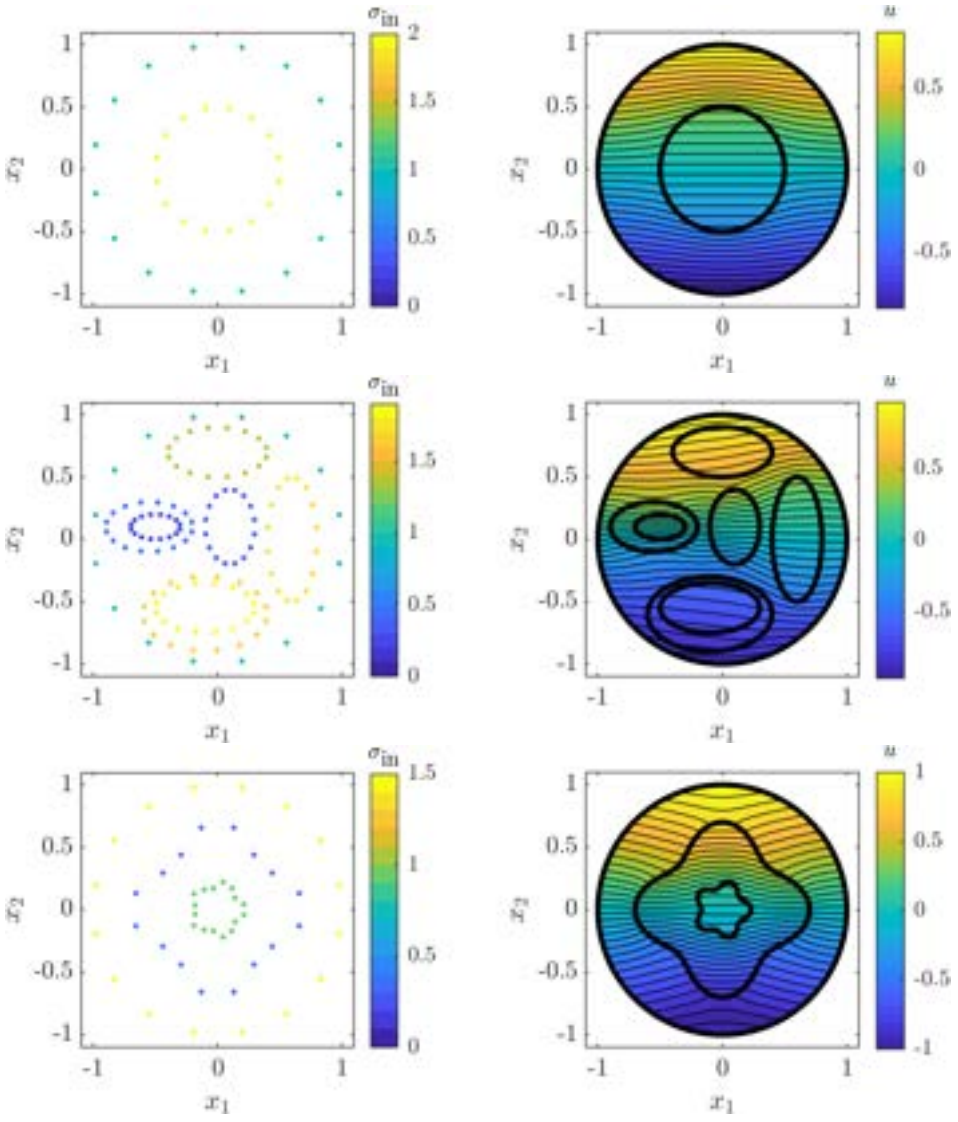

Figure 3.4: Conductivity σ for the problem (left) and potential u computed using our solver (right) for different test cases. The Neumann boundary data is $g(\theta) = \sin(\theta)$.

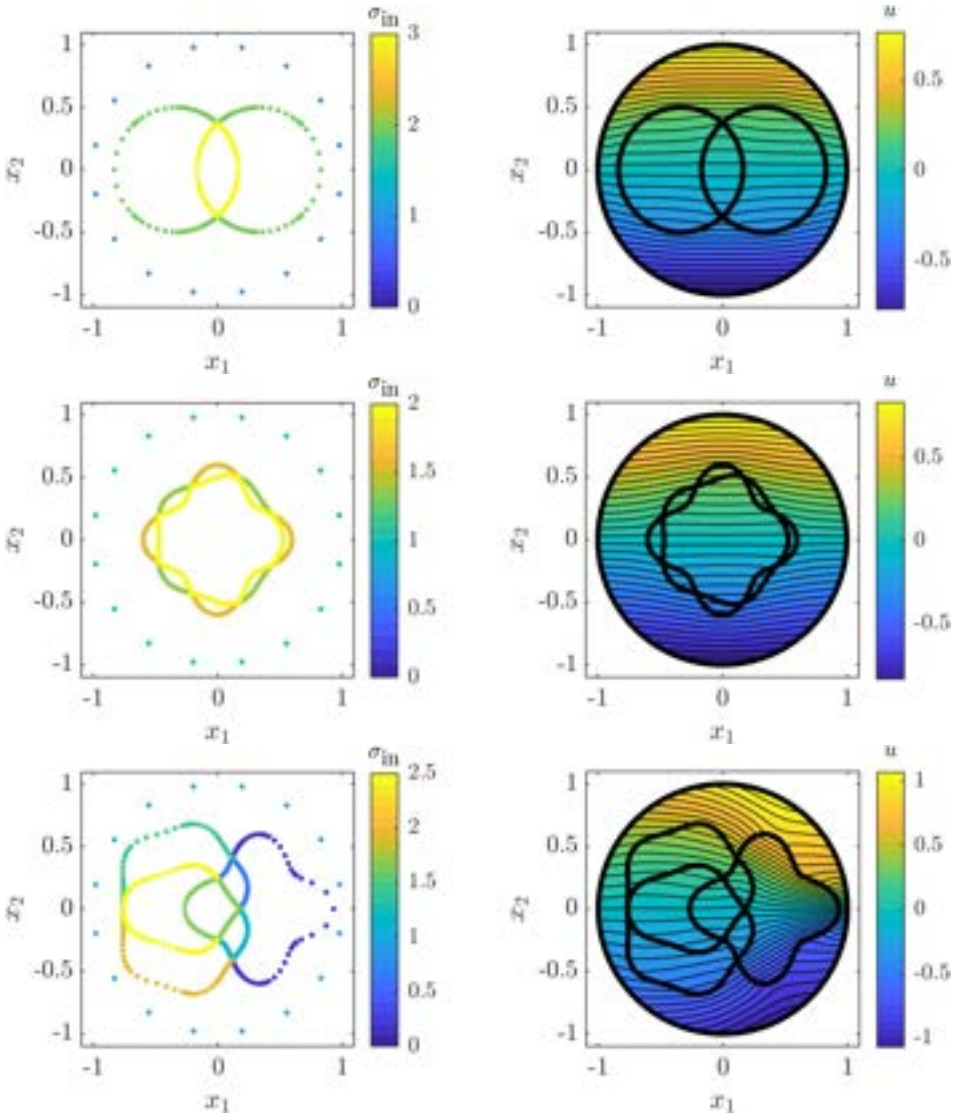

Figure 3.5: Conductivity σ for the problem (left) and potential u computed using our solver (right) for different test cases. The Neumann boundary data is $g(\theta) = \sin(\theta)$.

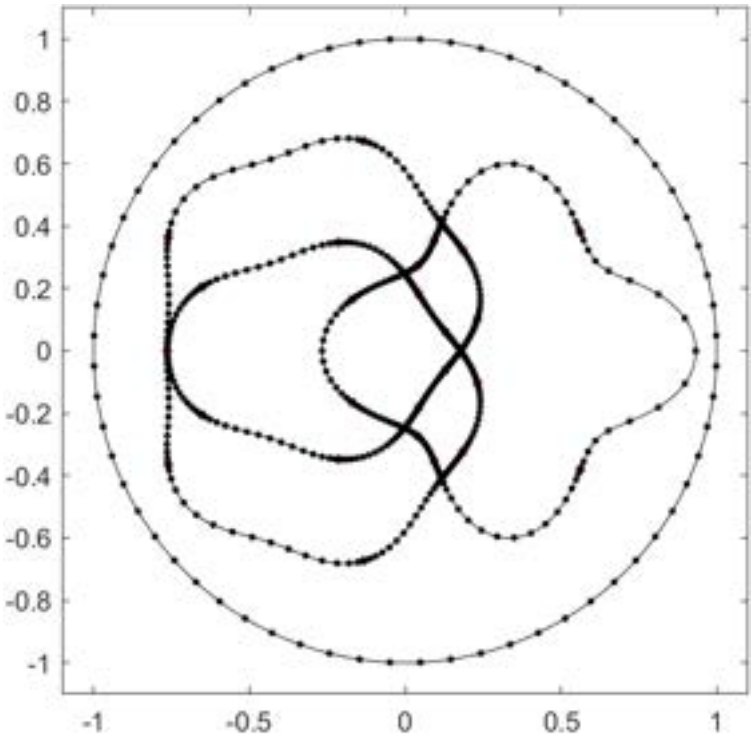

Figure 3.6: The automatically selected adaptive grid refinement (black dots are the quadrature nodes, red lines are the panel boundaries, black curves are interfaces) for a test case.

interface $\partial\Omega_i$. To compute $\sigma_{\text{out,background}}$, we look only at those interfaces that do not intersect $\partial\Omega_i$ and compute the winding number of those interfaces around an initial point on $\partial\Omega_i$. Only the regions whose interface has winding number 1 (and hence entirely contain $\partial\Omega_i$) contribute to $\sigma_{\text{out,background}}$.

If $\partial\Omega_i$ has no intersections with any other interface then we take $\sigma_{\text{out}} = \sigma_{\text{out,background}}$ and use a uniform grid. If $\partial\Omega_i$ does intersect other interfaces, then we find the points of intersection and split $\partial\Omega_i$ into panels at each point of intersection and use a dyadic grid between each successive intersection. On each such panel, σ_{out} will be constant. To find the value of σ_{out} on a panel we look ahead along the interface $\partial\Omega_i$ to find the first intersection with each other intersecting interface. At each such intersection point, to determine whether we have entered or exited a region, we compute the dot product between the tangent vector of the curve that we are on and the outward normal vector corresponding to the curve that we have intersected. If this dot product is negative then we have entered the region — else we have exited the region. On a panel, σ_{out} is then equal to $\sigma_{\text{out,background}}$ plus the contributions from the intersecting regions that the panel is inside.

At every grid point, the value of σ_{in} is equal to σ_{out} plus the contribution to the conductivity corresponding to the region whose boundary we are on. We will discuss how to find the points of intersection in Section 3.3.2.

3.3.2 *Locating Intersection Points for General Interfaces*

We need to develop an efficient method for computing intersection points for general interfaces, *i.e.*, for general curves $\vec{x}_1, \vec{x}_2$ parameterized by q_1, q_2 we need to find all points such that $\vec{x}_1(q_1) = \vec{x}_2(q_2)$.

To find all such points, we place a fine square mesh over our domain. We select each small square whose boundary intersects $\vec{x}_1$ and $\vec{x}_2$ in alternating order. For each selected small square, we use one of the intersection points between $\vec{x}_1$ and the boundary of the small square as the initial guess and use Newton's method or MATLAB's `fsolve` to find the precise intersection point. Finally, we compile a list of all intersection points and remove any duplicates.

4

CONCLUSIONS

A novel integral equation based method is presented to solve the elliptic partial differential equation problem for the electrostatic potential with piecewise constant conductivity and Neumann boundary conditions in dimension two. A system of well-conditioned integral equations for the charge densities is derived and used to solve the problem. This indirect method is comparatively simple owing to the smoothness of the kernel of the resulting integral operator.

We develop an atypical combination of approaches to address the close evaluation problem of evaluating single layer potentials at a point near a boundary. When the evaluation point is not near or on a single layer, we evaluate the single layer potentials using the same quadrature as used to solve the integral equations. When the evaluation point is near or on a single layer, we approximate the curve with line segments near the evaluation point and employ an analytic expression for the single layer potential on a line segment.

Additionally, we describe how the non-uniqueness of the Neumann electrical conductivity problem can be resolved by selecting the solution where the single layers have no net charge. We impose this condition by adjusting the kernel in the integral equations. This has the benefit that it does not change the dimensionality of the system to be solved and differs from the usual approach of adjoining additional conditions or rows to the system.

Our method of solving the elliptic partial differential equation problem is shown to be fast and efficient for several test cases. Our method is also shown to easily handle problems of significant complexity involving possibly hundreds of different regions of constant conductivity. This is enabled by efficient quadratures for smooth kernels, adaptively refining the quadrature grids, and utilizing the fast multipole method to speed up the calculation of distant quadrature nodes.

Our numerical method is supported by a robust analytical foundation. We provide theoretical results for our system of integral equations. We establish existence and uniqueness to this system of equations and we derive regularity for the charge densities along each interface. We show that assuming the interface has C^k regularity and the injected current

on the outer boundary lies in L^2, then the charge density on any inner interface is of regularity H^k. This is a novel analytical result.

Furthermore, we generalize our results by considering the case in which the piecewise constant regions of conductivity overlap. We study the behaviour of the solution to leading order at points of intersection between two transversely intersecting interfaces of regions of piecewise constant conductivity. This vastly increases the space of domains we can study. In particular, interfaces can be piecewise C^k with corners.

When regions overlap, the integrands are no longer smooth and instead contain weak singularities at the points of intersection between the interfaces. Using a dyadic grid, our adaptive quadrature grid refinement results in robust solutions to this situation. Further improvements could be made if we understood the asymptotics of the integrands by selecting a grid specifically chosen to account for the precise asymptotics of the change densities. Nevertheless, we successfully solve several test cases in a fast and efficient manner.

The numerical work on overlapping regions is also supported by analytic work on the elliptic partial differential equation problem for the electrostatic potential with overlapping regions of piecewise constant conductivity. We show that the electrostatic potential near a point of intersection between general intersecting curves and intersecting half-lines are identical to leading order. This is done in two steps. Firstly, a change of coordinates is performed that will convert the general intersecting curves to straight half-lines. Secondly, the electrostatic potential is solved for on this modified domain. We derive analytic bounds in L^2 on the asymptotic behaviour of the electrostatic potential near points of intersection.

Immediate work will commence to find analytic results to investigate the extent to which the piecewise constant conductivity case is a good approximation for the smooth conductivity case. Promising numerical work presented in this thesis suggests that smooth conductivities can be well approximated by piecewise constant conductivities and we would like to derive more formal results on this topic. We will also work on finding the effect of the angle of intersection on the order of convergence for the charge densities at points of intersection between general intersecting curves.

Future work could explore using the presented method to develop an inverse solver to solve the inverse conductivity problem. In the inverse conductivity problem, one seeks to reconstruct the unknown conductivity inside a body on whose boundary current and voltage measurements are made. A common technique for solving the inverse conductivity problem is to iteratively solve for the hypothesized conductivity. This process begins by making measurements of the voltage on the boundary of the

body for specified injections of current and then making an initial guess for the conductivities. The forward solver is run with this initial guess for the conductivities and the specified injections of current and the resulting voltages are recorded. The guess for the conductivities is then updated to minimize an objective function involving the differences between the measurements voltages and the numerically computed voltages from the forward solver. This process is repeated (requiring many forward solves) until the value of the objective function is sufficiently small. A good reconstruction of the unknown conductivity given a finite set of boundary measurements has several real-world applications including in the fields of medical imaging, geological imaging, and industrial processes imaging.

Another application of our method could be in solving fluid flow through porous media in fluid mechanics. This problem models the flow of fluids like water through porous media such as sponges, wood, and sand filters. The effective fluid permeability of the media would be analogous to the conductivity in the electrical conductivity problem. The pressure drop across the medium leads to a flow rate and is likewise analogous to the voltage leading to the current in the electrical conductivity problem. In porous media the regions are more likely than not to contain overlapping regions of effective fluid permeability.

Additional future work is to adapt the method to solve the three dimensional version of the problem. In the three dimensional problem, the resulting integral operator kernel is no longer smooth and the integral equations are more singular. The three dimensional problem would naturally be of significant importance for the medical imaging technique of electrical impedance tomography and other real-world applications.

BIBLIOGRAPHY

[ABH+15] Martin Alnæs, Jan Blechta, Johan Hake, August Johansson, Benjamin Kehlet, Anders Logg, Chris Richardson, Johannes Ring, Marie E Rognes, and Garth N Wells, *The FEniCS project version 1.5*, Archive of Numerical Software **3** (2015), no. 100, 9–23.

[ACL+20] Juan Pablo Agnelli, Aynur Cöl, Matti Lassas, Rashmi Murthy, Matteo Santacesaria, and Samuli Siltanen, *Classification of stroke using neural networks in electrical impedance tomography*, Inverse Problems **36** (2020), no. 11, 115008.

[aKB21] Ludvig af Klinteberg and Alex H Barnett, *Accurate quadrature of nearly singular line integrals in two and three dimensions by singularity swapping*, BIT Numerical Mathematics **61** (2021), no. 1, 83–118.

[Ale88] G. Alessandrini, *Stable determination of conductivity by boundary measurements*, Applicable Analysis **27** (1988), 153–172.

[ALS20] Yuri Flores Albuquerque, Antoine Laurain, and Kevin Sturm, *A shape optimization approach for electrical impedance tomography with point measurements*, Inverse Problems **36** (2020), no. 9, 095006.

[AMS22] Simon R Arridge, Peter Maaß, and Carola-Bibiane Schönlieb, *Deep learning for inverse problems*, Oberwolfach Reports **18** (2022), no. 1, 745–789.

[AP06] K. Astala and L. Päivärinta, *Calderón's inverse conductivity problem in the plane*, Annals of Mathematics **163** (2006), 265–299.

[Atk97] Kendall E. Atkinson, *The numerical solution of integral equations of the second kind*, Cambridge Monographs on Applied and Computational Mathematics, Cambridge University Press, 1997.

[AX17] Anthony P Austin and Kuan Xu, *On the numerical stability of the second barycentric formula for trigonometric interpolation in shifted equispaced points*, IMA Journal of Numerical Analysis **37** (2017), no. 3, 1355–1374.

[Bar14] Alex H Barnett, *Evaluation of layer potentials close to the boundary for Laplace and Helmholtz problems on analytic planar domains*, SIAM Journal on Scientific Computing **36** (2014), no. 2, A427–A451.

[BBP96] L. Borcea, J. G. Berryman, and G. C. Papanicolaou, *High-contrast impedance tomography*, Inverse Problems **12** (1996), 835–858.

[BGR10] James Bremer, Zydrunas Gimbutas, and Vladimir Rokhlin, *A nonlinear optimization procedure for generalized Gaussian quadratures*, SIAM Journal on Scientific Computing **32** (2010), no. 4, 1761–1788.

[BKIN07] Gregory Boverman, Bong Seok Kim, David Isaacson, and Jonathan C Newell, *The complete electrode model for imaging and electrode contact compensation in electrical impedance tomography*, 2007 29th Annual International Conference of the IEEE Engineering in Medicine and Biology Society, IEEE, 2007, pp. 3462–3465.

[BL01] J Thomas Beale and Ming-Chih Lai, *A method for computing nearly singular integrals*, SIAM Journal on Numerical Analysis **38** (2001), no. 6, 1902–1925.

[BM04] Jutta Bikowski and Jennifer L Mueller, *Electrical impedance tomography and the fast multipole method*, Image Reconstruction from Incomplete Data III, vol. 5562, SPIE, 2004, pp. 129–140.

[BMPS18] Elena Beretta, Stefano Micheletti, Simona Perotto, and Matteo Santacesaria, *Reconstruction of a piecewise constant conductivity on a polygonal partition via shape optimization in eit*, Journal of Computational Physics **353** (2018), 264–280.

[Bru01] M. Bruhl, *Explicit characterization of inclusions in electrical impedance tomography*, SIAM Journal on Mathematical Analysis **32** (2001), 1327–1341.

[BT04] Jean-Paul Berrut and Lloyd N Trefethen, *Barycentric Lagrange interpolation*, SIAM Review **46** (2004), no. 3, 501–517.

[BWV15] Alex Barnett, Bowei Wu, and Shravan Veerapaneni, *Spectrally accurate quadratures for evaluation of layer potentials close to the boundary for the 2D Stokes and Laplace equations*, SIAM Journal on Scientific Computing **37** (2015), no. 4, B519–B542.

[Cal80] A.P. Calderón, *On an inverse boundary value problem*, In Seminar on Numerical Analysis and its Applications to Continuum Physics, Soc. Brasileira de Matemàtica (1980), 65–73.

[CDH16] Christian Constanda, Dale Doty, and William Hamill, *Boundary integral equation methods and numerical solutions*, vol. 232, Springer, 2016.

[CII90] Margaret Cheney, David Isaacson, and Eli L Isaacson, *Exact solutions to a linearized inverse boundary value problem*, Inverse Problems **6** (1990), no. 6, 923.

[CIN+90] M. Cheney, D. Isaacson, J. C. Newell, S. Simske, and J. Goble, *Noser: An algorithm for solving the inverse conductivity problem*, International Journal of Imaging systems and technology **2** (1990), 66–75.

[CIN99] M. Cheney, D. Isaacson, and J. C. Newell, *Electrical impedance tomography*, SIAM Review **41** (1999), 85–101.

[CK13] David Colton and Rainer Kress, *Integral equation methods in scattering theory*, SIAM, 2013.

[CM20] Michael Capps and Jennifer L Mueller, *Reconstruction of organ boundaries with deep learning in the d-bar method for electrical impedance tomography*, IEEE Transactions on Biomedical Engineering **68** (2020), no. 3, 826–833.

[Cos88] Martin Costabel, *Boundary integral operators on Lipschitz domains: elementary results*, SIAM journal on Mathematical Analysis **19** (1988), no. 3, 613–626.

[CPS04] S. Ciulli, M.K. Pidcock, and C. Sebu, *An integral equation method for the inverse conductivity problem*, Physics Letters A **325** (2004), 253–267.

[CT04] Tony F. Chan and Xue-Cheng Tai, *Level set and total variation regularization for elliptic inverse problems with discontinuous coefficients*, Journal of Computational Physics **193** (2004), no. 1, 40–66.

[CZ99] Zhiming Chen and Jun Zou, *An augmented lagrangian method for identifying discontinuous parameters in elliptic systems*, SIAM Journal on Control and Optimization **37** (1999), no. 3, 892–910.

[DM88] Leonard Michael Delves and Julie L Mohamed, *Computational methods for integral equations*, CUP Archive, 1988.

[dMFH00] Jan C. de Munck, Theo J. C. Faes, and Rob M. Heethaar, *The boundary element method in the forward and inverse problem of electrical impedance tomography*, IEEE transactions on Biomedical Engineering **47** (2000), 792–800.

[DZB+05] Guoya Dong, J Zou, Richard H Bayford, Xinshan Ma, Shankai Gao, Weili Yan, and Manling Ge, *The comparison between fvm and fem for eit forward problem*, IEEE Transactions on Magnetics **41** (2005), no. 5, 1468–1471.

[DZKK10] A. M. Denisov, E. V. Zakharov, A. V. Kalinin, and V. V. Kalinin, *Numerical solution of an inverse electrocardiography problem for a medium with piecewise constant electrical conductivity*, Computational Mathematics and Mathematical Physics **50** (2010), 1172–1177.

[EGK13] Charles L Epstein, Leslie Greengard, and Andreas Klöckner, *On the convergence of local expansions of layer potentials*, SIAM Journal on Numerical Analysis **51** (2013), no. 5, 2660–2679.

[Eva10] Lawrence C. Evans, *Partial differential equations*, American Mathematical Society, Providence, R.I., 2010.

[Fla21] Flatiron Institute, *Flatiron institute fast multipole libraries*, 2021, [Online; accessed 2021-10-15].

[FY20a] Yuwei Fan and Lexing Ying, *Solving electrical impedance tomography with deep learning*, Journal of Computational Physics **404** (2020), 109119.

[FY20b] Yuwei Fan and Lexing Ying, *Solving electrical impedance tomography with deep learning*, Journal of Computational Physics **404** (2020), 109119.

[Gar20] Henrik Garde, *Reconstruction of piecewise constant layered conductivities in electrical impedance tomography*, Communications in Partial Differential Equations **45** (2020), no. 9, 1118–1133.

[GB13] Adrianna Gillman and Alex Barnett, *A fast direct solver for quasi-periodic scattering problems*, Journal of Computational Physics **248** (2013), 309–322.

[GGM93] Anne Greenbaum, Leslie Greengard, and GB McFadden, *Laplace's equation and the dirichlet-neumann map in multiply connected domains*, Journal of Computational Physics **105** (1993), no. 2, 267–278.

[GHL14] Leslie Greengard, Kenneth L Ho, and June-Yub Lee, *A fast direct solver for scattering from periodic structures with multiple material interfaces in two dimensions*, Journal of Computational Physics **258** (2014), 738–751.

[GJL14] Matthias Gehre, Bangti Jin, and Xiliang Lu, *An analysis of finite element approximation in electrical impedance tomography*, Inverse Problems **30** (2014), no. 4, 045013.

[Gon09] Pedro Gonnet, *Adaptive quadrature re-revisited*, Lulu. com, 2009.

[GR87] Leslie Greengard and Vladimir Rokhlin, *A fast algorithm for particle simulations*, Journal of Computational Physics **73** (1987), no. 2, 325–348.

[GR09] Christophe Geuzaine and Jean-François Remacle, *Gmsh: A 3-D finite element mesh generator with built-in pre-and post-processing facilities*, International journal for numerical methods in engineering **79** (2009), no. 11, 1309–1331.

[Har19] Bastian Harrach, *Uniqueness and lipschitz stability in electrical impedance tomography with finitely many electrodes*, Inverse Problems **35** (2019), no. 2, 024005.

[Hel11a] Johan Helsing, *The effective conductivity of arrays of squares: large random unit cells and extreme contrast ratios*, Journal of Computational Physics **230** (2011), no. 20, 7533–7547.

[Hel11b] ———, *The effective conductivity of random checkerboards*, Journal of Computational Physics **230** (2011), no. 4, 1171–1181.

[HH18] Sarah Jane Hamilton and Andreas Hauptmann, *Deep d-bar: Real-time electrical impedance tomography imaging with deep neural networks*, IEEE Transactions on Medical Imaging **37** (2018), no. 10, 2367–2377.

[HHHK19] Sarah J Hamilton, Asko Hänninen, Andreas Hauptmann, and Ville Kolehmainen, *Beltrami-net: domain-independent deep d-bar learning for absolute imaging with electrical impedance tomography (a-eit)*, Physiological Measurement **40** (2019), no. 7, 074002.

[HKM+17] Andreas Hauptmann, Ville Kolehmainen, Nguyet Minh Mach, Tuomo Savolainen, Aku Seppänen, and Samuli Siltanen, *Open 2d electrical impedance tomography data archive*, arXiv preprint arXiv:1704.01178 (2017), 1–15.

[HO08a] Johan Helsing and Rikard Ojala, *On the evaluation of layer potentials close to their sources*, Journal of Computational Physics **227** (2008), no. 5, 2899–2921.

[HO08b] _____, *On the evaluation of layer potentials close to their sources*, Journal of Computational Physics **227** (2008), no. 5, 2899–2921.

[HS10] Bastian Harrach and Jin Keun Seo, *Exact shape-reconstruction by one-step linearization in electrical impedance tomography*, SIAM Journal on Mathematical Analysis **42** (2010), no. 4, 1505–1518.

[HU13a] Bastian Harrach and Marcel Ullrich, *Monotonicity-based shape reconstruction in electrical impedance tomography*, SIAM Journal on Mathematical Analysis **45** (2013), 3382–3403.

[HU13b] Bastian Harrach and Marcel Ullrich, *Monotonicity-based shape reconstruction in electrical impedance tomography*, SIAM Journal on Mathematical Analysis **45** (2013), no. 6, 3382–3403.

[HW08] George C Hsiao and Wolfgang L Wendland, *Boundary integral equations*, Springer, 2008.

[HX11] George C Hsiao and Liwei Xu, *A system of boundary integral equations for the transmission problem in acoustics*, Applied Numerical Mathematics **61** (2011), no. 9, 1017–1029.

[Isa88] V. Isakov, *On uniqueness of recovery of a discontinuous conductivity coefficient*, Communications on Pure and Applied Mathematics **41** (1988), 865–877.

[KBGO13] Andreas Klöckner, Alexander Barnett, Leslie Greengard, and Michael O'Neil, *Quadrature by expansion: A new method for the evaluation of layer potentials*, Journal of Computational Physics **252** (2013), 332–349.

[KG07] Andreas Kirsch and Natalia Grinberg, *The factorization method for inverse problems*, vol. 36, Oxford University Press, Oxford, England, 2007.

[Kir05] Andreas Kirsch, *The factorization method for a class of inverse elliptic problems*, Mathematische Nachrichten **278** (2005), no. 3, 258–277.

[KLMS08] Kim Knudsen, Matti Lassas, Jennifer Mueller, and Samuli Siltanen, *Reconstructions of piecewise constant conductivities by the d-bar method for electrical impedance tomography*, Journal of Physics: Conference Series **124** (2008), no. 1, 012029.

[KLMS09] Kim Knudsen, Matti Lassas, Jennifer L Mueller, and Samuli Siltanen, *Regularized d-bar method for the inverse conductivity problem*, Inverse Problems and Imaging **35** (2009), no. 4, 599.

[KLV07] Klaus Knödel, Gerhard Lange, and Hans-Jürgen Voigt, *Environmental geology: handbook of field methods and case studies*, Springer Science & Business Media, 2007.

[Kre14] Rainer Kress, *Linear integral equations*, 3 ed., vol. 82, Springer, 2014.

[KV84] R. V. Kohn and M. Vogelius, *Determining conductivity by boundary measurements*, Communications on Pure and Applied Mathematics **37** (1984), 289–298.

[KV85] ———, *Determining conductivity by boundary measurements II: Interior results*, Communications on Pure and Applied Mathematics **38** (1985), 643–667.

[Liu09a] Yijun Liu, *Fast multipole boundary element method: theory and applications in engineering*, Cambridge university press, 2009.

[Liu09b] ———, *Fast multipole boundary element method: Theory and applications in engineering*, Cambridge University Press, 2009.

[LL94] R. J. LeVeque and Z. Li, *The immersed interface method for elliptic equations with discontinuous coefficients and singular sources*, SIAM Journal on Numerical Analysis **31** (1994), 1019–1044.

[LÖS18] Sebastian Lunz, Ozan Öktem, and Carola-Bibiane Schönlieb, *Adversarial regularizers in inverse problems*, Advances in Neural Information Processing Systems **31** (2018), 1–15.

[Mar19] Per-Gunnar Martinsson, *Fast direct solvers for elliptic pdes*, SIAM, 2019.

[MS03] Jennifer L Mueller and Samuli Siltanen, *Direct reconstructions of conductivities from boundary measurements*, SIAM Journal on Scientific Computing **24** (2003), no. 4, 1232–1266.

[MTF15] Q Marashdeh, FL Teixeira, and L-S Fan, *Electrical capacitance tomography*, Industrial Tomography, Elsevier, 2015, pp. 3–21.

[Nac96a] Adrian I Nachman, *Global uniqueness for a two-dimensional inverse boundary value problem*, Annals of Mathematics (1996), 71–96.

[Nac96b] A.I. Nachman, *Global uniqueness for a two-dimensional inverse boundary value problem*, Annals of Mathematics **143** (1996), 71–96.

[Neu77] Carl Neumann, *Untersuchungen über das logarithmische und newton'sche potential*, BG Teubner, 1877.

[NMIA11] Mohamed MS Nasser, Ali HM Murid, M Ismail, and EMA Alejaily, *Boundary integral equations with the generalized neumann kernel for laplace's equation in multiply connected regions*, Applied Mathematics and Computation **217** (2011), no. 9, 4710–4727.

[Nys30] Evert J Nyström, *Über die praktische auflösung von integralgleichungen mit anwendungen auf randwertaufgaben*, Acta Mathematica **54** (1930), 185–204.

[ON08] Yoshihiro Otani and Naoshi Nishimura, *An fmm for periodic boundary value problems for cracks for helmholtz'equation in 2d*, International Journal for Numerical Methods in Engineering **73** (2008), no. 3, 381–406.

[PAB14] Carlos Pérez-Arancibia and Oscar P Bruno, *High-order integral equation methods for problems of scattering by bumps and cavities on half-planes*, JOSA A **31** (2014), no. 8, 1738–1746.

[Pet12] Ivan Georgievich Petrovsky, *Lectures on partial differential equations*, Courier Corporation, 2012.

[Reb93] Stefano Rebay, *Efficient unstructured mesh generation by means of Delaunay triangulation and Bowyer-Watson algorithm*, Journal of Computational Physics **106** (1993), no. 1, 125–138.

[SMI00] Samuli Siltanen, Jennifer Mueller, and David Isaacson, *An implementation of the reconstruction algorithm of a nachman for the 2d inverse conductivity problem*, Inverse Problems **16** (2000), no. 3, 681.

[SS86] Youcef Saad and Martin H Schultz, *Gmres: A generalized minimal residual algorithm for solving nonsymmetric linear systems*, SIAM Journal on Scientific and Statistical Computing **7** (1986), no. 3, 856–869.

[SSBS88] A. J. Suroviec, S. S. Stuchly, J. R. Barr, and A. Swarup, *Dielectric properties of breast carcinoma and the surrounding tissues*, IEEE transactions on Biomedical Engineering **35** (1988), 257–263.

[SU87] J. Sylvester and G. A. Uhlmann, *A global uniqueness theorem for an inverse boundary value problem*, Annals of Mathematics **125** (1987), 153–169.

[TA77] A. N. Tikhonov and V. Y. Arsenin, *Solutions of ill-posed problems*, V. H. Winston & Sons, 1977.

[TNM+14] Renato S. Tavares, Flávio A. Nakadaira, Filho Marcos, S.G. Tsuzuki, Thiago C. Martins, and Raul Gonzalez Lima, *Discretization error and the eit forward problem*, IFAC Proceedings **47** (2014), 7535–7540.

[TSA24] Teemu Tyni, Adam R Stinchcombe, and Spyros Alexakis, *A boundary integral equation method for the complete electrode model in electrical impedance tomography with tests on experimental data*, SIAM Journal on Imaging Sciences **17** (2024), no. 1, 672–705.

[WJMT15] Grady B Wright, Mohsin Javed, Hadrien Montanelli, and Lloyd N Trefethen, *Extension of Chebfun to periodic functions*, SIAM Journal on Scientific Computing **37** (2015), no. 5, C554–C573.

[WLC19] Zhun Wei, Dong Liu, and Xudong Chen, *Dominant-current deep learning scheme for electrical impedance tomography*, IEEE Transactions on Biomedical Engineering **66** (2019), no. 9, 2546–2555.

[WYW05] Haitao Wang, Zhenhan Yao, and Pengbo Wang, *On the preconditioners for fast multipole boundary element methods for 2d multi-domain elastostatics*, Engineering Analysis with Boundary Elements **29** (2005), no. 7, 673–688.

[YB13] Wenjun Ying and J. Thomas Beale, *A fast accurate boundary integral method for potentials on closely packed cells*, Communications in Computational Physics **14** (2013), no. 4, 1073–1093.

[YNK01] Ken-ichi Yoshida, Naoshi Nishimura, and Shoichi Kobayashi, *Application of new fast multipole boundary integral equation method to crack problems in 3d*, Engineering Analysis with Boundary Elements **25** (2001), no. 4-5, 239–247.

[YP02] WQ Yang and Lihui Peng, *Image reconstruction algorithms for electrical capacitance tomography*, Measurement Science and Technology **14** (2002), no. 1, R1.

[ZG03] Y. Zou and Z. Guo, *A review of electrical impedance techniques for breast cancer detection*, Medical Engineering & Physics **25** (2003), 79–90.

[ZK09] EV Zakharov and Alexander Viktorovich Kalinin, *Method of boundary integral equations as applied to the numerical solution of the three-dimensional dirichlet problem for the laplace equation in a piecewise homogeneous medium*, Computational Mathematics and Mathematical Physics **49** (2009), no. 7, 1141–1150.

Appendices

A

ASYMPTOTIC BEHAVIOUR OF HARMONIC FUNCTIONS DEFINED ON CONES

We wish to study the asymptotic behaviours of harmonic functions defined on cones of angle $2\pi n$ for some $n \in (0,1]$. The metric on the cone is $g = dr^2 + r^2 d\phi^2$. We seek a solution to the PDE

$$\partial_r^2 u + \frac{1}{r}\partial_r u + \frac{1}{r^2}\partial_\phi^2 u = 0. \tag{A.1}$$

defined on the cone.

Lemma A.1. *There exists an H^1 solution to Eq. (A.1) of the form*

$$u(r,\phi) = C_0 A_0 + \sum_{k=1}^{\infty} C_k r^{\frac{k}{n}} \left(A_k \cos\left(\frac{k}{n}\phi\right) + B_k \sin\left(\frac{k}{n}\phi\right)\right). \tag{A.2}$$

for some constants $\{A_k\}_{k\geq 0}, \{B_k\}_{k\geq 1}, \{C_k\}_{k\geq 0}$.

Proof. We use separation of variables to find a solution. Substitute $u(r,\phi) = f(r)\ell(\phi)$ into the PDE Eq. (A.1) to obtain

$$f''(r)\ell(\phi) + \frac{1}{r}f'(r)\ell(\phi) + \frac{1}{r^2}f(r)\ell''(\phi) = 0. \tag{A.3}$$

Dividing by $\frac{1}{r^2}f(r)\ell(\phi)$ yields

$$\frac{r^2 f''(r)}{f(r)} + \frac{r f'(r)}{f(r)} + \frac{\ell''(\phi)}{\ell(\phi)} = 0. \tag{A.4}$$

Thus, there exists a constant λ such that

$$\frac{r^2 f''(r)}{f(r)} + \frac{r f'(r)}{f(r)} = -\frac{\ell''(\phi)}{\ell(\phi)} = \lambda. \tag{A.5}$$

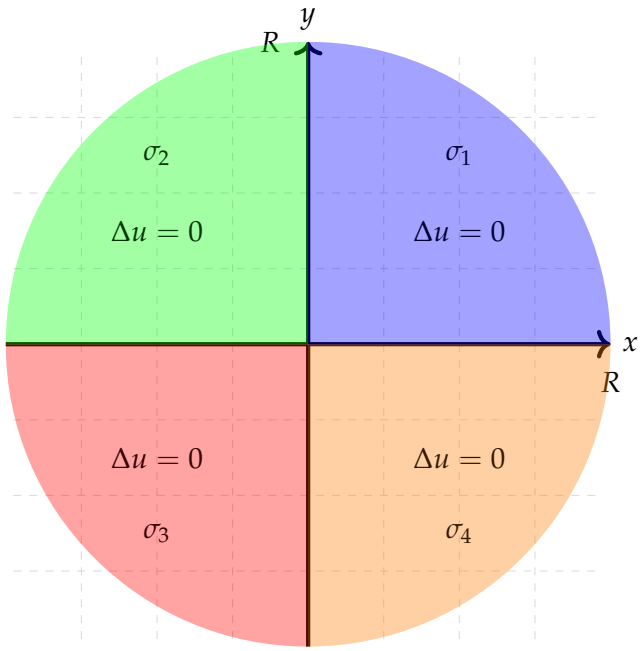

Figure A.1: The domain bounded by two half lines at a right angle.

We obtain two ODEs

$$r^2 f''(r) + r f'(r) - \lambda f(r) = 0, \tag{A.6}$$

$$\ell''(\phi) + \lambda \ell(\phi) = 0. \tag{A.7}$$

For Eq. (A.7), we seek solutions that are $2\pi n$-periodic, *i.e.*,

$$\ell(\phi) = \ell(\phi + 2\pi n), \quad \text{for } \lambda = \frac{k^2}{n^2},\ k = 0, 1, 2 \ldots. \tag{A.8}$$

We obtain a sequence of solutions of the form

$$\ell_k(\phi) = A_k \cos\left(\frac{k}{n}\phi\right) + B_k \sin\left(\frac{k}{n}\phi\right), \qquad k = 0, 1, 2, \ldots \tag{A.9}$$

for some arbitrary constants A_k's and B_k's. Substituting $\lambda = \frac{k^2}{n^2}$ into the ODE for r Eq. (A.6) we get an Euler equation

$$r^2 f''(r) + r f'(r) - \frac{k^2}{n^2} f(r) = 0, \qquad k = 0, 1, 2, \ldots. \tag{A.10}$$

We seek solutions of the form: $f(r) = r^\alpha$. Subbing this into the Euler equation Eq. (A.10) yields the equation

$$\alpha^2 - \frac{k^2}{n^2} = 0, \qquad k = 0, 1, 2, \ldots. \tag{A.11}$$

Hence $\alpha = \pm\frac{k}{n}$ for $k = 0, 1, 2, \ldots$ and we get a sequence of solutions

$$f_k(r) = C_k r^{\frac{k}{n}} + D_k r^{-\frac{k}{n}}, \qquad k = 1, 2, 3, \ldots \tag{A.12}$$

$$f_0(r) = C_0 + D_0 \ln r, \qquad k = 0 \tag{A.13}$$

for some arbitrary constants C_k's and D_k's. Since we require our function to have finite H^1-norm as $r \to 0$, we require that $D_k = 0$ for all $k \geq 0$. Our solution is then

$$u(r, \phi) = C_0 A_0 + \sum_{k=1}^{\infty} C_k r^{\frac{k}{n}} \left(A_k \cos\left(\frac{k}{n}\phi\right) + B_k \sin\left(\frac{k}{n}\phi\right)\right). \tag{A.14}$$

□

We note that to leading order the solution Eq. (A.14) is

$$u(r, \phi) = c_0 + c_1 r^{\frac{1}{n}} \cos\left(\frac{1}{n}\phi\right) + c_2 r^{\frac{1}{n}} \sin\left(\frac{1}{n}\phi\right) + \mathcal{O}(r^{\frac{2}{n}}) \tag{A.15}$$

for some constants c_0, c_1, c_2.

We consider the case of Fig. A.1 and define a new metric $g' = \sigma(d_x^2 + d_y^2)$, *i.e.*, the conductivity multiplied by the Euclidean metric where the cone angle is the ratio between the circumferences of the circle $C_{r=\rho}$ with respect to g' and with respect to ρ. In the case of Fig. A.1 where the lines intersect at right angles, this ratio is equal to $2\pi \sum_{i=1}^{4} \sigma_i$.

For Fig. A.1 the solution on each sector is like (proof similar to that of the removable singularity theorem)

$$u(r, \phi) = ar^\alpha \cos(\alpha\phi) + br^\alpha \sin(\alpha\phi) \tag{A.16}$$

$$= \lambda r^\alpha \cos(\alpha\phi + \theta). \tag{A.17}$$

We impose the interface matching conditions (continuity of potential and current), $u_- = u_+$ and $\sigma_- \partial_{\boldsymbol{n}} u_- = \sigma_+ \partial_{\boldsymbol{n}} u_+$, to find a particular combination of parameters that works.

Across the positive y-axis, $u_1 = u_2$ implies

$$\lambda_1 r^{\alpha_1} \cos(\alpha_1 \frac{\pi}{2} + \theta_1) = \lambda_2 r^{\alpha_2} \cos(\alpha_2 \frac{\pi}{2} + \theta_2). \tag{A.18}$$

Since this must be true for all positive r we get that $\alpha_1 = \alpha_2$.

Across the positive y-axis, the condition that $\sigma_- \partial_{\boldsymbol{n}} u_- = \sigma_+ \partial_{\boldsymbol{n}} u_+$ implies that

$$\sigma_1 \frac{1}{r} \partial_\phi u_1 = -\sigma_2 \frac{1}{r} \partial_\phi u_2, \tag{A.19}$$

i.e.,

$$-\sigma_1 \lambda_1 r^{\alpha_1 - 1} \sin(\alpha_1 \frac{\pi}{2} + \theta_1) = -\sigma_2 \lambda_2 r^{\alpha_2 - 1} \sin(\alpha_2 \frac{\pi}{2} + \theta_2) \tag{A.20}$$

Multiplying by r we get

$$\frac{\lambda_1 r^{\alpha_1}}{\lambda_2 r^{\alpha_2}} = \frac{\cos(\alpha_2 \frac{\pi}{2} + \theta_2)}{\cos(\alpha_1 \frac{\pi}{2} + \theta_1)} \tag{A.21}$$

$$= \frac{\sigma_2 \sin(\alpha_2 \frac{\pi}{2} + \theta_2)}{\sigma_1 \sin(\alpha_2 \frac{\pi}{2} + \theta_1)} \tag{A.22}$$

Considering the matching conditions across the other interfaces, we get

$$\alpha_1 = \alpha_2 = \alpha_3 = \alpha_4 := \alpha \tag{A.23}$$

and the equations

$$\frac{\lambda_1}{\lambda_2} = \frac{\cos(\alpha\frac{\pi}{2} + \theta_2)}{\cos(\alpha\frac{\pi}{2} + \theta_1)} \tag{A.24}$$

$$= \frac{\sigma_2 \sin(\alpha\frac{\pi}{2} + \theta_2)}{\sigma_1 \sin(\alpha\frac{\pi}{2} + \theta_1)} \tag{A.25}$$

$$\frac{\lambda_2}{\lambda_3} = \frac{\cos(\alpha\pi + \theta_3)}{\cos(\alpha\pi + \theta_2)} \tag{A.26}$$

$$= \frac{\sigma_3 \sin(\alpha\pi + \theta_3)}{\sigma_2 \sin(\alpha\pi + \theta_2)} \tag{A.27}$$

$$\frac{\lambda_3}{\lambda_4} = \frac{\cos(\alpha\frac{3\pi}{2} + \theta_4)}{\cos(\alpha\frac{3\pi}{2} + \theta_3)} \tag{A.28}$$

$$= \frac{\sigma_4 \sin(\alpha\frac{3\pi}{2} + \theta_4)}{\sigma_3 \sin(\alpha\frac{3\pi}{2} + \theta_3)} \tag{A.29}$$

$$\frac{\lambda_4}{\lambda_1} = \frac{\cos(\theta_1)}{\cos(\alpha 2\pi + \theta_4)} \tag{A.30}$$

$$= \frac{\sigma_1 \sin(\theta_1)}{\sigma_4 \sin(\alpha 2\pi + \theta_4)} \tag{A.31}$$

Without loss of generality, we choose $\lambda_1 = 1$ leading to a system of 8 equations for the 8 unknowns $(\lambda_2, \lambda_3, \lambda_4, \theta_1, \theta_2, \theta_3, \theta_4, \alpha)$.

Using the sum and difference trig identities we can rewrite the system Eqs. (A.24) to (A.31):

$$\frac{\lambda_1}{\lambda_2} = \frac{\cos(\alpha\frac{\pi}{2})\cos(\theta_2) - \sin(\alpha\frac{\pi}{2})\sin(\theta_2)}{\cos(\alpha\frac{\pi}{2})\cos(\theta_1) - \sin(\alpha\frac{\pi}{2})\sin(\theta_1)} \tag{A.32}$$

$$= \frac{\sigma_2}{\sigma_1}\frac{\sin(\alpha\frac{\pi}{2})\cos(\theta_2) + \cos(\alpha\frac{\pi}{2})\sin(\theta_2)}{\sin(\alpha\frac{\pi}{2})\cos(\theta_1) + \cos(\alpha\frac{\pi}{2})\sin(\theta_1)} \tag{A.33}$$

$$\frac{\lambda_2}{\lambda_3} = \frac{\cos(\alpha\pi)\cos(\theta_3) - \sin(\alpha\pi)\sin(\theta_3)}{\cos(\alpha\pi)\cos(\theta_2) - \sin(\alpha\pi)\sin(\theta_2)} \tag{A.34}$$

$$= \frac{\sigma_3}{\sigma_2}\frac{\sin(\alpha\pi)\cos(\theta_3) + \cos(\alpha\pi)\sin(\theta_3)}{\sin(\alpha\pi)\cos(\theta_2) + \cos(\alpha\pi)\sin(\theta_2)} \tag{A.35}$$

$$\frac{\lambda_3}{\lambda_4} = \frac{\cos(\alpha\frac{3\pi}{2})\cos(\theta_4) - \sin(\alpha\frac{3\pi}{2})\sin(\theta_4)}{\cos(\alpha\frac{3\pi}{2})\cos(\theta_3) - \sin(\alpha\frac{3\pi}{2})\sin(\theta_3)} \tag{A.36}$$

$$= \frac{\sigma_4}{\sigma_3}\frac{\sin(\alpha\frac{3\pi}{2})\cos(\theta_4) + \cos(\alpha\frac{3\pi}{2})\sin(\theta_4)}{\sin(\alpha\frac{3\pi}{2})\cos(\theta_3) + \cos(\alpha\frac{3\pi}{2})\sin(\theta_3)} \tag{A.37}$$

$$\frac{\lambda_4}{\lambda_1} = \frac{\cos(\theta_1)}{\cos(\alpha 2\pi)\cos(\theta_4) - \sin(\alpha 2\pi)\sin(\theta_4)} \tag{A.38}$$

$$= \frac{\sigma_1}{\sigma_4}\frac{\sin(\theta_1)}{\sin(\alpha 2\pi)\cos(\theta_4) + \cos(\alpha 2\pi)\sin(\theta_4)} \tag{A.39}$$

Lemma A.2. *There exists a solution to system Eq. (A.32)–Eq. (A.39) with* $\alpha \in [0, 1]$.

Proof. First, we will show that for any solution with $\alpha = \alpha^*$, we also have a solution with $\alpha = \alpha^* + 2$.

Assume there is a solution to system Eq. (A.32)–Eq. (A.39) with some $\alpha = \alpha^*$. Then, taking $\alpha = \alpha^* + 2$ and the same θ_i's and using the properties that $\sin(x + \pi) = -\sin(x)$ and $\cos(x + \pi) = -\cos(x)$, we have

$$\frac{\cos((\alpha^*+2)\frac{\pi}{2})\cos(\theta_2) - \sin((\alpha^*+2)\frac{\pi}{2})\sin(\theta_2)}{\cos((\alpha^*+2)\frac{\pi}{2})\cos(\theta_1) - \sin((\alpha^*+2)\frac{\pi}{2})\sin(\theta_1)}$$

$$= \frac{\cos(\alpha^*\frac{\pi}{2}+\pi)\cos(\theta_2) - \sin(\alpha^*\frac{\pi}{2}+\pi)\sin(\theta_2)}{\cos(\alpha^*\frac{\pi}{2}+\pi)\cos(\theta_1) - \sin(\alpha^*\frac{\pi}{2}+\pi)\sin(\theta_1)} \tag{A.40}$$

$$= \frac{\cos(\alpha^*\frac{\pi}{2})\cos(\theta_2) - \sin(\alpha^*\frac{\pi}{2})\sin(\theta_2)}{\cos(\alpha^*\frac{\pi}{2})\cos(\theta_1) - \sin(\alpha^*\frac{\pi}{2})\sin(\theta_1)} \tag{A.41}$$

$$= \frac{\lambda_1}{\lambda_2} \tag{A.42}$$

Similarly, for $\alpha = \alpha^* + 2$ and the same θ_i's, the other equations in system Eq. (A.32)–Eq. (A.39) are also satisfied.

Second, we will show that for any solution with $\alpha = \alpha^*$, we have a solution with $\alpha = -\alpha^*$.

Assume there is a solution to system Eq. (A.32)–Eq. (A.39) with some $\alpha = \alpha^*$ and θ_i^*'s. Then, taking $\alpha = -\alpha^*$ and $\theta_i = -\theta_i^*$ and using the properties that $\sin(x)$ is odd and $\cos(x)$ is even, we have

$$\begin{aligned}
&\frac{\cos(-\alpha^*\frac{\pi}{2})\cos(-\theta_2^*) - \sin(-\alpha^*\frac{\pi}{2})\sin(-\theta_2^*)}{\cos(-\alpha^*\frac{\pi}{2})\cos(-\theta_1^*) - \sin(-\alpha^*\frac{\pi}{2})\sin(-\theta_1^*)} \\
&= \frac{\cos(\alpha^*\frac{\pi}{2})\cos(\theta_2^*) - \sin(\alpha^*\frac{\pi}{2})\sin(\theta_2^*)}{\cos(\alpha^*\frac{\pi}{2})\cos(\theta_1^*) - \sin(\alpha^*\frac{\pi}{2})\sin(\theta_1^*)} && \text{(A.43)} \\
&= \frac{\lambda_1}{\lambda_2} && \text{(A.44)}
\end{aligned}$$

Similarly, for $\alpha = -\alpha^*$ and the same θ_i's, the other equations in system Eq. (A.32)–Eq. (A.39) are also satisfied.

Hence, there is a solution to system Eq. (A.32)–Eq. (A.39) with $\alpha \in [0, 1]$. □

B

SOLVING AS A CONTRACTION MAPPING

B.0.1 *Condition for Contraction Mapping.*

We state a useful condition for a linear map $T : L^2(\mathbb{S}^1) \to L^2(\mathbb{S}^1)$ to yield a contraction mapping.

Consider the map T defined by a kernel function $K(x, y)$:

$$T[f](x) = \int_{\mathbb{S}^1} K(x,y) f(y) dy. \tag{B.1}$$

Then:

Lemma B.1. *If* $\int_{\mathbb{S}^1} \int_{\mathbb{S}^1} |K(x,y)|^2 dxdy = \delta < 1$ *the operator* T *is a contraction mapping, meaning that:*

$$\|T[f]\|_{L^2(\mathbb{S}^1)} \leq \delta \|f\|_{L^2(\mathbb{S}^1)}. \tag{B.2}$$

Proof. Note that:

$$\|T[f]\|_{L^2(\mathbb{S}^1)} = \int_{\mathbb{S}^1} \left[\int_{\mathbb{S}^1} K(x,y) f(y) dy \right]^2 dx \leq \int_{\mathbb{S}^1} \int_{\mathbb{S}^1} [K(x,y)]^2 dy \cdot \int_{\mathbb{S}^1} [f(y)]^2 dydx$$
$$\leq \left[\int_{\mathbb{S}^1} [f(y)]^2 dy \right] \cdot \int_{\mathbb{S}^1} \int_{\mathbb{S}^1} [K(x,y)]^2 dydx \tag{B.3}$$

Thus a sufficient condition to get a contraction mapping is precisely that:

$$\int_{\mathbb{S}^1} \int_{\mathbb{S}^1} [K(x,y)]^2 dydx < 1 \tag{B.4}$$

□

B.0.2 *A Boundary Integral Formulation*

We describe a boundary integral formulation for two concentric circular regions of constant conductivity. The domain for this inverse conductivity problem is shown in Fig. B.1.

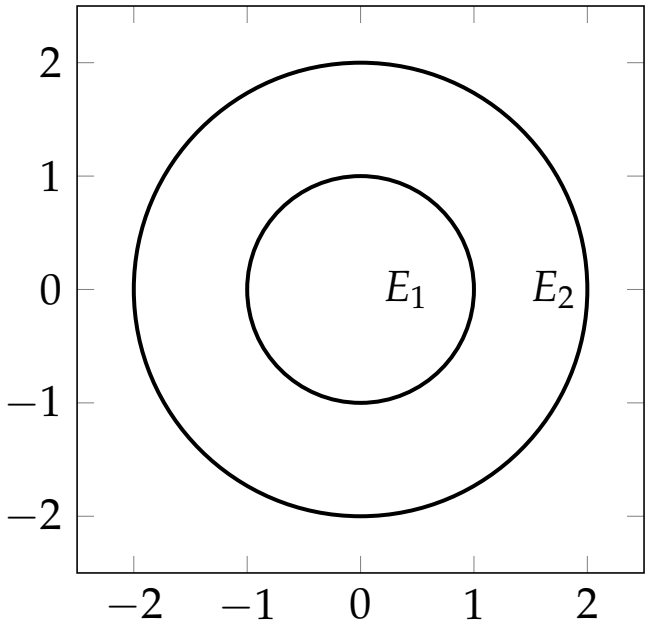

Figure B.1: Domain for inverse conductivity problem with two concentric circular regions of constant conductivity, $\Omega_i = \cup_{j=1}^{i} E_j$ for $i = 1, 2$.

Consider the problem

$$\Delta u = 0 \text{ on } \Omega_2 \setminus \partial\Omega_1 \tag{B.5}$$

$$\sigma_2 \partial_\nu u = g(\theta) \text{ on } \partial\Omega_2 \tag{B.6}$$

$$u_- = u_+ \text{ on } \partial\Omega_1 \tag{B.7}$$

$$\sigma_1 \partial_{\nu^-} u = \sigma_2 \partial_{\nu^+} u \text{ on } \partial\Omega_1 \tag{B.8}$$

We choose to represent the solution as the sum of two single layer potentials

$$u(\mathbf{x}) = \mathcal{S}_{\partial\Omega_1}[\gamma_1](\mathbf{x}) + \mathcal{S}_{\partial\Omega_2}[\gamma_2](\mathbf{x}). \tag{B.9}$$

The single layer potential is defined as

$$\mathcal{S}_\Gamma[\gamma](\mathbf{x}) = \int_\Gamma G(\mathbf{x}, \mathbf{y})\gamma(\mathbf{y}) ds_{\mathbf{y}}, \tag{B.10}$$

with the two-dimensional free space Green's function

$$G(\mathbf{x}, \mathbf{y}) = \frac{1}{2\pi} \log |\mathbf{x} - \mathbf{y}|. \tag{B.11}$$

The single layer potential is harmonic off of Γ, continuous across Γ, and has a known jump in normal derivative across Γ. To describe what happens

to the normal derivative on Γ, we need to define the Neumann-Poincaré operator

$$\mathcal{K}_\Gamma^*[\gamma](\mathbf{x}) := \frac{1}{2\pi}\int_\Gamma \frac{(\mathbf{x}-\mathbf{y})\cdot\mathbf{n}(\mathbf{x})}{|\mathbf{x}-\mathbf{y}|^2}\gamma(\mathbf{y})\, ds_\mathbf{y}, \quad \mathbf{x}\in\Gamma. \tag{B.12}$$

A standard result from potential theory is that

$$\partial_{\nu^\pm}\mathcal{S}_\Gamma[\gamma](\mathbf{y}) = \mathcal{K}_\Gamma^*[\gamma](\mathbf{y}) \pm \frac{1}{2}\gamma(\mathbf{y}), \tag{B.13}$$

which we can use to obtain equations for γ_1 and γ_2 by enforcing the boundary conditions.

We parameterize the two boundary curves as $\partial\Omega_i : \mathbf{x} = (R_i\cos(\theta_i), R_i\sin(\theta_i))^T$ for $i = 1, 2$.

The Neumann boundary condition with $\mathbf{x}\in\partial\Omega_2$ gives

$$\sigma_2\left[-\frac{1}{2}\gamma_2(\theta) + \mathcal{K}^*_{\partial\Omega_2}[\gamma_2](\mathbf{x}) + \frac{\partial}{\partial n}\mathcal{S}_{\partial\Omega_1}[\gamma_1](\mathbf{x})\right] = g(\theta), \tag{B.14}$$

and the jump interface condition for $\mathbf{x}\in\partial\Omega_1$ gives

$$\begin{aligned}&\sigma_1\left[-\frac{1}{2}\gamma_1(\theta) + \mathcal{K}^*_{\partial\Omega_1}[\gamma_1](\mathbf{x}) + \frac{\partial}{\partial n}\mathcal{S}_{\partial\Omega_2}[\gamma_2](\mathbf{x})\right] \\ =&\sigma_2\left[+\frac{1}{2}\gamma_1(\theta) + \mathcal{K}^*_{\partial\Omega_1}[\gamma_1](\mathbf{x}) + \frac{\partial}{\partial n}\mathcal{S}_{\partial\Omega_2}[\gamma_2](\mathbf{x})\right].\end{aligned} \tag{B.15}$$

The kernel of the Neumann-Poincaré operator is constant on a circle:

$$\begin{aligned}&\mathcal{K}_\Gamma^*[\gamma](\theta) \\ &= \frac{1}{2\pi}\int_0^{2\pi} \frac{((R\cos(\theta), R\sin(\theta))^T - (R\cos(\theta'), R\sin(\theta'))^T)\cdot(\cos(\theta),\sin(\theta))^T}{|((R\cos(\theta), R\sin(\theta))^T - (R\cos(\theta'), R\sin(\theta'))^T)|^2}\gamma(\theta')\ R d\theta' \qquad \text{(B.16)}\\ &= \frac{R}{2\pi}\int_0^{2\pi}\frac{R - R\cos(\theta-\theta')}{2R^2 - 2R^2\cos(\theta-\theta')}\gamma(\theta')d\theta' \qquad \text{(B.17)}\\ &= \frac{1}{4\pi}\int_0^{2\pi}\gamma(\theta')d\theta'. \qquad \text{(B.18)}\end{aligned}$$

We compute the normal derivative of the single layer potentials. The normal derivative points in the radial direction. For $\mathbf{x} \in \partial\Omega_i : \mathbf{x} = (R_i \cos(\theta_i), R_i \sin(\theta_i))^T$,

$$\frac{\partial}{\partial n_i}\mathcal{S}_{\partial\Omega_j}\left[\gamma_j\right](\mathbf{x}) = \frac{\partial}{\partial n_i}\int_{\partial\Omega_j}\frac{1}{2\pi}\log|\mathbf{x}-\mathbf{y}|\gamma_j(\mathbf{y})dS_{\mathbf{y}} \tag{B.19}$$

$$= \frac{\partial}{\partial n_i}\int_0^{2\pi}\frac{1}{2\pi}\log\Big|(R_i\cos(\theta_i), R_i\sin(\theta_i))^T - \left(R_j\cos(\theta_j), R_j\sin(\theta_j)\right)^T\Big|\,\gamma_j\left(\theta_j\right)R_j d\theta_j \tag{B.20}$$

$$= \frac{\partial}{\partial n_i}\int_0^{2\pi}\frac{1}{2\pi}\log\Big|\big(R_i\cos(\theta_i) - R_j\cos(\theta_j), R_i\sin(\theta_i) - R_j\sin(\theta_j)\big)^T\Big|\,\gamma_j\left(\theta_j\right)R_j d\theta_j \tag{B.21}$$

$$= \frac{\partial}{\partial n_i}\int_0^{2\pi}\frac{1}{2\pi}\log\Big(\left(R_i\cos(\theta_i) - R_j\cos(\theta_j)\right)^2 + \left(R_i\sin(\theta_i) - R_j\sin(\theta_j)\right)^2\Big)^{1/2}\gamma_j\left(\theta_j\right)R_j d\theta_j \tag{B.22}$$

$$= \frac{\partial}{\partial n_i}\int_0^{2\pi}\frac{1}{4\pi}\log\Big(\left(R_i\cos(\theta_i) - R_j\cos(\theta_j)\right)^2 + \left(R_i\sin(\theta_i) - R_j\sin(\theta_j)\right)^2\Big)\gamma_j\left(\theta_j\right)R_j d\theta_j \tag{B.23}$$

$$= \int_0^{2\pi}\frac{\partial}{\partial R_i}\frac{1}{4\pi}\log\left(R_i^2 + R_j^2 - 2R_iR_j\cos(\theta_i-\theta_j)\right)\gamma_j\left(\theta_j\right)R_j d\theta_j \tag{B.24}$$

$$= \int_0^{2\pi}\frac{R_j}{2\pi}\frac{R_i - R_j\cos\left(\theta_i-\theta_j\right)}{R_i^2 + R_j^2 - 2R_iR_j\cos\left(\theta_i-\theta_j\right)}\gamma_j(\theta_j)d\theta_j \tag{B.25}$$

$$= \int_0^{2\pi}K_{i,j}(\theta_i-\theta_j)\gamma_j(\theta_j)d\theta_j \tag{B.26}$$

where

$$K_{i,j}(\theta) = \frac{R_j}{2\pi}\frac{R_i - R_j\cos\left(\theta\right)}{R_i^2 + R_j^2 - 2R_iR_j\cos\left(\theta\right)}. \tag{B.27}$$

Let

$$C_i := \int_0^{2\pi}\gamma_i(\theta)d\theta, \quad i = 1, 2. \tag{B.28}$$

The two linear integral equations for γ_1 and γ_2 become

$$-\frac{\sigma_2}{2}\gamma_2(\theta) + \frac{\sigma_2}{4\pi}C_2 + \sigma_2 \int_0^{2\pi} K_{1,2}(\theta - \theta')\gamma_1(\theta')d\theta' = g(\theta) \tag{B.29}$$

$$\frac{\sigma_1 + \sigma_2}{2}\gamma_1(\theta) + \frac{\sigma_2 - \sigma_1}{4\pi}C_1 + (\sigma_2 - \sigma_1) \int_0^{2\pi} K_{2,1}(\theta - \theta')\gamma_2(\theta')d\theta' = 0. \tag{B.30}$$

Integrate Eq. (B.29) and Eq. (B.30) in θ from 0 to 2π to obtain

$$\frac{R_2}{R_1}C_1 = \int_0^{2\pi} g(\theta)\, d\theta \tag{B.31}$$

$$\sigma_2 C_1 = 0. \tag{B.32}$$

We get that $C_1 = 0$. Since our solution is only defined up to an additive constant, we can take $C_2 = 0$. Thus, there is no net charge density around each boundary.

Solving for γ_1 in the second equation we get

$$\gamma_1(\theta) = \frac{2(\sigma_1 - \sigma_2)}{\sigma_1 + \sigma_2} \int_0^{2\pi} K_{2,1}(\theta - \theta')\gamma_2(\theta')d\theta'. \tag{B.33}$$

Substituting this result into the first equation we get

$$g(\theta) = -\frac{\sigma_2}{2}\gamma_2(\theta) + \sigma_2 \int_0^{2\pi} K_{1,2}(\theta - \theta') \left[\frac{2(\sigma_1 - \sigma_2)}{\sigma_1 + \sigma_2} \int_0^{2\pi} K_{2,1}(\theta' - \theta'')\gamma_2(\theta'')d\theta''\right] d\theta' \tag{B.34}$$

$$= -\frac{\sigma_2}{2}\gamma_2(\theta) + \frac{2\sigma_2(\sigma_1 - \sigma_2)}{\sigma_1 + \sigma_2} \int_0^{2\pi} \int_0^{2\pi} K_{1,2}(\theta - \theta')K_{2,1}(\theta' - \theta'')\gamma_2(\theta'')d\theta''d\theta'. \tag{B.35}$$

Multiplying by $-2/\sigma_2$ we get:

$$-\frac{2}{\sigma_2}g(\theta) = \gamma_2(\theta) - \frac{4(\sigma_1 - \sigma_2)}{\sigma_1 + \sigma_2} \int_0^{2\pi} \int_0^{2\pi} K_{1,2}(\theta - \theta')K_{2,1}(\theta' - \theta'')\gamma_2(\theta'')d\theta''d\theta' \tag{B.36}$$

$$= (I - T)[\gamma_2](\theta) \tag{B.37}$$

where

$$
\begin{aligned}
&T[\gamma_2](\theta) \\
&= \frac{4(\sigma_1-\sigma_2)}{\sigma_1+\sigma_2}\int_0^{2\pi}\int_0^{2\pi} K_{1,2}(\theta-\theta')K_{2,1}(\theta'-\theta'')\gamma_2(\theta'')d\theta''d\theta' && \text{(B.38)}\\
&= \frac{4(\sigma_1-\sigma_2)}{\sigma_1+\sigma_2}\int_0^{2\pi}\int_0^{2\pi}\left(\frac{R_2}{2\pi}\frac{R_1-R_2\cos(\theta-\theta')}{R_1^2+R_2^2-2R_1R_2\cos(\theta-\theta')}\right. \\
&\qquad\left.\frac{R_1}{2\pi}\frac{R_2-R_1\cos(\theta'-\theta'')}{R_1^2+R_2^2-2R_1R_2\cos(\theta'-\theta'')}\gamma_2(\theta'')\right)d\theta''d\theta' && \text{(B.39)}\\
&= \frac{r}{\pi^2}\frac{(\sigma_1-\sigma_2)}{\sigma_1+\sigma_2}\int_0^{2\pi}\int_0^{2\pi}\frac{r-\cos(\theta-\theta')}{r^2+1-2r\cos(\theta-\theta')}\frac{1-r\cos(\theta'-\theta'')}{r^2+1-2r\cos(\theta'-\theta'')}d\theta'\gamma_2(\theta'')d\theta'' && \text{(B.40)}
\end{aligned}
$$

in which $r = R_1/R_2$.

By switching the order of integration and explicitly evaluating the integrals, we find that

$$
T[\gamma_2](\theta) = \int_0^{2\pi}\left(\frac{1}{2\pi}+a_2\sigma_1 r+\frac{b_2\sigma_1}{\pi}\frac{r^2}{1+r}\frac{r^2-\cos(\theta-\theta')}{1+r^4-2r^2\cos(\theta-\theta')}\right)\gamma_2(\theta')d\theta', \tag{B.41}
$$

in which $r = R_2/R$.

By Eq. (B.4), in order to show that T is a contraction mapping, it suffices to show that

$$
\int_0^{2\pi}\int_0^{2\pi}\left(\frac{1}{2\pi}+a_2\sigma_1 r+\frac{b_2\sigma_1}{\pi}\frac{r^2}{1+r}\frac{r^2-\cos(\theta-\theta')}{1+r^4-2r^2\cos(\theta-\theta')}\right)^2 d\theta'd\theta < 1. \tag{B.42}
$$

B.0.3 *Inverting an Integral Equation*

Interior Dirichlet Problem. Find a function u that is harmonic in D, is continuous in $\bar{D}$, and satisfies the boundary condition

$$
u = f \quad \text{on } \partial D
$$

where f is a given continuous function.

Let $K : C(\partial D) \to C(\partial D)$ be the integral operators given by

$$
(K\varphi)(x) := 2\int_{\partial D}\varphi(y)\frac{\partial\Phi(x,y)}{\partial v(y)}ds(y), \quad x \in \partial D \tag{B.43}
$$

where $\Phi(x,y) = \frac{1}{2\pi} \ln \frac{1}{|x-y|}$ is the fundamental solution to Laplace's equation.

Neumann [Neu77] gave the first rigorous proof for the existence of a solution to the two-dimensional interior Dirichlet problem in a strictly convex domain of class C^2. By completely elementary means he established that the successive approximations

$$\varphi_{n+1} := \frac{1}{2}\varphi_n + \frac{1}{2}K\varphi_n - f, \quad n = 0,1,2,\ldots$$

with arbitrary $\varphi_0 \in C(\partial D)$ converge uniformly to the unique solution φ of the integral equation $\varphi - K\varphi = -2f$. In functional analytic terms his proof amounted to showing that the operator L given by $L := \frac{1}{2}(I+K)$ is a contraction with respect to the norm

$$\|\varphi\| := \left| \sup_{z\in\partial D} \varphi(z) - \inf_{z\in\partial D} \varphi(z) \right| + \alpha \sup_{z\in\partial D} |\varphi(z)| \tag{B.44}$$

where $\alpha > 0$ is appropriately chosen. This norm is equivalent to the maximum norm.

If our kernel K does not lead to a contraction mapping then we can consider another kernel $\widetilde{K}$

$$\widetilde{K}(\theta,\theta') = K(\theta,\theta') - \frac{\int_0^{2\pi} K(\theta,\theta'')\, d\theta''}{2\pi} \tag{B.45}$$

This is because we require $\int_0^{2\pi} \gamma_1(\theta)\, d\theta = 0$ and

$$\widetilde{T}[\gamma_1](\theta) = \int_0^{2\pi} K(\theta,\theta')\gamma_1(\theta')\, d\theta' \tag{B.46}$$

$$= \int_0^{2\pi} K(\theta,\theta') \left[\gamma_1(\theta') - \frac{\int_0^{2\pi} \gamma_1(\theta'')\, d\theta''}{2\pi} \right] d\theta' \tag{B.47}$$

$$= \int_0^{2\pi} \left[K(\theta,\theta') - \frac{\int_0^{2\pi} K(\theta,\theta'')\, d\theta''}{2\pi} \right] \gamma_1(\theta') d\theta' \tag{B.48}$$

$$= \int_0^{2\pi} \widetilde{K}(\theta,\theta')\gamma_1(\theta')\, d\theta'. \tag{B.49}$$

Then

$$\widetilde{T}[\gamma_1](\theta) = \int_0^{2\pi} \frac{b_2\sigma_1}{2\pi(1+r)} \left(2r^2 \frac{r^2 - \cos(\theta-\theta')}{1+r^4-2r^2\cos(\theta-\theta')} - 1\right) \gamma_1(\theta')d\theta' \tag{B.50}$$

$$= \int_0^{2\pi} \frac{b_2\sigma_1}{2\pi(1+r)} \left(\frac{r^4-1}{1+r^4-2r^2\cos(\theta-\theta')}\right) \gamma_1(\theta')d\theta' \tag{B.51}$$

$$= \int_0^{2\pi} \frac{b_2\sigma_1}{2\pi} \left(\frac{(r-1)(r^2+1)}{1+r^4-2r^2\cos(\theta-\theta')}\right) \gamma_1(\theta')d\theta' \tag{B.52}$$

To show that $\widetilde{K}$ yields a contraction mapping it suffices to show that

$$\int_0^{2\pi}\int_0^{2\pi} \left[\frac{b_2\sigma_1}{2\pi}\left(\frac{(r-1)(r^2+1)}{1+r^4-2r^2\cos(\theta-\theta')}\right)\right]^2 d\theta' d\theta < 1 \tag{B.53}$$

We compute the double integral in (B.53) numerically in MATLAB and plot the results in Fig. B.2 along with the largest (in absolute value) eigenvalue of the kernel

$$\widetilde{K}(\theta,\theta') = \frac{b_2\sigma_1}{2\pi}\left(\frac{(r-1)(r^2+1)}{1+r^4-2r^2\cos(\theta-\theta')}\right). \tag{B.54}$$

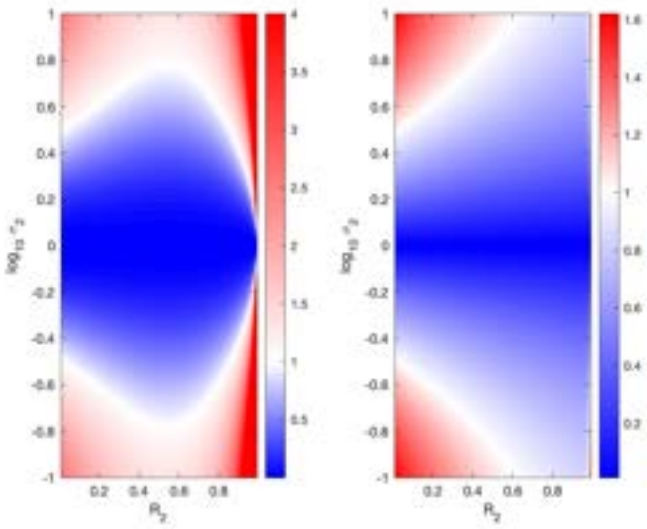

Figure B.2: On the left, integral computed numerically for different radii R_2 and conductivities σ_2 of the small disk where the large disk has radius $R = 1$ and conductivity $\sigma_1 = 1$. On the right, the largest (in absolute value) eigenvalue of the kernel.

The integral in (B.53) can be expressed as an integral of one variable because the function depends on the difference $(\theta - \theta')$ and is 2π-periodic. So once you find the inner integral in $d\theta'$, you get a constant. And the next integral in $d\theta$ just yields a factor 2π.

MATHEMATICA computes the inner integral explicitly with:

```
Integrate[((r-1)*(r^2+1)/(1+r^4-2*r^2*Cos[theta]))^2,{theta
    ↪ ,0,2*Pi},Assumptions->0<r&&r<1]
```

to give:

$$2\pi(1+r^4)/(1-r)/(1+r)^3/(1+r^2). \tag{B.55}$$

The double integral of the square of the adjusted kernel then becomes

$$4\sigma_1^2(\sigma_1-\sigma_2)^2/(\sigma_1+\sigma_2)^2(1+r^4)/(1-r)/(1+r)^3/(1+r^2) \tag{B.56}$$

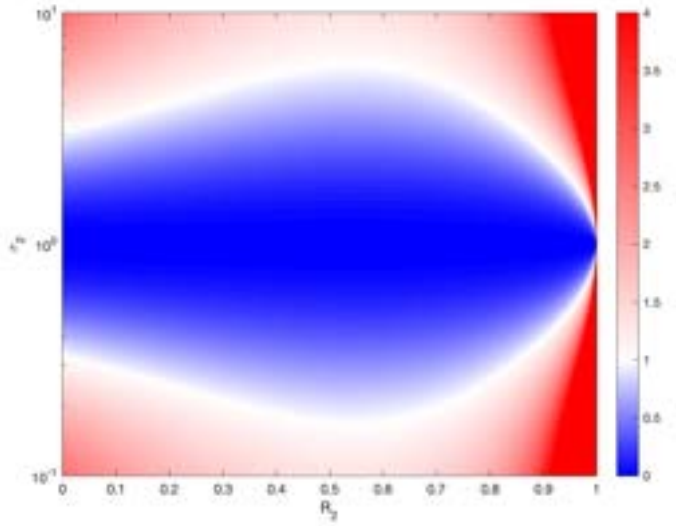

Figure B.3: Integral computed numerically for different radii R_2 and conductivities σ_2 of the small disk where the large disk has radius $R = 1$ and conductivity $\sigma_1 = 1$.

We plot this integral with $\sigma_1 = 1, R = 1$ (so that $r = R_2$) for different values of σ_2 and R_2 in Fig. B.3. In the blue region of the plot, the integral is less than 1 which is a sufficient condition for a contraction mapping. Thus, we can invert the integral equation

$$(I - T)[\gamma_1](\theta) = -2g(\theta) \tag{B.57}$$

by considering the series

$$[\gamma_1](\theta) = (I - T)^{-1}[-2g(\theta)] \tag{B.58}$$
$$= [I + T + T^2 + \dots][-2g(\theta)]. \tag{B.59}$$

We can truncate the series after the Nth term to approximate γ_1

$$[\gamma_1](\theta) \approx [I + T + T^2 + \cdots + T^N][-2g(\theta)]. \tag{B.60}$$

We want to find an explicit expression for the error for this approximation. This will require us to find an explicit formula for $T^N[g](\theta)$. We compute the following:

$$T[g](\theta) = \int_0^{2\pi} \frac{b_2\sigma_1}{2\pi} \left(\frac{(r-1)(r^2+1)}{1 + r^4 - 2r^2\cos(\theta - \theta')} \right) g(\theta')d\theta' \tag{B.61}$$

$$T^2[g](\theta)$$
$$= \int_0^{2\pi} \frac{b_2\sigma_1}{2\pi} \left(\frac{(r-1)(r^2+1)}{1 + r^4 - 2r^2\cos(\theta - \theta')} \right) T[g](\theta')d\theta' \tag{B.62}$$
$$= \left(\frac{b_2\sigma_1}{2\pi} \right)^2 \int_0^{2\pi} \int_0^{2\pi} \left(\frac{(r-1)(r^2+1)}{1 + r^4 - 2r^2\cos(\theta - \theta')} \right)$$
$$\cdot \left(\frac{(r-1)(r^2+1)}{1 + r^4 - 2r^2\cos(\theta' - \theta'')} \right) g(\theta'')d\theta' d\theta'' \tag{B.63}$$

We can define $T^N[g](\theta)$ recursively

$$T^N[g](\theta) = \int_0^{2\pi} \frac{b_2\sigma_1}{2\pi} \left(\frac{(r-1)(r^2+1)}{1 + r^4 - 2r^2\cos(\theta - \theta')} \right) T^{N-1}[g](\theta')d\theta'. \tag{B.64}$$

COLOPHON

This thesis was typeset using the typographical look-and-feel `classicthesis` developed by André Miede and Ivo Pletikosić.

The style was inspired by Robert Bringhurst's seminal book on typography "*The Elements of Typographic Style*".